# A VID-BASED STRATEGY FOR THE SYNTHESIS OF ARMCHAIR AROMATIC BELTS

TIEGUANG YAO

# A VID-Based Approach to Synthesize Armchair Aromatic Belts

Tieguang Yao

# A VID-Based Strategy for the Synthesis of Armchair Aromatic Belts

By

Tieguang Yao

B.Sc., Hons. Peking University, Beijing, China, 2003

A thesis submitted to the School of Graduate Studies in partial fufillment of the requirements for the degree of Doctor of Philosophy

Department of Chemistry

Memorial University

St. John's, Newfoundland and Labrador, Canada

March 2009

# Abstract

A molecular belt is considered to be an assembly of atoms that has two continuous, nonintersecting edges and a width that is small in relation to its circumference. Molecular belts having surfaces consisting entirely of a polycyclic aromatic framework are referred to "aromatic belts".

Aromatic belts have stood as challenging synthetic targets for many years. Several approaches to synthesize aromatic belts have been reported. To date, no aromatic belts has been successfully synthesized rationally by assembling small building blocks.

Bodwell's group has developed a method, valence isomerization followed by dehydrogenation (VID), which can accomplish the formation of highly nonplanar (and thus strained) pyrene units.

A strategy for the synthesis of cyclophenacene-type aromatic belts (or armchair SWNCT segments) that relies upon a VID reaction is described, and progress toward achieving this goal is presented.

# Acknowledgements

I would like to thank my supervisor, Prof. Graham J. Bodwell for providing me such a wonderful opportunity to join his group his enthusiasm and encouragement throughout the past years.

I am also grateful to my supervisory committee members, Prof. Paris Geoghiou and Prof. David Thompson for valuable suggestions and help during the past years.

The present and past members of the Bodwell group are also acknowledged for their collaboration and help: Hao Yu, Dr. Baozhong Zhang, Brad Merner, Amit Kudale, Salah Al-dukhi, Ahn-Thu Dang, Jennifer Swyers, Penchal Reddy Nandaluru, Yixi Yang, Venkata Ramana, Dr. Teizi Satou, Krista Hawco, Jamie Kendall, Greg Manning, Chad Warford, Patty Merner, and Marisa Chard.

Guang Chen is gratefully acknowledged for the valuable discussion of the calculation in Appendix A.

I would like to acknowledge all of the faculty, staff, and graduate students in Chemistry Department, especially Prof. Paris E. Georghiou, Prof. Sunil Pansare, Prof. Yuming Zhao and their research groups for their kind cooperation.

Acknowlegements are also extended to Dave Miller, Linda Winsor, Dr. Celine Schneider, Julie Collins, and Kai Zhang, and Li Wang for their assistance with the NMR, MS, and other characterizations.

I also appreciate financial support from the School of Graduate Studies and Memorial University.

# Table of Contents

# List of Figures

# List of Schemes

# List of Tables

# List of Abbreviations and Symbols Used

| | |
|---|---|
| Ac | acetyl |
| APCI | atmosphere pressure chemical ionization |
| Bu | butyl |
| BuLi | *n*-butyllithium |
| Calcd | calculated |
| cat. | Catalytic |
| CNT | carbon nanobube |
| d | doublet (in NMR) |
| dd | doublet of doublets |
| DBU | 1,8-diazabicyclo[5.4.0]undec-7-ene |
| DDQ | 2,3-dichloro-5,6-dicyano-1,4-benzoquinone |
| DIBAL-H | diisobutylaluminum hydride |
| DMA | *N,N*-dimethylacetamide |
| DMPD | 1,3-dimethyl-2-phenyl-1,3,2-diazaphospholidine |
| Et | ethyl |
| HRMS | high-resolution mass spectrometry |
| h | hours |
| h$\nu$ | light |
| HPLC | high-performance liquid chromatography |
| Hz | hertz |
| IBX | 2-iodoxybenzoic acid |

| | |
|---|---|
| IR | infrared (spectroscopy) |
| *J* | coupling constant (Hz) |
| K | Kelvin |
| kcal | kilocalorie(s) |
| kJ | kilojoule(s) |
| m | multiplet (in NMR) |
| m | medium (in IR) |
| Me | methyl |
| MHz | megahertz |
| min | minute(s) |
| mp | melting point |
| NBS | *N*-bromosuccinimide |
| NMR | nuclear magnetic resonance (spectroscopy) |
| Ph | phenyl |
| ppm | parts per million |
| q | quartet (in NMR) |
| $R_f$ | retention factor (in TLC) |
| Rt | room temperature |
| s | singlet (in NMR) |
| s | strong (in IR) |
| SWCNT | single-walled carbon nanotube |
| t | triplet (in NMR) |
| TCDI | 1,1'-thiocarbonyldiimidazole |

| | |
|---|---|
| THF | tetrahydrofuran |
| TLC | thin layer chromatography |
| TMS | trimethylsilyl |
| | tetramethylsilane (in NMR) |
| Ts | *p*-toluenesulfonyl |
| UV-Vis | ultraviolet-visible (spectroscopy) |
| VID | valence isomerization-dehydrogenation |
| w | weak (in IR) |

# Chapter 1

# Introduction

## 1.1 Aromatic Belts

For the purpose of this thesis, a molecular belt will be considered to be an assembly of atoms that has two continuous, nonintersecting edges and a width that is small in relation to its circumference. This definition immediately disqualifies systems such as cyclodextrins, e.g., (**1-1**)[1] and cyclic phenylene acetylenes, e.g., (**1-2**)[2] because the two edges intersect (Figure 1.01). Numerous examples of molecular belts have been reported, e.g., cucurbiturils (**1-3**),[3] and virtually all of these systems have some $sp^3$-hybridized atoms in their frameworks, especially the edges. Special cases among molecular belts are those that have only $sp^2$-hybridized atoms in their surfaces. Although a variety of structural motifs can conceivably fall into this category, molecular belts having surfaces consisting entirely of a polycyclic aromatic framework have been by far the subjects of the greatest interest. Such systems are often referred to as "aromatic belts".

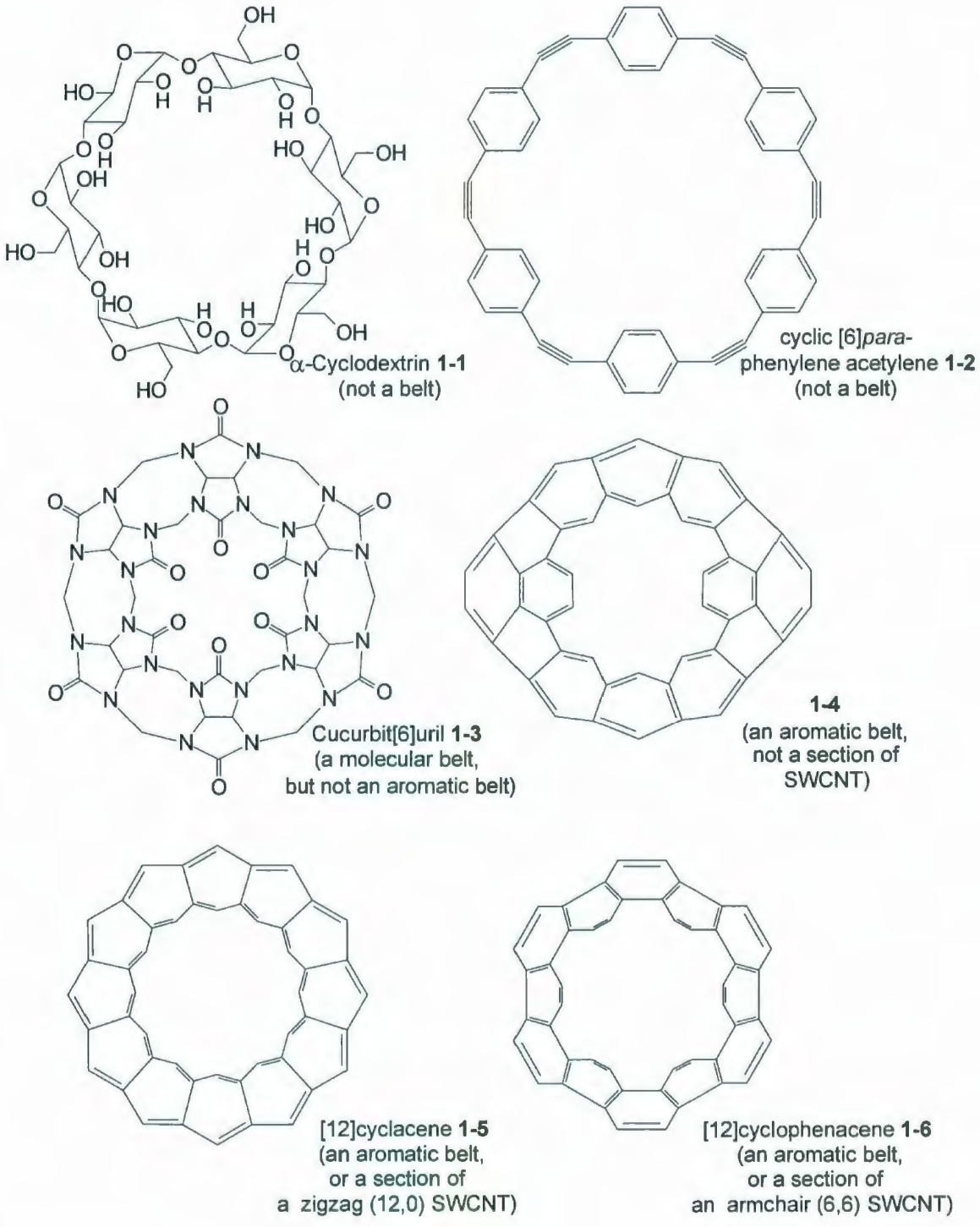


**Figure 1.01.** Some examples of aromatic belts, molecular belts, and non-belts.

Aromatic belts can also be viewed as segments of single-walled carbon nanotubes (SWCNT). As such, there is a direct relationship between the roll-up motif in SWCNTs[4] and the roll-up motif of aromatic belts. Cyclacenes (**1-5**), which are substructures of "zigzag" nanotubes, are derived from rolling up linear acenes (or [*n*]acenes), and cyclophenacenes (**1-6**), which are substructures of "armchair nanotubes", are derived from rolling up [*n*]phenacenes (Figure 1.02). A broad range of chiral aromatic belts, which correspond to chiral SWCNTs, are also possible, but such systems will not be discussed in this thesis.

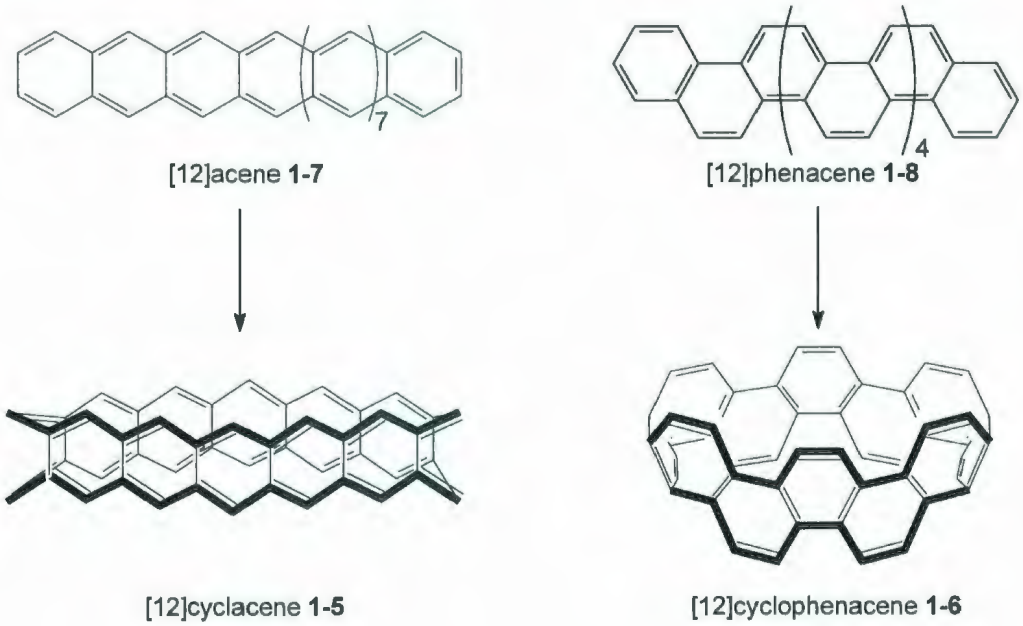


**Figure 1.02.** The roll-up motifs of cyclacenes and cyclophenacenes.

The trigonal planar geometry of an $sp^2$-hybridized carbon atom and the cyclic nature of a belt are structurally at odds with one another. In other words, a polycyclic aromatic system such as an [*n*]acene or an [*n*]phenacene has a lowest energy conformation that is planar. However, the rolling up process requires the adoption of a nonplanar conformation. As the degree of nonplanarity increases, the strain energy increases and the aromatic stabilization energy (ASE) decreases. These two major energetic factors will be important in determining the stability of a particular aromatic belt.

Some aromatic belts also map onto the surfaces of various fullerenes, and can be viewed as segments of fullerenes (Figure 1.03). The belt that maps on the equator of $C_{60}$ is [10]cyclophenacene. Interestingly, the belt that maps onto the equator of $D_{5h}$-$C_{70}$ and the equatorial region of $D_{5d}$-$C_{80}$ has the same structure, but it adopts different conformations ($D_{5h}$ and $C_{5v}$ symmetry, respectively). The next higher homolog of this belt maps onto the equator of $D_{6h}$-$C_{84}$. This series of belts, which will be discussed later, was originally proposed by Vögtle.[5]

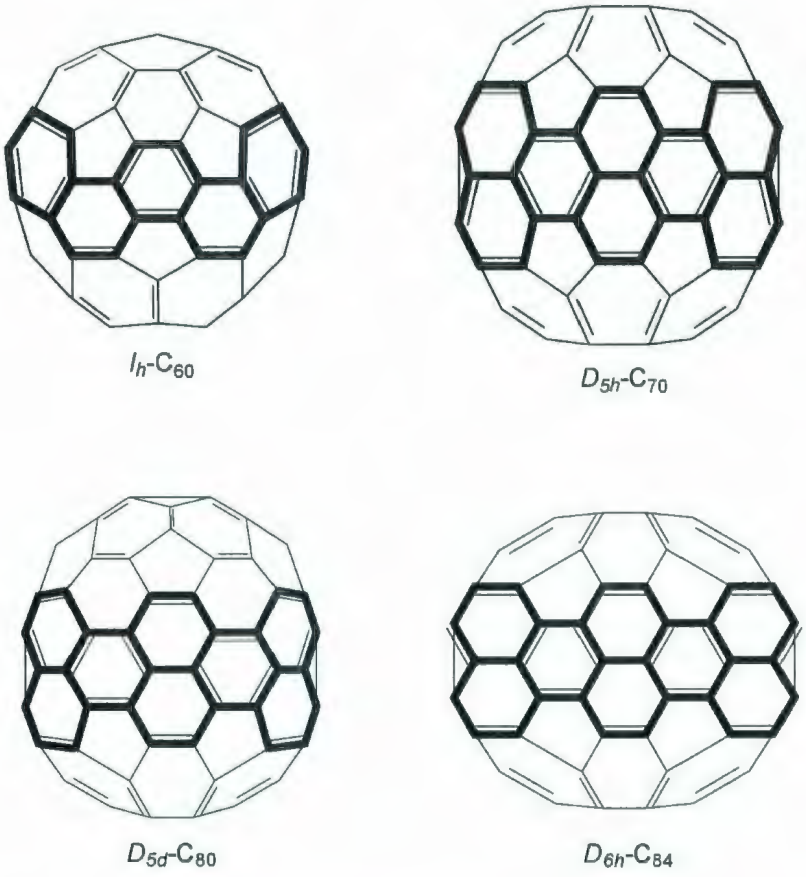


**Figure 1.03.** Aromatic belts that maps onto fullerenes.

## 1.2 Theoretical Studies of Aromatic Belts

The aromaticity of aromatic belts can be estimated qualitatively from their Clar structures.[6] The maximum number of isolated aromatic sextets indicates the relative aromatic stability of linear and cyclic polyacenes (Figure 1.04). As shown, [12]acene (**1-7**), as an example of the [*n*]acenes, has only one aromatic sextet, and [12]phenacene (**1-8**), as an example of [*n*]phenacenes, has six aromatic sextets. This result gives a reasonable assumption that [*n*]phenacenes are more

stable than the corresponding [*n*]acenes. On the other hand, [12]cyclacene (**1-5**) has no aromatic sextets, but [12]cyclophenacene (**1-6**) has six. Therefore, cyclophenacenes are expected to be more stable than cyclacenes, primarily due to greater aromatic stabilization energy (ASE). The expectation of greater stability immediately flags the cyclophenacene motif as being synthetically more attractive than the cyclacene motif.

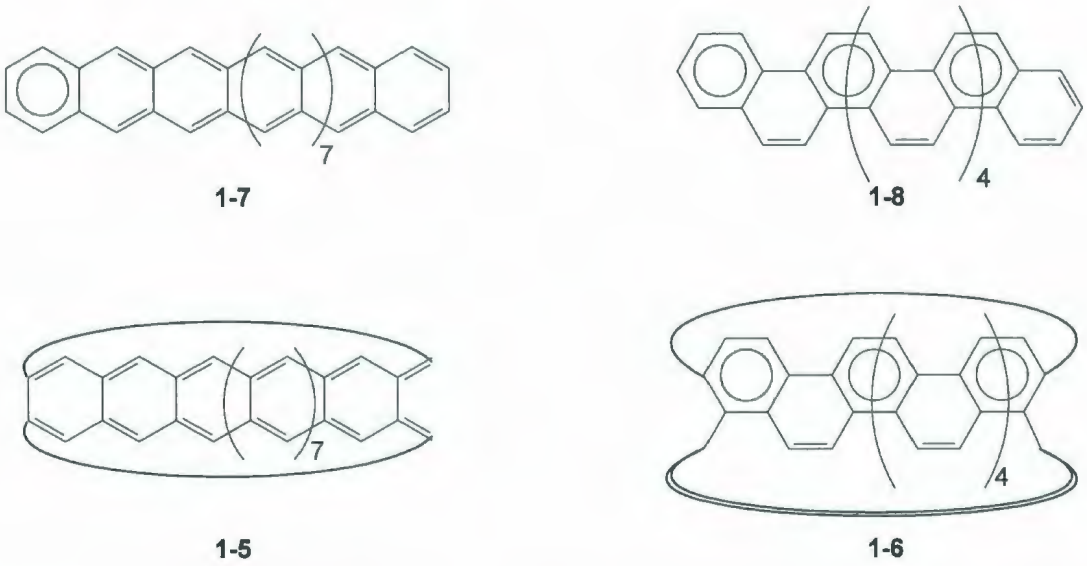


**1-7** **1-8**

**1-5** **1-6**

**Figure 1.04.** Clar structures of [12]acene (**1-7**), [12]cyclacene (**1-5**), [12]phenancene (**1-8**), and [12]cyclophenacene (**1-6**).

Calculations also supported this simple analysis. Aihara analyzed the topological resonance energy (TRE), resonance energy per ⑥-electron (REPE), and the percentage resonance energy (%RE) ("good measures of aromatic stabilization")[7,8] of [*n*]acenes, [*n*]phenacenes, [*n*]cyclacenes, and [*n*]cyclophenacenes to predict their relative aromaticity.[8] For example, in the case

of [12]cyclacene **1-5** and [12]cyclophenacene **1-6**, the %RE of **1-5** is 1.341, and %RE of **1-6** is 2.573. Calculations of other [*n*]acenes, [*n*]phenacenes, [*n*]cyclacenes, and [*n*]cyclophenacenes based on TRE, REPE, and %RE also follow the same trend, leading to the same expectation of relative aromaticity of cyclacenes and cyclophenacenes.

### 1.3 Previous Attempts at the Synthesis of Aromatic Belts

A number of synthetic approaches toward aromatic belts have been reported in the past decades. Cyclacenes, cyclophenacenes and other motifs have all been the subject of study. The most popular strategy involves the formation of a relatively unstrained molecular belt by a double Diels-Alder reaction, followed by aromatization. To synthesize the molecular belt precursor, two types of double Diels-Alder reactions were most frequently reported (Scheme 1.01). The first strategy employs a molecule containing both a diene unit and a dienophile unit, which has been called an "AB-type monomer".[9] Self-reaction of such a system generally leads to the formation of a cyclic dimer and/or higher cyclic oligomers, as well as linear oligomers/polymers. The second strategy is a double Diels-Alder reaction involving a bis(diene) and a bis(dienophile) to afford the bis(cycloadduct).

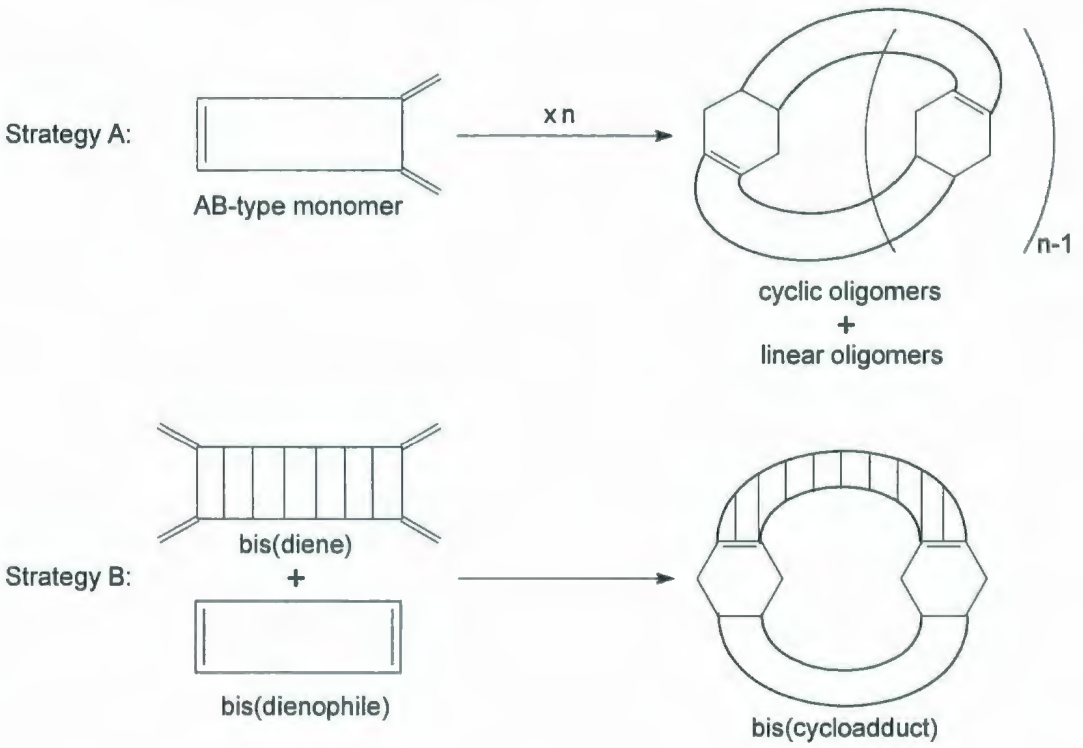


**Scheme 1.01.** Two frequently reported strategies to synthesize molecular belts based on Diels-Alder reactions.

Schlüter reported the synthesis of two belt-shaped frameworks by application of Strategy A. The first molecular belt was compound **1-14**, which is a potential precursor to a highly strained [6]cyclacene (Scheme 1.02).[9] The synthesis of **1-14** proceeded through a Diels-Alder reaction between diene **1-9** and 1,4-benzoquinone (**1-10**) to afford compound **1-11**, which was then oxidized to afford compound **1-12** (reaction conditions and yield were not given). The orbital symmetry-allowed ring-opening of the cyclobutene ring in **1-12** afforded intermediate **1-13**, which self-reacted to afford the desired cyclic dimer **1-14**

(70%) along with polymers in a ratio of 4:1. No attempt to convert **1-14** into an aromatic belt has been reported.

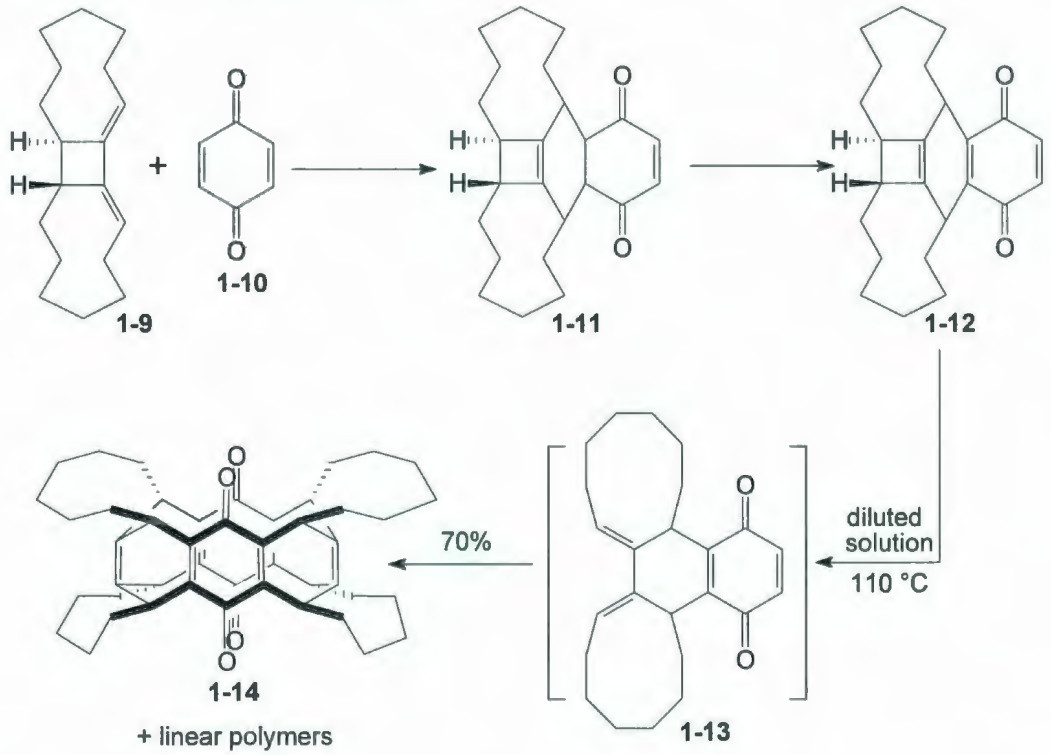


**Scheme 1.02.** Schlüter's synthesis of molecular belt **1-14**.

The second target, **1-20**, embodies the carbon framework of [18]cyclacene.[10] The first key step of the synthesis (Scheme 1.03) was a Diels-Alder reaction between diene **1-15** and dienophile **1-16** to give **1-17**, which was then converted into dienophile **1-18** by treatment with *n*-BuLi (benzyne formation) in the presence of furan. Compound **1-18** was then converted into cyclic trimer **1-20** in 4 steps, the last of which was *in situ* generation and self-reaction of monomer **1-19**. Compound **1-20** was found to be in equilibrium with linear oligomers under the reaction conditions.

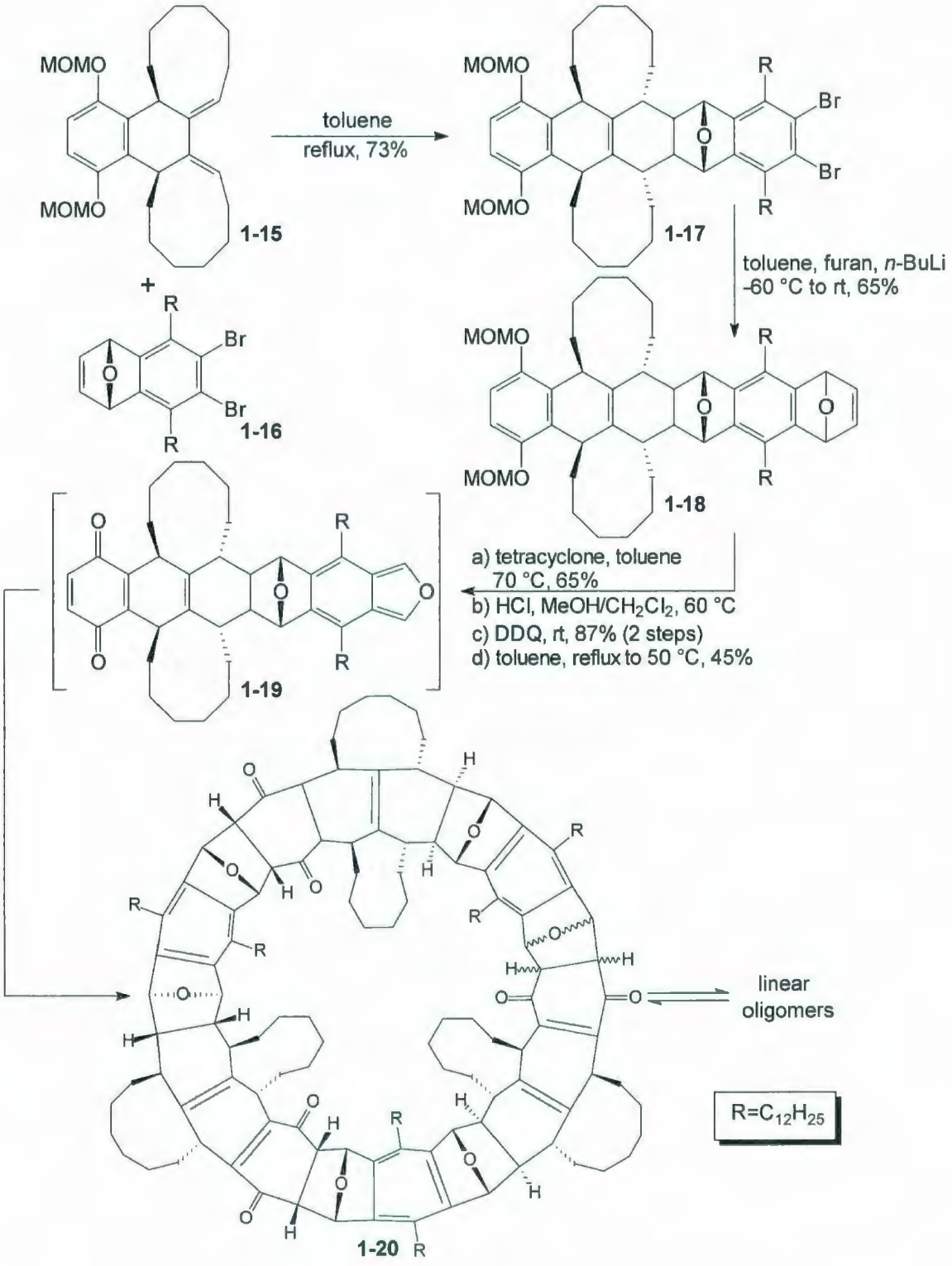


**Scheme 1.03.** Schlüter's synthesis of molecular belt **1-20**.

Klärner and coworkers reported the synthesis of a series of frameworks of [12]-, [13]-, and [14]cyclacenes using Strategy B to assemble the requisite carbon atoms of desired macrocycles.[11] Bis(diene) **1-21** reacted with bis(dienophile) **1-22a** and **1-22b** under high pressure to afford molecular belts **1-1-23a** and **1-23b** in 50-60% yield (Scheme 1.04). These systems possess the framework of [12]cyclacene. Bis(diene) **1-24** was reacted with bis(dienophile) **1-25** under the same conditions to afford inseparable 1:1 mixture of compounds $C_{2h}$-**1-26** and $C_{2v}$-**1-26**, which embody the skeleton of [14]cyclacene (Scheme 1.05). The framework of [13]cyclacene was also synthesized using this method (not shown). The aromatization of these molecular belts was not reported, since the methano bridges essentially rule out conversion of the molecular belts to cyclacenes.

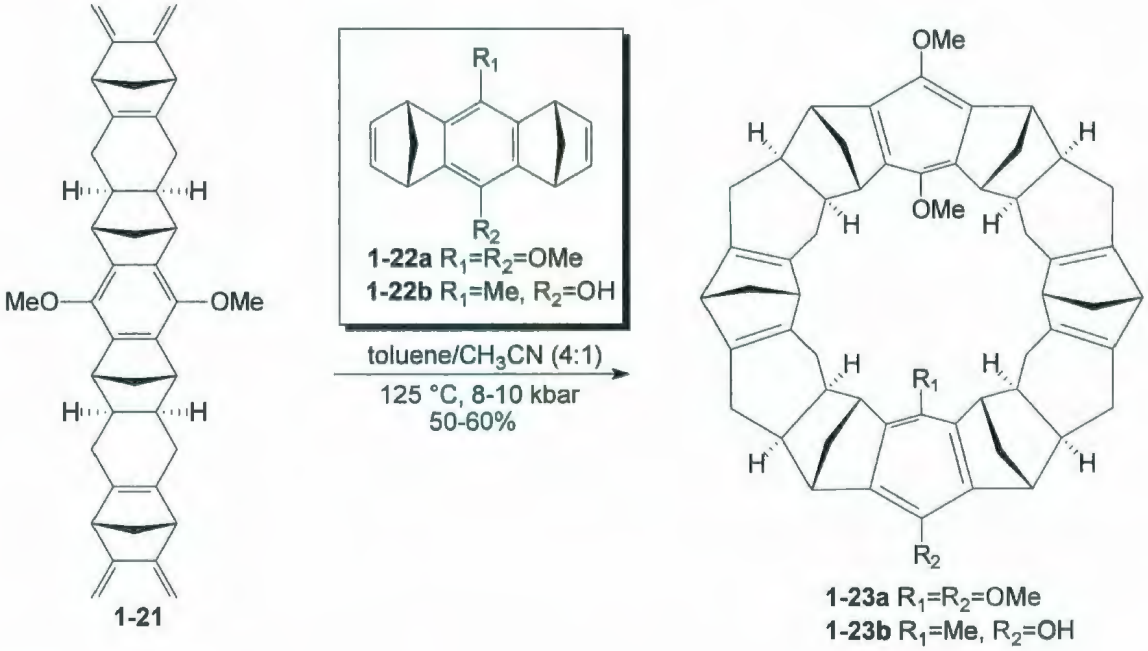


**Scheme 1.04.** Klärner's synthesis of the frameworks of [12]cyclacene.

Although no attempt to aromatize belts **1-23** and **1-26** was reported, these pioneering achievements established the viability of the Diels-Alder approach for the formation of molecular belts.

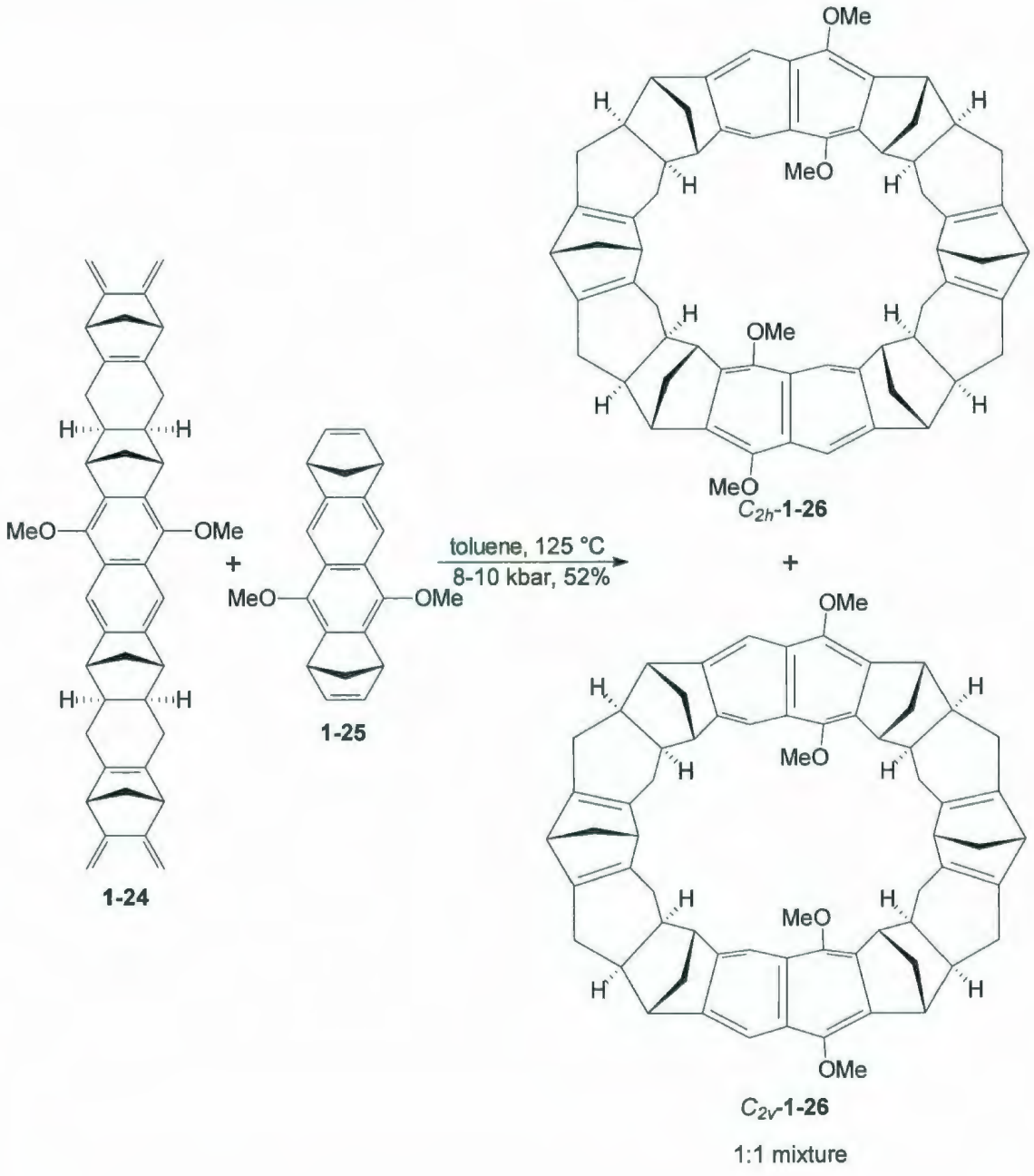


**Scheme 1.05.** Klärner's synthesis of the frameworks of [14]cyclacene.

Stoddart also pursued a synthesis of [12]cyclacene based on a double Diels-Alder approach (Strategy B) to build the skeleton of the molecular belt **1-32** (Scheme 1.06).[12] In this case, the only one of ten possible diastereoisomeric 2:1 adducts, i.e., bis(diene) **1-30**, was synthesized in good yield (80%) by the reaction of bis(diene) **1-29** and bis(dienophile) **1-28** in a 2.5:1 ratio. Compound **1-30** was then reacted with bis(dienophile) **1-28** under high pressure to furnish molecular belt **1-32** "presumably" through intermediate **1-31** in 36% yield. Partial deoxygenation occurred upon treatment with $TiCl_4/LiAlH_4$ to give compound **1-33** (34%) and subsequent acid-catalyzed dehydration afforded the less symmetric isomer of octahydro[12]cyclacene (**1-34**) consisting of one benzene, two naphthalene, and one anthracene substructures in 56% isolated yield (Scheme 1.07). The preference for the formation of isomer **1-34** to the exclusion of others presumably reflects the most favorable balance between maximization of ASE and minimization of strain energy. Treatment of **1-34** with $Li/NH_{3(l)}$ afforded highly symmetric [12]collarene (a dodecahydro[12]cyclacene) (**1-35**). MS analysis showed clearly a molecular ion at *m/z* 612 with little fragmentation. $^1H$ NMR analysis also supported the formation of **1-35**.

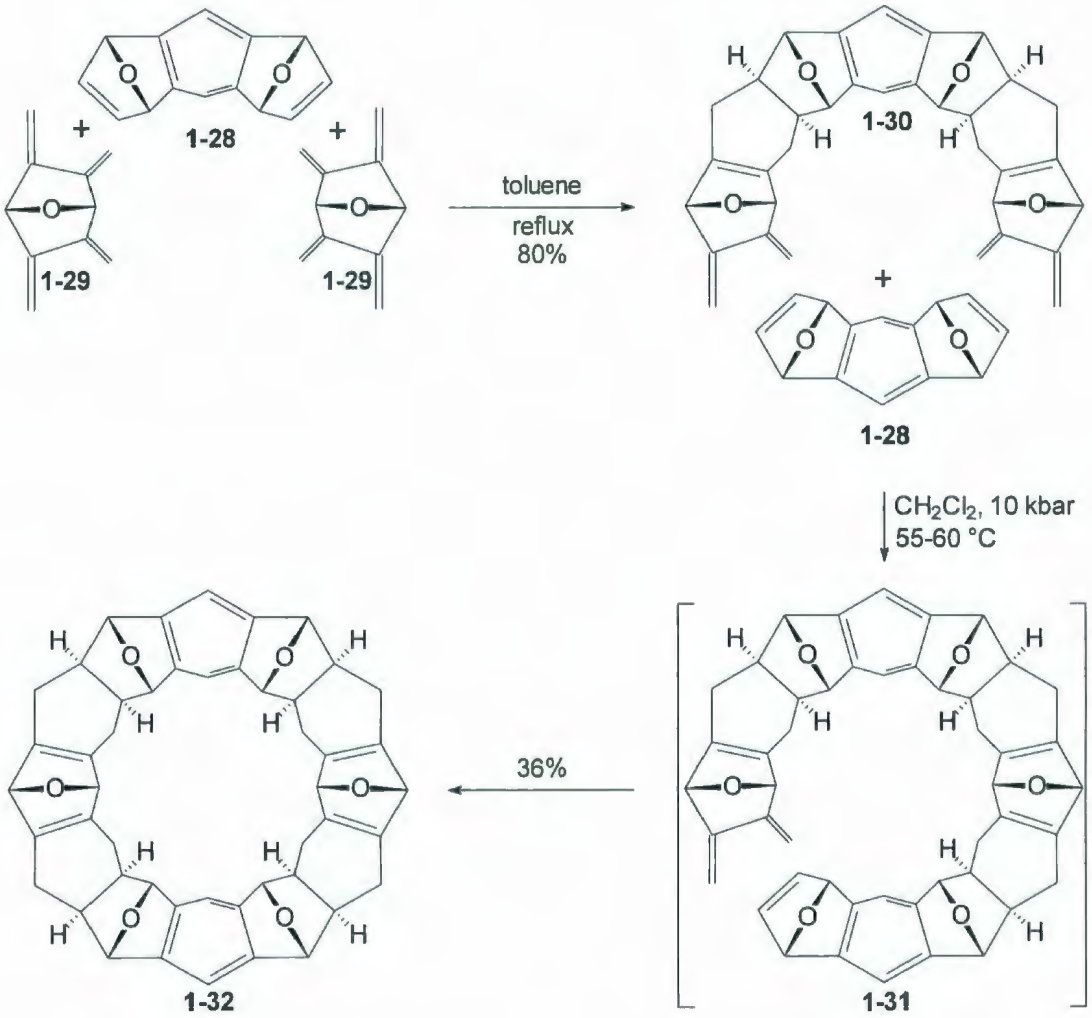


**Scheme 1.06.** Stoddart's synthesis of molecular belts **1-32**.

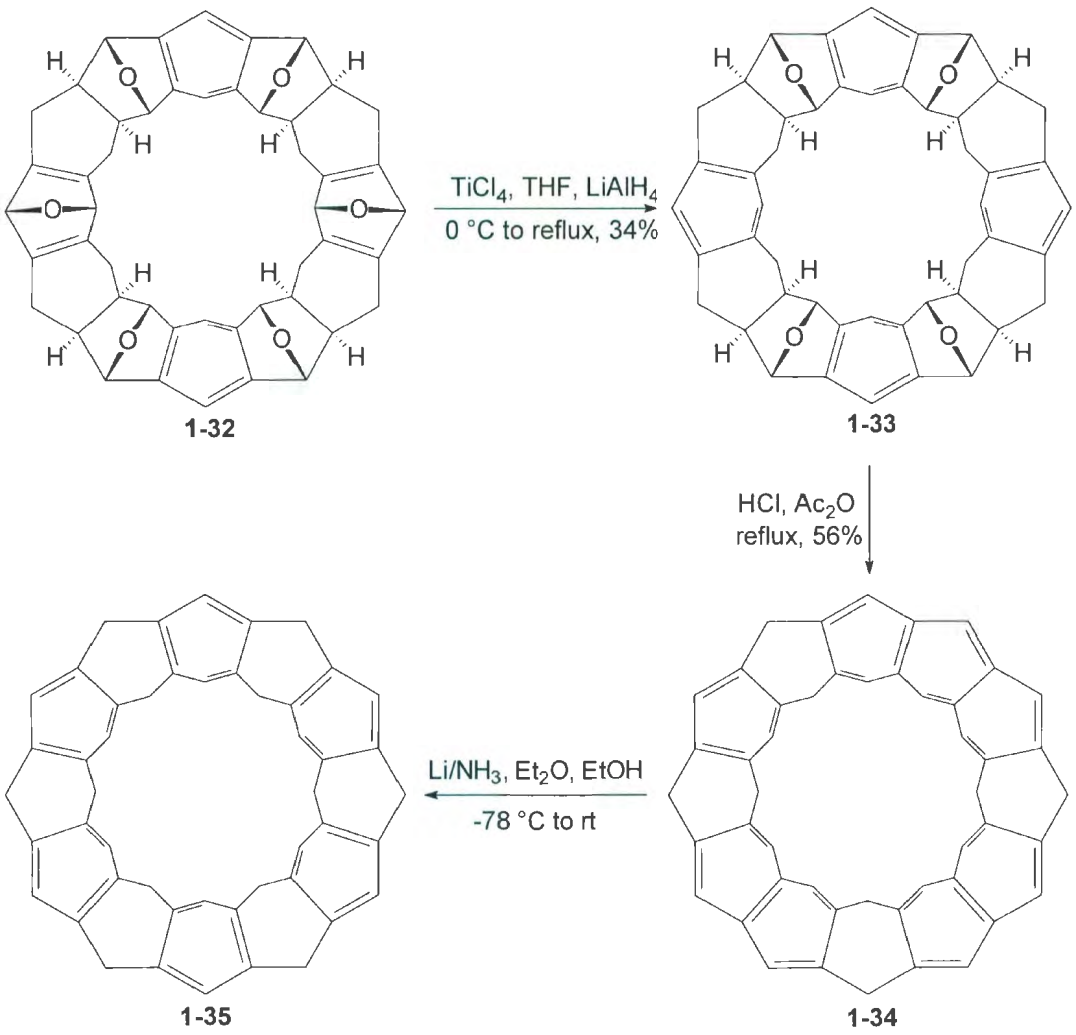


**Scheme 1.07.** Stoddart's synthesis toward [12]cyclacene and collarene.

Cory also reported attempts to synthesize [8]cyclacenes using a double Diels-Alder (Strategy B) to assemble the requisite carbon framework of [8]cyclacene (Scheme 1.08).[13] The reaction between bis(diene) **1-36** and bis(dienophile) **1-37** afforded molecular belt **1-38** in an impressive 69% yield when separate dioxane solutions of the diene and dienophile were added simultaneously to refluxing dioxane. Macrocyclic cyclophane **1-38** has two existing aromatic rings and functionality that could conceivably be used to effect aromatization. Although extra unsaturation could be introduced by epoxidation and dehydration (i.e., via **1-39**, **1-40**), dehydrogenation with DDQ (i.e., **1-41**), or oxidation with PCC and oxygen (i.e., **1-42**, **1-43**), the complete conversion of **1-38** into an [8]cyclacene (or [8]cyclacenequinone) has not yet been reported (Scheme 1.09).[14] Considering that [8]cyclacene is a relatively small (and thus strained) belt, this is not surprising.

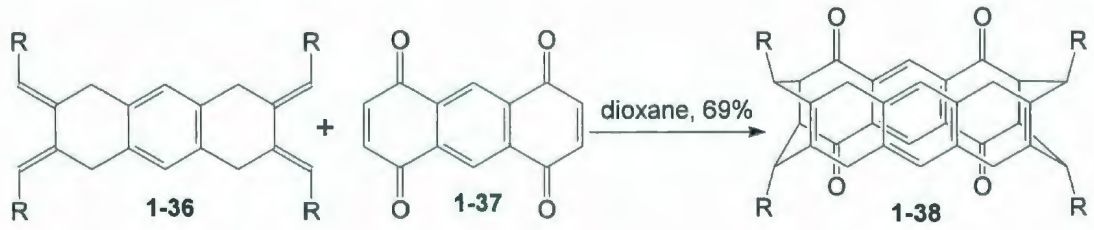


**Scheme 1.08.** Cory's synthesis of molecular belt **1-38**.

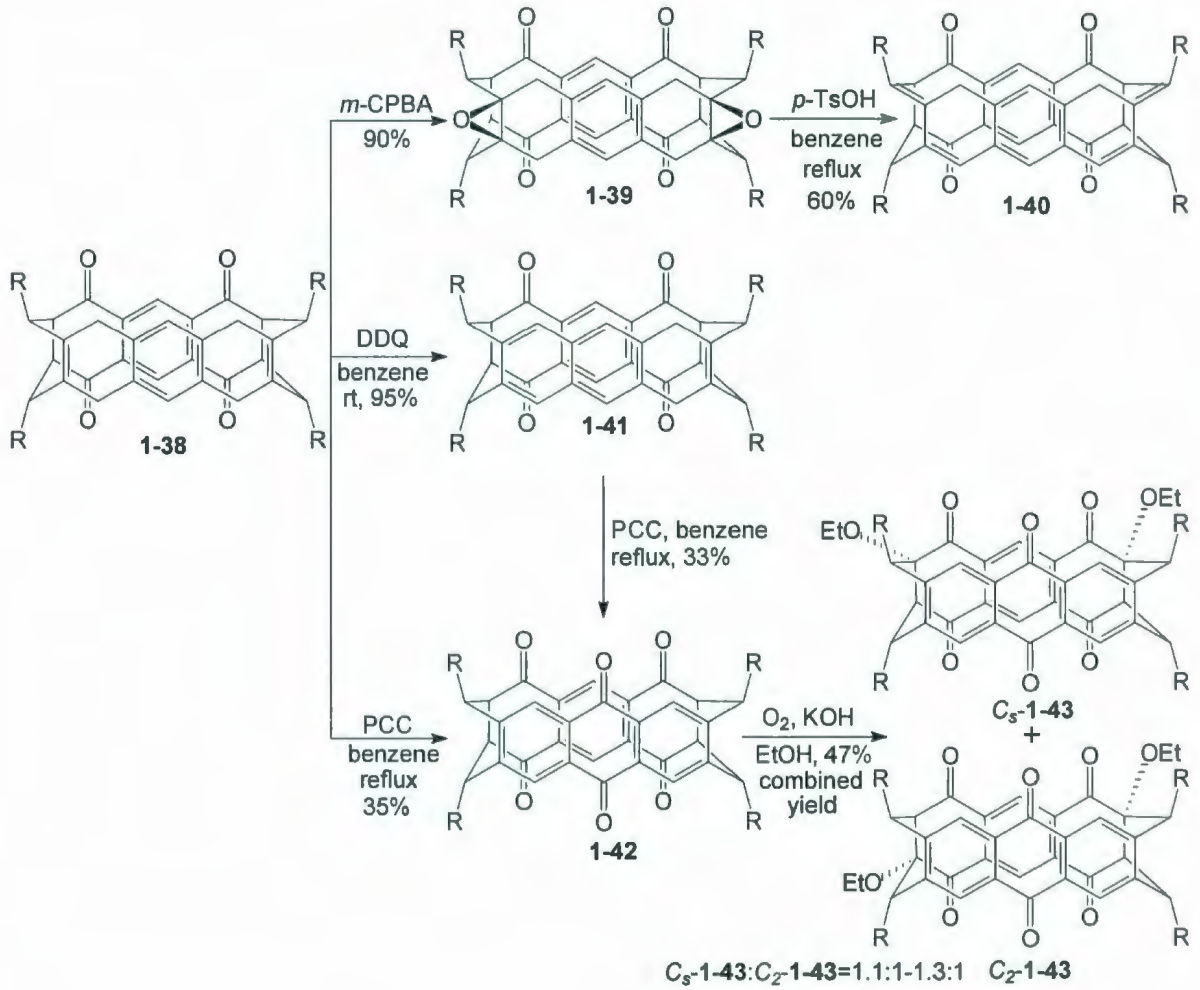


**Scheme 1.09.** Cory's attempts to synthesize [8]cyclacene from **1-38**.

Schlüter reported an attempt to synthesize aromatic belt **1-57**, which he refers to as a "double-stranded cycle" (Scheme 1.11-1.13).[15] The carbon skeleton of this belt maps onto the surface of $D_2$-$C_{84}$. Again, the synthesis relied upon a double Diels–Alder reaction (strategy A) to build the "double–stranded cycles". The key feature of this approach was that the target belt consists of alternating naphthalene and anthracene units, in which every fusion is 1,8- with respect to the naphthalene systems (*peri*-fusion) and 2,3- with respect to the anthracene systems. As a result, four five-membered rings are present on the surface of **1-57**. The departure from the pure cyclacene motif was anticipated to bring with it enhanced stability. The synthesis of the fully unsaturated ladder polymer **1-47** by dehydrogenation of polymer **1-46** by treatment with DDQ, which came from self-reaction of **1-44** in the presence of anti-oxidant **1-45**, provided grounds for optimism that the same chemistry could be applied to the synthesis of aromatic belt **1-57** (Scheme 1.10).[16]

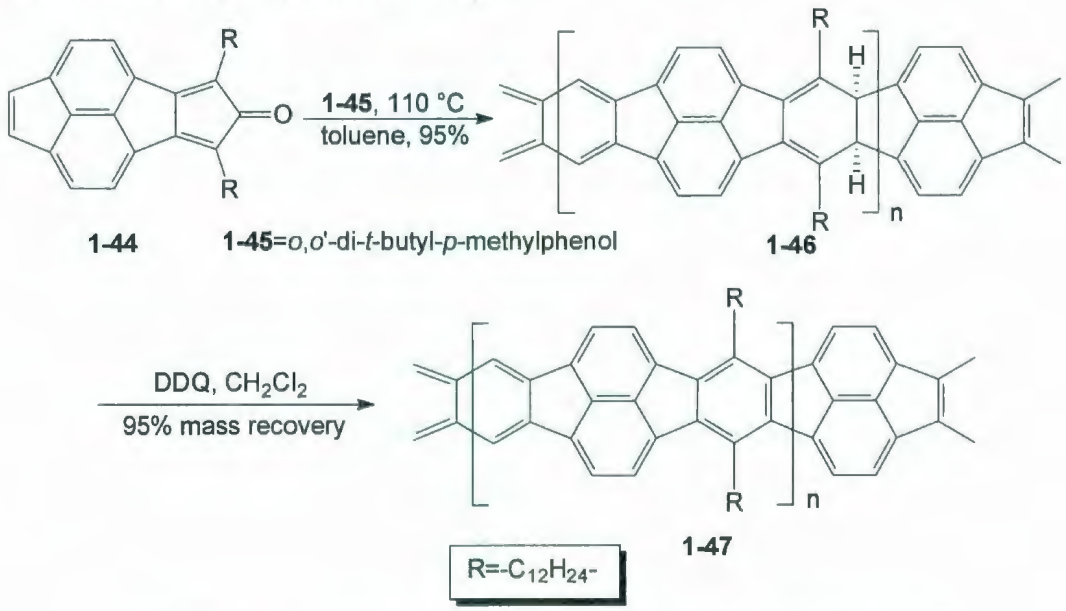


**Scheme 1.10.** Schlüter's synthesis of ladder polymer **1-47**.

The synthesis proceeded through the reaction between dihydropyracylene (**1-48**) and isobenzofuran precursor **1-49** to afford the *endo* and *exo* isomers of **1-50** in a ratio of 4:1 in 90% combined yield (Scheme 1.11).[15] The isomers were then separated. After dehydrogenation of **1-50** by treatment with DDQ, the two diastereomers were independently reacted with *n*-BuLi to afford a benzyne intermediate, which underwent Diels-Alder reaction with the solvent (furan). The reaction of *endo*-**1-50** gave a mixture of *syn* and *anti* diastereomeric oxanorbornenes *endo-syn*-**1-51**, *endo-anti*-**1-51** in a ratio of 1.5:1 in 53% combined yield, and the reaction of *exo*-**1-50** gave a mixture of *syn* and *anti* isomers *exo-syn*-**1-51**, *exo-anti*-**1-51** in 1:1 ratio in 50% combined yield. Each diastereomer of **1-51** was then individually reacted with tetracyclone (2,3,4,5-tetraphenylcyclopentadienone) to afford the corresponding Diels-Alder adduct **1-52** (20%). These reactions proceeded completely stereoselectively in an *exo* fashion on the face of the dienophile opposite to the oxygen atoms.[15] Each of the four diastereomers of **1-52** was then individually heated in toluene to generate monomers **1-53**, which then self-reacted to give the same macrocycle **1-54** (Scheme 1.12).

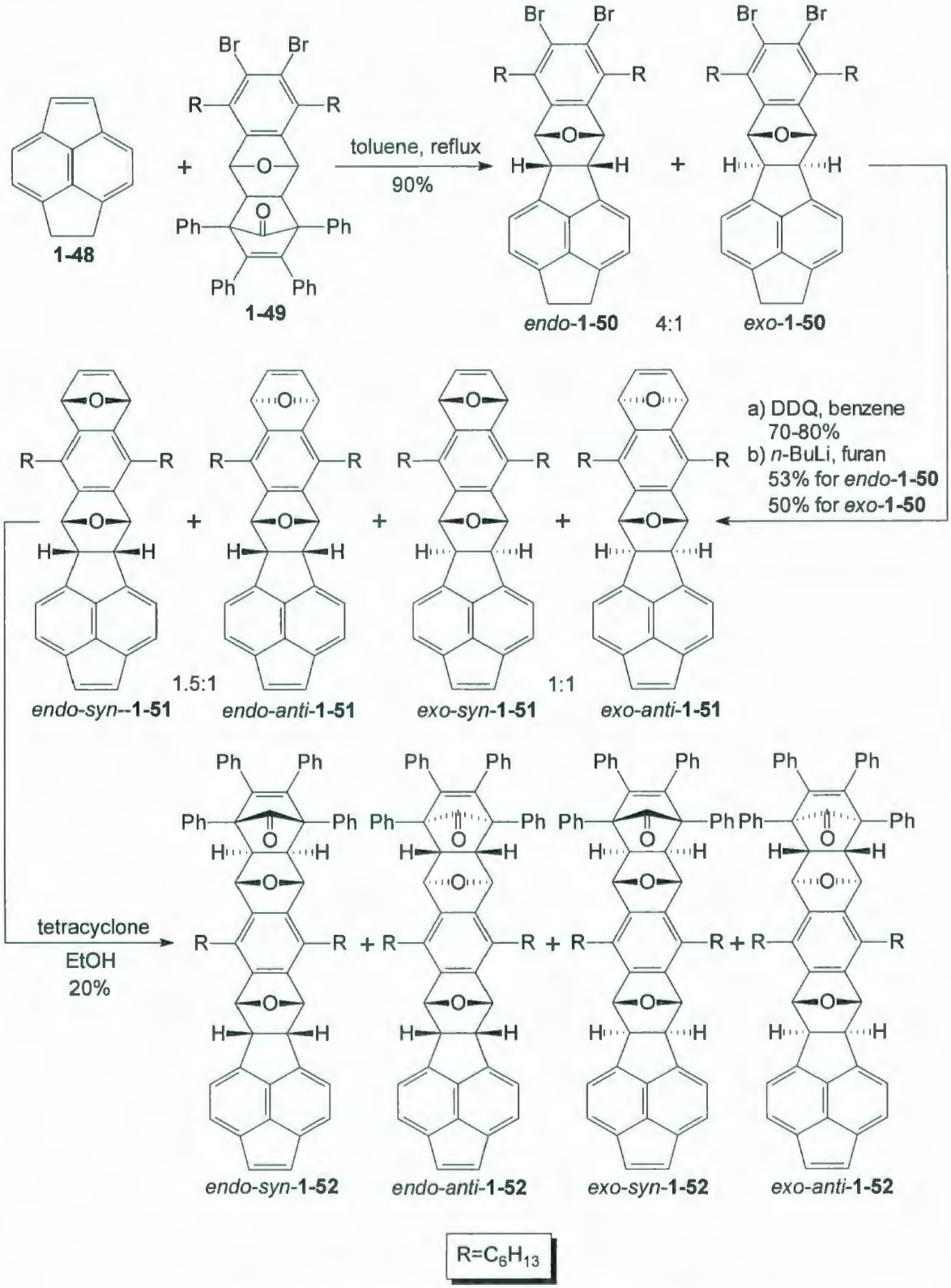


**Scheme 1.11.** Schlüter's synthesis of building blocks **1-52**.

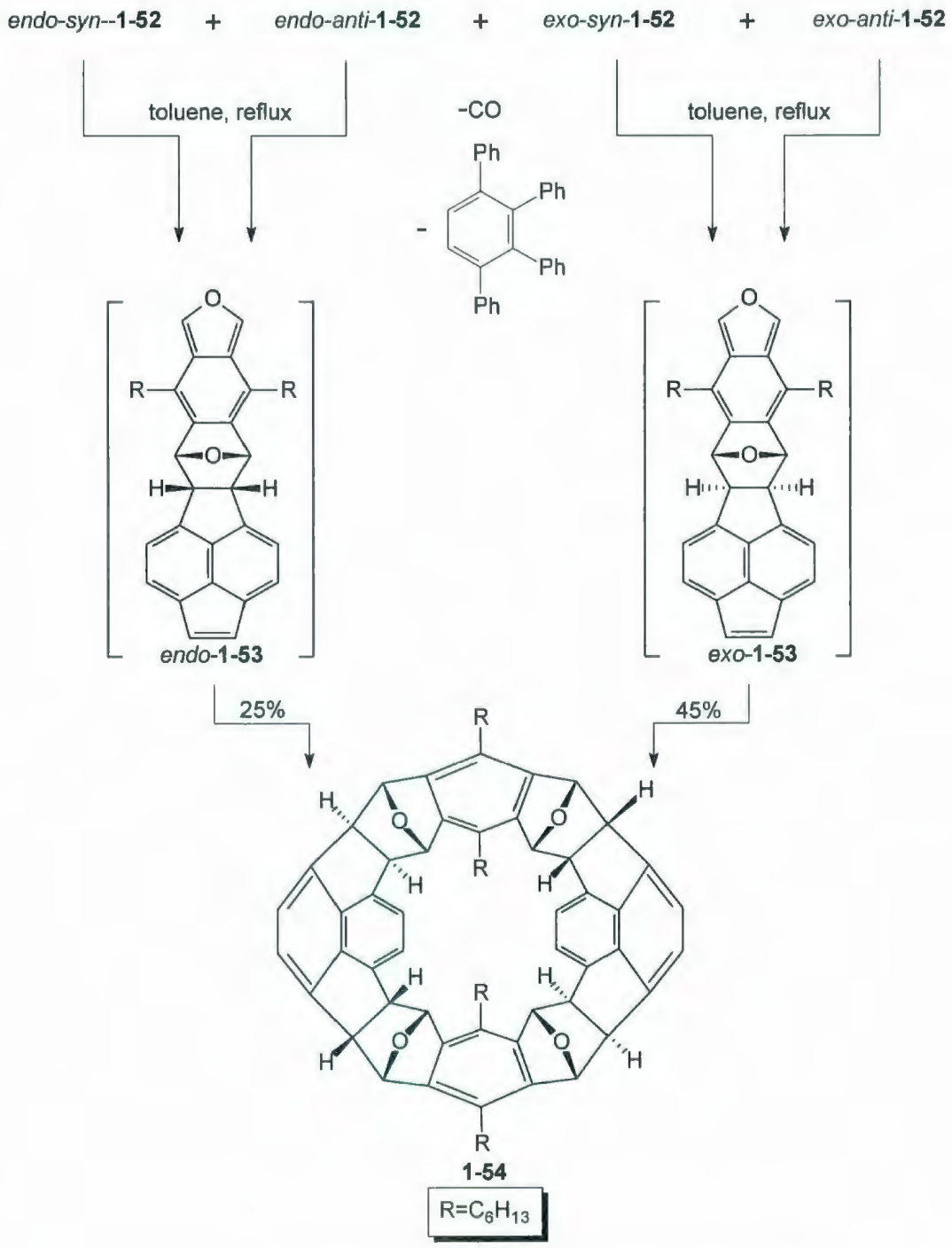


**Scheme 1.12.** Schlüter's synthesis of molecular belt **1-54**.

In principle, fourfold dehydration of **1-54** should afford aromatic belt **1-57** and, at first glance, Schlüter's belt motif appears to have better chances of giving a stable belt than the [*n*]cyclacenes because of the localization of the anthracene and naphthalene units. However, attempts to achieve this transformation by treatment of **1-54** with *p*-TsOH afforded macrocycle **1-55**, the product of twofold dehydration, in 49% yield (Scheme 1.13). No trace of the desired belt **1-57** was detected. However, an intractable black solid formed during this reaction and Schlüter speculated that this might be follow-on products of the target belt **1-57**. Molecular belt **1-55** was converted into tetraacetate **1-56** (80%) by reaction of **1-55** with acetic anhydride in the presence of a trace amount of $ZnCl_2$.[17] Fourfold elimination of acetic acid from **1-56** under mass spectrometric conditions was then investigated.[18] The molecular ions of the protonated aromatic belt **1-57** (*m/z*=933), single hydrated belt **1-57** (*m/z*=950) were indeed detected; but double hydrated **1-57** (*m/z*=968) was not detected. However, Schlüter was careful to point out that the correct mass does not distinguish the protonated aromatic belt **1-57** from any protonated rearranged products, such as **1-62** and **1-63** (Figure 1.05), in which migration of a hydrogen atom from a benzylic position to the belt skeleton introduces $sp^3$ hybridization and would therefore be expected to relieve strain.

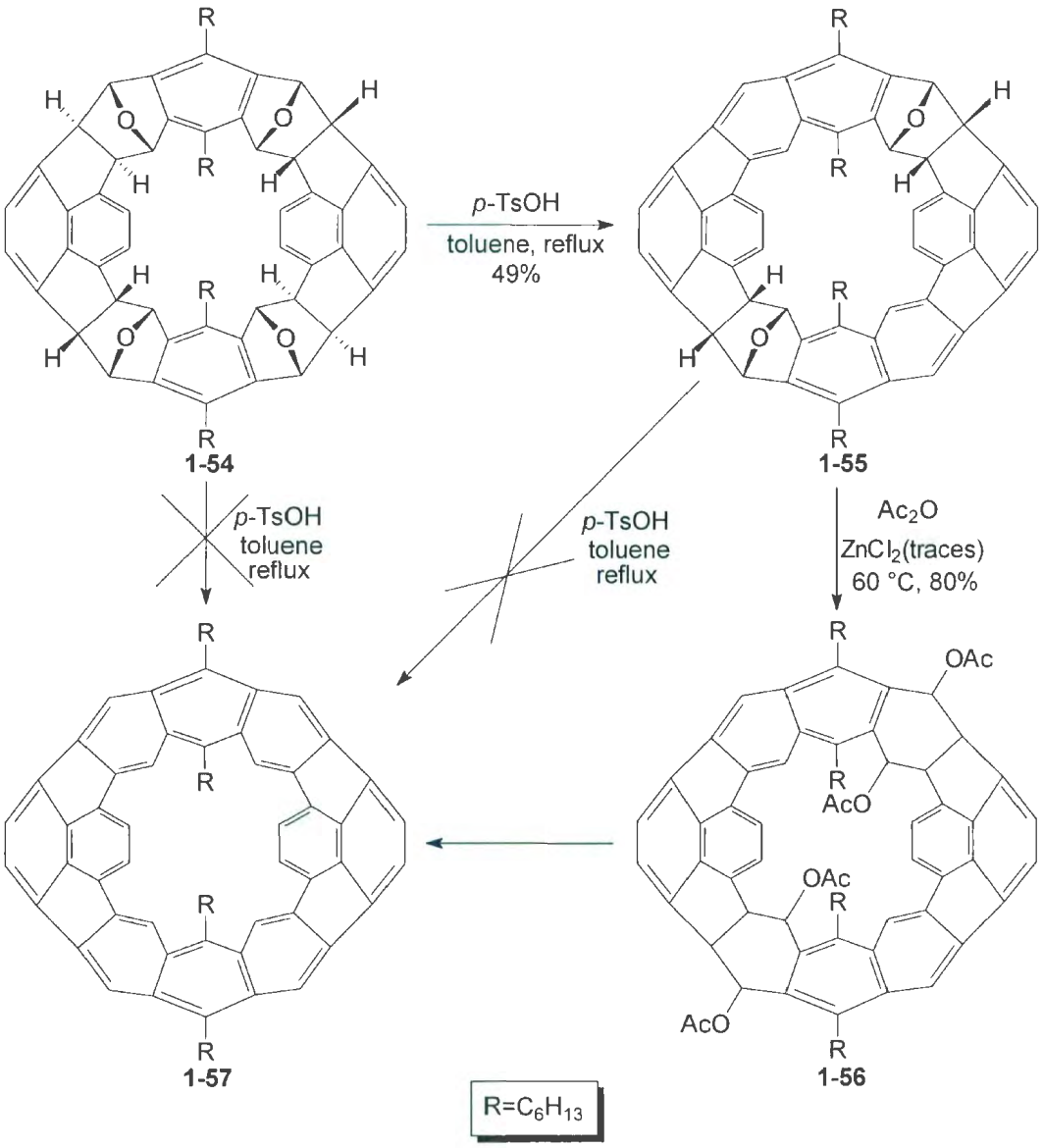


**Scheme 1.13.** Schlüter's attempts to synthesize aromatic belt **1-57**.

The energetics of the aromatization of molecular belts **1-55** and **1-56** to furnish belt **1-57** was then investigated using high-level computational studies.[18] The addition of water and hydrogen to anthracene was calculated at the G3 computational level and the addition to 1-57a was compared with the same respective additions to antheracene through isodesmic reactions. The method of the calculation of the rearrangement of 1-57a was not mentioned. To simplify the calculations, the tetraethyl substituted model **1-57a** was chosen (Figure. 1.05). Remarkably, the calculations suggested that the addition of one water molecule to **1-57a** was exothermic by 20.0 kcal $mol^{-1}$ and the addition of two water molecules to **1-57a** was exothermic by 42.2 kcal $mol^{-1}$. Hydrogenation of **1-57a** (one equivalent of hydrogen) was calculated to be exothermic by 38.8 kcal $mol^{-1}$ and hydrogenation with two equivalents of hydrogen was calculated to be exothermic by 80.2 kcal $mol^{-1}$. Rearrangement of belt **1-57a** to **1-62** (one rearrangement) and **1-63** (two rearrangements) resulted in similar structural changes to those observed upon mono- and dihydrogenation, but changes in energy were not reported. Although it was not taken to be conclusive evidence, it was suggested that the absence of doubly hydrated **1-57** in the MS analysis of the reactions described in Scheme 1.13 might be because singly rearranged **1-57** was formed but not belt **1-57**. It thus appears as though even just an isolated anthracene unit (let alone a full cyclacene) in an aromatic belt could be expected to be the source of instability.

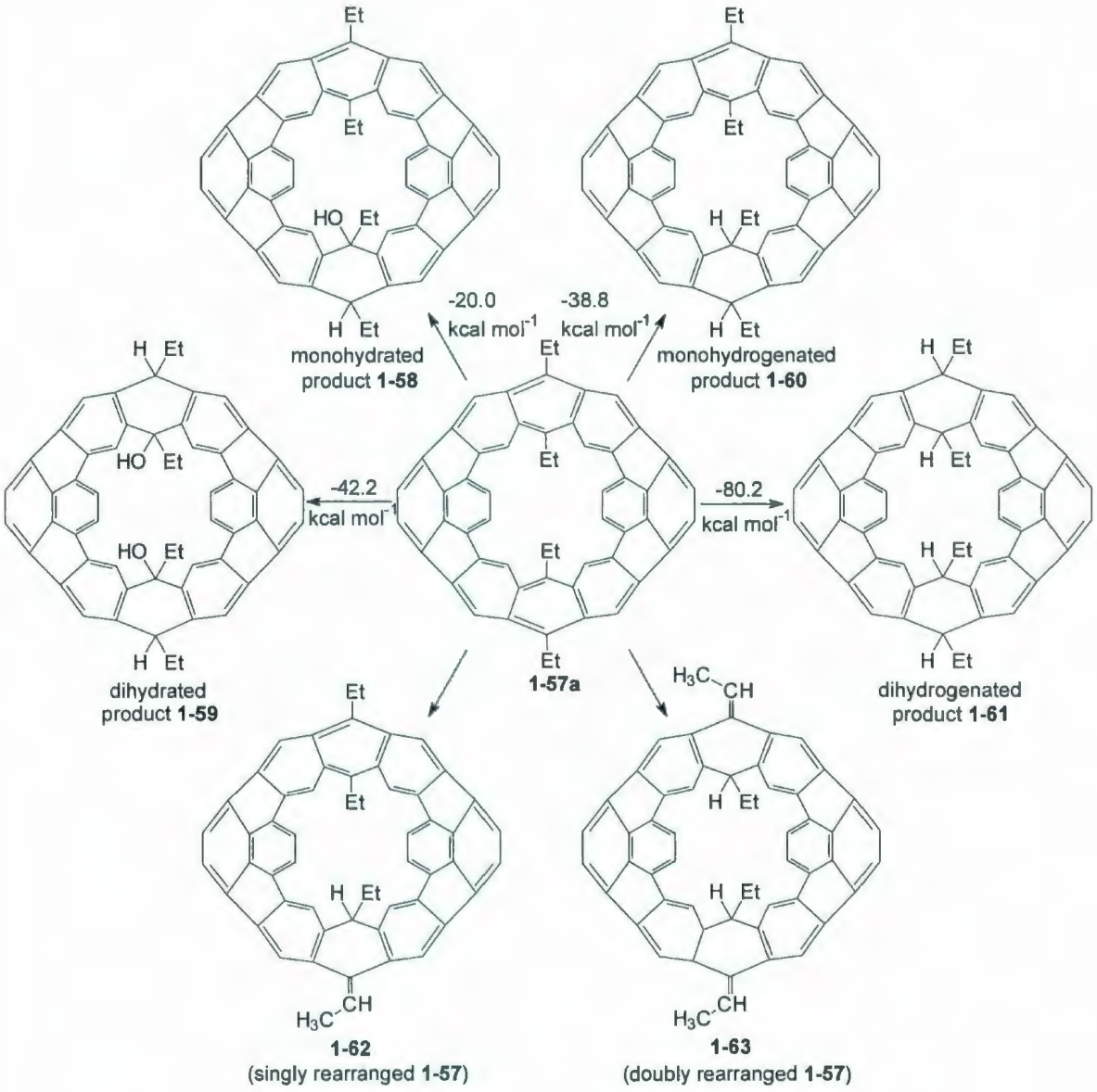


**Figure 1.05.** Theoretical study of a model of aromatic belt **1-57**.

Gleiter and co-workers accomplished the synthesis of a series of belts **1-65** – **1-68**, which he classifies as cyclacenes (Scheme 1.14).[19] The innate tub-shaped geometry of the eight-membered rings allows the macrocyclic skeleton to form without the build-up of excessive strain. On the other hand, it can be argued

that the innately nonaromatic character of the eight-membered rings rules out these belts as being aromatic belts. However, this is not to say that these systems are not important in the context of molecular belts. The synthesis culminated a remarkable one-pot operation, which involved the treatment of dibenzocyclooctadiyne **1-64**[20] with $CpCo(CO)_2$ under irradiation with UV light. This photoinduced transition-metal-catalyzed threefold cyclodimerization furnished the target belt-shaped molecules **1-65** – **1-68** in 14, 41, 12, and 8% yield, respectively.

Gleiter later reported the synthesis of a fully conjugated, purely hydrocarbon "cyclacene", i.e., $[6.8]_3$cyclacene **1-73**, which is the smallest, as well as the most strained one, in the $[6.8]_n$ series (Scheme 1.15).[21] As with **1-65** – **1-68**, the eight-membered rings are a key structural feature. Their nonplanar nature avoids strain, but their nonaromatic nature disqualifies them as being aromatic belts.

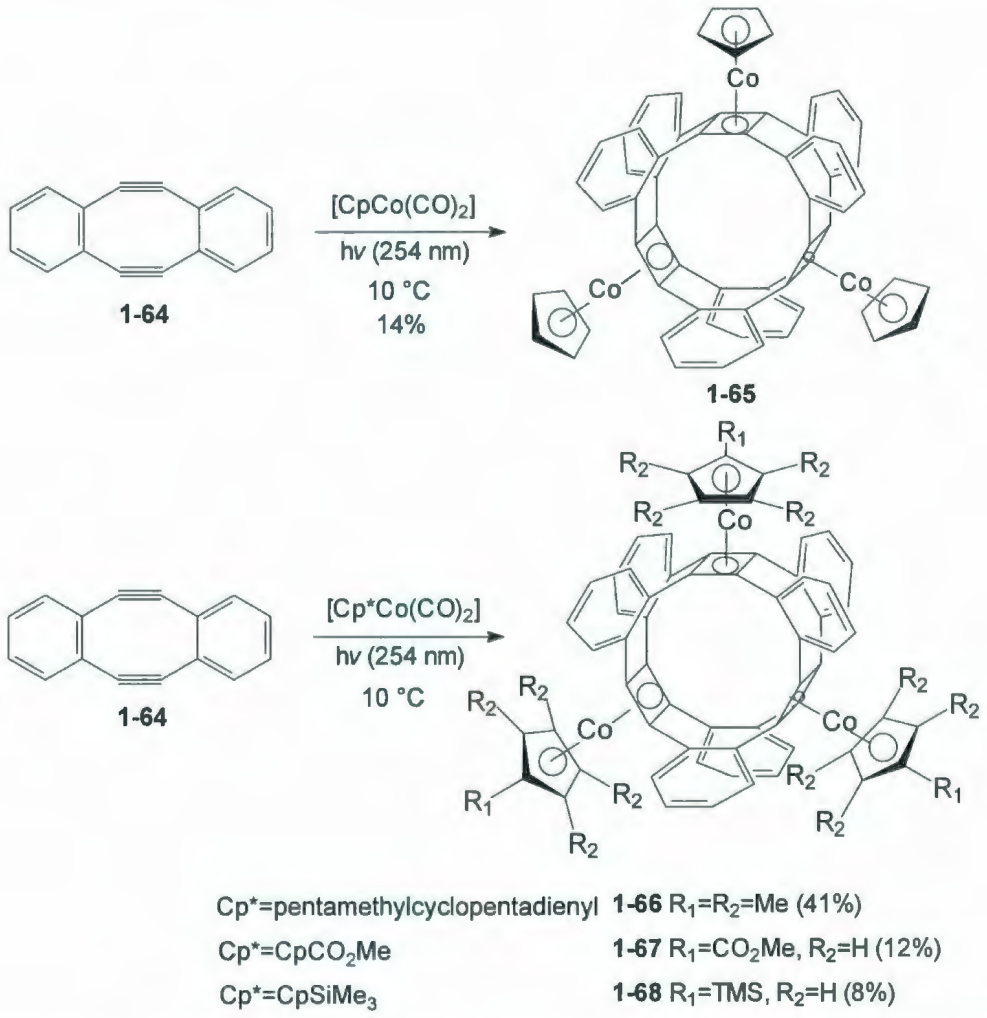


**Scheme 1.14.** Gleiter's synthesis of a series of Co conjugated belts **1-65** – **1-68**.

The first key step in the synthesis was the self-Wittig reaction of compound **1-69**, which was synthesized in 3 steps from 1,5-bis(chloromethyl)-2,4-dimethylbenzene (not shown) (Scheme 1.15).[22,23] Cyclic triene **1-70** was obtained in a 1:32 ratio of *Z,Z,Z* and *E,Z,Z* isomers (*Z,Z,Z*)-**1-70** and (*E,Z,Z*)-**1-70** in 7% combined yield. The mixture of the *E,Z,Z* and *Z,Z,Z* isomer was then converted into the pure *Z,Z,Z* isomer (*Z,Z,Z*)-**1-70** (85%) upon irradiation with UV light. Free radical bromination of **1-70** using NBS, followed by oxidation of the

resulting hexabromide **1-71** with IBX, furnished the hexaaldehyde **1-72** (14% yield, over 2 steps). Threefold intramolecular McMurry reaction of **1-72** resulted in the formation of cyclacene **1-73** (8%). Although the overall yield is very low, the synthesis has the advantage of being very short (requiring nine steps from *m*-xylene).

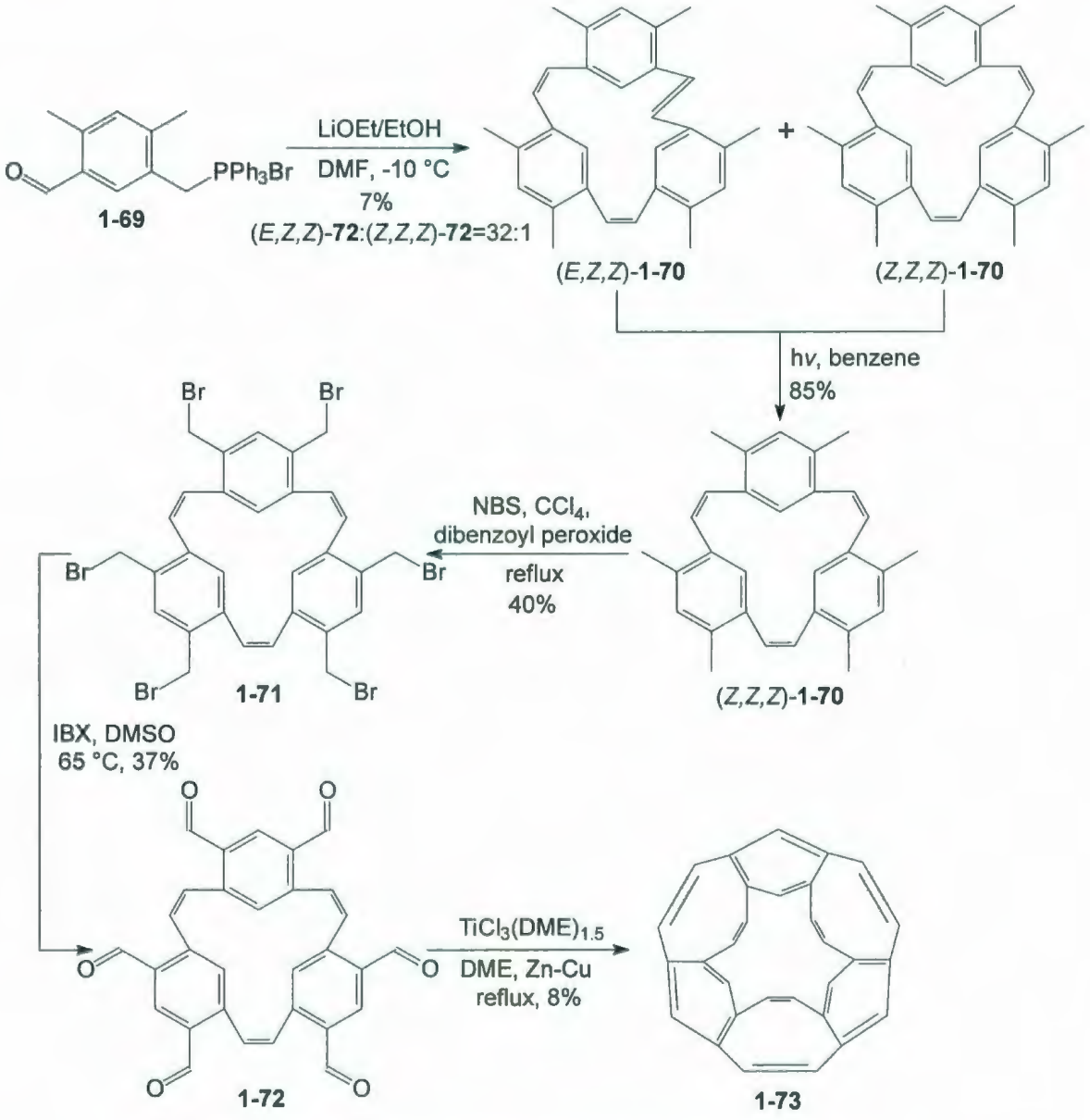


**Scheme 1.15.** Gleiter's synthesis of $[6,8]_3$cyclacene (**1-73**).

Cyclophenacenes have also been the subject of synthetic work. Vollhardt and coworkers reported the synthesis of compound **1-76** via tris(benzocyclobutadieno)benzene **1-74**, which is a noteworthy system because of the bond fixation in its central ring (a 1,3,5-cyclohexatriene rather than a benzene) (Scheme 1.16).[24] The synthesis started from stereoselective hydrogenation of **1-74**, which was synthesized from hexabromobenzene in four steps,[25] to give compound **1-75** (87%). The mild conditions reflected the high degree of bond localization and strain in **1-74**. Compound **1-75** was then cleanly and stereospecifically isomerized to *all-Z*-triene **1-76** upon heating at 125-160 °C in $C_6D_6$ in a sealed tube for several days. No attempt to aromatize **1-76** to afford [6]cyclophenacene was reported.

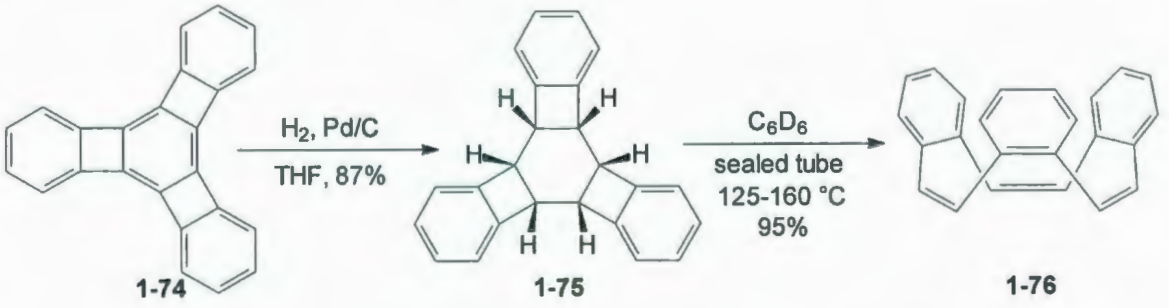


**Scheme 1.16.** Vollhardt's synthesis of tribenzo[12]annulene **1-76**.

Iyoda also reported an approach to such aromatic belts through *Z,Z,Z*-tribenzo[12]annulene **1-76** (Scheme 1.17).[26] The intention was to perform multifold stilbene-phenanthrene type transformations to generate the belts. Two strategies for the synthesis of the belt precursors were reported. This first strategy involved a nickel-catalyzed cyclotrimerization of dibromide **1-77** to give a

mixture of isomers **1-75** and **1-78** (ratio not given), followed by a thermal ring-opening reaction of the *all-cis*-trimer at reflux in *o*-dichlorobenzene. Again, no attempt to convert **1-75** into the corresponding belt was reported and this is not surprising in view of the small size of the macrocycle.

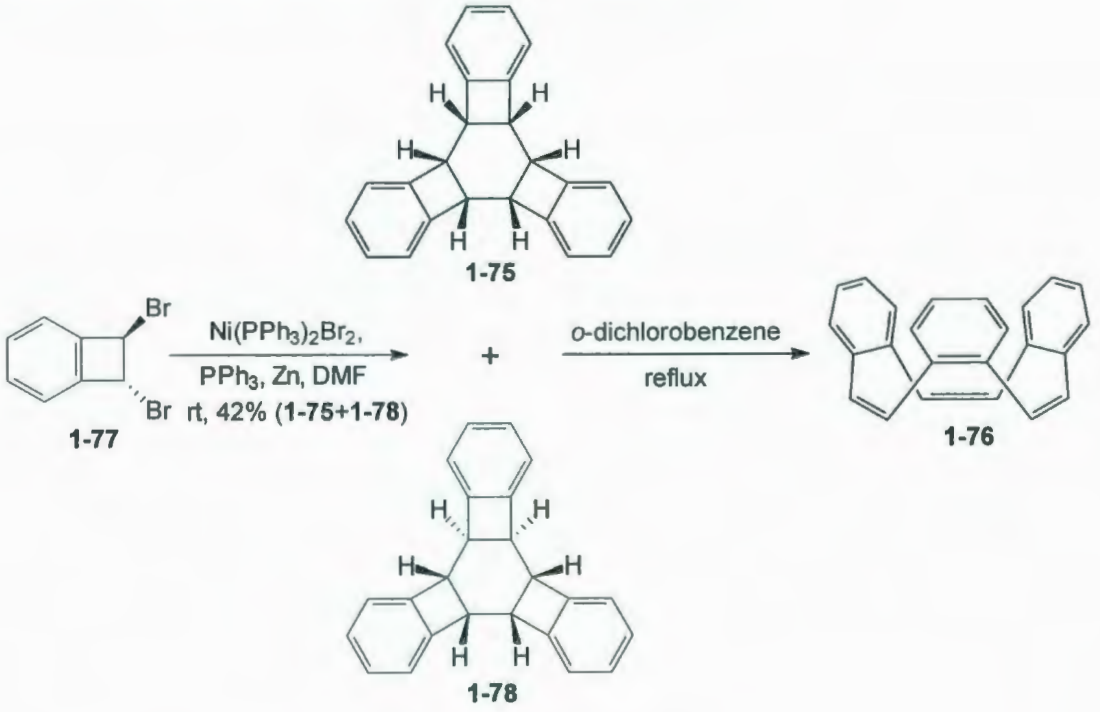


**Scheme 1.17.** Iyoda's synthesis of tribenzo[12]annulene **1-76**.

To overcome the problem associated with the first strategy, Iyoda and Kuwatani later reported an approach to such aromatic belts through a series of *all-Z*-"[*n*]benzo[4*n*]annulenes" **1-76** (scheme 1.18).[27,28] This strategy was based on an intramolecular pinacol coupling of the corresponding linear oligomeric *all-Z*-stilbene dialdehydes **1-79** to furnish the corresponding diols **1-80** (Scheme 1.18). Although a mixture of *threo*-**1-80** and *erythro*-**1-80** was obtained, the

undesired *threo*-**1-80** could be successfully converted into the desired *erythro*-**1-80** by Swern oxidation to the corresponding α-diketone (not shown) followed by $NaBH_4$ reduction. The carbon-carbon double bond in the target molecule **1-76** was then installed by a Corey-Winter reaction of the corresponding thionocarbonate **1-81** with DMPD.

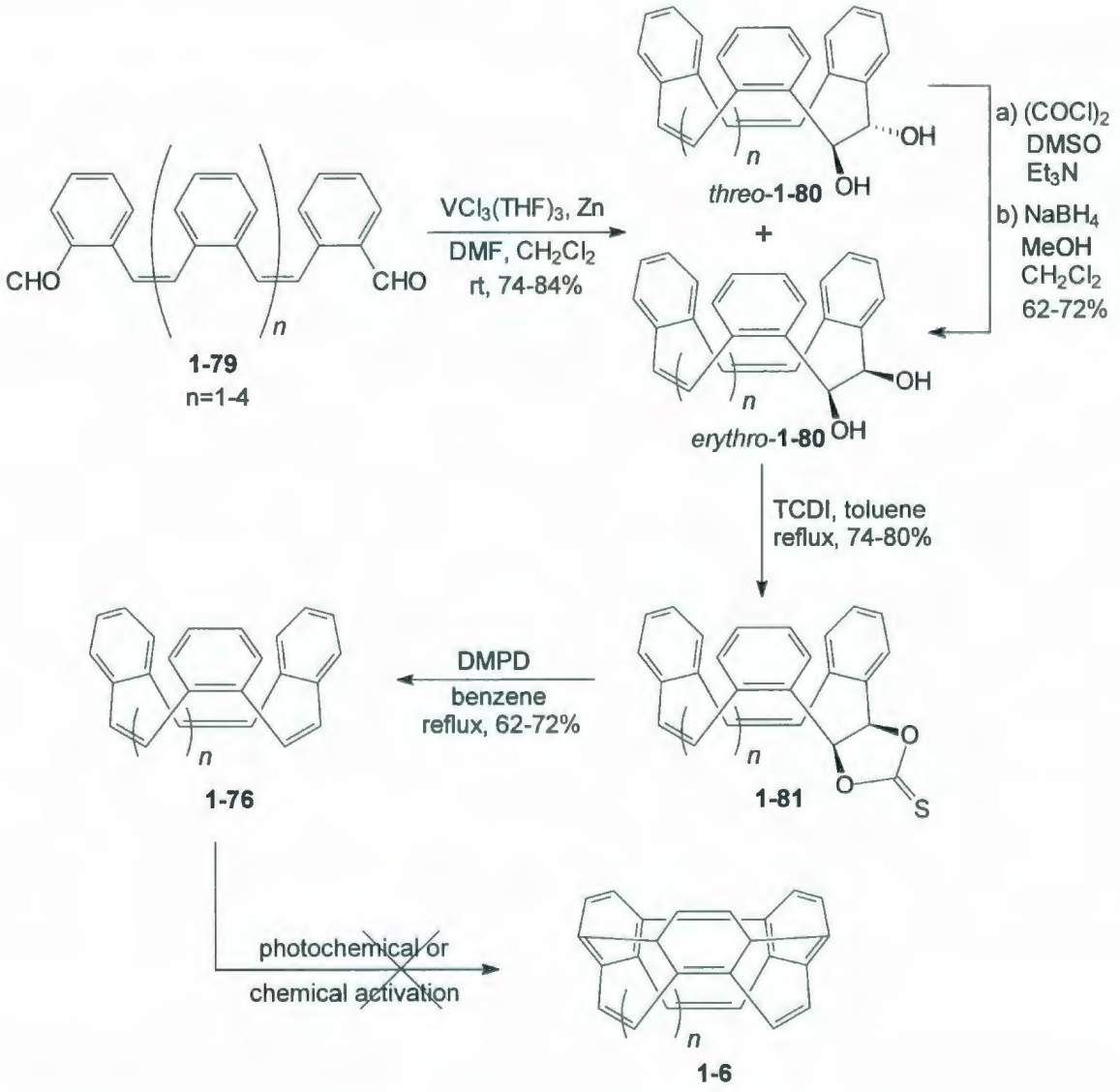


**Scheme 1.18.** Iyoda and Kuwatani's approach to synthesize cyclophenacenes.

Vögtle proposed a series of belts **1-82** as "interesting targets" [5] before the discovery of the fullerenes (1985) and nanotubes (1991) (Figure. 1.06). He also reported the synthesis of a potential precursor of belt **1-82** (n= –1).[29] It is noteworthy that these belts, which are segments of (*n,n*) armchair SWCNTs, were proposed in 1983, i.e., prior to the discovery of the fullerenes (1985) and CNTs (1991). The synthesis commenced with compound **1-83**, which was coupled with another molecule of **1-83** in the presence of NaTsNH to afford tetraester **1-84** (20-26%) (Scheme 1.19). Compound **1-84** was then reduced with $LiAlH_4$. The resulting alcohols were acylated to afford tetraacetate **1-85** (75%). The subsequent bromination of **1-85** gave tetrabromide **1-86** (75%). A second key building block, tetrathiol **1-87**, was obtained by reaction of **1-86** with thiourea in 79% yield. Compound **1-86** and **1-87** were then coupled in the presence of $Cs_2CO_3$ to afford **1-88** ($D_{2h}$ symmetry) along with a $C_{2v}$ isomer **1-89** in 3.4% combined yield. No attempt to synthesize belt **1-82** from **1-88** was reported. Considering the small size of the belt, the low yield of **1-88** and the number of synthetic steps needed to get to **1-82**, this is not surprising.

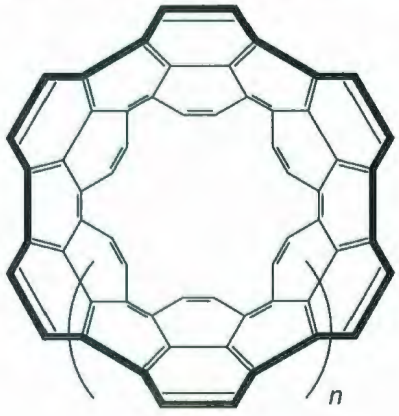


**1-82**

**Figure 1.06.** Vögtle's belts **1-82**.

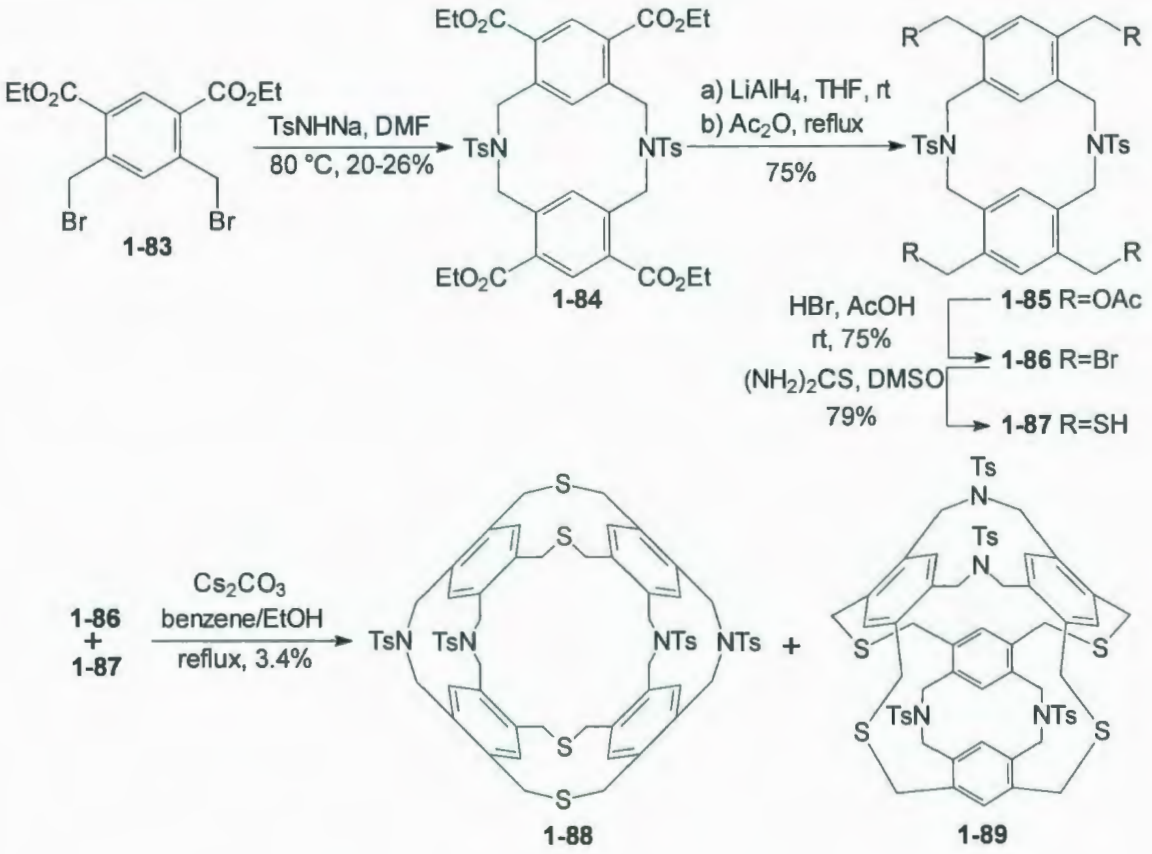


**Scheme 1.19.** Vögtle's synthesis of molecular belts **1-88** and **1-89**.

Nakamura and co-workers are the only group to have synthesized molecules that contain a simple aromatic belt, i.e., several capped cyclo[10]phenacenes (Scheme 1.20).[30] This synthesis is unique in that the aromatic belts were not constructed during the synthesis, but rather unmasked through functionalization of the starting material, $C_{60}$. The actual construction of the belt occurred during the production of $C_{60}$. This work not only demonstrated that capped cyclo[10]phenacenes are stable, but also provided information about their structure and properties.

As mentioned above, the synthesis started with $C_{60}$, which was treated with MeMgBr/CuBr·$Me_2S$ followed by $NH_4Cl$ to afford the cyclopentadiene derivative **1-90** (92%), which is the product of a fivefold organocuprate addition reaction (Scheme 1.20). Attempts to convert **1-90** directly into the target **1-91** failed, because reaction of **1-90** with PhMgBr/CuBr·$Me_2S$ generated the corresponding cyclopentadienyl anion, which was unreactive toward further addition under a variety of conditions. This problem was then overcome by "protecting" the acidic hydrogen atom on the cyclopentadiene ring by replacing it with a cyano group. This was accomplished by sequential treatment of **1-90** with *t*-BuOK and TsCN. This afforded nitrile **1-92** in 63% yield. Not only did the presence of the cyano group solve the problem of the acidic proton, but its electron-withdrawing nature also increased the electrophilicity of the 50π-electron system in compound **1-92**. The reaction of **1-92** with PhMgBr/CuBr·$Me_2S$ now proceeded smoothly to afford **1-93** (14%), which has a cyclo[10]phenacene system. The target molecule, carbon-capped fullerene **1-91**, was then generated by the removal of the protective cyano group under reductive conditions (82%). Penta-oxygenated derivative **1-94** was obtained from compound **1-91** upon treatment with potassium hydride followed by exposure to molecular oxygen (42%).

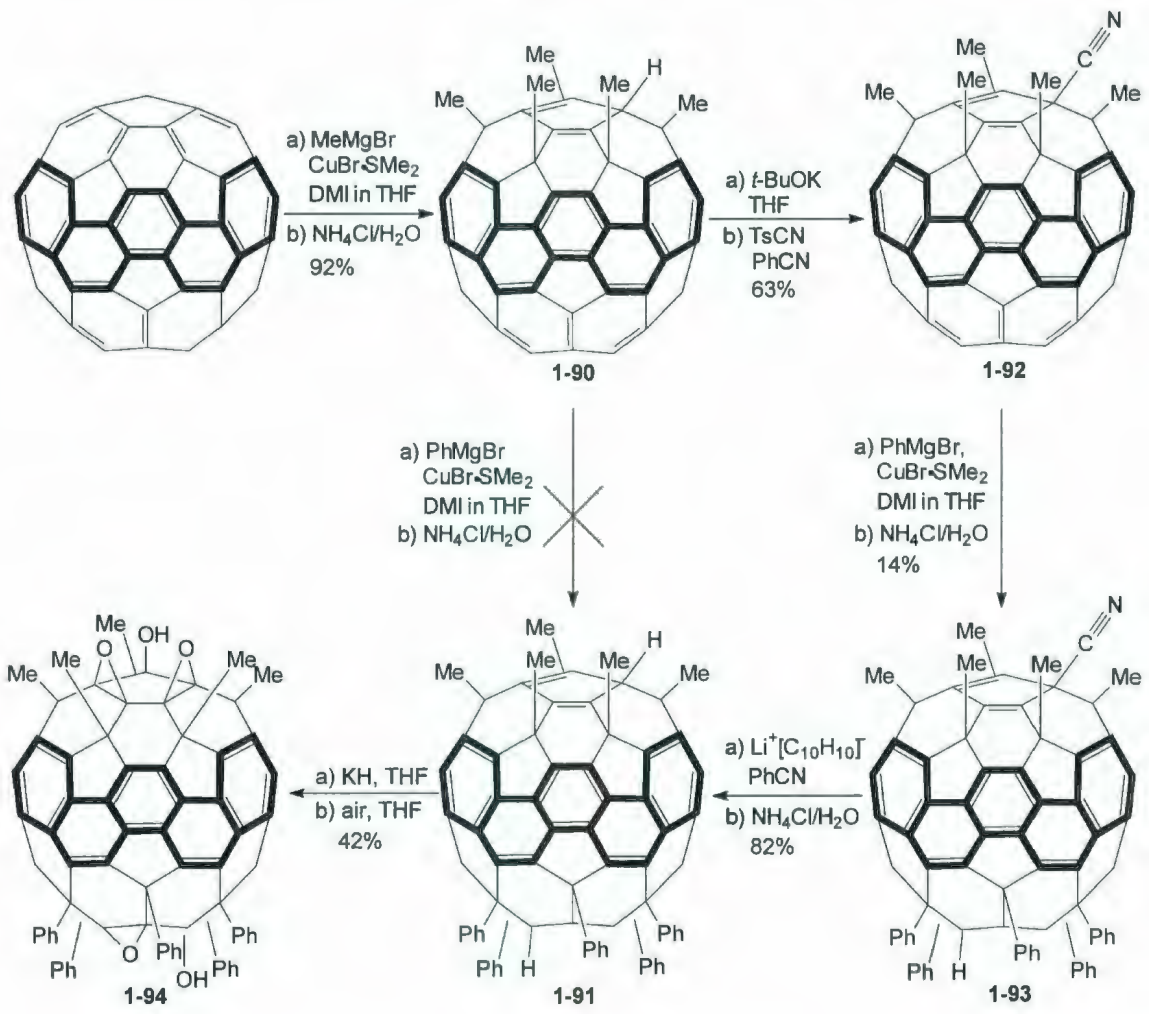


**Scheme 1.20.** Nakamura's synthesis of derivatives of [10]cyclophenacene.

Another series of cyclophenacene derivatives of [60]fullerene, called "double-decker buckyferrocenes", were also synthesized by Nakamura's group (Scheme 1.21).[31] The pentamethyl-pentaphenyl compound **1-95** was synthesized by treatment of either cyclophenacene compound **1-91** or its precursor cyanofullerene **1-93** with $[CpFe(CO)_2]_2$ in benzonitrile at 185 °C. The loss of hydride and cyano group was led by the electron transfer from the Fe complex to

the cyclophenacene unit, followed by intramolecular electron transfer to the cyclopentadienyl unit. The decamethyl substituted compound **1-97** was furnished from the pentamethyl buckyferrocene **1-96** in the presence of MeMgBr/CuBr·$Me_2S$. The synthesis of "double-decker buckyferrocene" **1-97** was then accomplished by reaction of the resulting ferrocene (not shown) with $[CpFe(CO)_2]_2$ in benzonitrile at 185 °C.

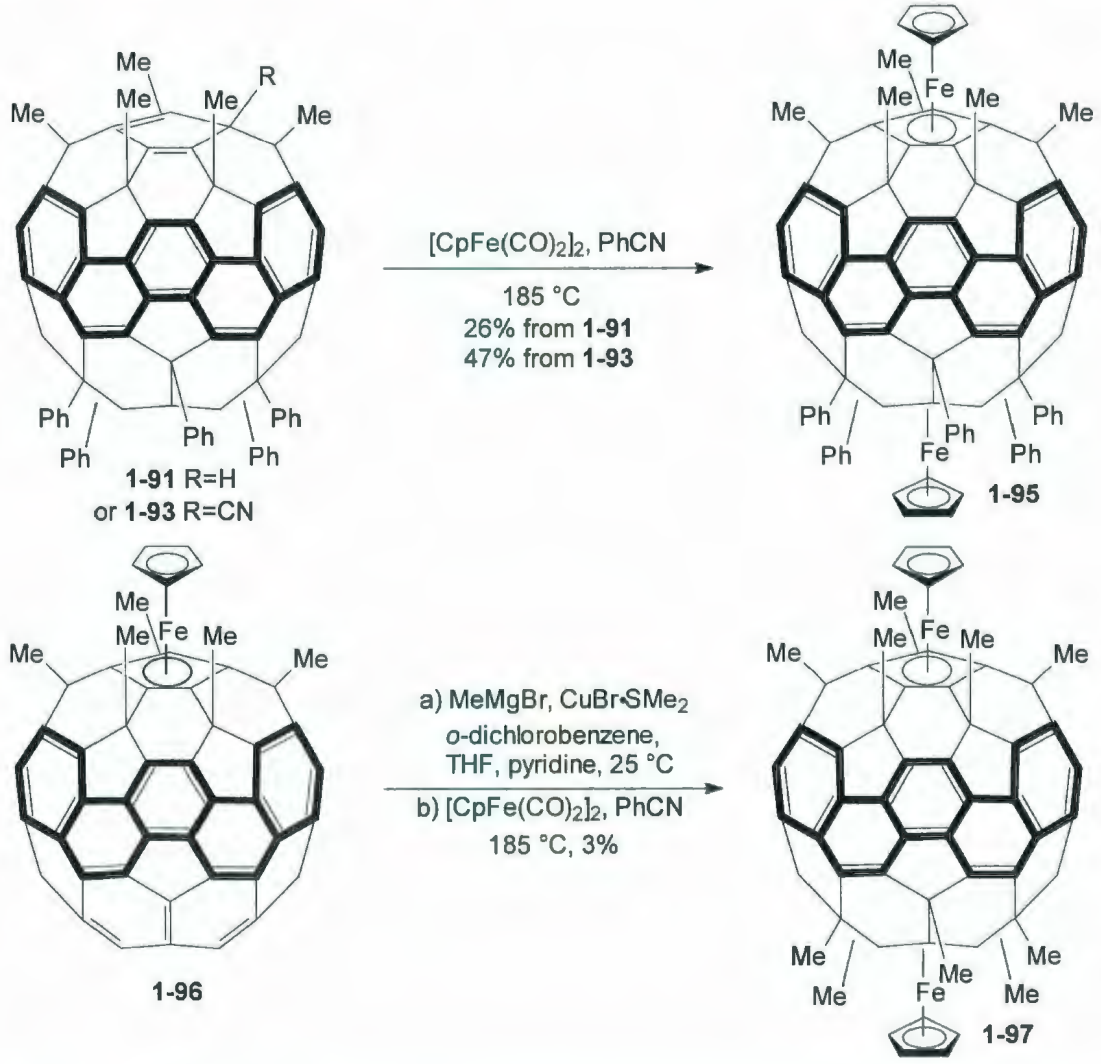


**Scheme 1.21.** Nakamura's synthesis of "double-decker buckyferrocenes" **1-95** and **1-97**.

Other groups are (or have been) engaged in research aimed at the synthesis of aromatic belts, but substantial progress towards these goals has not yet been reported. Scott's group[32] and Goroff's group[33] are targeting cyclophenacenes using approaches related to Iyoda's. Miller is attempting to exploit the reversible addition of $C_{60}$ to pentacene to synthesize cyclacenes. Hughes[34] is targeting somewhat thicker cyclophenacenes (segments of armchair (*n*,*n*)nanotubes) using chemistry popularized by Müllen for the synthesis of large graphene substructures. Clearly, this is an area of growing interest[35].

## 1.4 References


1. Szejtli, J. *Chem. Rev.* **1998**, *98*, 1743.
2. Kuwase, T.; Kurata, H. *Chem. Rev.* **2006**, *106*, 5250.
3. Lee, J. W.; Samal, S.; Selvapalam, N.; Kim, H. J.; Kim, K. *Acc. Chem. Res.* **2003**, *36*, 621.
4. White, C. T.; Mintmire, J. W. *J. Phys. Chem. B* ***2005***, *109*, 52.
5. Vögtle, F. *Top. Curr. Chem.* **1983**, *115*, 157.
6. (a) Clar, E. *Polycyclic Hydrocarbons*; Academic Press: London **1964**. (b) Clar, E. *The aromatic sextet*; Wiley: New York **1972**.
7. Gutman, I.; Milun, M.; Trinajstic, N. *J. Am. Chem. Soc.* **1977**, *99*, 1692.
8. Aihara, J. *J. Chem. Soc. Perkin Trans. 2,* **1994**, 971.
9. Godt, A.; Enkelmann, V. E.; Schlüter, A. D. *Angew. Chem. Int. Ed.* **1989**, *28*, 1680.
10. Kintzel, O.; Luger, P.; Weber, M.; Schlüter, A. D. *Eur. J. Org. Chem.* **1998**, 99.
11. Benkhoff, J.; Boese, R.; Klärner, F. G.; Wigger, A. E. *Tetrahedron Lett.* **1994**, *35*, 73.
12. Ashton, P. R.; Brown, G. R.; Isaacs, N. S.; Giuffrida, D.; Kohnke, F. H.; Mathias, J. P.; Slawin, A. M. Z.; Smith, D. R.; Stoddart, J. F.; Williams D. J. *J. Am. Chem. Soc.* **1992**, *114*, 6330.
13. Cory, R. M.; McPhail, C. L.; Dikmans, A. J.; Vittal, J. J. *Tetrahedron Lett.* **1996**, *37*, 1983.

14. Cory, R. M.; McPhail, C. L. *Tetrahedron Lett.* **1996**, *37*, 1987.

15. Neudorff, W. D.; Lentz, D.; Anibarro, M.; Schlüter, A. D. *Chem. Eur. J.* **2003**, *9*, 2745.

16. Schlüter, A. D.; Löffler, M.; Enkelmann, V. *Nature*, **1994**, *368*, 831.

17. Stuparu, M.; Lentz, D.; Rüegger, H.; Schlüter, A. D. *Eur. J. Org. Chem.* **2007**, 88.

18. Denekamp, C. D.; Etinger, A.; Amrein, W.; Stanger, A.; Stuparu, M.; Schlüter, A. D. *Chem. Eur. J.* **2008**, *14*, 1628.

19. Hellbach, B.; Rominger, F.; Gleiter, R. *Angew. Chem. Int. Ed.* **2004**, *43*, 5846.

20. Orita, A.; Hasegawa, D.; Nakano, T.; Otera, J. *Chem. Eur. J.* **2002**, *8*, 2000.

21. Esser, B.; Rominger, F.; Gleiter, R. *J. Am. Chem. Soc.* **2008**, *130*, 6716.

22. Gerisch, M.; Krumper, J. R.; Bergman, R. G.; Tilley, T. D. *Organometallics* **2003**, *22*, 47.

23. Wood, J. H.; Tung, C. C.; Perry, M. A.; Gibson, R. E. *J. Am. Chem. Soc.* **1950**, *72*, 2992.

24. Mohler, D. L.; Vollhardt, K. P. C.; Wolff, S. *Angew. Chem. Int. Ed.* **1990**, *29*, 1151.

25. Diercks, R.; Vollhardt, K. P. C. *J. Am. Chem. Soc.* **1986**, *108*, 3150.

26. Iyoda, M.; Kuwatani, Y.; Yamauchi, T.; Oda, M. *J. Chem. Soc., Chem. Commun.* **1988**, 65.

27. Kuwatani, Y.; Yoshida, T.; Kusaka, A.; Iyoda, M. *Tetrahedron Lett.* **1999**, *41*, 359.

28. Kuwatani, Y.; Igarashi, J.; Iyoda, M. *Tetrahedron Lett.* **2004**, *45*, 359.

29. Schröder, A.; Karbach, D.; Güther, R.; Vögtle, F. *Chem. Ber.* **1992**, *125*, 1881.

30. Nakamura, E.; Tahara, K.; Matsuo, Y.; Sawamura, M. *J. Am. Chem. Soc.* **2003**, *125*, 2834.

31. Matsuo, Y.; Tahara, K.; Nakamura, E. *J. Am. Chem. Soc.* **2006**, *128*, 7154.

32. http://www2.bc.edu/~scottla/

33. http://www.chem.stonybrook.edu/ngoroff.html

34. http://www.uvm.edu/~tshughes/?Page=group/research.html

35. Reviews: (a) In *Advances in Theoretically Interesting Molecules*; Thummel, R. P., Ed.; JAI Press: Greenwich, **1998**; Vol. IV, p 53. (b) *Chem. Rev.* **2006**, *106*, 5274.

# Chapter 2

# The Bodwell Group's Approach to Aromatic Belts

For over a decade, the Bodwell group has been exploiting valence isomerization/dehydrogenation (VID) reactions of tethered [2.2]metacyclophane-1,9-dienes such as **2-1** to synthesize (2,7)pyrenophanes **2-3** having nonplanar pyrene systems via 10b,10c-dihydropyrenophanes **2-2** (Scheme 2.01). To date, over twenty pyrenophanes have been successfully synthesized using this methodology (Figure 2.01).[1-5]

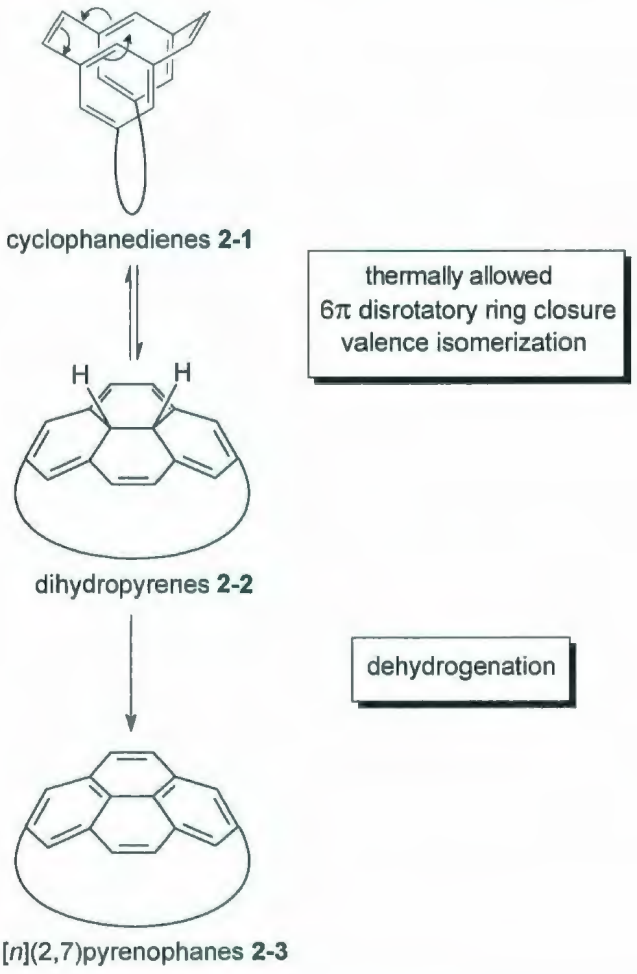


**Scheme 2.01.** The VID reactions in the synthesis of [*n*](2,7)pyrenophanes.

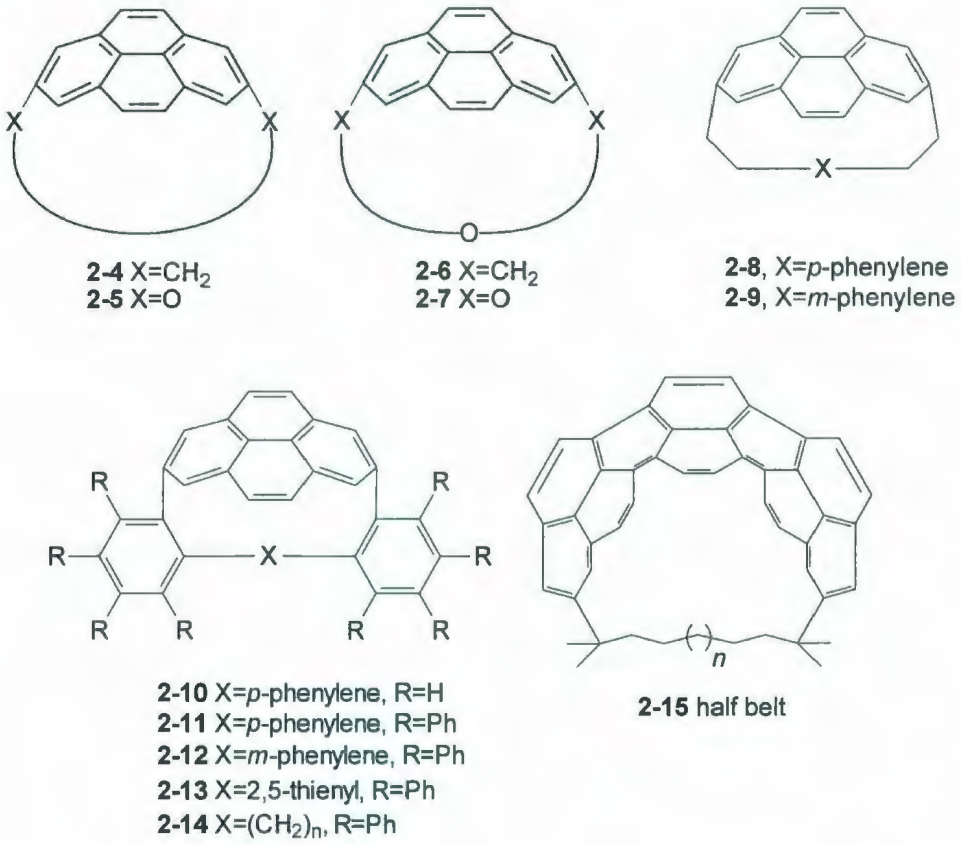


**2-4** X=$CH_2$
**2-5** X=O

**2-6** X=$CH_2$
**2-7** X=O

**2-8**, X=*p*-phenylene
**2-9**, X=*m*-phenylene

**2-10** X=*p*-phenylene, R=H
**2-11** X=*p*-phenylene, R=Ph
**2-12** X=*m*-phenylene, R=Ph
**2-13** X=2,5-thienyl, R=Ph
**2-14** X=$(CH_2)_n$, R=Ph

**2-15** half belt

**Figure 2.01.** Pyrenophanes previously synthesized by the Bodwell group.

The VID methodology has proved to be very powerful for the generation of nonplanar (and therefore strained) pyrene systems, even those that are severely distorted from planarity, under mild conditions. The success of the VID reaction in this regard can be attributed to several factors, which operate cooperatively to favor the reaction. First, in the tethered metacyclophanediene **2-1**, the [2.2]metacyclophanediene unit is held in the *syn* conformation by the tether (provided the number of carbon atoms in the tether is less than 12).[7] As such, the valence isomerization, which is a 6π-electron electrocyclic ring closure, is

suprafacial. This means that, unlike the analogous valence isomerizations of *anti*-[2.2]metacyclophanedienes,[8] *cis*-stilbenes,[9] and (*Z*)-1,2-dithienylethenes,[10] it is thermally allowed. The enforced proximity of the two reacting carbon atoms and the high level of preorganization also serve to keep $<G^{\ddagger}$ low. Furthermore, thermodynamically, the valence isomerization of simple *syn*-[2.2]metacyclophanedienes to their corresponding *cis*-10b,10c-dihydropyrenes is known to be favorable, even when a 12-atom tether is present.[7] Although the ASE of two benzene rings is lost (~29 kcal $mol^{-1}$ per ring)[11] in this step, a new carbon-carbon bond is formed (~84 kcal $mol^{-1}$)[12] and a [14]annulene is generated. Suresh and Koga calculated the $E_{aromatization}$ (an aromaticity index based on isodesmic reactions) of *trans*-10b,10c-dihydropyrene (33 kcal $mol^{-1}$), and benzene (29 kcal $mol^{-1}$) among others.[13] $E_{aromatization}$ correlated well with other indices of aromaticity, including the ASE. This means that the conversion of *anti*-[2.2]metacyclophanediene into 10b,10c-dihydropyrene involves the loss of 2 % 29 kcal $mol^{-1}$ ($E_{aromatization}$ of benzene) and the gain of 33 kcal $mol^{-1}$ ($E_{aromatization}$ of dihydropyrene) and 84 kcal $mol^{-1}$ from the formation of a new carbon-carbon bond. Assuming that there is only a small change in strain energy for this valence isomerization, it would appear to be an energetically favored process (~49 kcal $mol^{-1}$).

*cis*-Dihydropyrenophanes such as **2-2** are naturally "saucer-shaped" because of the eclipsed ethano unit that is embedded within the 14π periphery.[14] This means that the VID reaction is not accompanied by the build-up of as much

strain as there would be in an innately planar $\pi$ system, e.g., in a *trans*-dihydropyrenophane. In other words, a *cis*-dihydropyrene unit can accommodate a shorter bridge than a *trans*-dihydropyrene. It is important that the valence isomerization is a reversible reaction. Thus, even when the *cis*-dihydropyrenophane is energetically disfavored by the presence of a short tether, the irreversible dehydrogenation step may still have the opportunity to proceed via the small proportion of the *cis*-dihydropyrenophane. The dehydrogenation results in the formation of a nonplanar pyrene system, which has a lowest-energy conformation that is planar. This means that dehydrogenation must bring with it an increase in strain energy. On the other hand, the ASE of *cis*-dihydropyrenes (~33 kcal $mol^{-1}$) is replaced with the ASE of a pyrene system (78!1 kcal $mol^{-1}$) (caution, different calculation).[15] Cyrański and co-workers recently showed that the ASE of pyrene is only weakly diminished upon bending out of planarity.[13] Even in severely distorted systems, the majority of the ASE is still available to help drive the reaction. Of course, enthalpic changes associated with changes in bonding are of major importance in the dehydrogenation step, but the particular case of pyrene formation is favored by the large amount of the ASE that accompanies it, even in nonplanar systems.

The general strategy involves four stages (Scheme 2.02). Stage 1 is the construction of a tetrasubstituted molecular "board" **2-16**. Stage 2 involves functional group interconversions and the union of two boards to afford a large cyclophane **2-17** with four bridges. Stage 3 is the conversion of **2-17** into the

corresponding [2.2.2.2]cyclophanetetraene **2-18** and the final stage, Stage 4, is the VID reaction of **2-18** to afford a belt **2-19**.

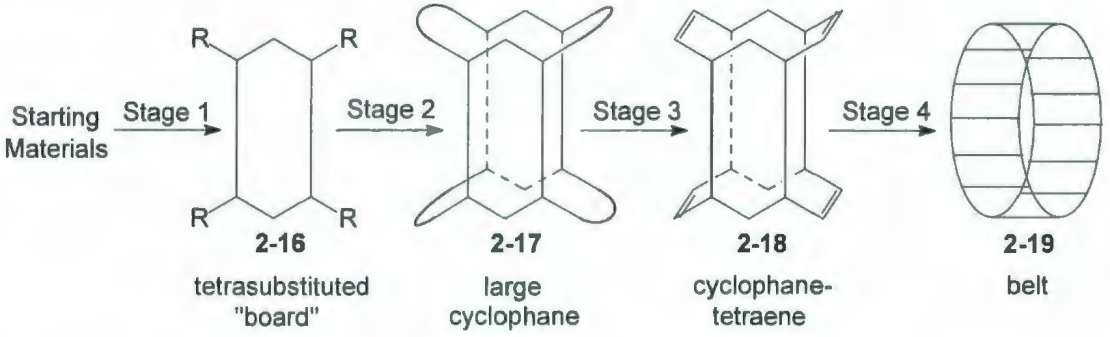


**Scheme 2.02.** Four stages of Bodwell's strategy to synthesize aromatic belts.

The first belt to be targeted by the Bodwell group was $D_{6h}$-symmetric **1-82** (introduced in Chapter 1), which was first proposed by Vögtle and maps onto the equator of $D_{6h}$-$C_{84}$.[16] Retrosynthetic application of Stage 4 of the general strategy (along with additional dehydrogenation) affords cyclophanetetraene **2-20** (Scheme 2.03).[17] Partial saturation of the two boards was anticipated to promote solubility throughout the synthesis. The retrosynthesis then leads back via Stages 3 and 2 to molecular board **2-21**, which was thus established as the target for Stage 1 of the synthesis. Molecular board **2-21** was to be synthesized from layered [2.2]metacyclophane **2-22**, which was expected to be accessible from tetrathiacyclophane **2-23**, itself the product of coupling of dibromodiester **2-24** with tetrathiol **2-25**.

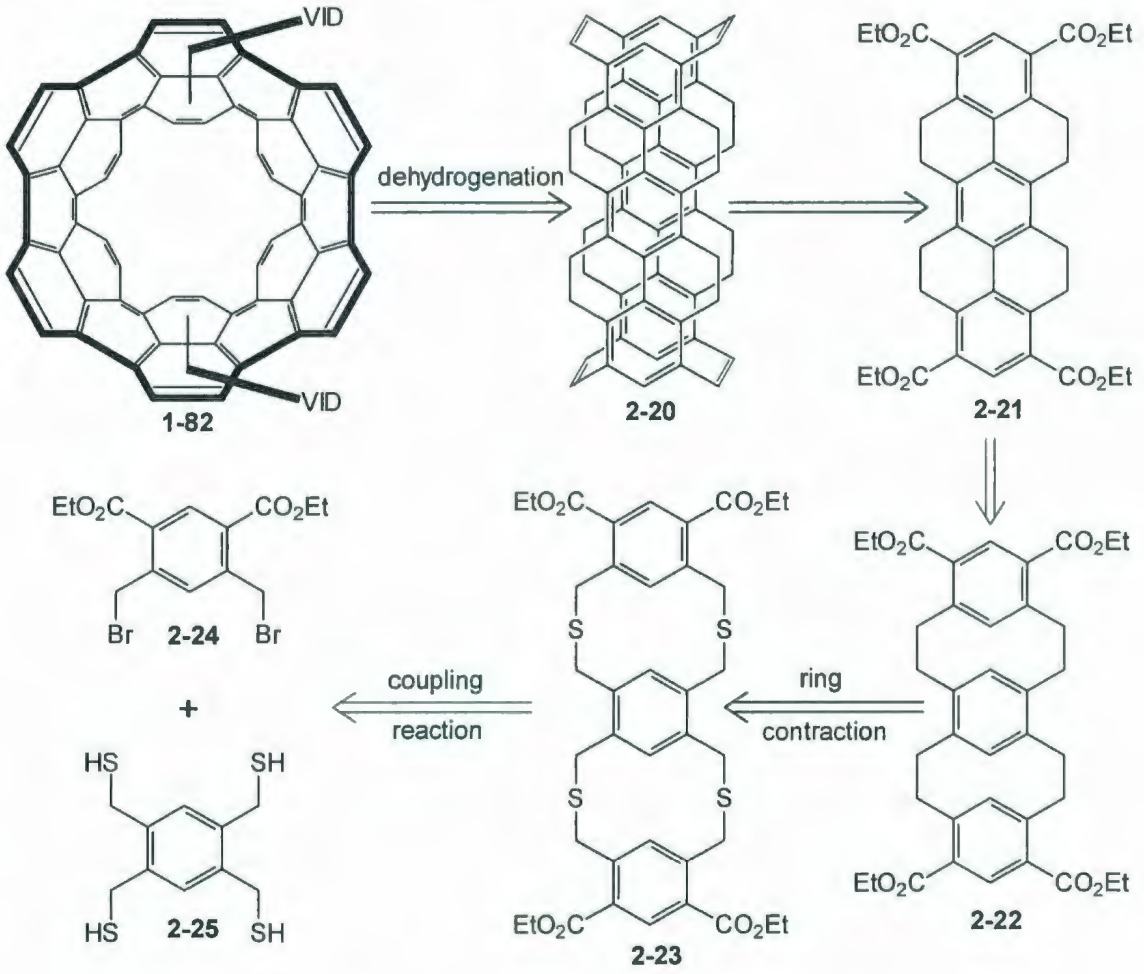


**Scheme 2.03.** Retrosynthetic analysis of $D_{6h}$-**1-82**.

The attempted synthesis of molecular board **2-21** started from *m*-xylene (**2-26**), which was bromomethylated to afford **2-27** (56% yield, Scheme 2.04).[17] Dibromide **2-27** was then reacted with sodium acetate to afford diacetate **2-28** (99%), saponification of which was accomplished by treatment with aqueous KOH. Oxidation of the resulting crude diol (not shown) using $KMnO_4$ then afforded diacid **2-29** (80%, 2 steps). Esterification of **2-29** via the bis(acid chloride) gave diester **2-30** (76%). A twofold free-radical benzylic bromination of

**2-30** gave dibromide **2-24** (40%) as one of the partners of the planned coupling reaction. The other partner, tetrathiol **2-25**, was synthesized by reaction of commercially available tetrabromide **2-31** with thiourea, followed by treatment of the resulting tetrakis(isothiouronium) salt with aqueous KOH. The coupling reaction of dibromide **2-24** and tetrathiol **2-25** gave, as expected, a mixture of two tetrathiacyclophanes, which were separated by careful column chromatography to give the desired isomer **2-23** (13%) and the unwanted isomer **2-32** (19%). Further investigation of functional group interconversions of the ester groups was not attempted due to the acid sensitivity of cyclophane **2-23**. Attention was then focused on the ring contraction of cyclophane **2-23**, leaving functional group interconversion the ester groups until a later stage in the synthesis. Unfortunately, none of numerous attempts to achieve ring contractions (Stevens rearrangement, Wittig rearrangement, photolytic sulfur extrusion, oxidation/pyrolysis, benzyne Stevens rearrangement) afforded the desired tetraene **2-33** or hydrogenated derivative **2-22** (Scheme 2.05).

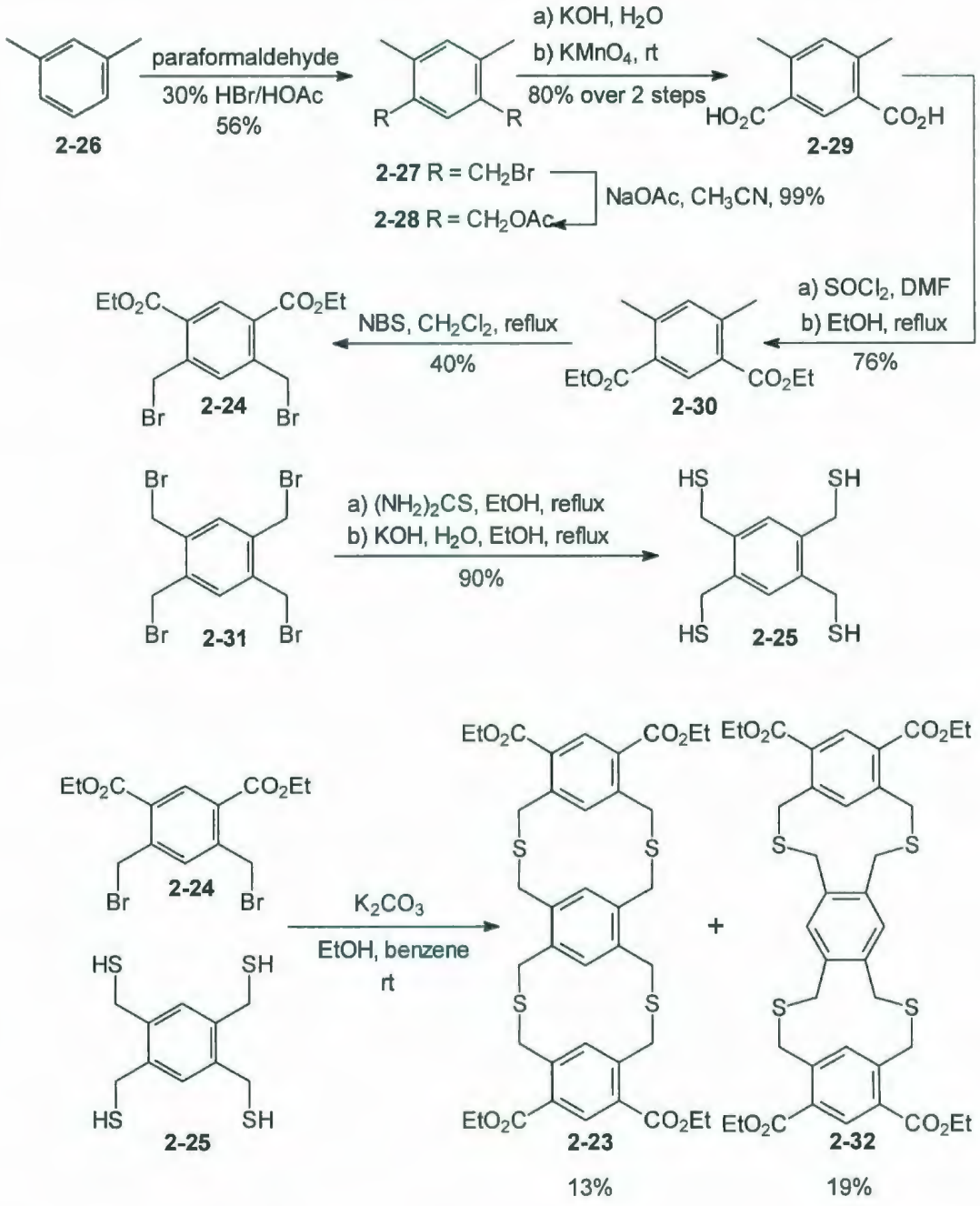


**Scheme 2.04.** Synthesis of tetrathiacyclophane **2-23**.

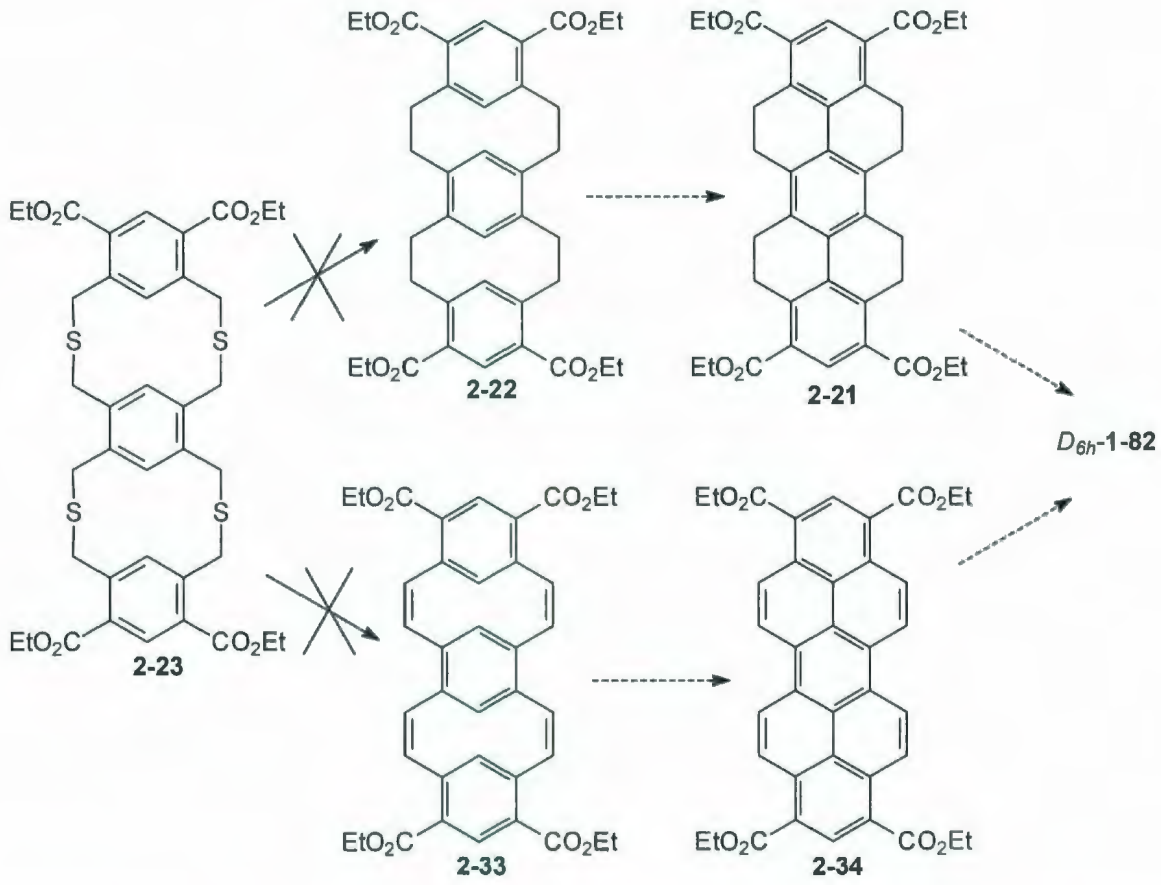


**Scheme 2.05.** Attempted conversion of **2-23** into molecular board **2-21** and **2-34**.

Since the molecular boards **2-21** and **2-34** were several steps away from the desired aromatic belt, synthetically useful quantities would certainly be required. In view of the synthetic problems encountered *en route* to **2-21**, a simpler and synthetically less challenging board was therefore needed. Board **2-35** was then identified as a viable target. In its average (planar) conformation, **2-35** has lower ($C_{2h}$) symmetry than the previously targeted board **2-21** ($D_{2h}$). Due to its lower symmetry, taking **2-21** through the general strategy leads to two isomeric belts, $C_{2h}$-**2-36** and $D_2$-**2-36** rather than one (**2-21**) (Scheme 2.06). As

before, it was anticipated that the nonaromatic rings, which were included for the sake of maintaining solubility, would be aromatized by DDQ during the key VID step (Stage 4).

The Bodwell group has reported an initial attempt to synthesize the parent aromatic belts **2-36** via a dibenzo[*a*,*h*]anthracene board motif **2-35**.[18] The retrosynthetic analysis took the board **2-35** back to dibromide **2-37** via a twofold direct arylation reaction,[19] and then back to tetraesterdiyne **2-38**, which could be synthesized from starting materials **2-39** – **2-41** using Sonogashira chemistry (Scheme 2.07).

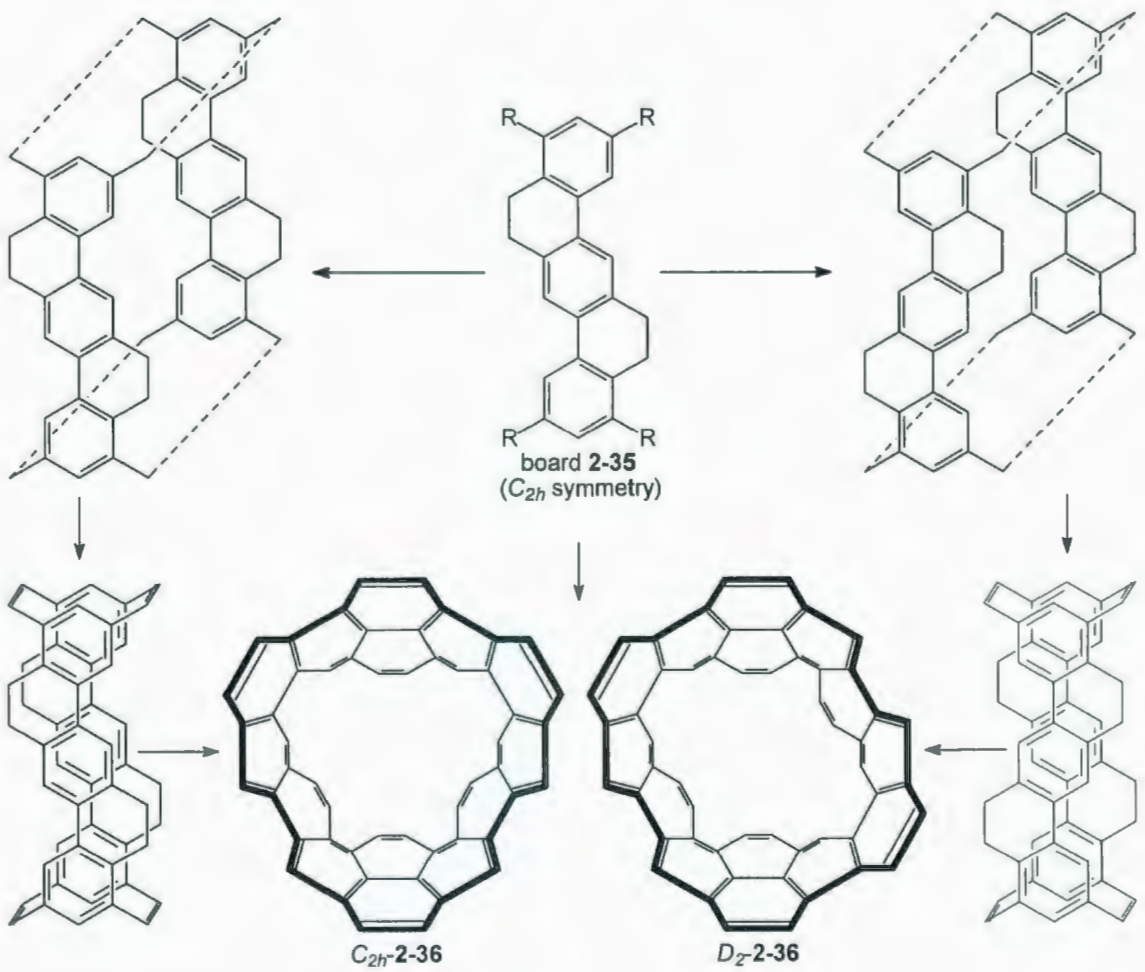


**Scheme 2.06.** The origin of two isomers from one molecular board.

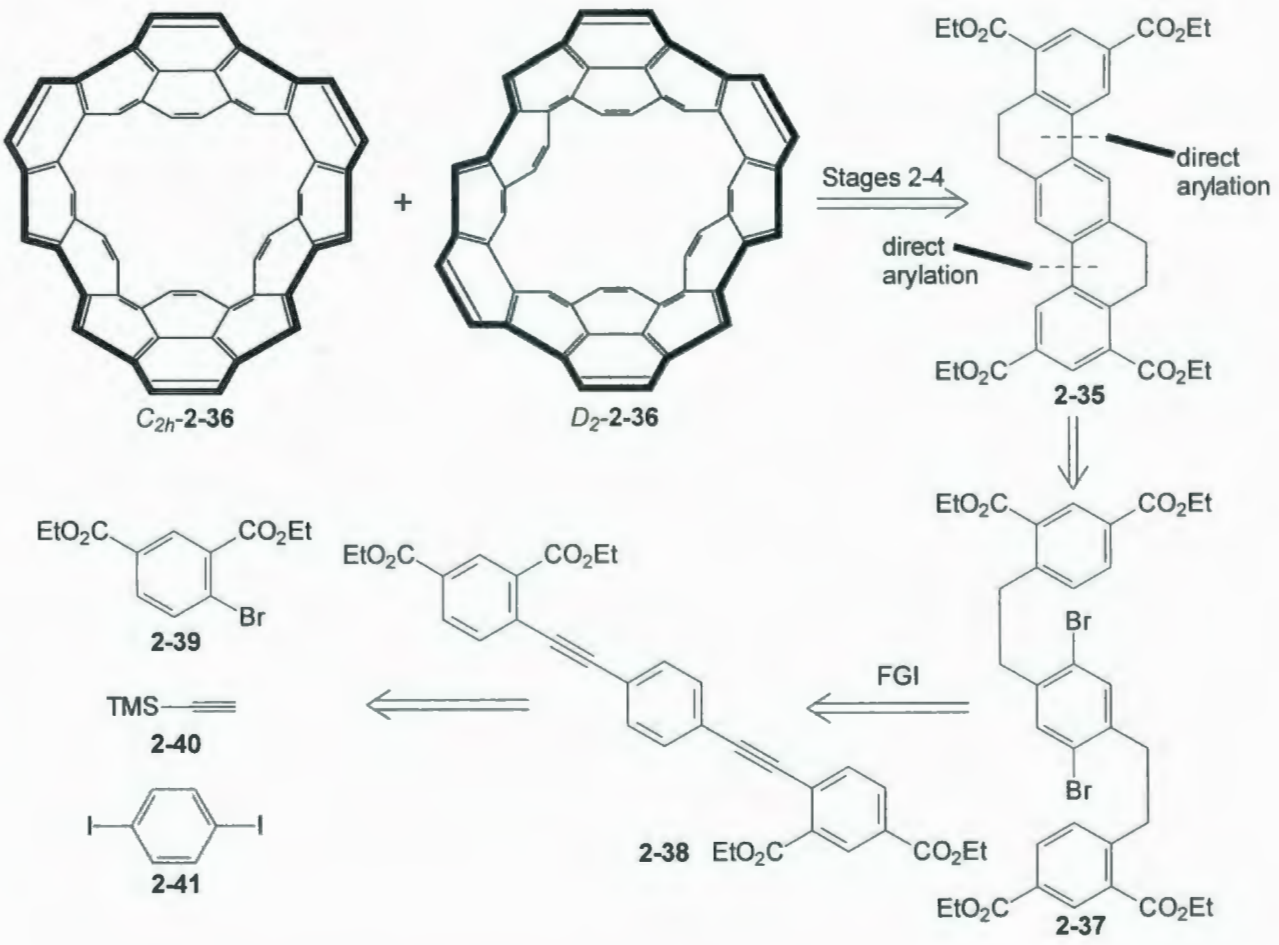


**Scheme 2.07.** Retrosynthetic analysis of aromatic belts **2-35**.

The synthesis started with the Sonogashira reaction of 1,4-diiodobenzene (**2-41**) and trimethylsilyl acetylene (**2-40**) to afford protected diyne **2-42** (Scheme 2.08). Deprotection of **2-42** furnished diyne **2-43** in quantitative yield over two steps. Bromide **2-39** was synthesized by esterification of 4-bromoisophthalic acid (**2-44**) (98%). Diyne **2-43** was then reacted with bromide **2-39** under Sonogashira conditions to afford tetraesterdiyne **2-38** (55%). Hydrogenation of **2-38** in the presence of Pd/C gave compound **2-44** (100%), which was then

regioselectively brominated on the more electron-rich ring to afford dibromide **2-37** as the substrate for the direct arylation reaction. After some optimization, it was found that the direct arylation could give the desired molecular board **2-35** in high yield (91%). This completed Stage 1 of this approach.

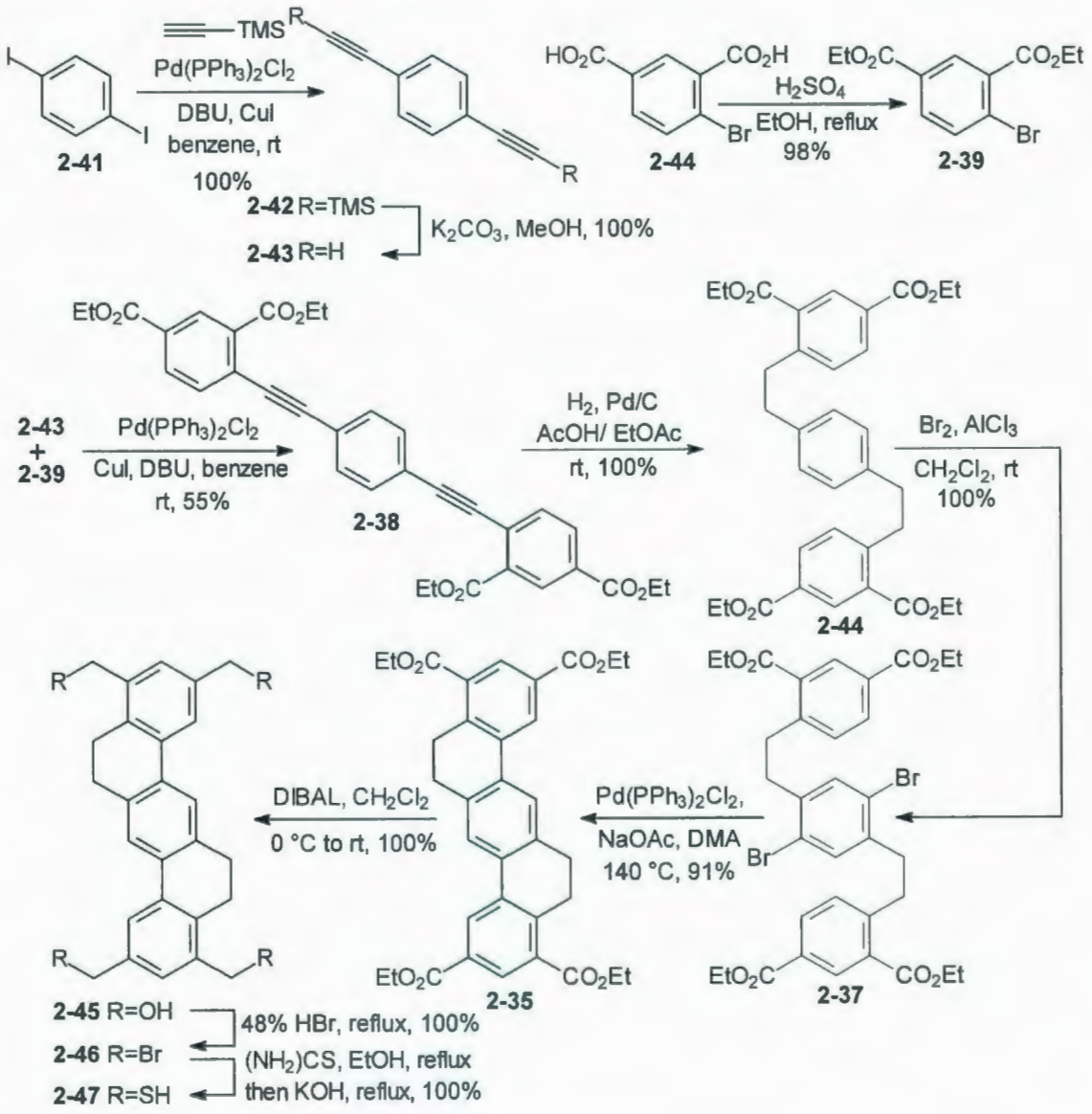


**Scheme 2.08.** Synthesis of appropriately functional molecular boards **2-46** and **2-47**.

Stage 2 commenced with the reduction of board **2-35** with DIBAL to afford tetraol **2-45**. Purification of the product was difficult due to its low solubility. This being the case, crude **2-45** was used directly in the next step, which was bromination with concentrated aqueous hydrobromic acid. This afforded tetrabromide **2-46** in high yield (100%, crude, two steps). Cursory attempts to synthesize tetrathiacyclophanes $C_{2h}$-**2-48** and $D_2$-**2-48** by treatment of **2-46** with $Na_2S/Al_2O_3$ failed, as did an attempted reaction between **2-46** and the crude tetrathiol **2-47** derived from it (Scheme 2.09). The problem was the solubility of tetrabromide **2-46**, which was not sufficient in common organic solvents for it to be used successfully in the following steps. Purification and characterization of tetrabromide **2-46** were also difficult.

Although this approach was unsuccessful, it established that the twofold direct arylation reaction was capable of generating the carbon skeleton of the dibenzo[*a*,*h*]anthracene board motif **2-21** in short order. If a solution to the solubility problem could be found, then this approach could be investigated further.

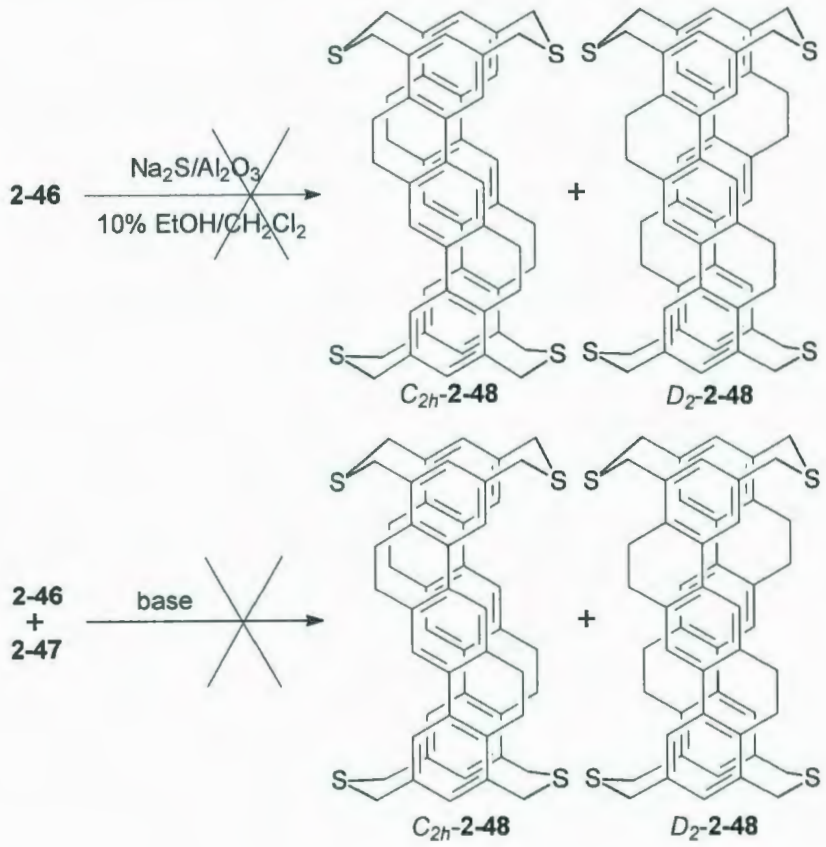


**Scheme 2.09.** Attempted synthesis of tetrathiacyclophanes **2-48**.

**Referenes:**


1. Bodwell, G. J.; Bridson, J. N.; Houghton, T. J.; Kennedy, J. W. J.; Mannion, M. *Angew. Chem. Int. Ed. Engl.* **1996**, *35*, 1320.
2. Bodwell, G. J.; Bridson, J. N. Houghton, T. J.; Kennedy, J. W. J.; Mannion, M. R. *Chem. Eur. J.* **1999**, *5*, 1823.
3. Bodwell, G. J.; Fleming, J. J.; Mannion, M. R.; Miller, D. O. *J. Org. Chem.* **2000**, *65*, 5360.
4. Bodwell, G. J.; Miller, D. O.; Vermeij, R. J. *Org. Lett.* **2001**, *3*, 2093.
5. Zhang, B.; Manning, G. P.; Dobrowolski, M. A.; Cyrańsk, M. K.; Bodwell, G. J. *Org. Lett.* **2008**, *10*, 273.
6. Merner, B. L.; Dawe, L. N.; Bodwell, G. J. *Angew. Chem. Int. Ed. Engl* **2009**, *48*, 1.
7. Bodwell, G. J.; Houghton, T. J.; Kennedy, J. W. J.; Mannion, M. R. *Angew. Chem. Int. Ed. Engl.* **1996**, *35*, 2121.
8. Mitchell, R. H.; Boekelheide, V. *J. Am. Chem. Soc.* **1974**, *96*, 1547. (In this citation, the disfavored *anti*-[2.2]metacyclophanediene was observed to convert thermally into *trans*-10b,10c-dihydropyrene. This is a notable exception to the Woodward-Hoffman rules.)
9. Caldwell, R. A.; Mizuno, K.; Hansen, P. E.; Vo, L. P.; Frentrup, M.; Ho, C. D. *J. Am. Chem. Soc.* **1981**, *103*, 7263.
10. Irie, M.; Mohri, M. *J. Org. Chem.* **1988**, *53*, 803.

11. Wodrich, M. D.; Wannere, C. S.; Mo, Y.; Jarowski, P. D.; Houk, K. N.; Schleyer, P. R. *Chem. Eur. J.* **2007**, *13*, 7731.

12. Smith, M. B.; March, J. Advanced Organic Chemistry, 5th edition, Wiley Inter-Science, 2001, page 24.

13. Suresh, C. H.; Koga, N. *Chem. Phys. Lett.* **2006**, 550.

14. Mitchell, R. H. *E. J. Org. Chem.* **1999**, 2695.

15. Wu, J.; Cyranski, M. K.; Dobrowolski, M. A.; Merner, B. L.; Bodwell, G. J.; Mo, Y.; Schleyer, P. V. R. *Mol. Phys.* **2009**, in press.

16. Vögtle, F. *Top. Curr. Chem.* **1983**, *115*, 157.

17. Vermeij. R. Ph.D. Thesis, Memorial University, 2001.

18. Yu, H. M.Sc. Thesis, Memorial University, 2004.

19. Hosoya, T.; Takashiro, E.; Matsumoto, T.; Suzuki, K. *J. Am. Chem. Soc.* **1994**, *116*, 1004.

# Chapter 3

## Synthesis of Aromatic Belts via Tetrasubstituted 5,6,12,13-Tetrahydrodibenzo[*a*,*h*]anthracene Boards

## 3.1 Synthesis of Aromatic Belts via a Dimethyl Substituted Molecular Board

The first attempt to synthesize aromatic belts by way of dibenzo[*a*,*h*]anthracene-based boards was unsuccessful due to the low solubility of some of the synthetic intermediates. The obvious solution to this problem was the introduction of solubilizing groups on the boards.

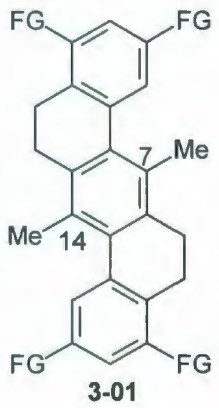


**3-01**

**Figure 3.01.** Dimethyl substituted molecular board **3-01**.

Although several positions are available for substitution, it was decided to introduce alkyl substituents on the central ring, i.e., at C-7 and C-14 positions as shown in structure **3-01** (Figure 3.01). In reaching this decision, two points were important. First, it was anticipated that the existing synthetic route could be used with only minor modifications. Second, the solubilizing groups are far away from the functional groups (FG) that will be used later to form the cyclophane system and, ultimately, the belt (Stages 2-4). As such, steric hindrance due to the solubilizing groups should be minimized. However, one potential problem was

identified immediately. The presence of the two solubilizing groups dictated that the twofold direct arylation reaction would be required to form a hexasubstituted benzene ring and no such reaction had been reported at that time. To test the viability of this reaction, methyl groups were employed initially.

Synthetic work commenced with 1,4-diiodo-2,5-dimethylbenzene (**3-02**), which was synthesized according to a literature procedure (Scheme 3.01).[1] Reaction of **3-02** with trimethylsilylacetylene under Sonogashira conditions gave the protected diyne **3-03** (90%). Deprotection of **3-03** by treatment with $K_2CO_3$ then afforded diyne **3-04** (98%). Another Sonogashira reaction between diyne **3-04** and bromide **2-39** furnished tetraesterdiyne **3-05** (72%), in which all of the skeletal atoms required for the desired board **3-01** are present. Catalytic hydrogenation of **3-05** in the presence of Pd/C afforded tetraester **3-06** (91%). Regioselective bromination on the most electron-rich ring then afforded dibromide **3-07** (80%) as the substrate for the crucial twofold arylation reaction.

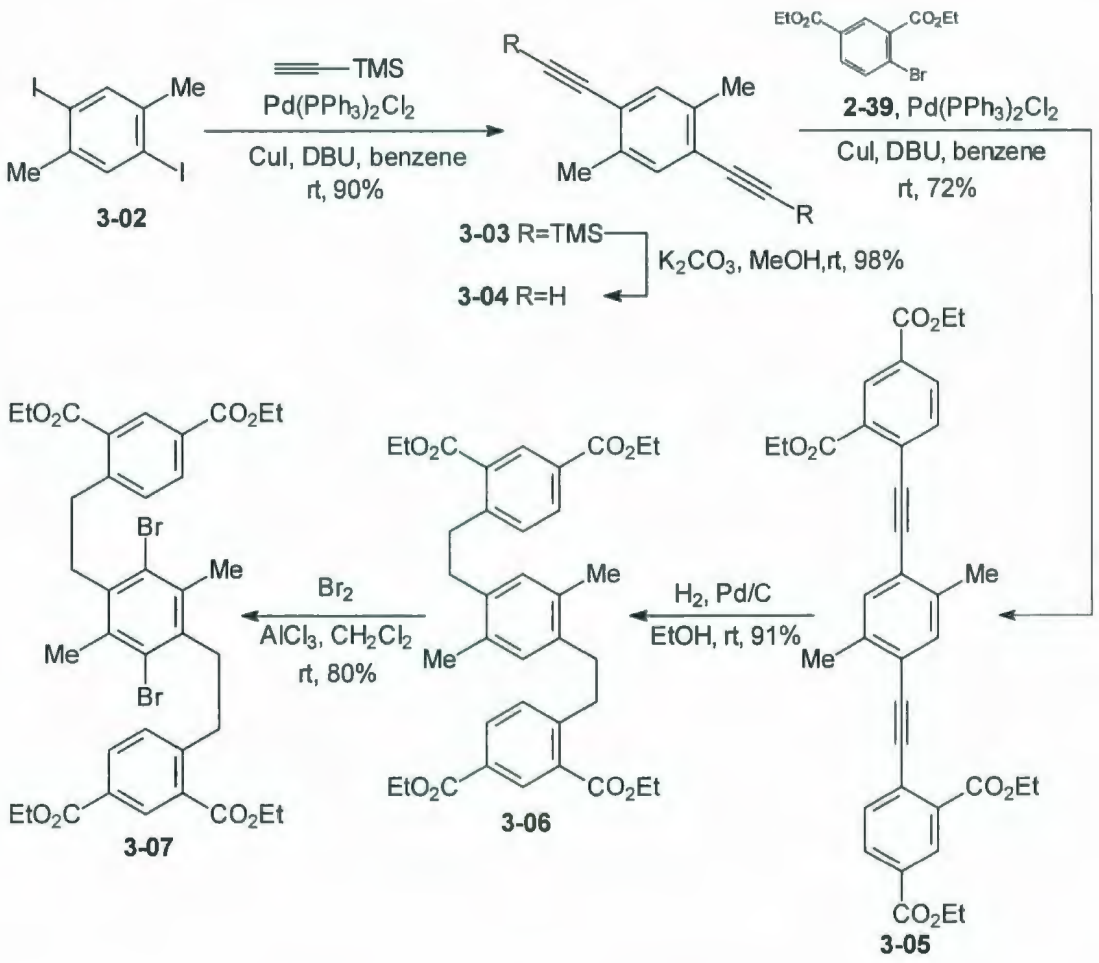


**Scheme 3.01.** Synthesis of dibromide **3-07**.

Subjection of **3-07** to the conditions employed for the previous twofold direct arylation reaction (**2-37** to **2-35**, Scheme 2.08) resulted in the formation of only traces amount of newly-formed compounds (TLC analysis) (Table 3.01, Entry 1). Increasing the reaction time from 2 h to 48 h did not give a significantly different result at 140 °C or 150 °C (Table 3.01, Entries 2, 3). When the temperature of the oil bath was increased to 180 °C, all of **3-07** was consumed after 48 h, but only intractable materials were produced (Table 3.01, Entry 4).

However, when the reaction time at 180 °C was decreased from 48 hours to 2 hours, the desired product **3-08** was isolated in 9% yield (Table 3.01, Entry 6). When a large amount of catalyst was loaded, the yield increased to 41% (Table 3.01, Entry 8).

**Table 3.01.** Optimization of the twofold direct arylation leading to **3-08**.

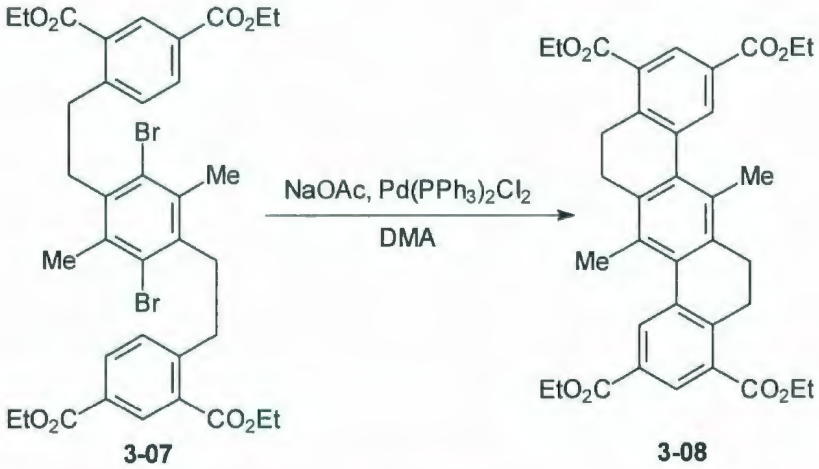


**3-07** **3-08**

| Entry | Oil bath Temperature (°C) | Time (h) | mol% of Catalyst | Result |
|---|---|---|---|---|
| 1 | 140 | 2 h | 10 | Little progress-impure **3-07** was recovered |
| 2 | 140 | 48 h | 10 | Little progress-impure **3-07** was recovered |
| 3 | 150 | 48 h | 10 | Little progress-impure **3-07** was recovered |
| 4 | 180 | 48 h | 10 | Intractable products |
| 5 | 180 | 24 h | 10 | Intractable products |
| 6 | 180 | 2 h | 10 | Board **3-08** isolated in 9% yield |
| 7 | 180 | 2 h | 50 | Board **3-08** isolated in 26% yield |
| 8 | 180 | 2 h | 70 | Board **3-08** isolated in 41% yield |

Based on a suggestion by Prof. Keith Fagnou (University of Ottawa),[2] the use of potassium instead of sodium bases was investigated, as was the use of a more elaborate ligand (Table 3.02). $K_2CO_3$ proved to be a good choice for this

reaction. An initial reaction was performed using 10 mol% $Pd(OAc)_2$, 20 mol% ligand **3-09**.[2] After 18 h at reflux, a complex mixture had formed (Table 3.02, Entry 1). However, when the reaction time was decreased to 30 min and $Pd(OAc)_2$ with ligand **3-06** was employed, the desired product was isolated in 45% yield (Table 3.02, Entry 2). Replacing the combination of $Pd(OAc)_2$ and **3-09** with just $Pd(PPh_3)_2Cl_2$ afforded the desired product **3-08** in 62% yield (Table 3.02, Entry 4). With both catalysts, the yield increased significantly with the scale (Table 3.02, Entries 3, 5), whether this is a real increase in yield or a consequence of being able to isolate the product by crystallization is unclear. At this point, $Pd(PPh_3)_2Cl_2$ was identified as the catalyst of choice for this reaction. This completed Stage 1 of the synthesis.

Stage 2 began with the reduction of **3-08** with DIBAL to afford tetraol **3-10** (100%, crude) (Scheme 3.02). Although **3-10** appeared to be more soluble than **2-45** (the parent tetraol) in DMSO, its solubility was still limited, which made purification and characterization difficult. Therefore, the crude material was used directly in the next step, i.e., bromination in aqueous HBr at reflux to give tetrabromide **3-11** (80%, crude, 2 steps). Gratifyingly, tetrabromide **3-11** exhibited better solubility than the parent dibromide **2-46** in DMSO. Nevertheless, **3-11** was still not a freely-soluble compound, so it was also used as obtained from the bromination reaction. The purity of the crude product was $\lambda$ 90% according to its $^1H$ NMR spectrum.

**Table 3.02.** Optimization of the twofold direct arylation leading to **3-08**.

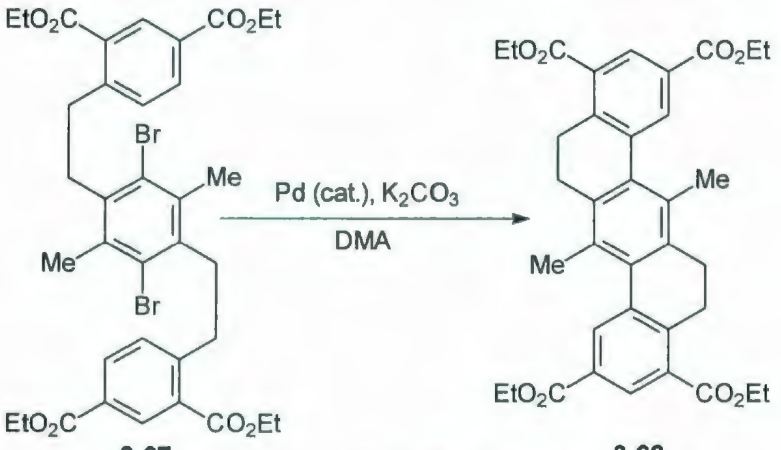


**3-07** **3-08**

Ligand:

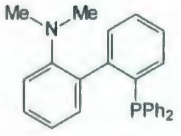


**3-09**

| Entry | Catalyst | Ligand | Time (h) | Scale | Yield of **3-08** (%) |
|---|---|---|---|---|---|
| 1 | $Pd(OAc)_2$, 10% | 20% | 18 | 57 mg | A complex mixture |
| 2 | $Pd(OAc)_2$, 10% | 20% | 0.5 | 57 mg | 45 |
| 3 | $Pd(OAc)_2$, 10% | 20% | 0.5 | 285 mg | 62 |
| 4 | $Pd(PPh_3)_2Cl_2$, 10% | n/a | 0.75 | 285 mg | 62 |
| 5 | $Pd(PPh_3)_2Cl_2$, 10% | n/a | 0.5 | 1.14 g | 81 |

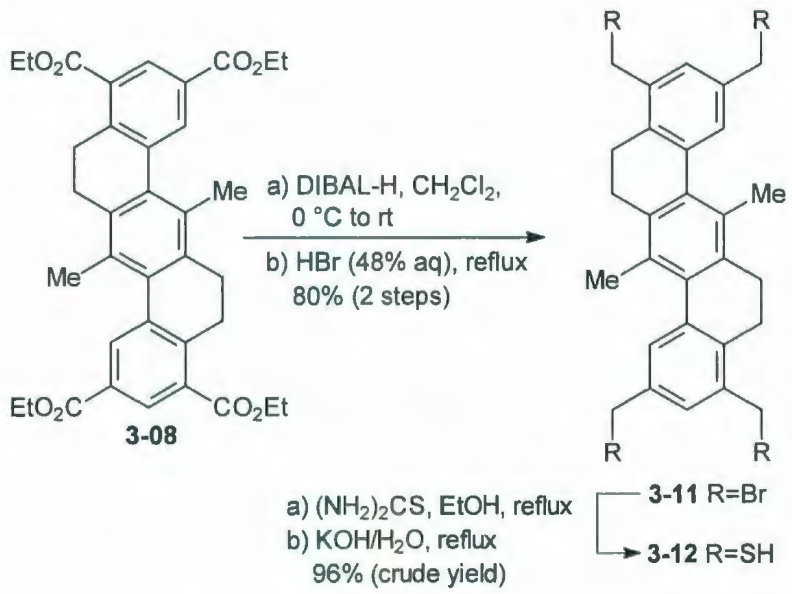


**Scheme 3.02.** Synthesis of appropriately functional molecular boards **3-11** and **3-12**.

With this precursor in hand, the coupling reaction to synthesize tetrathiacyclophanes $C_{2h}$-**3-13** and $D_2$-**3-13**, the key step in Stage 2, was attempted (Scheme 3.03). Reaction of **3-11** with $Na_2S/Al_2O_3$ in 10% $EtOH/CH_2Cl_2$ resulted in no reaction, presumably due to the low solubility of the substrate **3-11**. An alternative high dilution coupling of tetrabromide **3-11** and the corresponding tetrathiol **3-12** (synthesized from **3-11** by treatment with thiourea, followed by treatment with aqueous KOH) (96%, crude yield, Scheme 3.02) was investigated. Both starting materials were not sufficiently soluble in benzene (the standard solvent for this reaction) to be used successfully in this reaction.

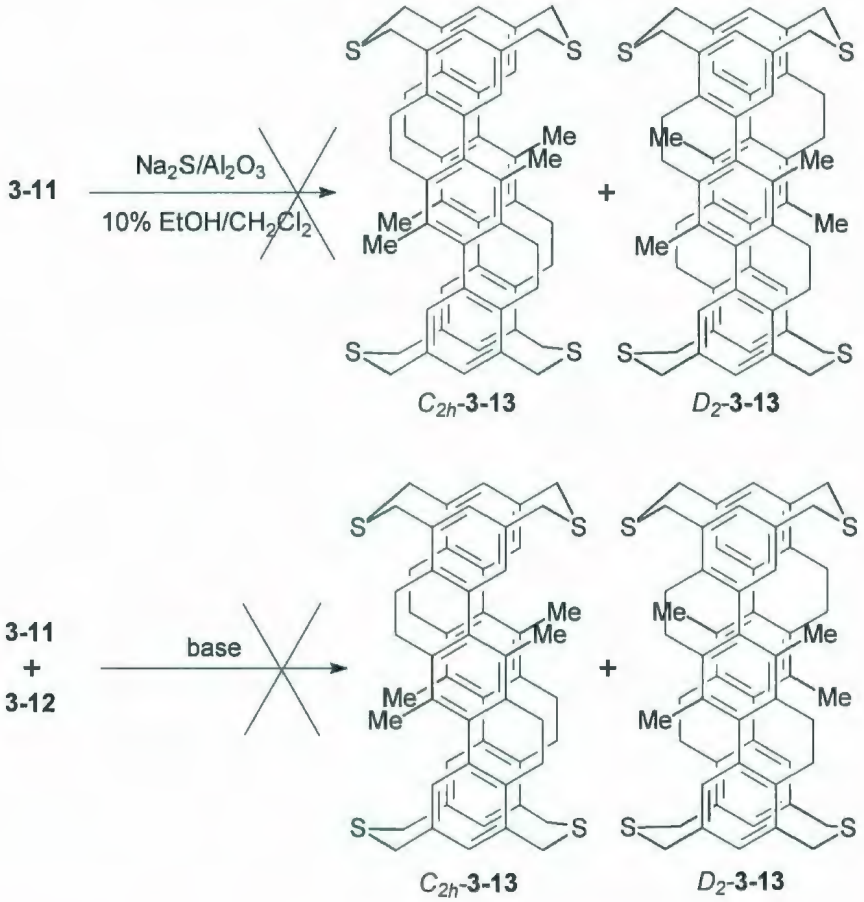


**Scheme 3.03.** Attempted synthesis of tetrathiacyclophanes **3-13**.

As with the parent boards, poor solubility brought the approach involving dimethyl-substituted boards to an end at Stage 2. However, two important lessons were learned. First, even two methyl groups resulted in a small, but significant increase in the solubility of the tetraol and tetrabromide intermediates. The introduction of longer solubilizing groups was therefore expected to solve the solubility problem. Second, the success of the twofold direct arylation reaction established that the synthesis of the hexasubstituted central ring could be accomplished without any major difficulty.

### 3.2 Synthesis of Aromatic Belts via a Didecyl-substituted Molecular Board

*n*-Decyl solubilizing groups were chosen for the next attempt to synthesize aromatic belts. Since diyne **3-14** was available in the Bodwell laboratory,[3] it was envisaged that this compound could simply replace diyne **3-02** in the previous synthetic pathway. However, reaction between bromide **2-39** and diyne **3-14** under Sonogashira conditions resulted in the formation of a complex mixture (Scheme 3.04).

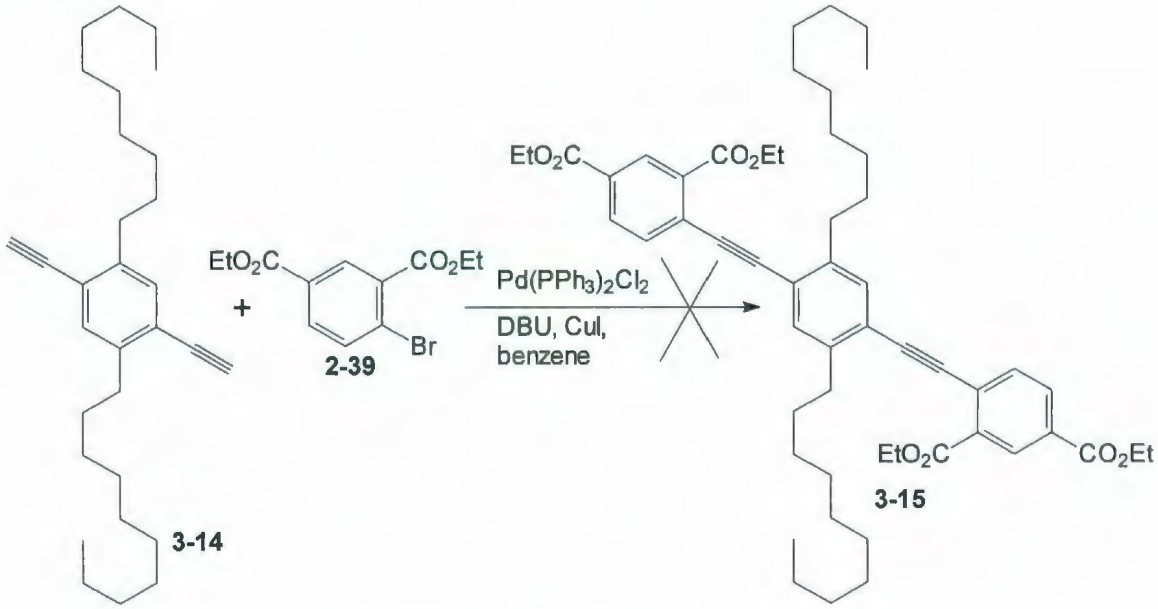


**Scheme 3.04.** Attempted synthesis of diynetetraester **3-15**.

Rather than attempting to modify/optimize this reaction, an alternative approach was investigated (Scheme 3.05). 1,4-Didecyl-2,5-diiodobenzene (**3-16**) was synthesized from 1,4-diiodobenzene (**2-41**) by a series of reactions consisting of Sonogashira reaction with 1-decyne to afford **3-17** (86%), catalytic

hydrogenation to give **3-18** (96%) and electrophilic aromatic substitution to give **3-16** (35%). This diiodide was then reacted under Sonogashira conditions with alkyne **3-19**, which was synthesized in 2 steps from bromide **2-39** according to the procedures described by Yu.[4] This reaction also afforded a complex mixture. Another problem was that the synthesis of **3-19** was difficult to scale up. Therefore, work on this particular synthesis pathway was abandoned in favor of the investigation of a different route in which the solubilizing groups were introduced at a later stage in the synthesis.

Tetraester **2-44** was synthesized according to Yu's procedures (Scheme 2.08)[4] and it was then halogenated to prepare for the attachment of the solubilizing groups. Bromination of **2-44** according to Yu's procedure afforded **2-37** quantitatively with complete regioselectivity (Scheme 3.06). Sonogashira reaction between dibromide **2-37** and 1-decyne then afforded the desired product **3-20** in 75% yield after reacting in benzene at reflux for 2 d (Scheme 3.06). In an attempt to increase the yield of tetraesterdiyne **3-20** and/or shorten the reaction time, **2-44** was first iodinated chemo- and regioselectively according to Yu's procedures[4] to give diiodide **3-21** (83%) and was then subjected to Sonogashira reaction with 1-decyne. This reaction afforded tetraesterdiyne **3-20** (70%) after reacting in benzene at room temperature for 6 h.

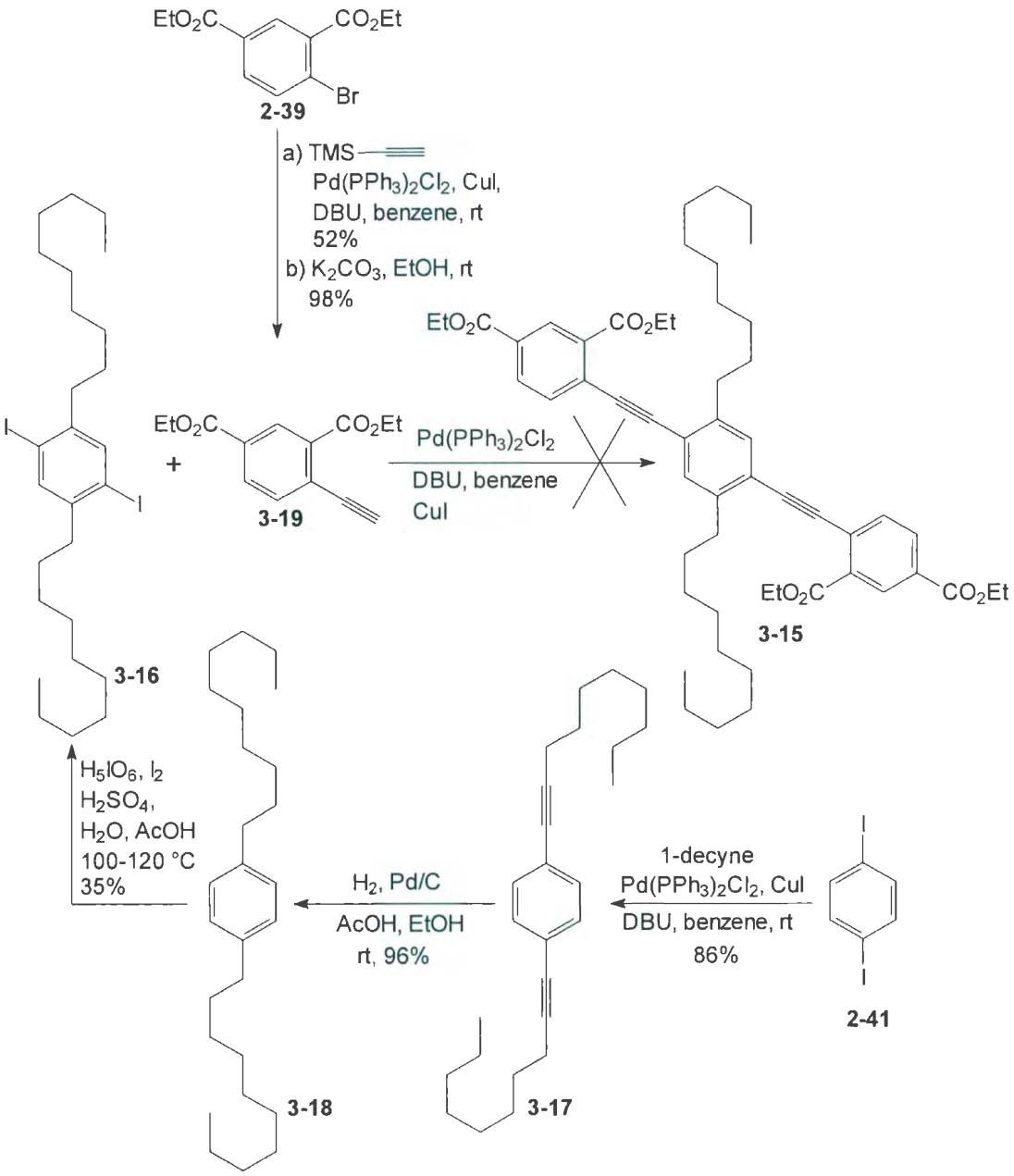


**Scheme 3.05.** Attempted synthesis of diynetetraester **3-15**.

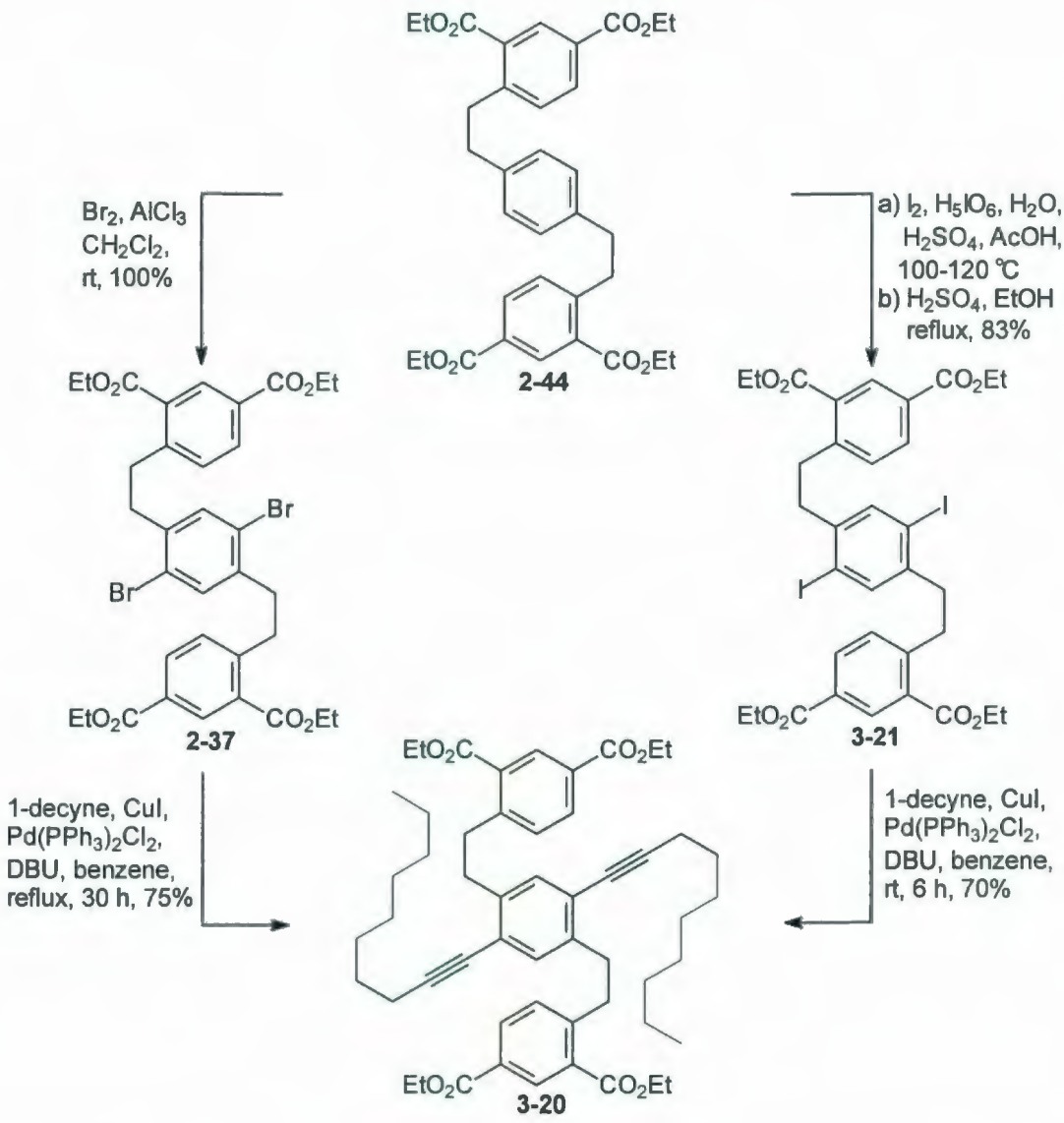


**Scheme 3.06.** Synthesis of diynetetraester **3-20**.

Catalytic hydrogenation of **3-20** in the presence of Pd/C gave compound **3-22** (92%) (Scheme 3.07). Subsequent bromination of **3-22** upon treatment with $Br_2$ (2.5 equivalents) and $AlCl_3$ in $CH_2Cl_2$ gave a mixture of the desired dibromide **3-24** and monobromide **3-23** in a 7:1 ratio (estimated by $^1H$ NMR analysis of the

crude product). Somewhat surprisingly, extension of the time of the reaction and the use of 10 equivalents of $Br_2$ gave essentially the same result. For this reason, iodination was not investigated at this point. Instead, other bromination conditions were investigated. Treatment of **3-22** with $Br_2$ (as both the reagent and solvent) and a catalytic amount of iodine at room temperature gave the desired dibromide **3-23** in 100% crude yield (Scheme 3.08). Other conditions using $Br_2$ in $H_2O$ gave **3-23** in 87% yield. Practically, the use of $Br_2/H_2O$ was found to be more convenient and this method was used subsequently.

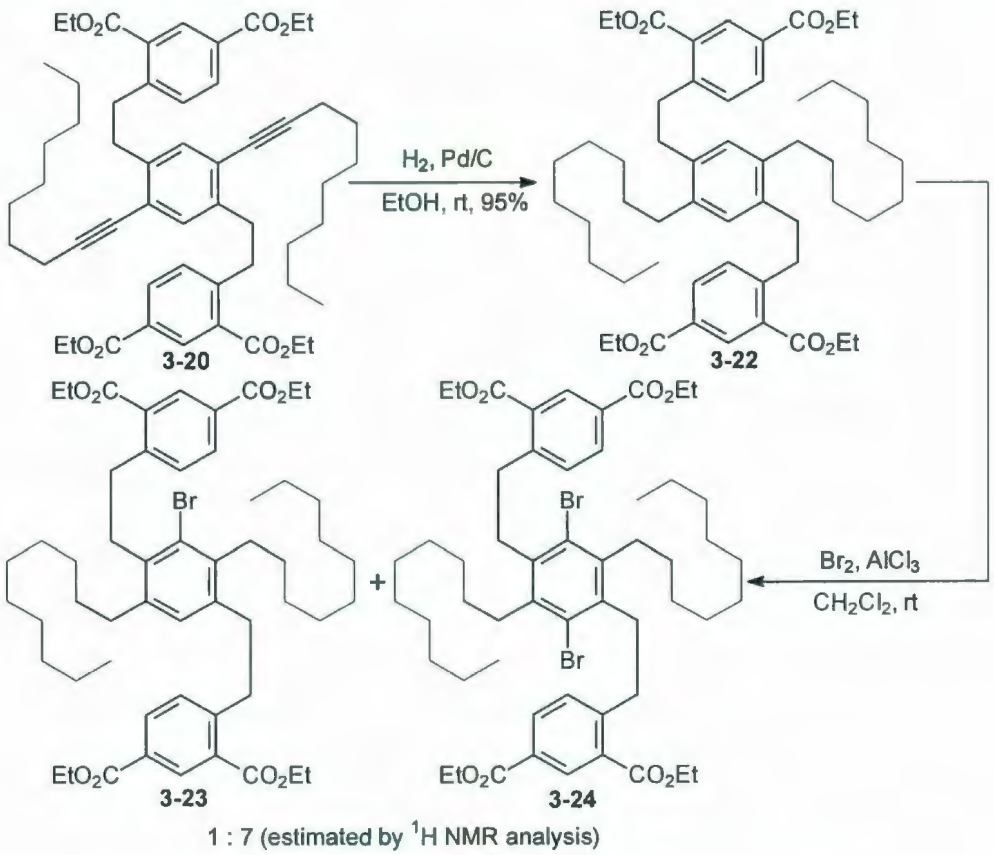


**Scheme 3.07.** Attempted synthesis of dibromide **3-24**.

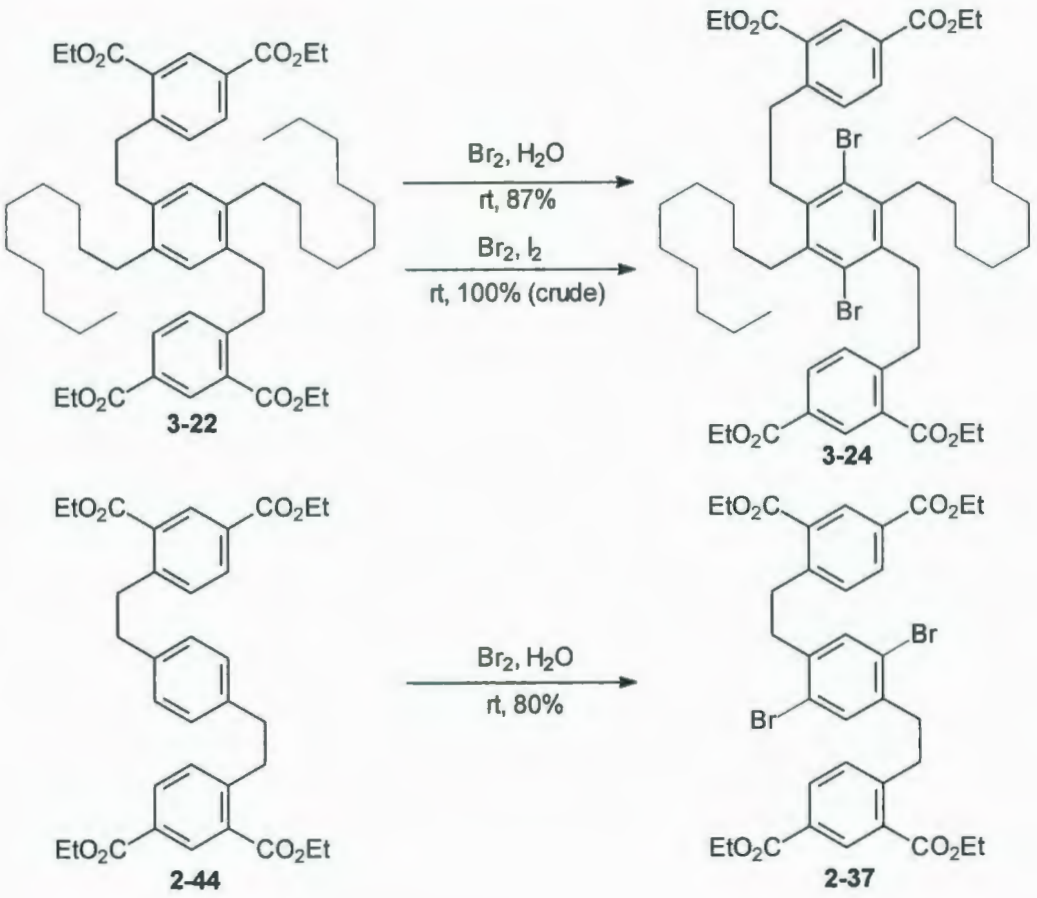


**Scheme 3.08.** Synthesis of dibromides **3-24** and **2-37** using $Br_2/H_2O$.

Employment of the $Br_2/H_2O$ to synthesize compound **2-37** was then attempted (Scheme 3.08) and this method afforded **2-37** in 80% yield when excess (10 equivalents) $Br_2$ was employed. No trace of tri- and tetrabromides, which formed using $Br_2/AlCl_3$ when the number of equivalents of $Br_2$ even slightly exceeded 2.0,[4] were observed. The use of $Br_2/H_2O$ was also found to be practically more convenient and was therefore used for larger scale reactions.

Twofold direct arylation reaction of **3-24** using the same conditions as for the synthesis of **3-08** furnished molecular board **3-25** (Scheme 3.09). The isolated yield of this reaction was somewhat variable (generally 50-70%) and appeared to depend on the efficiency of the crystallization of the impure chromatographed product. No attempt was made to optimize this reaction. The reduction of **3-25** by DIBAL then gave the desired tetraol **3-26**. Bromination of **3-26** by treatment with aqueous HBr at reflux afforded a black, intractable product. However, the use of $PBr_3$ in $CH_2Cl_2$ gave the desired tetrabromide **3-27** (80%, 2 steps).

Although the solubilities of **2-46**, **3-11** (the parent tetrabromides) and **3-27** were not measured, it was obvious that **3-27** was much more soluble than either **2-46** or **3-11** in common organic solvents such as $CH_2Cl_2$ and $CHCl_3$.

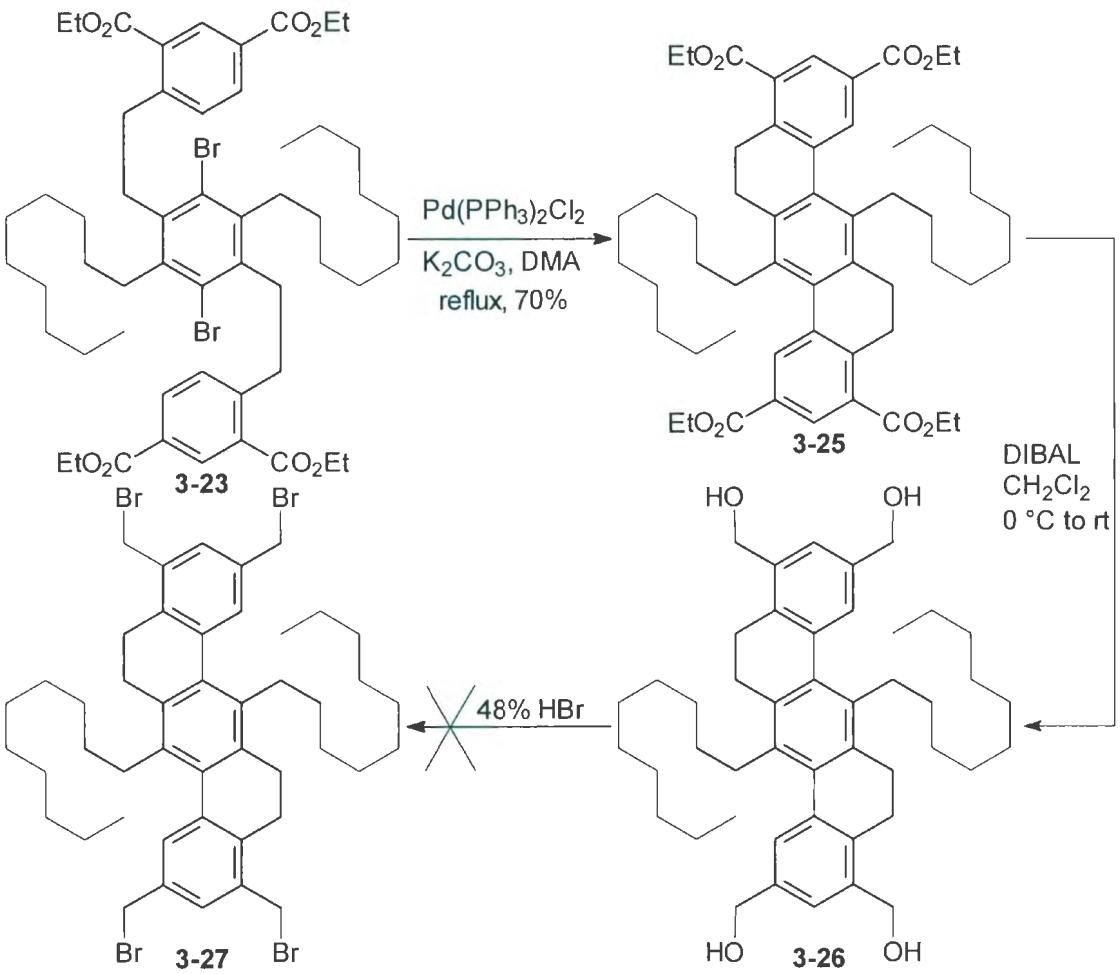


**Scheme 3.09.** Synthesis of tetraester **3-25** and attempted synthesis of tetrabromide **3-27**.

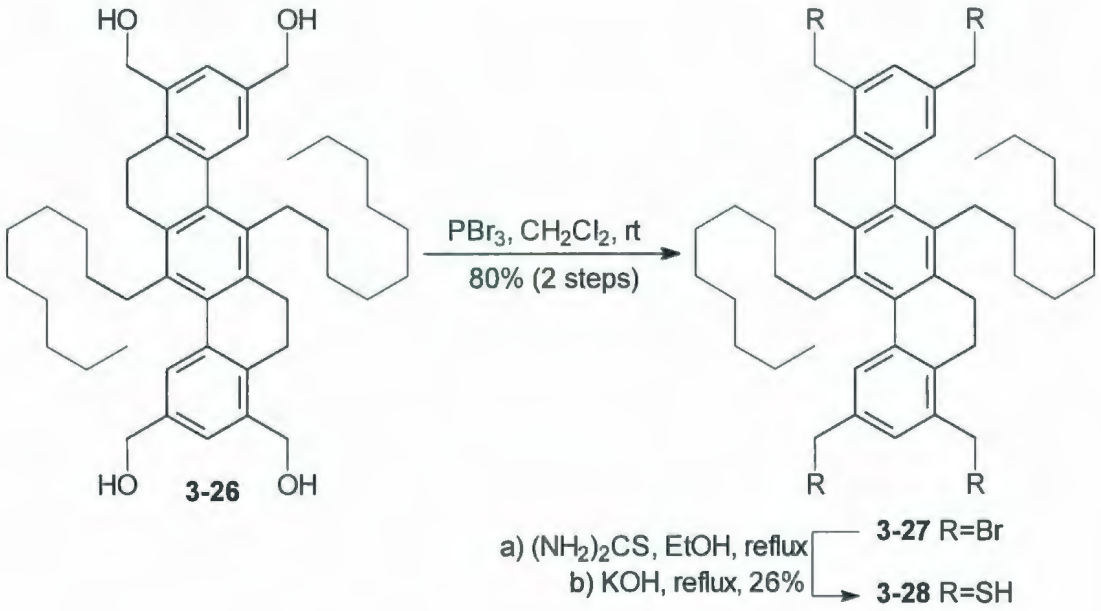


**Scheme 3.10.** Synthesis of molecular boards **3-27** and **3-28**.

The key reaction in Stage 2, which was anticipated to generate large cyclophanes, was attempted at this point. In the case of Vögtle's synthesis of cyclophane **1-88** (Scheme 1.19, p.34) and the previous attempts to synthesize aromatic belt **1-82** in the Bodwell group (Scheme 2.04), the coupling reaction between bromides and thiols was employed to generate thiacyclophanes. This suggested the bromide-thiol coupling reaction would be a good choice to synthesize cyclophane **3-29**. It was anticipated that this reaction would not be especially problematic. Although the first C-S-C bridge formation of **3-29** between **3-27** and **3-28** was an intermolecular reaction, all subsequent bridge formations were intramolecular. Tetrabromide **3-27** was reacted with thiourea followed by KOH to afford tetrathiol **3-28** (26%) (Scheme 3.10). Attempted high-dilution

coupling of tetrabromide **3-27** and tetrathiol **3-28** under basic conditions gave a crude product, the mass spectrum of which exhibited only a very weak cluster of peaks corresponding to the molecular formula of tetrathiacyclophane **3-29**. None of the desired product could be isolated by column chromatography.

The use of $Na_2S/Al_2O_3$,[5] which had proved to be an effective method in the Bodwell group to synthesize dithiacyclophanes from tetrabromides,[6-10] was then attempted. This reaction afforded a mixture of the desired tetrathiacyclophanes $C_{2h}$-**3-29** and $D_2$-**3-29** (up to 54%). Separation of $C_{2h}$-**3-29** and $D_2$-**3-29** by HPLC was attempted, but was not successful. Nevertheless, this constituted the first successful completion of Stage 2. No other linear oligomers or cyclic oligomers (not shown) were detected by mass spectrometry. The $^1$H NMR spectrum was very complex, which was not surprising. At first glance, there are ten unique benzylic protons (two pairs of diasterotopic $CH_2S$ protons, a pair of diastereotopic $CH_2$ protons of the side chain and four chemically inequivalent protons in each board ethano unit), most of which are highly coupled. Any conformational process in the board moieties (twisting of the four 9,10-dihydrophenanthrene units) and in the $CH_2$-S-$CH_2$ bridges (pseudochair/pseudoboat interconversions) would greatly complicate the already complicated situation. Furthermore, the sample consists of two constitutional isomers, which would be expected to have similar and equally complex $^1$H NMR spectra. As such, MS was the only method that could easily provide evidence for the formation of **3-29**.

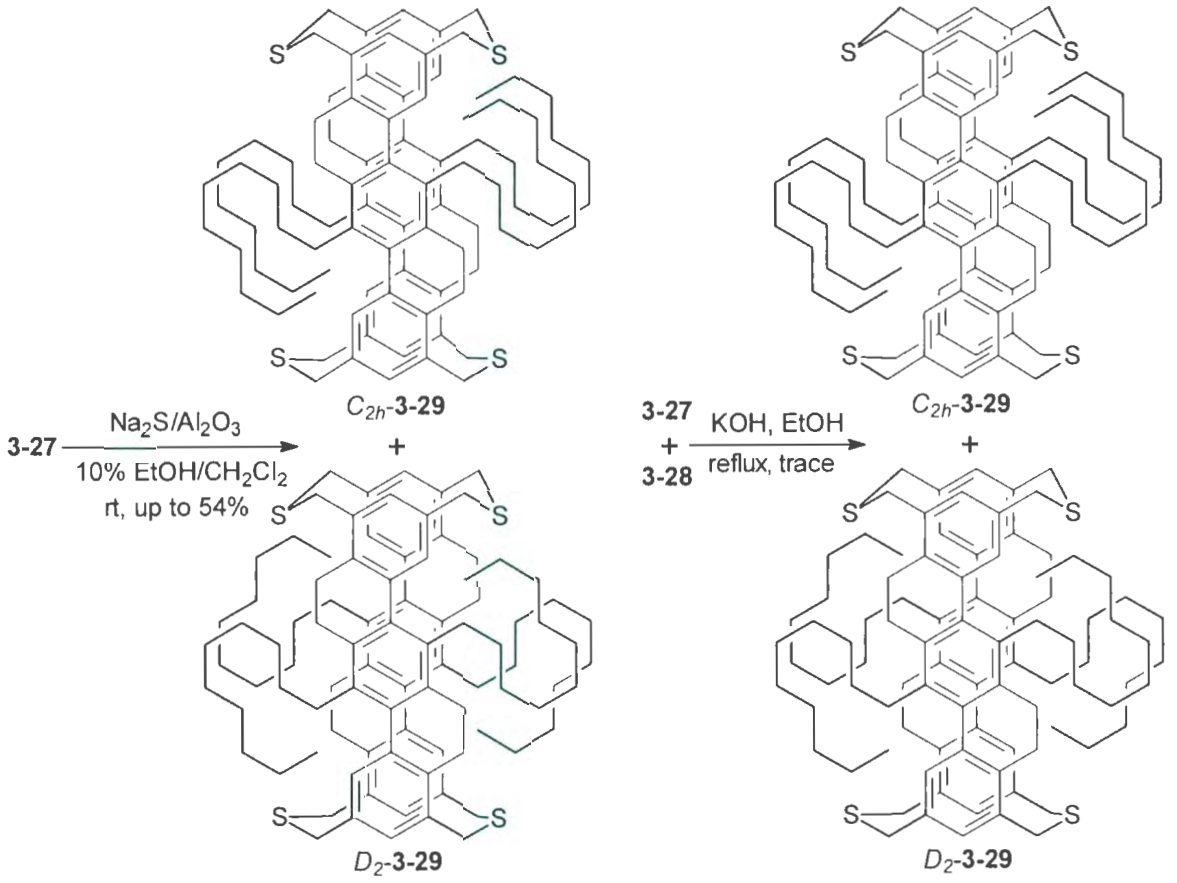


**Scheme 3.11.** Synthesis of tetrathiacyclophane **3-29**.

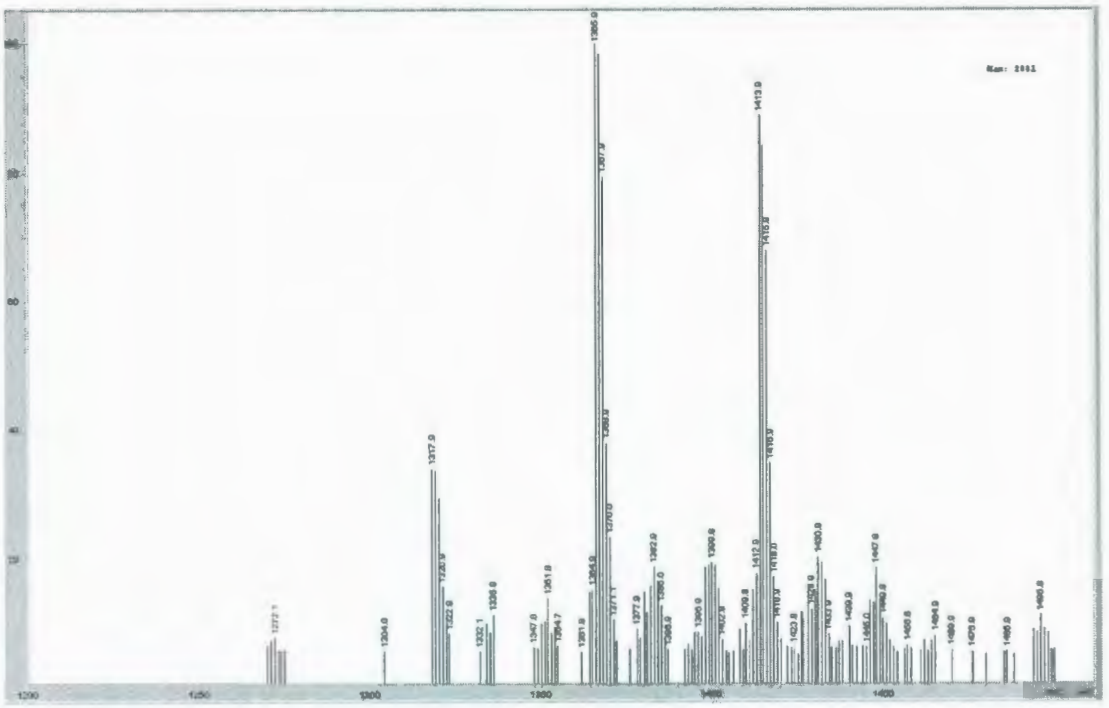

**Figure 3.02.** APCI (positive) mass spectrum of **3-31**.

Despite only having MS evidence (albeit reasonable evidence) for the formation of **3-29**, work on Stage 3 (tetrathiacyclophane to cyclophanetetraene) was then initiated. Tetrathiacyclophane **3-29** was reacted with Borch reagent ($(MeO)_2CHBF_4$) to give the corresponding tetrakis(methylsulfonium tetrafluoroborate) **3-30**, which was then treated with *t*-BuOK to bring about a thia-Stevens rearrangement to afford compound **3-31** (28%) (Scheme 3.12). The thia-Stevens rearrangement of *syn*-2,11-dithia[3.3]metacyclophanes is known to afford mixtures of methylthio-substituted [2.2]metacyclophanes in which the SMe substituents can be attached to benzylic carbons of either the same aromatic ring or opposite aromatic rings (positional isomers).[11] Furthermore, an individual SMe group can be oriented in a pseudoaxial or pseudoequatorial fashion

(stereoisomers). Thus, in the case of **3-31**, there are 148 possible isomers (140 pairs of enantiomers and 8 *meso*-diastereomers in total: 64 pairs of enantiomers and 8 *meso*-diastereomers come from $C_{2h}$-**3-31** and 76 pairs of enantiomers come from $D_2$-**3-31**) (See Appendix 3.01 for a discussion of the stereochemistry of this system). With up to 148 isomers present, it is not surprising that NMR spectroscopy was not useful for the identification and characterization of the products. MS again proved to be the only useful method. The low-resolution mass spectrum (APCI-positive) of a chomatographed product exhibited a cluster of peaks at 1413-1417, which showed an isotopic pattern that resembled the calculated pattern for $C_{96}H_{132}S_4$ (Figure 3.02). The clusters of peaks at *m/z*=1365–1370, and 1317–1320 correspond to the fragments arising from the loss of SMe groups. Due to the high molecular masses observed, high-resolution mass spectra could not be obtained.

Fourfold *S*-methylation of a chromatographed sample of **3-31** with Borch reagent was then performed with the intention of generating tetrakis(dimethylsulfonium tetrafluoroborate) salt **3-32** (Scheme 3.13). The crude product of this reaction was treated with *t*-BuOK to induce a Hofmann elimination to provide cyclophanetetraene (23%). The low-resolution mass spectrum (APCI positive) of the chomatographed product exhibited a cluster of peaks at 1221-1224, which showed an isotopic pattern that closely resembled the calculated pattern for $C_{92}H_{116}$ (Figure 3.03). Despite the low yields for the conversion of **3-29**

to **3-33** (tetrathiacyclophane to cyclophanediene), Stage 3 had now been completed.

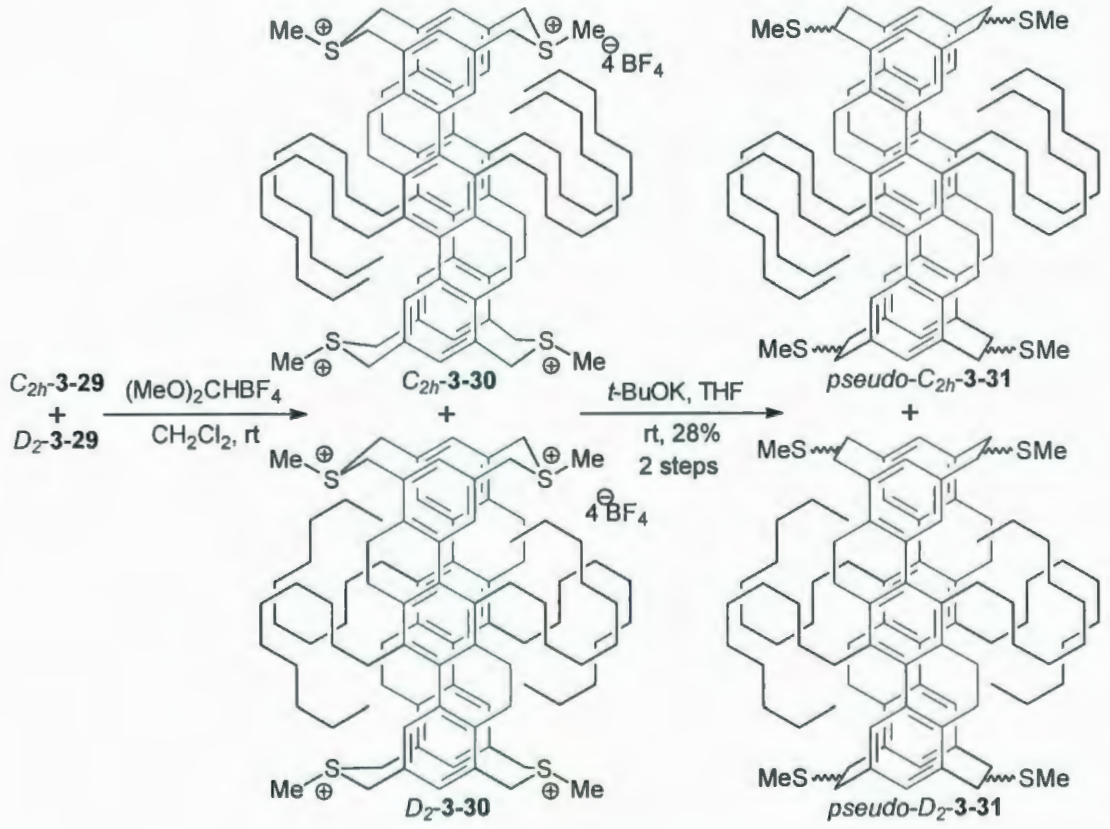


**Scheme 3.12.** Synthesis of **3-31**.

With tetraene **3-33** in hand, albeit in small quantities (λ 20 mg), Stage 4 of the general strategy was then investigated to complete the synthesis. In this case, dehydrogenation was expected to occur not only on the dihydropyrene units resulting from valence isomerization, but also on the partially saturated rings. Therefore, the removal of twelve hydrogen atoms was required in this step.

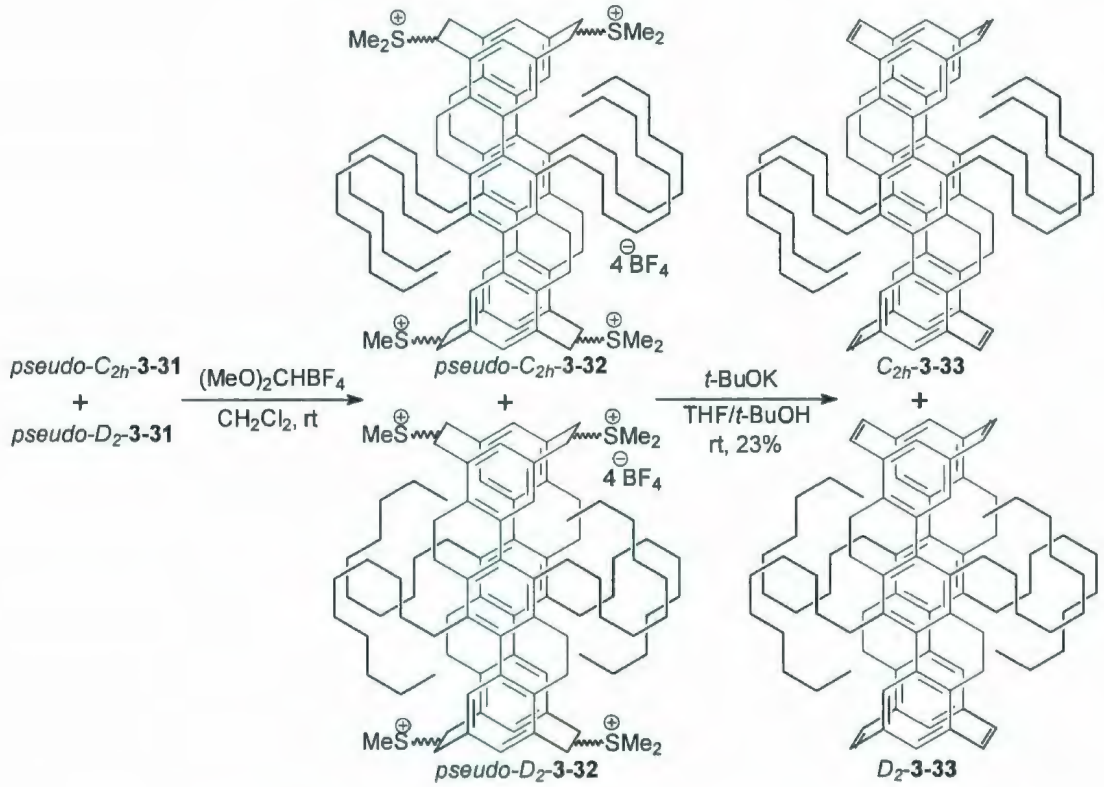


**Scheme 3.13.** Synthesis of tetraenes **3-33**.

Initially, tetraene **3-33** was reacted with DDQ (20 equivalents) in benzene at room temperature (Table 3.03, Entries 1, 2). TLC analysis indicated that the starting material ($R_f$ = 0.3, 5% EtOAc/hexanes) was fully consumed after 0.5 h. Two narrowly separated mobile spots had formed ($R_f$ = 0.2, 5% EtOAc/hexanes), which exhibited bright (green) fluorescence under 366 nm light. Column chromatography afforded <1 mg (traces) of a mixture of compounds. Mass spectrometric analysis confirmed that **3-33** had been fully consumed, and that a mixture of products corresponding to varying degrees of dehydrogenation had formed. Performing the reaction at reflux in benzene for 30 min did not give a

significantly different result (Table 3.03, Entry 3). Increasing the reaction time in either benzene or toluene at reflux for 48 h resulted in the eventual disappearance of the new mobile spots at $R_f$ = 0.3. If the desired belts **3-34** are indeed formed, it can be inferred that they have limited stability under the reaction conditions. When *m*-xylene or mesitylene were employed as the solvent and the temperature was increased to close to the boiling point of these two solvents, a peak at *m/z*=1205 (APCI, positive), which indicated the presence of a compound that has a structure with four protons less than the desired aromatic belts **3-34**, was detected by MS. The identity of this product(s) is unclear. One possibility is belts **3-35**, which is the result of dehydrogenation of one of the side chains of **3-34**, followed by a 6π electrocyclic ring-closing reaction to give **3-35** and another dehydrogenation.

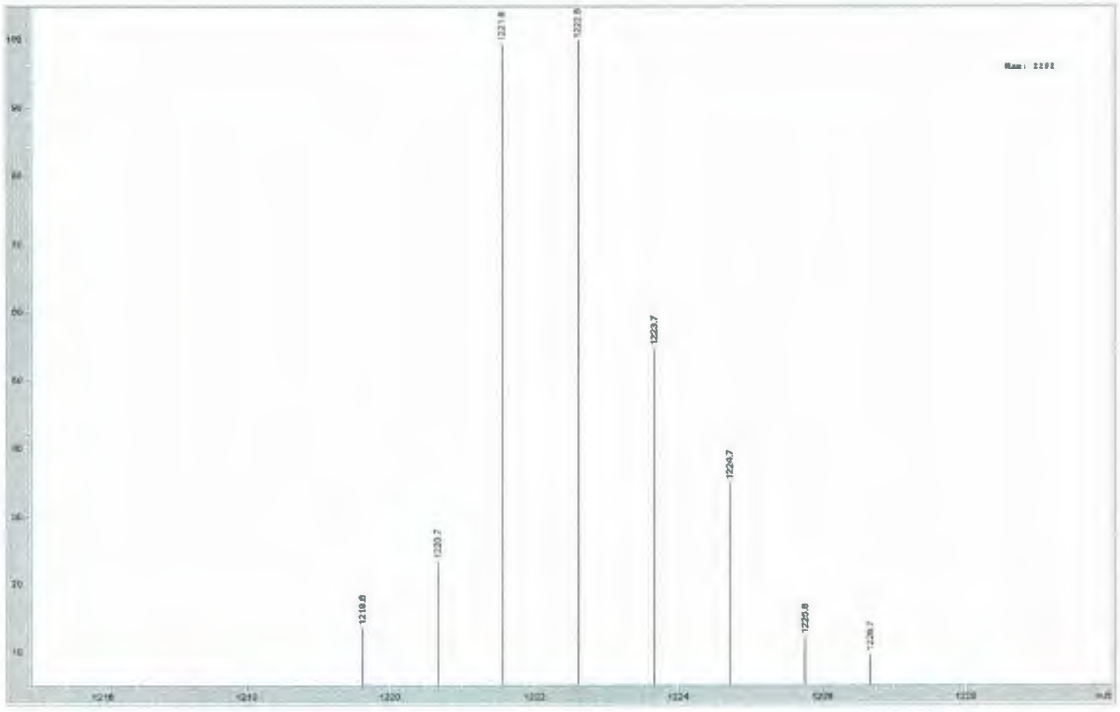

**Figure 3.03.** APCI (positive) mass spectrum of **3-33**.

**Table 3.03.** Attempted synthesis of aromatic belts **3-34**.

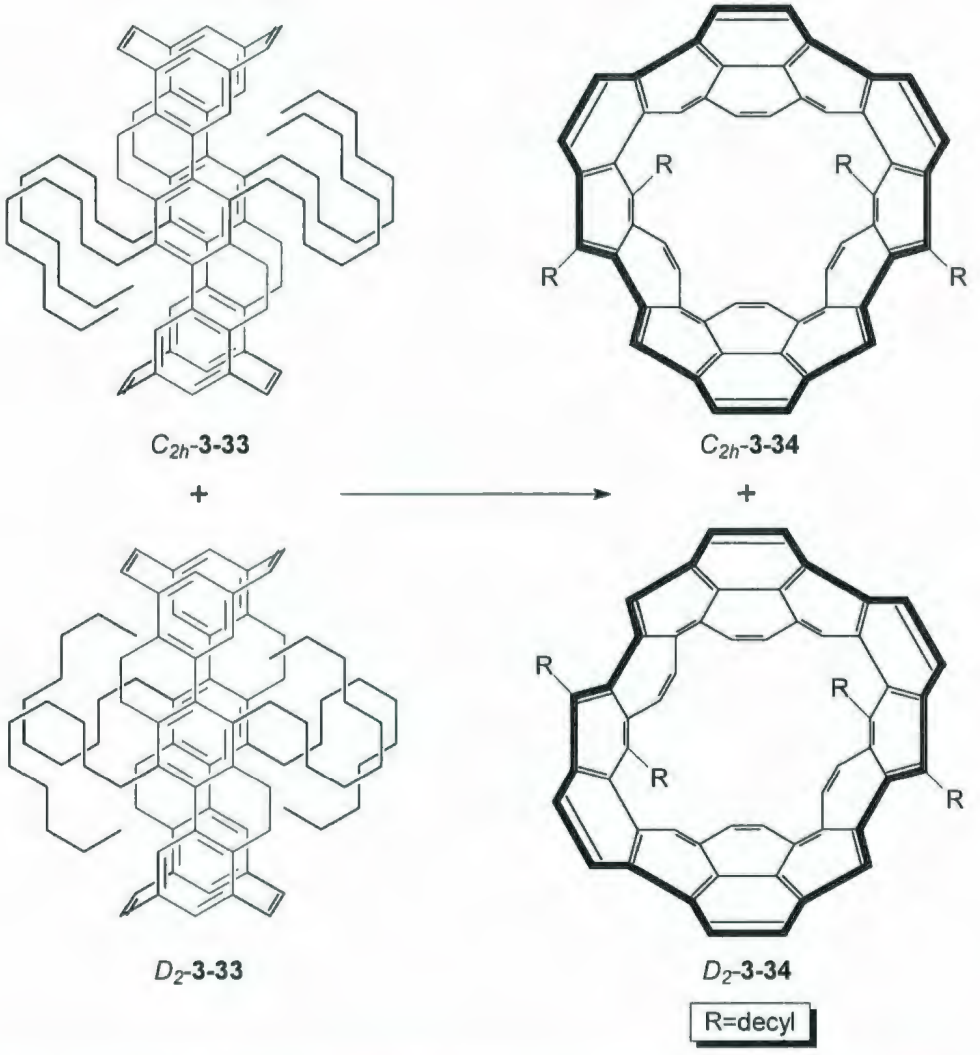


| Entry | Scale (mg, **3-34**) | Oxidant | Solvent | Temp | Time | MS Result |
|---|---|---|---|---|---|---|
| 1 | 10 | DDQ | benzene | rt | 0.5 h | 1209-1222 |
| 2 | 8 | DDQ | benzene | rt | 6 h | 1209-1222 |
| 3 | 8 | DDQ | benzene | reflux | 0.5 h | 1209-1222 |
| 4 | 12 | DDQ | benzene | reflux | 48 h | Unproductive consumption of **3-33** |
| 5 | 21 | DDQ | toluene | reflux | 48 h | Unproductive consumption of **3-33** |
| 6 | 1 | DDQ | *m*-xylene | 135 °C | 10 min | 1205 |
| 7 | 1 | DDQ | mesitylene | 160 °C | 1 min | 1205 |
| 8 | 9 | $Br_2$ | $CS_2$ | -20 °C | 0.5 h | Unproductive consumption of **3-33** |

The problems encountered during attempts to convert **3-33** to **3-34** may have their origin in either the VID reaction or the dehydrogenation of the partially saturated rings of the boards, which are the least aromatic rings of the dibenzo[*a*,*h*]anthracene (*cf.* the central ring of phenantharene).[12] To test the reactivity of the two positions, dehydrogenation of tetraester **3-25** by treatment with DDQ, in either benzene or toluene at both room temperature and at reflux, was attempted. In all cases, including reflux for 14 days, a mixture of unreacted starting material **3-25**, mono-reacted product, desired product **3-36** was obtained according to mass spectrometric analysis of the crude reaction mixtures. Isolation of each compound was not successful due to their similar mobility on silica gel. Although it is tempting to conclude that the dehydrogenation of the partially-saturated rings is responsible for the problematic conversion of **3-33** to **3-34**, it should be noted that the model system **3-25** bears electron-withdrawing groups, and it is known that electron-deficient arenes can be difficult to prepare by DDQ oxidation of a partially saturated precursor. In such cases, oxidants such as $Br_2/CS_2$ have proved to be more effective. Treatment of **3-25** with $Br_2$ in $CS_2$ was consequently tried. However, TLC analysis indicated that, after **3-25** was consumed, a complex mixture was formed.

Benzylic bromination of the side chain may have been a competing reaction. Whatever the case, it was evident that Stage 4 of this approach was difficult and that the next approach to aromatic belts **3-34** needed to involve "fully aromatic" boards such as **3-36**.

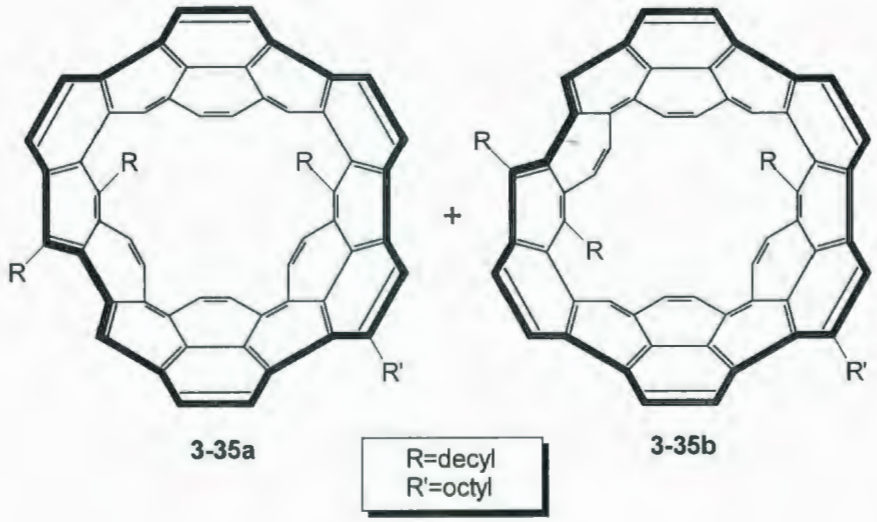


**Figure 3.04.** Belts **3-35**.

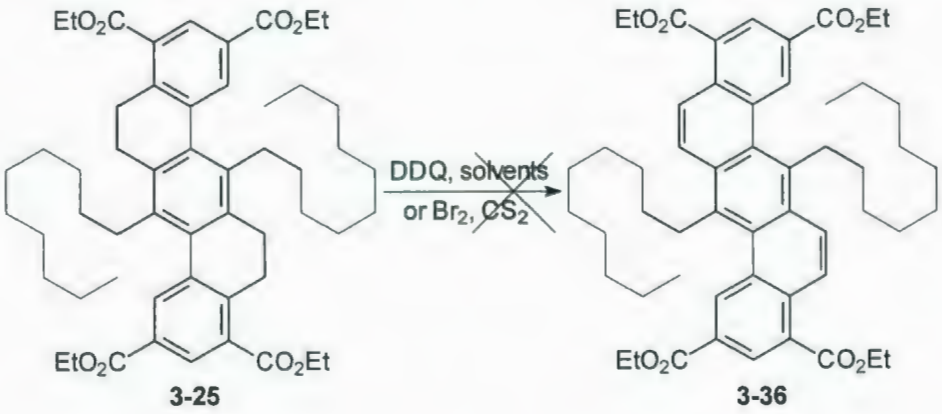


**Scheme 3.14.** Model study of the dehydrogenation reaction.

### 3.3 Experimental

**General.** All chemicals mentioned in this chapter were used as received from commercial sources unless otherwise indicated and were reagent grade. Merck silica gel 60 (particle size 40-63 μm, 230-400 mesh) was used for all column chromatography. The dimensions of the columns were recorded as diameter × height, and all solvent mixtures given for TLC retention factors were the same as those used for column chromatography unless specifically mentioned. TLC spots were visualized with a UV lamp (254 and 366 nm). Melting points were measured on a Fisher-Johns apparatus and are uncorrected. The recrystallization solvents were shown with the melting points. Mass spectrometric data were determined on an Agilent 1100 series LC/MSD instrument. $^{1}H$ NMR (500 MHz) and $^{13}C$ NMR (125.76 MHz) were recorded on a Bruker AVANCE instrument. IR spectra were obtained on a Bruker TENSOR 27 infrared spectrometer. HRMS (EI or CI) were measured on a GCT Premier instrument (Water Micromass technologies). THF was freshly distilled from sodium benzophenone ketyl. As a reaction solvent, $CH_2Cl_2$ was freshly distilled from $CaH_2$. Hexanes were distilled before use. Benzene was spectroscopic grade. Solvents were deoxygenated by bubbling $N_2$ through for 10 min.

**1,4-Dimethyl-2,5-bis((2,4-bis(ethoxycarbonyl)phenyl)ethynyl)benzene (3-05).**

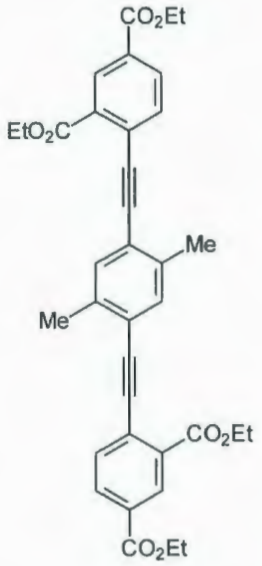


To a mixture of diethyl 4-bromoisophthalate (**2-39**) (1.80 g, 5.97 mmol), $Pd(PPh_3)_2Cl_2$ (0.042 g, 0.060 mmol) and CuI (0.045 g, 0.238 mmol) in benzene (25 mL) was added a mixture of 1,4-diethynyl-2,5-dimethylbenzene (**3-04**) (0.46 g, 3.0 mmol) and DBU (1.14 g, 7.46 mmol) in benzene (25 mL). The mixture was stirred at room temperature for 18 h. The resulting precipitate was removed by suction filtration and the filtrate was concentrated under reduced pressure. The residue was dissolved in $CH_2Cl_2$ (50 mL), washed with saturated aqueous $NH_4Cl$ solution (50 mL), washed with $H_2O$ (50 mL), washed with brine (50 mL), dried over $MgSO_4$ and concentrated under reduced pressure. The residue was recrystallized from EtOAc to afford **3-05** as a yellow solid (1.27 g, 2.14 mmol, 72%): $R_f$ ($CH_2Cl_2$) = 0.40; mp (EtOAc) 123.0–125.0 °C; IR (neat) 2925 (m), 1723 (s), 1610 (w), 1467 (m), 1284 (m), 1229 (s), 1135 (m), 1181 (m), 1030 (m) $cm^{-1}$; $^1H$ NMR (500 MHz, $CDCl_3$) δ 8.53 (d, *J*=1.7 Hz, 2H), 8.04 (dd, *J*=8.1, 1.6 Hz, 2H), 7.24 (d, *J*=8.0 Hz, 2H), 6.90 (s, 2H), 4.45 (q, *J*=7.1 Hz, 4H), 4.44 (q, *J*=7.2 Hz, 4H), 2.53 (s, 6H), 1.43 (t, *J*=7.1 Hz, 12H); $^{13}C$ NMR (125 MHz, $CDCl_3$) δ 165.44, 165.36, 137.9, 134.2, 133.2, 132.2, 132.1, 131.4, 129.7, 128.0, 123.3, 96.4, 93.0, 61.53, 61.50, 20.0, 14.3 (2C); LCMS (APCI, positive) *m/z* (%): 597 (10), 596 (40), 595 (100,

$M^+$); UV/Vis ($CHCl_3$) $\lambda_{max}$ (log $\varepsilon$) nm 363 (4.32); Anal. calcd for $C_{36}H_{34}O_8$: 594.2254, found: 594.2271.

**1,4- Dimethyl-2,5-bis(2-(2,4-bis(ethoxycarbonyl)phenyl)ethyl)benzene (3-06).**

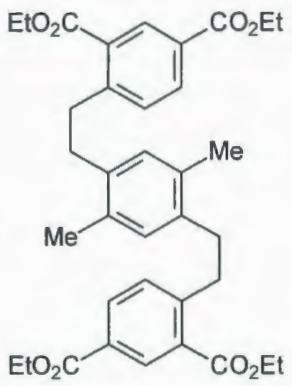


A mixture of 1,4-dimethyl-2,5-bis((2,4-bis(ethoxycarbonyl)phenyl)ethynyl)benzene (**3-05**) (10.60 g, 17.83 mmol), 10% Pd/C (3.74 g) in EtOH (400 mL) was stirred at room temperature under hydrogen for 24 h. The solvent was removed under reduced pressure, and the residue was taken up in $CH_2Cl_2$ (400 mL). Insoluble material was removed by suction filtration through a plug of $MgSO_4$. The filtrate was concentrated under reduced pressure to afford **3-06** as a white solid (9.81 g, 16.3 mmol, 91%). The product was of sufficient purity (>95% by $^1H$ NMR) for use in the next step. For characterization, a small sample of the product was recrystallized from EtOAc, which afforded **3-06** as a white solid: $R_f$ ($CH_2Cl_2$) = 0.4; mp (EtOAc) 122.0–124.0 °C; IR (neat) 2925 (m), 1723 (s), 1610 (w), 1467 (m), 1284 (m), 1229 (s), 1135 (m), 1181 (m), 1030 (m), $cm^{-1}$; $^1H$ NMR (500 MHz, $CDCl_3$) $\delta$ 8.53 (d, *J*=1.8 Hz, 2H), 8.05 (dd, *J*=8.0, 1.8 Hz, 2H), 7.27 (d, *J*=8.0 Hz, 2H), 6.93 (s, 2H), 4.40 (q, *J*=7.1 Hz, 4H), 4.39 (q, *J*=7.1 Hz, 4H), 3.27–3.22 (m, 4H), 2.86–2.82 (m, 4H), 2.23 (s, 6H), 1.42 (t, *J*=7.1 Hz, 6H), 1.41 (t, *J*=7.1 Hz, 6H); $^{13}C$ NMR (125 MHz, $CDCl_3$) $\delta$ 167.1, 166.1, 148.9, 137.5, 133.6, 132.6, 132.0, 131.5, 131.1, 130.6, 128.7, 61.40, 61.36, 35.6, 34.9, 18.9, 14.5 (2C); LCMS (APCI, positive) *m/z* (%): 603 (100, $M^+$), 604 (39); UV/Vis ($CHCl_3$)

$\lambda_{max}$ (log $\varepsilon$) nm 278 (3.31); Anal. calcd for $C_{36}H_{42}O_8$: C, 71.74; H, 7.02, found: C, 71.56; H, 7.01.

**1,4-Dibromo-2,5-bis(2-(2,4-bis(ethoxycarbonyl)phenyl)ethyl)-3,6-dimethylbenzene (3-07).**

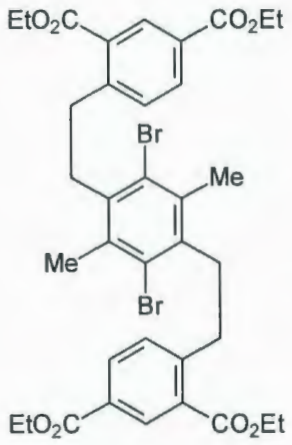


$Br_2$ (5.72 g, 35.8 mmol) was added to a mixture of $AlCl_3$ (13.02 g, 97.66 mmol) and 1,4-dimethyl-2,5-bis(2-(2,4-bis(ethoxycarbonyl)phenyl)ethyl)benzene (**3-06**) (9.81 g, 16.3 mmol) and $CH_2Cl_2$ (300 mL). The mixture was stirred at room temperature for 1 h and then quenched with saturated aqueous $NaHSO_3$ solution (100 mL). The organic layer was washed with $H_2O$ (300 mL), washed with brine (100 mL), dried over $MgSO_4$ and concentrated under reduced pressure. The residue was recrystallized from EtOAc to afford **3-07** as a white solid (9.90 g, 13.0 mmol, 80%): $R_f$ ($CH_2Cl_2$) = 0.5; mp (EtOAc) 199.0–201.0 °C; IR (neat) 2922 (m), 1720 (s), 1609 (w), 1468 (m), 1301 (m), 1285 (m), 1173 (s), 1132 (m), 1073 (m) $cm^{-1}$; $^1H$ NMR (500 MHz, $CDCl_3$) $\delta$ 8.51 (d, *J*=1.8 Hz, 2H), 8.08 (dd, *J*=8.0, 1.8 Hz, 2H), 7.44 (d, *J*=8.0 Hz, 2H), 4.41 (q, *J*=7.1 Hz, 4H), 4.40 (q, *J*=7.1 Hz, 4H), 3.27–3.22 (m, 8H), 2.52 (s, 6H), 1.42 (t, *J*=7.1 Hz, 6H), 1.41 (t, *J*=7.1 Hz, 6H); $^{13}C$ NMR (125 MHz, $CDCl_3$) $\delta$ 167.1, 166.1, 148.2, 138.8, 136.1, 132.7, 131.8, 131.5, 130.6, 129.1, 128.8, 61.5, 61.4, 37.4, 33.2, 21.9, 14.58, 14.56; LCMS (APCI, positive) *m/z* (%): 765 (5), 764 (17), 763 (26), 762 (22), 761

(48, $M^+$ ($^{81}Br$)($^{79}Br$)), 760 (11), 759 (26); Anal. calcd for $C_{36}H_{40}O_8Br_2$: C, 56.85, H, 5.30; found, C, 56.70, H, 5.26; UV/Vis ($CHCl_3$) $\lambda_{max}$ (log $\varepsilon$) nm 285 (3.42).

**7,14-Dimethyl-5,6,12,13-tetrahydrodibenzo[*a,h*]anthracene-2,4,9,11 tetracarboxylic acid tetraethyl ester (3-08).**

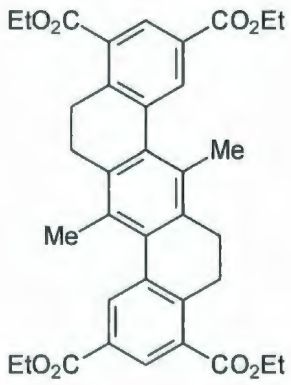


A mixture of 1,4-dibromo-2,5-bis(2-(2,4-bis(ethoxycarbonyl)phenyl)ethyl)-3,6-dimethylbenzene (**3-07**) (1.14 g, 1.50 mmol), $Pd(PPh_3)_2Cl_2$ (0.11 g, 0.15 mmol), $K_2CO_3$ (1.24 g, 9.00 mmol) and DMA (20 mL) in a 100 mL round-bottomed flask was stirred at room temperature for 5 min and then plunged into an oil bath preheated to 180 °C. Stirring was continued at this temperature for 40 min and then the heat resource was removed. The reaction mixture was cooled for 5 min and then put in a –20 °C freezer for 2 h. The resulting precipitate was collected by suction filtration. The filter cake was washed with 50% DMA in $H_2O$ and then taken up in $CH_2Cl_2$ (50 mL). The resulting solution was dried over $MgSO_4$ and concentrated under reduced pressure to afford **3-08** as an off-white solid (0.73 g, 1.22 mmol, 81%). For characterization, a small sample was recrystallized from EtOAc to afford **3-08** as a white solid: $R_f$ ($CH_2Cl_2$) = 0.4; mp (EtOAc) 232.0–233.0 °C; IR (neat) 2920 (s), 1718 (s), 1602 (w), 1467 (m), 1318 (m), 1221 (s) $cm^{-1}$; $^1H$ NMR (500 MHz, $CDCl_3$) $\delta$ 8.44 (d, *J*=1.7 Hz, 2H), 8.33 (d, *J*=1.7 Hz, 2H), 4.47–4.40 (m, 8H), 3.25–3.20 (m, 4H), 2.79–2.76 (m, 4H), 2.53 (s, 6H), 1.47–1.40 (m,

12H); $^{13}C$ NMR (125 MHz, $CDCl_3$) δ 167.5, 166.3, 146.6, 138.2, 137.0, 134.0, 133.3, 130.0, 129.6, 129.0, 127.6, 61.5, 61.4, 27.0, 26.5, 19.3, 14.6; LCMS (APCI, positive) *m/z* (%): 601 (8), 600 (37), 599 (100, $M^+$), 598 (68); UV/Vis ($CHCl_3$) $\lambda_{max}$ (log ε) nm 306 (4.18); Anal. calcd for $C_{36}H_{38}O_8$: C, 72.22, H, 6.40, found: C, 72.11, H, 6.44.

**7,14-Dimethyl-2,4,9,11-tetrakis(bromomethyl)-5,6,12,13-tetrahydrodibenz[*a,h*]anthracene (3-11).**

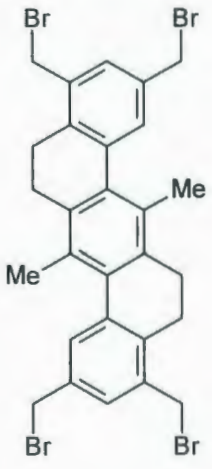


To a solution of 7,14-dimethyl-5,6,12,13-tetrahydrodibenz[*a,h*]anthracene-2,4,9,11 tetracarboxylic acid tetraethyl ester (**3-08**) (0.78 g, 1.3 mmol) in $CH_2Cl_2$ (20 mL) was added a solution of DIBAL-H in $CH_2Cl_2$ (1.0 M, 20.8 mL) at 0 °C. The reaction was allowed to warm to room temperature and stir for 18 h and then quenched by adding water (20 mL) followed by aqueous HCl solution (1.0 M, 10 mL) dropwise at 0 °C. The precipitate was collected by suction filtration, which afforded crude **3-10** as a white solid. A mixture of crude **3-10** (0.62 g, 1.3 mmol) in 48% aqueous HBr solution (60 mL) was refluxed for 2.5 h. The resulting solid was collected by suction filtration to afford **3-11** as a tan solid (0.75 g, 1.1 mmol, 80%): mp 270 °C (dec.); $^1H$ NMR (500 MHz, DMSO-$d_6$) 7.58 (s, 2H), 7.48 (s, 2H), 4.86 (s, 4H), 4.76 (s, 4H), 2.78–2.70 (m, 8H), 2.50 (s, 6H), 2.49 (s, 6H). Due to insufficient solubility in DMSO, $^{13}C$ NMR analysis was not possible. LCMS (APCI, positive) *m/z* (%): 687 (8), 686 (17), 685 (22), 684 (56), 683 (42), 682 (85), 681

(44), 680 (68), 679 (25), 678 (29), 677 (7), 676 (6), 622 (13), 621 (33), 620 (32), 619 (99), 618 (42), 617 (100), 616 (23), 615 (38). Due to the low solubility in $CHCl_3$, UV/Vis analysis was unavailable for this compound.

**7,14-Dimethyl-2,4,9,11-tetrakis(thiomethyl)-5,6,12,13-tetrahydrodibenz[*a,h*]anthracene (3-12).**

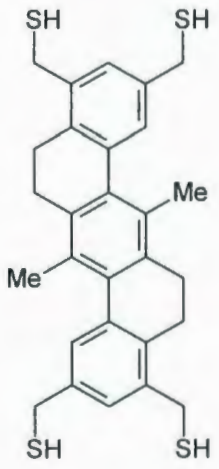


A mixture of 7,14-dimethyl-2,4,9,11-tetrakis(bromomethyl)-5,6,12,13-tetrahydrodibenz[*a,h*]anthracene (**3-11**) (0.075 g, 0.11 mmol) and thiourea (0.034 g, 0.45 mmol) in EtOH (15 mL) was heated at reflux for 2 h. A solution of KOH (0.062 g, 1.10 mmol) in $H_2O$ (5 mL) was then added. The reaction was refluxed for a further 1.5 h and quenched with 9.0 M $H_2SO_4$. The resulting solid was collected by suction filtration to afford **3-12** as a tan solid (0.052 g, 0.10 mmol, 96 %): mp. 280 °C (dec.); $^1$H NMR (500 MHz, $CDCl_3$) 7.39 (s, 2H), 7.20 (s, 2H), 3.84 (d, *J*=7.1 Hz, 4H), 3.76 (d, *J*=7.1 Hz, 4H), 2.84 (t, *J*=8.0 Hz, 2H), 2.78 (t, *J*=8.0 Hz, 2H), 2.75-2.72 (m, 4H), 2.72-2.69 (m, 4H), 2.47 (s, 6H). Due to insufficient solubility in DMSO, the result of $^{13}$C NMR analysis was not obtained; LCMS (APCI, positive) *m/z* (%): 497 (8), 496 (11), 495 (22, $M^+$), 494 (8), 493 (8), 492 (8), 491 (7), 480 (9), 479 (15), 478 (32), 477 (7), 476 (8), 476 (6), 475 (6), 464 (8), 463 (21), 462 (39), 461 (100), 460 (19), 459 (26), 458 (5), 457 (5); Due to the low solubility in $CHCl_3$, UV/Vis analysis was unavailable for this compound.

**1,4-Bis(2-(2,4-bis(ethoxycarbonyl)phenyl)ethyl)-2,5-bis(octylethynyl)benzene (3-20).**

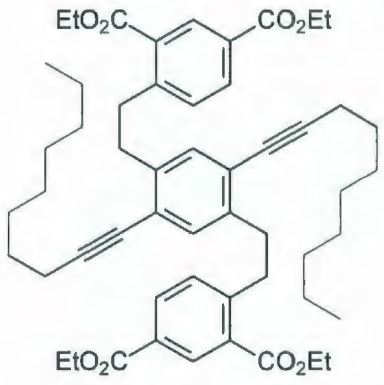


To a mixture of 1,4-dibromo-2,5-bis(2-(2,4-bis(ethoxycarbonyl)phenyl)ethyl)benzene (**2-37**) (35.35 g, 48.26 mmol), $Pd(PPh_3)_2Cl_2$ (1.69 g, 2.41 mmol), CuI (0.92 g, 4.82 mmol) in benzene (400 mL) was added 1-decyne (16.68 g, 120.6 mmol) and DBU (22.04 g, 144.8 mmol) with stirring under $N_2$ protection. The reaction was stirred at reflux under $N_2$ for 6 h. $Pd(PPh_3)_2Cl_2$ (0.34 g, 0.48 mmol), CuI (0.18 g, 0.92 mmol), 1-decyne (1.18 g, 24.4 mmol), and DBU (4.40 g, 28.9 mmol) were then added to the reacting system. The mixture was stirred at reflux for a further 24 h. Insoluble material (an off-white solid) was removed by suction filtration. The filtrate was concentrated under reduced pressure. The residue was dissolved in $CH_2Cl_2$ (400 mL) and the organic layers were washed with saturated aqueous $NH_4Cl$ solution (300 mL), washed with $H_2O$ (300 mL), washed with brine (100 mL), dried over $MgSO_4$ and concentrated under reduced pressure. The crude product was subjected to column chromatography to give **3-20** as an off-white solid (24.17 g, 59%). Mixed fractions containing the product were concentrated under reduced pressure and the residue was subjected to recrystallization from EtOH (75 mL) to give **3-20** as an off-white solid (6.66 g, 16%, combined yield = 75%). Both batches of the product were of sufficient purity (>95% by $^1H$ NMR) for use in the next step. For characterization, a small sample of the product was recrystallized from EtOH (1–

3 times), which afforded **3-20** as a white solid: $R_f$ ($CH_2Cl_2$) = 0.60; mp (EtOH) = 67.5–69.5 °C; IR (neat) 2926 (s), 1721 (s), 1609 (m), 1453 (m), 1284 (m), 1172 (s) $cm^{-1}$; $^1H$ NMR (500 MHz, $CDCl_3$) δ 8.54 (d, *J*=1.9 Hz, 2H), 8.04 (dd, *J*=8.0, 1.9 Hz, 2H), 7.26 (d, *J*=8.0 Hz, 2H), 7.21 (s, 2H), 4.41 (q, *J*=7.0 Hz, 4H), 4.39 (q, *J*=7.1 Hz, 4H), 3.32-3.29 (m, 4H), 3.03–3.00 (m, 4H), 2.43 (t, *J*=7.1 Hz, 4H), 1.59 (quint, *J*=7.4 Hz, 4H), 1.46–1.39 (m, 16H), 1.31–1.25 (m, 16H), 0.87 (t, *J*=6.0 Hz, 6H); $^{13}C$ NMR (125 MHz, $CDCl_3$) δ 167.10, 166.11, 148.7, 140.8, 132.7, 132.5, 132.1, 131.5, 130.5, 128.6, 123.0, 95.3, 79.3, 61.39, 61.33, 35.7, 35.5, 32.1, 29.40, 29.37, 29.27, 29.1, 22.8, 19.9, 14.6 (2C), 14.3; LCMS (APCI, positive) *m/z* (%): 866 (23), 865 (65), 864 (100), 849 (9), 848 (29), 847 (48, $M^+$), 844 (7), 843 (12); UV/Vis ($CHCl_3$) $\lambda_{max}$ (log ε) nm 277 (4.23), 309 (3.34); Anal. calcd for $C_{54}H_{70}O_8$: C, 76.56, H; 8.33, found: C, 76.05; H, 8.39.

**1,4-Didecyl-2,5-bis(2-(2,4-bis(ethoxycarbonyl)phenyl)ethyl)benzene (3-22).**

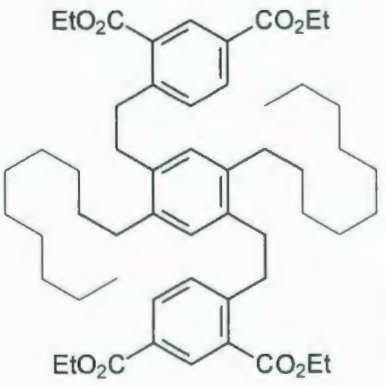


A mixture of Pd/C (6.12 g) and 1,4-bis(2-(2,4-bis(ethoxycarbonyl)phenyl)ethyl)-2,5-bis(octylethynyl)benzene (**3-20**) (22.07 g, 26.05 mmol) and EtOH (400 mL) was stirred at room temperature under hydrogen for 7 d. The solvent was removed under reduced pressure and the residue was taken up in $CH_2Cl_2$ (400 mL). Insoluble material was removed by suction filtration through a plug of $MgSO_4$. The filtrate was concentrated under reduced pressure to afford **3-22** as an off-white solid (20.55

g, 24.03 mmol, 92%). The product was of sufficient purity (>95% by $^1$H NMR) for the use in the next step. For characterization, a small sample of the product was recrystallized from EtOH, which afforded **3-22** as a white solid: $R_f$ ($CH_2Cl_2$) = 0.6; mp (EtOH) 71.0–73.0 °C, IR (neat) 2925 (m), 1723 (s), 1610 (w), 1467 (m), 1284 (m), 1229 (s), 1135 (m), 1181 (m), 1030 (m) cm$^{-1}$; $^1$H NMR (500 MHz, $CDCl_3$) δ 8.53 (d, *J*=1.9 Hz, 2H), 8.04 (dd, *J*=8.0, 1.9 Hz, 2H), 7.24 (d, *J*=8.0 Hz, 2H), 6.90 (s, 2H), 4.41 (q, *J*=7.1 Hz, 4H), 4.40 (q, *J*=7.1 Hz, 4H), 3.28-3.25 (m, 4H), 2.89–2.86 (m, 4H), 2.54–2.51 (m, 4H), 1.52–1.46 (m, 4H), 1.49–1.43 (m, 12H), 1.35–1.26 (m, 28H), 0.87 (t, *J*=7.0 Hz, 6H); $^{13}$C NMR (125 MHz, $CDCl_3$) δ 167.1, 166.1, 148.9, 138.3, 136.8, 132.5, 132.0, 131.6, 130.5, 130.3, 128.6, 61.38, 61.34, 36.5, 34.3, 32.5, 32.1, 31.8, 30.0, 29.9, 29.8, 29.7, 29.6, 22.9, 14.56, 14.54, 14.3; LCMS (APCI, positive) *m/z* (%): 857 (3), 856 (10), 855 (16, $M^+$), 839 (12), 838 (36), 837 (59), 825 (18), 824 (57), 823 (100), 810 (16), 809 (30), 795 (17); $\lambda_{max}$ (log ε) nm 281 (3.89); Anal. calcd for $C_{54}H_{78}O_8$: C, 75.84, H, 9.19, found: C, 75.98, H, 9.22.

**1,4-Dibromo-2,5-didecyl-3,6-bis(2-(2,4-bis(ethoxycarbonyl)phenyl)ethyl)benzene (3-24).**

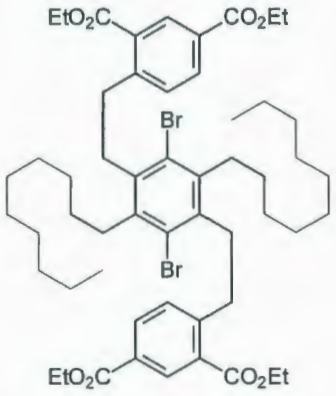


$Br_2$ (38.39 g, 240.3 mmol) was added to a mixture of 1,4-didecyl-2,5-bis(2-(2,4-bis(ethoxycarbonyl)phenyl)ethyl)benzene (**3-22**) (20.55 g, 24.03 mmol) and $H_2O$ (500 mL) in one portion at room temperature. The mixture was mechanically stirred at room temperature for 24 h. The reaction was quenched with saturated aqueous $NaHSO_3$ solution (100 mL) and then $CH_2Cl_2$ (300 mL) was added. The aqueous layer was extracted with $CH_2Cl_2$ (100 mL). The combined organic layers were washed with $H_2O$ (400 mL), washed with brine (100 mL), dried over $MgSO_4$ and concentrated under reduced pressure. The residue was recrystallized from EtOH (200 mL) to afford **3-24** as a white solid (21.06 g, 20.91 mmol, 87%); $R_f$ ($CH_2Cl_2$) = 0.40; mp (ethanol) 125.0–127.0 °C; IR (neat) 2922 (m), 1720 (s), 1609 (w), 1468 (m), 1301 (m), 1285 (m), 1173 (s), 1132 (m), 1073 (m) $cm^{-1}$; $^1H$ NMR (500 MHz, $CDCl_3$) δ 8.54 (d, *J*=1.9 Hz, 2H), 8.10 (dd, *J*=8.0, 1.9 Hz, 2H), 7.49 (d, *J*=8.1 Hz, 2H), 4.41 (q, *J*=7.1 Hz, 4H), 4.40 (q, *J*=7.1 Hz, 4H), 3.29–3.26 (m, 4H), 3.20–3.17 (m, 4H), 2.97–2.94 (m, 4H), 1.49–1.41 (m, 16H), 1.35–1.26 (m, 28H), 0.88 (t, *J*=7.1 Hz, 6H); $^{13}C$ NMR (125 MHz, $CDCl_3$) δ 166.9, 166.0, 148.5, 140.9, 138.9, 132.7, 131.9, 131.5, 130.4, 128.9, 128.8, 61.42, 61.39, 36.8, 35.0, 33.9, 32.1, 30.1, 30.0, 29.9, 29.8, 29.7, 29.6, 22.9, 14.6 (2C), 14.3; LCMS (APCI, positive) *m/z* (%): 1017 (8), 1016 (23), 1015 (45), 1014 (42), 1013 (77, $M^+$ ($^{81}Br$)($^{79}Br$)), 1012 (23), 1011 (35), 1002

(12), 1001 (22), 1000 (22), 999 (35), 998 (10), 997 (17), 989 (7), 988 (17), 987 (31), 986 (28), 985 (53), 984 (14), 983 (23), 975 (8), 974 (23), 973 (37), 972 (31), 971 (54), 970 (14), 969 (26), 961 (7), 960 (30), 959 (64), 958 (56), 957 (100), 956 (23), 955 (43); UV/Vis ($CHCl_3$) $\lambda_{max}$ (log $\varepsilon$) nm 284 (3.90); Anal. calcd for $C_{54}H_{76}O_8Br_2$: C, 64.03, H, 7.56, found: C, 64.05; H, 7.56.

**7,14-Didecyl-5,6,12,13-tetrahydrodibenz[*a,h*]anthracene-2,4,9,11-tetracarboxylic acid tetraethyl ester (3-25).**

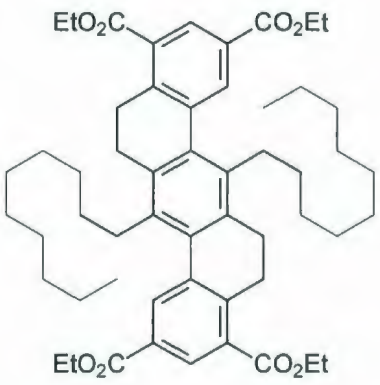


A mixture of $Pd(PPh_3)_2Cl_2$ (0.216 g, 0.308 mmol), 1,4-dibromo-2,5-didecyl-3,6-bis(2-(2,4-bis(ethoxycarbonyl)phenyl)ethyl)benzene (**3-24**) (3.12 g, 3.08 mmol), $K_2CO_3$ (2.55 g, 18.5 mmol) and DMA (60 mL) in a 250 mL round-bottomed flask was stirred at room temperature for 5 min and then plunged into an oil bath preheated to 180 °C. Stirring was continued at this temperature for 40 min. The flask was removed from the oil bath and allowed to stand for 5 min before being placed in a –20 °C freezer for at least 2 h. Insoluble material was then removed by suction filtration and the filter cake was rinsed with EtOAc (3 × 10 mL). The filtrate was diluted with ethyl acetate (50 mL) and $H_2O$ (100 mL) and the layers were separated. The aqueous layer was extracted with EtOAc (3 × 50 mL). The combined organic layers were washed with $H_2O$ (3 × 100 mL), washed with brine (50 mL), dried over $MgSO_4$ and concentrated under reduced pressure.

The residue was subjected to column chromatography (4 × 10 cm, $CH_2Cl_2$), which afforded an oily yellow solid (2.43 g). Recrystallization from ethanol afforded **3-25** as a white solid (1.82 g, 2.14 mmol, 70%): $R_f$ ($CH_2Cl_2$) = 0.3; mp (ethanol) 128.0–129.0 °C; IR (neat) 2920 (s), 1718 (s), 1602 (w), 1467 (m), 1318 (m), 1221 (s) $cm^{-1}$; $^1H$ NMR (500 MHz, $CDCl_3$) δ 8.48 (d, *J*=1.6 Hz, 2H), 8.26 (d, *J*=1.6 Hz, 2H), 4.43 (q, *J*=7.1 Hz, 4H), 4.41 (q, *J*=7.1 Hz, 4H), 2.81–2.78 (m, 6H), 1.72–1.68 (m, 4H), 1.45 (t, *J*=7.2 Hz, 6H), 1.39 (t, *J*=7.1 Hz, 6H), 1.33–1.26 (m, 28H), 0.87 (t, *J*=7.0 Hz, 6H); $^{13}C$ NMR (125 MHz, $CDCl_3$) δ 167.5, 166.2, 146.9, 138.0, 137.6, 134.6, 134.0, 132.8, 129.8, 129.8, 127.7, 61.5, 61.3, 32.1, 31.5, 31.0, 30.1, 30.0, 29.9, 29.6, 29.5, 27.2, 26.4, 22.9, 14.6 (2C), 14.3; LCMS (APCI, positive) *m/z* (%): 853 (21) 852 (60), 851 (100, $M^+$), 824 (35), 823 (62), 822 (21); UV/Vis ($CHCl_3$) $\lambda_{max}$ (log ε) nm 304 (4.06); HRMS ($EI^+$): calcd for $C_{54}H_{74}O_8$ 850.5384, found 850.5392.

**7,14-Didecyl-2,4,9,11-tetrakis(bromomethyl)-5,6,12,13-tetrahydrodibenz[*a,h*]anthracene (3-27).**

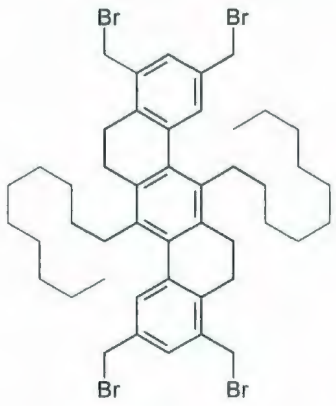


To a solution of 7,14-didecyl-5,6,12,13-tetrahydrodibenz[*a,h*]anthracene-2,4,9,11-tetracarboxylic acid tetraethyl ester (**3-25**) (13 mg, 0.015 mmol) in distilled $CH_2Cl_2$ (3 mL) was added a solution of DIBAL-H in $CH_2Cl_2$ (1.0 M, 0.24 mL) at 0 °C. The reaction was allowed to warm to room temperature and stir for 18 h. The reaction was quenched by adding $H_2O$ (3 mL)

followed by aqueous HCl solution (1.0 M, 5 mL) dropwise at 0 °C. The precipitate was collected by suction filtration to afford **3-26** as a white solid. The crude material was of sufficient purity for the use in the next step. To a mixture of crude 7,14-didecyl-2,4,9,11-tetrakis(hydroxymethyl)-5,6,12,13-tetrahydrodibenz[*a,h*]anthracene **3-26** (150 mg, 0.22 mmol) in $CH_2Cl_2$ (25 mL) was added $PBr_3$ (89 mg, 0.33 mmol) in one portion at room temperature. The reaction was stirred at room temperature for 24 h and then quenched with $H_2O$ (15 mL). The organic layer was then dried over $MgSO_4$ and concentrated under reduced pressure. The residue was subjected to column chromatography (1.5 × 5 cm, 50% hexanes in $CH_2Cl_2$), which afforded **3-27** as a white solid (200 mg, 18 mmol, 80%). For characterization, a small sample of **3-27** was recrystallized from heptane, which afforded **3-27** as a white solid: $R_f$ (50% hexanes in $CH_2Cl_2$) = 0.7, mp (heptane) 168.0–170.5 °C; IR (neat) 2919 (m), 1607 (w), 1471 (m), 1424 (w), 1209 (m) $cm^{-1}$; $^1H$ NMR (500 MHz, $CDCl_3$) 7.45 (d, *J*=1.0 Hz, 2H), 7.31 (d, *J*=1.0 Hz, 2H), 4.62 (s, 4H), 4.50 (s, 4H), 2.85–2.81 (m, 12H), 1.69 (m, 4H), 1.45–1.41 (m, 4H), 1.30–1.22 (m, 24H), 0.88 (t, *J*=6.9 Hz, 6H); $^{13}C$ NMR (125MHz, $CDCl_3$) δ 140.1, 137.8, 137.6, 135.1, 135.0, 134.3, 134.1, 130.2, 128.8, 33.6, 32.1, 32.0, 31.6, 31.1, 30.2, 29.96, 29.93, 29.85, 29.71, 29.58, 26.3, 25.4, 22.9, 14.3; LCMS (APCI, positive) *m/z* (%): 940.05 (10), 939.15 (20), 938.10 (31.4), 937.05 (74), 936.15 (56), 935.10 (100, $M^+$ $(^{81}Br)_2(^{79}Br)_2$), 934 (43), 933 (77), 932 (19), 931 (19); UV/Vis ($CHCl_3$) $\lambda_{max}$ (log ε) nm 303 (3.95); Anal. calcd for $C_{46}H_{62}Br_4$: C, 59.12, H, 6.69, found: C, 59.33, H, 6.71.

**7,14-Didecyl-2,4,9,11-tetrakis(thiomethyl)-5,6,12,13-tetrahydrodibenz[*a,h*]anthracene (3-28).**

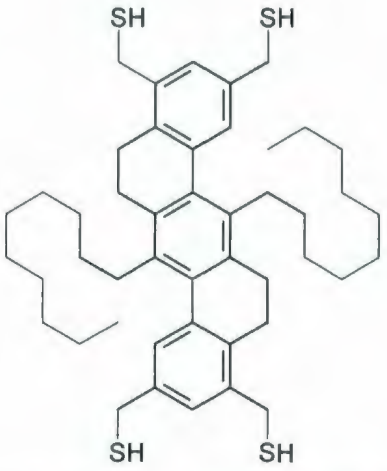


A mixture of 7,14-dimethyl-2,4,9,11-tetrakis(bromomethyl)-5,6,12,13-tetrahydrodibenz[*a,h*]anthracene (**3-27**) (0.200 g, 0.214 mmol) and thiourea (0.067 g, 0.877 mmol) and EtOH (20 mL) was heated at reflux for 3.5 h, and then a deoxygenated solution of KOH (0.120 g, 2.14 mmol) in $H_2O$ (7 mL) was added. The mixture was heated at reflux for 1.5 h, cooled to room temperature and placed into a –20 °C freezer (2 h). The mixture was quenched by 9.0 M $H_2SO_4$ (4 mL). The precipitate was collected by suction filtration and subjected to column chromatography (2 × 7 cm, 50% $CH_2Cl_2$ in hexane) to afford **3-28** as a yellow gel (0.042 g, 0.056 mmol, 26 %): IR (neat) 2919 (m), 1607 (w), 1471 (m), 1424 (w), 1209 (m) $cm^{-1}$; $^1H$ NMR (500 MHz, $CDCl_3$) 7.34 (s, 2H), 7.17 (s, 2H), 3.85 (d, *J*=7.1 Hz, 4H), 3.75 (d, *J*=7.1 Hz, 4H), 2.86–2.80 (m, 12H), 1.79–1.71 (m, 8H), 1.44–1.40 (m, 4H), 1.37–1.23 (m, 24H), 0.88 (t, *J*=7.1 Hz, 6H); $^{13}C$ NMR (125MHz, DMSO-d6) δ 138.2, 137.7, 137.4, 137.2, 137.1, 135.3, 133.9, 127.87, 127.82, 126.9 (2C), 32.1, 31.7, 30.2, 30.0, 29.8, 29.2, 27.2, 26.7, 25.3, 22.9, 14.38, 14.30; LCMS (APCI, positive) *m/z* (%): 750 (12) 749 (32), 748 (56), 747 (100, $M^+$), 746 (35), 716 (14), 715 (30), 714 (34), 713 (64), 683 (13), 682 (27), 681 (60), 680 (35), 679 (66); HRMS ($EI^+$): calcd for $C_{46}H_{66}S_4$ 746.4047, found 746.4039.

**7,8,14,15,22,23,29,30-Octahydro-6,13,24,31-tetradecyl-2,19,36,39-tetrathia[2$_4$](2,4,9,11)dibenzo[*a,h*]anthracenophane (*C$_{2h}$*-3-29) and 7,8,14,15,24,25,31,32-octahydro-6,13,23,30-tetradecyl-2,19,36,39-tetrathia[2$_4$](2,4,9,11)(4,2,11,9)dibenzo[*a,h*]anthracenophane (*D$_2$*-3-29).**

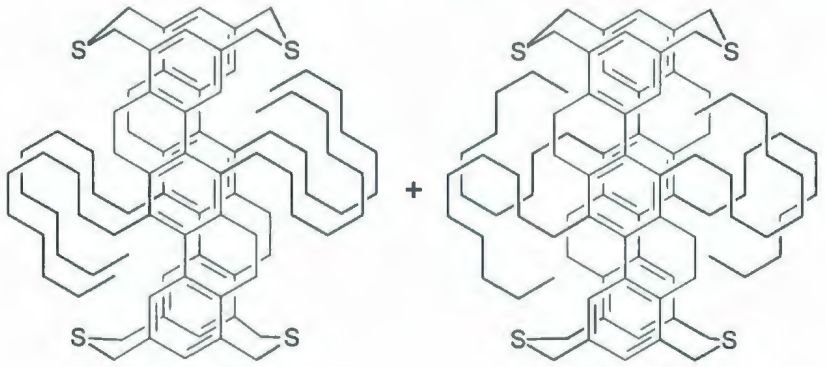


*C$_{2h}$*-**3-29** *D$_2$*-**3-29**

To a solution of the 7,14-didecyl-2,4,9,11-tetrakis(bromomethyl)-5,6,12,13-tetrahydrodibenz[*a,h*]anthracene (**3-27**) (2.30 g, 2.46 mmol) in 10% EtOH/$CH_2Cl_2$ (75 mL) was added $Na_2S/Al_2O_3$ (14.76 g, 39.40 mmol) at room temperature in 4 roughly equal portions over 4 d. Insoluble material was removed by suction filtration and the filtrate was concentrated under reduced pressure. The residue was subjected to column chromatography (4 × 25 cm, 10% EtOAc in hexanes), which afforded **3-29** as a white solid (0.50 g, 0.75 mmol, 30%): $R_f$ (10% EtOAc in hexanes) = 0.5; LCMS (APCI, positive) *m/z* (%): 1362 (18) 1361 (58), 1360 (65), 1359 (99), 1358 (71), 1357 (100, $M^+$), 1356 (8), 1355 (19).

**6,7,13,14,20,21,27,28-Octahydro-5,12,22,29-tetradecyl-1,17/18,33/34,35/36-tetrakis(methylthio)[2$_4$](2,4,9,11)dibenzo[*a,h*]anthracenophane (*pseudo*-$C_{2h}$-3-31) and 6,7,13,14,22,23,29,30-octahydro-5,12,21,28-tetradecyl-1/2,17/18,33/34,35/36-tetrakis(methylthio)[2$_4$](2,4,9,11)(4,2,11,9)dibenzo[*a,h*]anthracenophane (*pseudo*-$D_2$-3-31).**

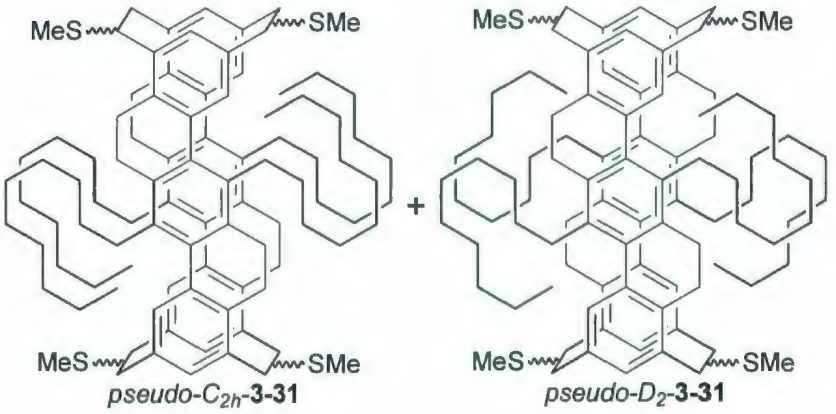

*pseudo*-$C_{2h}$-**3-31** *pseudo*-$D_2$-**3-31**

To a solution of a mixture of 7,8,14,15,22,23,29,30-octahydro-6,13,24,31-tetradecyl-2,19,36,39-tetrathia[3$_4$](2,4,9,11)dibenzo[*a,h*]anthracenophane ($C_{2h}$-**3-29**) and 7,8,14,15,24,25,31,32-octahydro-6,13,23,30-tetradecyl-2,19,36,39-tetrathia[3$_4$](2,4,9,11)(4,2,11,9)dibenzo[*a,h*]anthracenophane ($D_2$-**3-29**) (0.36 g, 0.27 mmol) in $CH_2Cl_2$ (20 mL) was added $(MeO)_2CHBF_4$ (0.43 g, 2.65 mmol) by syringe at room temperature. The mixture was stirred for 3 h at room temperature and then concentrated under reduced pressure. EtOAc (20 mL) was added to the residue and the mixture was stirred at room temperature for 20 min. The precipitate was collected by suction filtration, dried on high vacuum for 6 h and then mixed with THF (10 mL) and *t*-BuOK (2.97 g, 26.5 mmol). The mixture was

stirred at room temperature overnight and then concentrated under reduced pressure. The residue was taken up in $CH_2Cl_2$ (50 mL), washed with $H_2O$ (50 mL × 2), washed with brine (50 mL) and concentrated under reduced pressure. The residue was subjected to column chromatography (2 × 10 cm, 10% EtOAc in hexanes), which afforded **3-31** as an waxy yellow solid (0.11 g, 0.076 mmol, 28%): $R_f$ (10% EtOAc in hexanes) = 0.5; LCMS (APCI, positive) *m/z* (%): 1417 (33) 1416 (40), 1415 (30), 1414 (30), 1413 (13, $M^+$), 1371 (18), 1370 (42), 1369 (66), 1368 (100), 1367 (70), 1366 (62), 1322 (30), 1321 (36), 1320 (39), 1319 (27), 1318 (21).

**6,7,13,14,20,21,27,28-Octahydro-5,12,22,29-tetradecyl-(1*Z*,17*Z*,33*Z*,35*Z*)-[2$_4$](2,4,9,11)dibenzo[*a,h*]anthracenophane-1,17,33,35-tetraene ($C_{2h}$-3-33), and 6,7,13,14,22,23,29,30-octahydro-5,12,21,28-tetradecyl-(1*Z*,17*Z*,33*Z*,35*Z*)-[2$_4$](2,4,9,11)(4,2,11,9)dibenzo[*a,h*]anthracenophane-1,17,33,35-tetraene ($D_2$-3-33).**

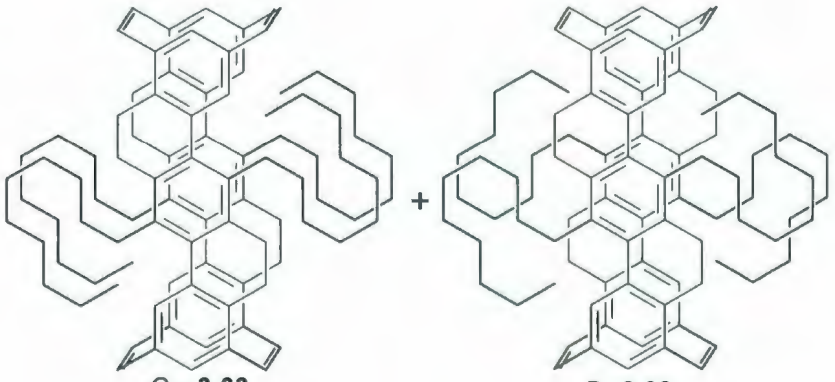

$C_{2h}$-3-33 + $D_2$-3-33

To a solution of 6,7,13,14,20,21,27,28-octahydro-5,12,22,29-tetradecyl-1,17/18,33/34,35/36-tetrakis(methylthio)[$2_4$](2,4,9,11)dibenzo[*a,h*]anthracenophane ($C_{2h}$-**3-31**) and 6,7,13,14,22,23,29,30-octahydro-5,12,21,28-tetradecyl-1/2,17/18,33/34,35/36-tetrakis(methylthio)[$2_4$](2,4,9,11)(4,2,11,9)dibenzo[*a,h*]anthracenophane ($D_2$-**3-31**) (0.11 g, 0.075 mmol) in $CH_2Cl_2$ (20 mL) was added $(MeO)_2CHBF_4$ by syringe. The mixture was stirred for 6 h at room temperature, concentrated under reduced pressure and dried on high vacuum for 6 h. The residue was mixed with 50% *t*-BuOH in THF (20 mL) and *t*-BuOK (0.84 g, 7.5 mmol). The mixture was stirred at room temperature overnight and then concentrated under reduced pressure. The residue was dissolved in $CH_2Cl_2$ (50 mL), washed with $H_2O$ (50 mL × 2), washed with brine (50 mL), dried over $MgSO_4$ and concentrated under reduced pressure. The residue was subjected to column chromatography (2 × 10 cm, 10% EtOAc in hexanes), which afforded **3-33** as an waxy yellow solid (0.021 g, 23%): $R_f$ (10% EtOAc in hexanes) = 0.3; LCMS (APCI, positive) *m/z* (%): 1222 (28), 1221 (100, $M^+$).

**3.4 Reference:**


1. Suzuki, H. *Organic Syntheses*; Wiley: New York, **1988**, Collect. Vol. VI, 700.
2. Campeau, L-C.; Parisien, M.; Leblanc, M.; Fagnou, K. *J. Am. Chem. Soc.* **2004**, *126*, 9186.
3. Zhang, B. Ph.D. Thesis, Memorial University, 2008.
4. Yu, H. Ms.C. Thesis, Memorial University, 2004.
5. Bodwell, G. J.; Houghton, T. J.; Koury, H. E.; Yarlagadda, B. *Synlett* **1995**, 751.
6. Bodwell, G. J.; Bridson, J. N.; Houghton, T. J.; Kennedy, J. W. J.; Mannion, M. *Angew. Chem. Int. Ed. Engl.* **1996**, *35*, 1320.
7. Bodwell, G. J.; Bridson, J. N. Houghton, T. J.; Kennedy, J. W. J.; Mannion, M. R. *Chem. Eur. J.* **1999**, *5*, 1823.
8. Bodwell, G. J.; Fleming, J. J.; Mannion, M. R.; Miller, D. O. *J. Org. Chem.* **2000**, *65*, 5360.
9. Bodwell, G. J.; Miller, D. O.; Vermeij, R. J. *Org. Lett.* **2001**, *3*, 2093.
10. Zhang, B.; Manning, G. P.; Dobrowolski, M. A.; Cyrańsk, M. K.; Bodwell, G. J. *Org. Lett.* **2008**, *10*, 273.
11. Mitchell, R. H.; Boekelheide, V. *J. Am. Chem. Soc.* **1974**, *96*, 1547.
12. Harvey, R. G. *Polycyclic Aromatic Hydrocarbons: Chemistry and Carcinogenicity;* Cambridge University Press: Cambridge **1991**.

# Chapter 4

# Synthesis of Aromatic Belts via Dibenzo[*a*,*h*]anthracene Boards

## 4.1 A strategy based on the stilbene-phenanthrene photocyclization

The attempted synthesis of aromatic belts via tetrahydrodibenzo[*a,h*]anthracene board **3-25** failed at Stage 4 of the general strategy. However, the observation of a cluster of peaks at the correct mass was cause for cautious optimism that the VID methodology was powerful enough to deliver the desired product. Thus an alternative synthetic approach involving the corresponding aromatized board **4-01** (Scheme 4.01, 4.02) was then investigated.

The new approach relied on the stilbene-phenanthrene photocyclization, which is also a VID reaction. Precedent for the synthesis of dibenzo[*a,h*]anthracenes using this methodology was reported by Laarhoven *et al.* (Scheme 4.03).[1] Interestingly, the substituents on the central benzene ring are not only required for the reaction to proceed,[2] but are also perfectly positioned as solubilizing groups for the dibenzo[*a,h*]anthracene product. In principle, the (*E,E*) (*E,Z*) and (*Z,Z*) isomers of **4-02** are all viable precursors to **4-01**, because the *E* configured alkenes equilibrate with their *Z* counterparts under the reaction conditions.[3] The (*E,E*) isomer, (*E,E*)-**4-02**, was expected to be accessible using Stille couplings (Scheme 4.01) or Wittig reactions, and the (*Z,Z*) isomer, (*Z,Z*)-**4-02**, was expected to be accessible by partial catalytic hydrogenation of **3-05** (Scheme 4.02).

Previous work in the Bodwell group showed that a Wittig-based approach to (*E,E*)-**4-02** was problematic,[4] so a Stille coupling based approach was investigated instead. Dimethyl-substituted board **4-01** was chosen as the initial target of the synthesis for the sake of synthetic ease. The synthesis started from alkyne **3-19**[4] and 1,4-diiodo-2,5-dimethylbenzene (**3-02**),[5] which were synthesized according to literature procedures. One-pot conditions (sequential hydrostannylation and Stille coupling)[6] were first attempted to synthesize compound (*E,E*)-**4-02** (Table 4.01). After stirring a mixture of **3-19** and **3-02** for 1 h in the presence of $Pd(PPh_3)_2Cl_2$ and $Bu_3SnH$ at room temperature, the reaction proceeded only as far as the hydrostannylation stage, affording the proximal hydrostannylated product **4-04** (88%) instead of the distal product **4-03**. The diiodide **3-02** was recovered quantitatively. Although the anticipated compound **4-03** was not obtained, the conversion of the undesired proximal isomer **4-04** into the desired (*E,E*)-**4-02** by way of a Heck-like reaction with diiodide **3-02**.[7] When the reaction time and temperature were increased, alkyne **3-19** and 1,4-diiodo-2,5-dimethylbenzene (**3-02**) were completely consumed, but only a complex mixture of products which could not be purified was obtained. A stepwise approach was then employed (Scheme 4.04). Hydrostannylation of alkyne **3-19** by treatment with $Bu_3SnH$ afforded compound **4-04** (98%). However, the subsequent attempted Heck-like reaction of **4-04** with **3-02** also afforded a complex mixture.

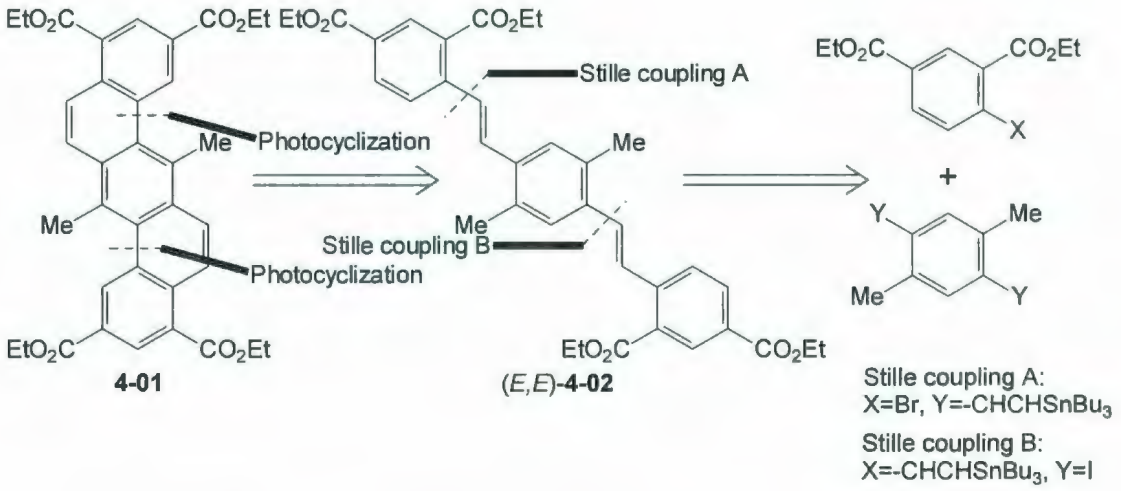


**Scheme 4.01.** Retrosynthetic analysis of molecular board **4-01**.

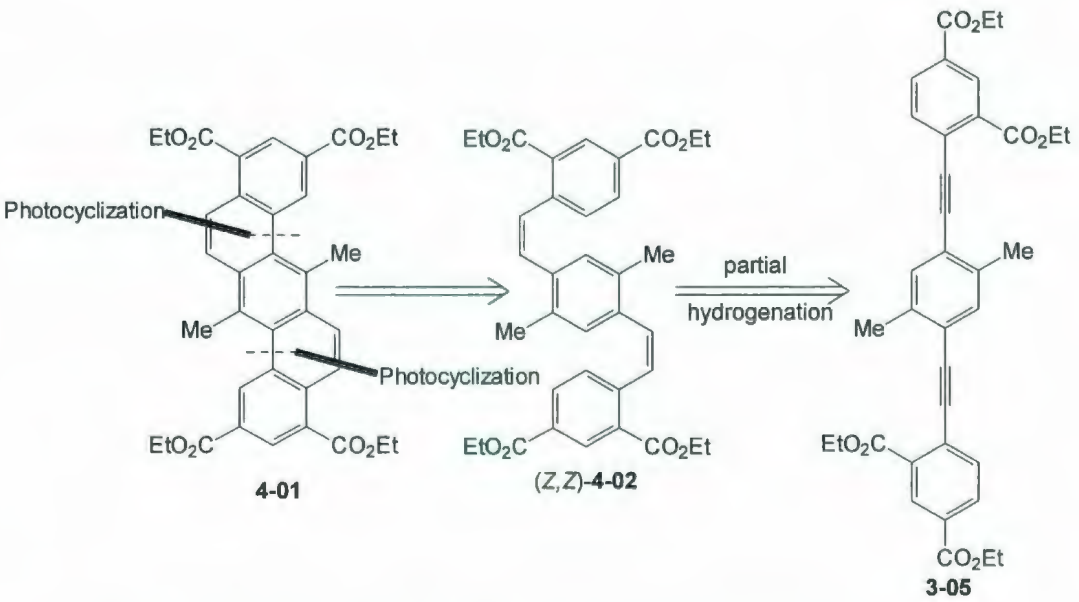


**Scheme 4.02.** Retrosynthetic analysis of molecular board **4-01**.

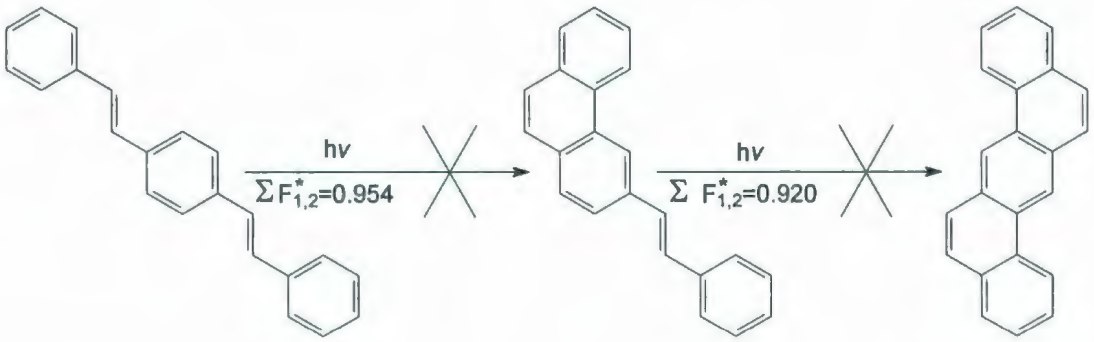


**Scheme 4.03.** Precedent for the synthesis of dibenzo[*a,h*]anthracene.

The approach was then modified by exchanging the key functionality of the two building blocks (Scheme 4.05). One-pot conditions were employed first, i.e., diyne **3-02** and bromide **2-39** were reacted in the presence of $Pd(PPh_3)_2Cl_2$ and $Bu_3SnH$. These conditions again afforded a complex mixture. Another stepwise procedure was then investigated. Unlike the previous hydrostannylation with **3-19**, treatment of diyne **3-02** with $Bu_3SnH$ afforded a complex mixture. Thus, the origin of the failure of this one-pot reaction was likely due to the problematic hydrostannylation of diyne **3-02**.

**Table 4.01.** Attempted synthesis of tetraesterdiene (*E,E*)-**4-02**.

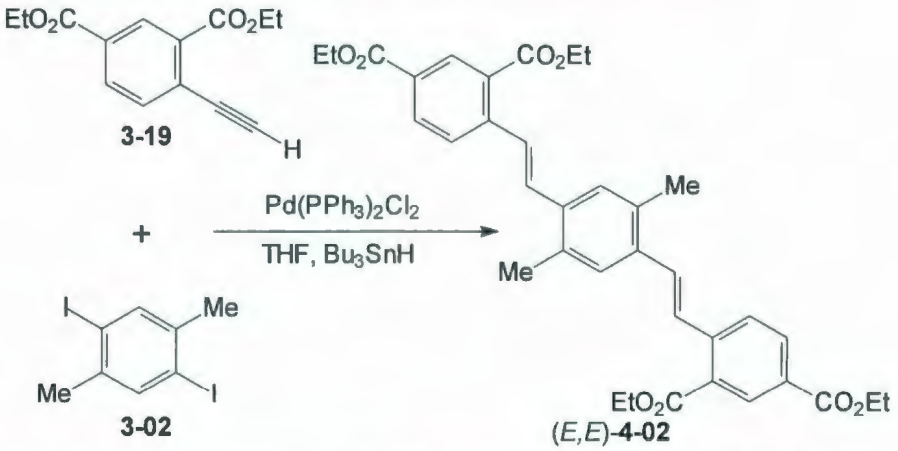


| mol of catalyst | temperature | time (h) | result |
|---|---|---|---|
| 0.0073 | 0 °C to rt | 1 h | **4-04** (88%), **3-02** (100% recovery) |
| 0.0073 | reflux | 24 h | complex mixture |
| 0.05 | reflux | 48 h | complex mixture |
| 0.2 | reflux | 48 h | complex mixture |

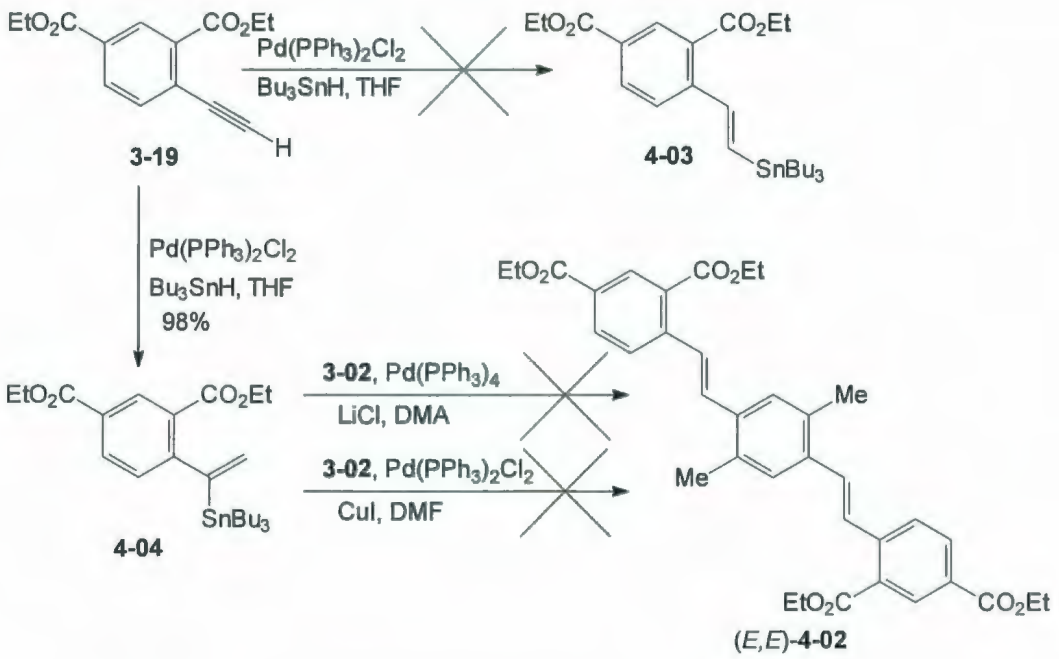


**Scheme 4.04.** Attempted synthesis of tetraesterdiene (*E,E*)-**4-02**.

Attention was then turned to the synthesis of (*Z,Z*)-**4-02**. Tetraesterdiyne **3-05** (see Scheme 3.01, p.63) was reacted with $H_2$ in the presence of $Pd/CaCO_3$ (Lindlar's catalyst) in hexane and this gave the desired product (*Z,Z*)-**4-02** (77%, Table 4.02, Entry 1). However, despite considerable effort, this result could not be repeated under identical conditions (Table 4.02, Entry 2), or under a variety of other conditions (Table 4.02, Entries 3-11). In all cases, **3-05** was recovered (>95%).

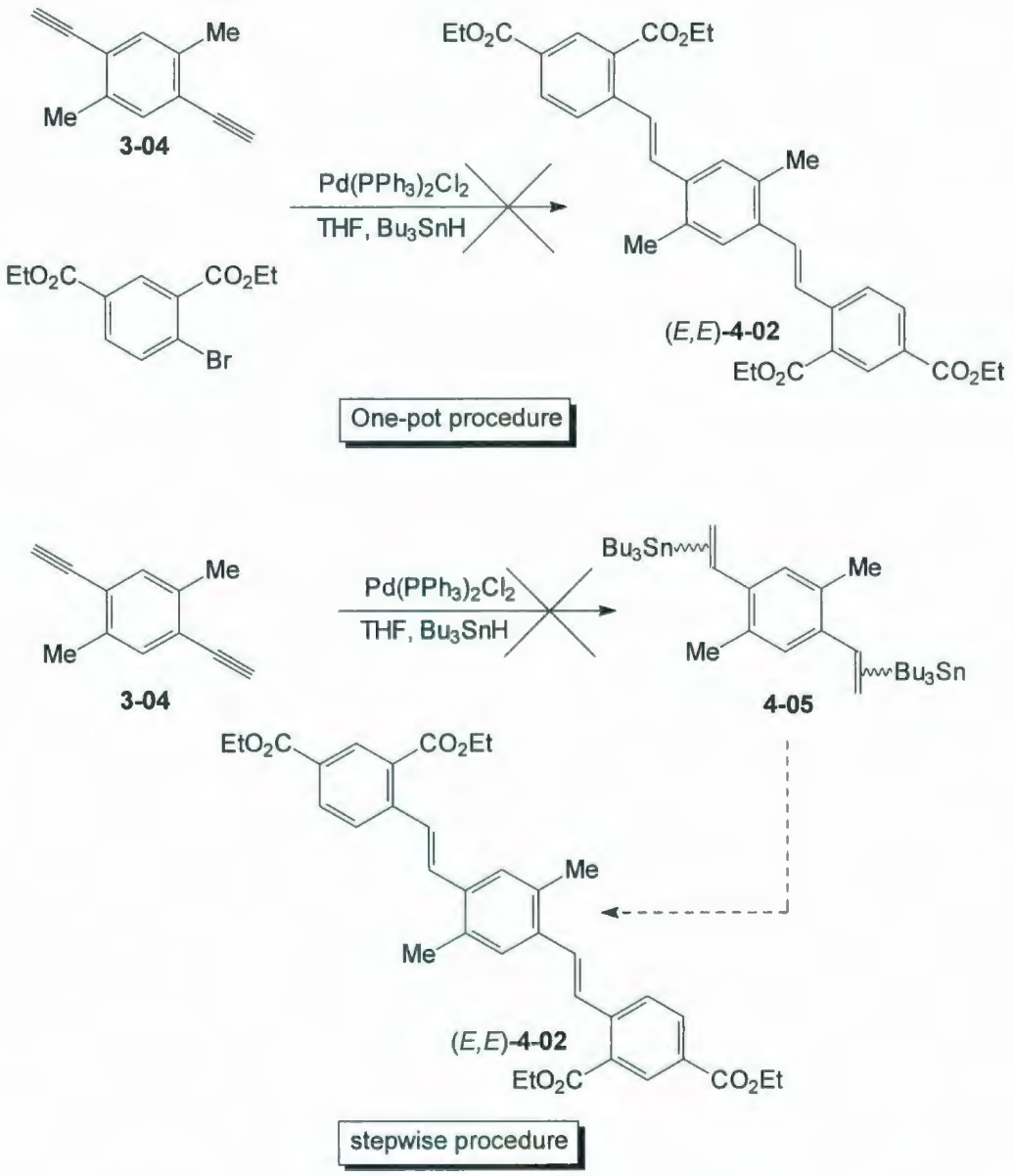


**Scheme 4.05.** Attempted synthesis of tetraesterdiene (*E,E*)-**4-02**.

**Table 4.02.** Attempted synthesis of tetraesterdiene (*Z,Z*)-**4-02**.

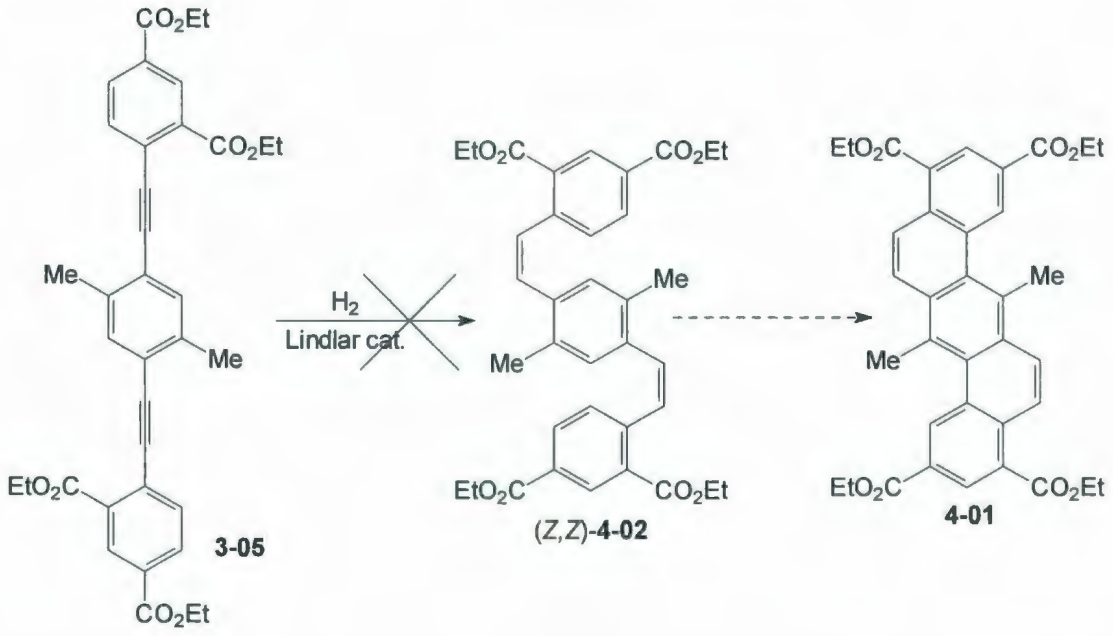


| Entry | solvents | additives | results |
|---|---|---|---|
| 1 | hexane | n/a | (*Z,Z*)-**4-02** (77%) |
| 2 | hexane | n/a | No reaction was detected |
| 3 | MeOH | n/a | No reaction was detected |
| 4 | $CH_2Cl_2$/MeOH | n/a | No reaction was detected |
| 5 | EtOAc | n/a | No reaction was detected |
| 6 | hexane | quinoline | No reaction was detected |
| 7 | MeOH | quinoline | No reaction was detected |
| 8 | EtOAc | quinoline | No reaction was detected |
| 9 | hexane/EtOH | quinoline | No reaction was detected |
| 10 | hexane/EtOH | EDA | No reaction was detected |
| 11 | hexane/EtOH | pyridine | No reaction was detected |

At this stage, therefore, work on this approach was concluded and the aromatization of the didecyl substituted board **3-25**, which had already been synthesized (see Scheme 3.09, p.76), was then reinvestigated.

## 4.2 Synthesis of aromatic belts 3-34

In general, the aromatization of partially-saturated polycyclic aromatic hydrocarbons can be accomplished using four types of reactions, i.e., oxidation, addition/elimination, substitution/elimination and catalytic dehydrogenation. The previous attempts to aromatize **3-25** by treatment with DDQ (oxidation) were unsuccessful (see Scheme 3.14, p.87). A cursory attempt to achieve the same result using $Br_2/CS_2$ (substitution/elimination) was also unsuccessful, giving a complex mixture of products (see Scheme 3.14, p.87). However, this reaction did appear to give some of the desired product **3-36** according to MS analysis (*m/z*=847). The use of free radical bromination followed by elimination of HBr was therefore reinvestigated. To minimize the competing benzylic bromination of side chains, tetraester **3-25** was chosen as the substrate for this work, since benzylic carbons having hydrogen atoms available exist at the C-2,4,9 and 11 positions on other building blocks, i.e., **3-26**, **3-27** and **3-28**.

Initial work focused on the use of $Br_2/CS_2$. The temperature and the number of equivalents of $Br_2$ were varied. At all temperatures investigated, the starting material **3-25** was completely consumed by the time the addition of $Br_2$ was complete. In each case, a cluster of peaks corresponding to the desired product **3-36** was observed by MS analysis, but $^1H$ NMR analysis indicated that a complex mixture had formed. Increasing the number of equivalents of $Br_2$ from 2.1 to 3.0 (Table 4.03, Entry 3) did not affect the outcome significantly according

to TLC, MS and $^1$H NMR analysis. Attempted purification of one of the resulting mixtures was not successful in all cases. In the hope that purification could be achieved at a later stage, the crude material was then carried though the subsequent DIBAL reduction, but, once again, an intractable product was obtained.

**Table 4.03.** Attempted synthesis of molecular board **3-36** using $Br_2/CS_2$.

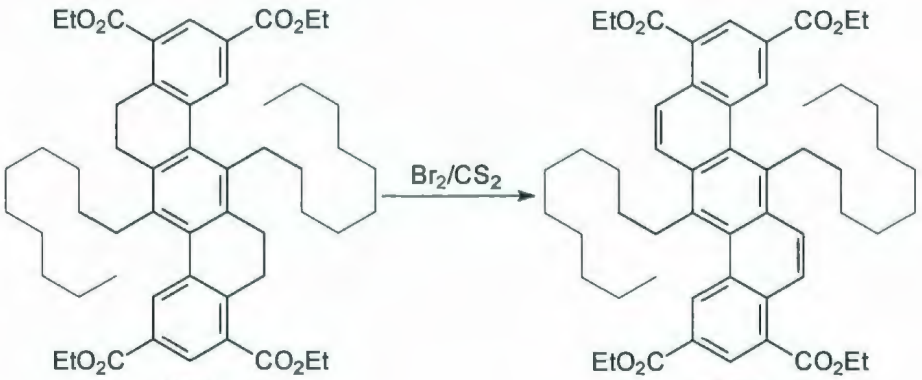


**3-25** **3-36**

| Entry | Temperature | Amount of $Br_2$ | Result |
|---|---|---|---|
| 1 | rt | 2.1 eq. | complex mixture |
| 2 | 0 °C | 2.1 eq. | complex mixture |
| 3 | -20 °C | 3.0 eq. | complex mixture |
| 4 | -20 °C | 2.1 eq. | complex mixture |
| 5 | -50 °C | 2.1 eq. | complex mixture |

Replacing $Br_2/CS_2$ with NBS/dibenzoyl peroxide in either benzene or $CH_2Cl_2$ was then investigated. Treatment of **3.25** with 2.0 equivalents of NBS afforded a mixture of the desired board **3-36**, mono-reacted product **4-06** (4:1, estimated by $^1$H NMR analysis) (Scheme **4**.06). When the amount of NBS was then increased to 2.5-3.0 equivalents, dibenzo[*a,h*]anthracene board **3-36** was

obtained in 30-60% yields after column chromatography. According to $^1$H NMR analysis, the chromatographed product contained a small amount of unidentified impurities (~5%). Pure **3-36** was obtained in 21% yield by crystallization from EtOH. However, it proved to be more convenient to proceed with the chromatographed product and purify at a later stage. Reaction of **3-36** with DIBAL using a standard work-up ($H_2O$ quench followed by the addition of 1 M HCl solution) resulted in the formation of an intractable mixture (Scheme 4.07). Omission of the addition of HCl solution afforded a product (presumably the desired product along with DIBAL-derived products) that was somewhat soluble in $CDCl_3$ and exhibited a $^1$H NMR spectrum consistent with the desired reduction product (i.e., tetraalcohol, **4-07**). However, the crude mass corresponded to >200% yield, presumably due to organoaluminum by-products. Bromination of the crude reduction product by treatment with $PBr_3$ in $CH_2Cl_2$ gave tetrabromide **4-08** in 10% overall yield after column chromatography from tetraester **3-36**. Purification of the chromatographed sample to remove the small amount of impurities was not attempted due to the low yield. However, treatment of **4-07** with 30% HBr in AcOH successfully afforded tetrabromide **4-08** in higher yield (50% from **3-36**, after crystallization) (Scheme 4.08).

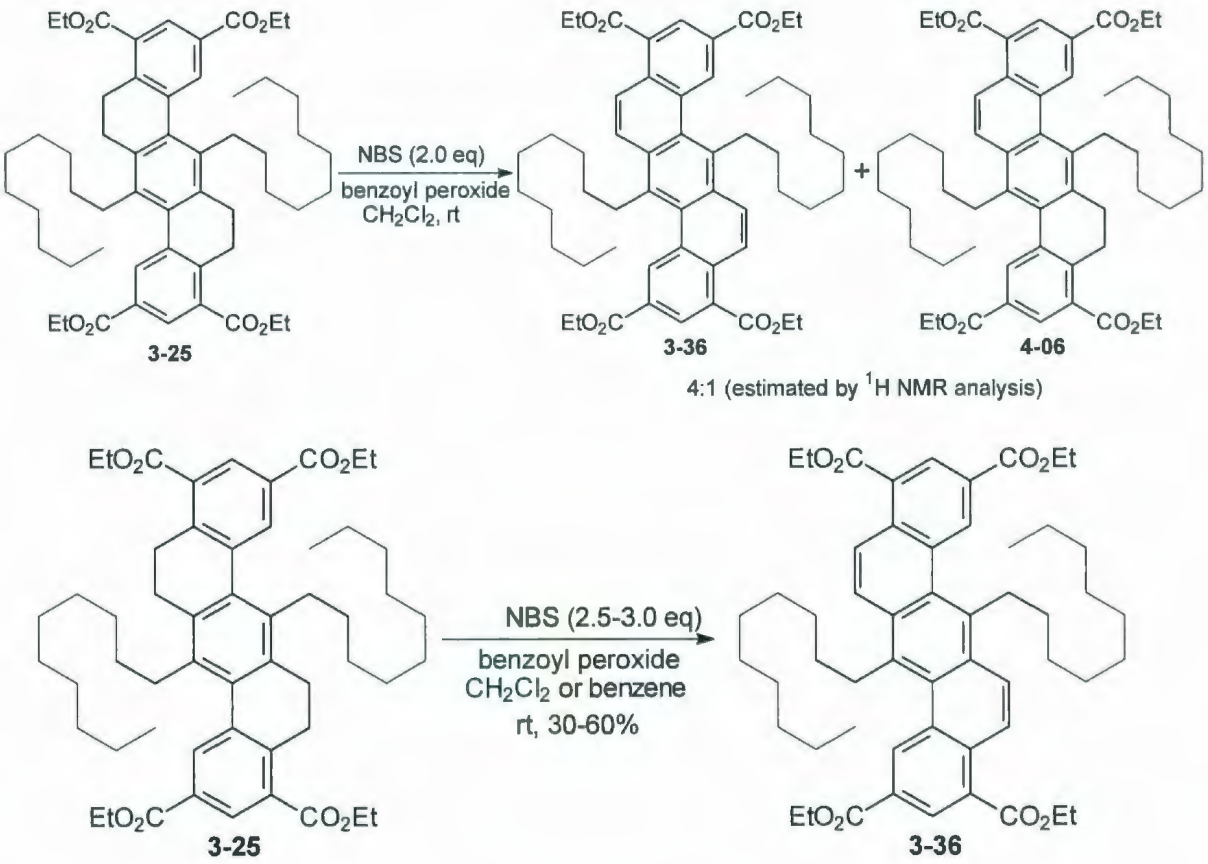


**Scheme 4.06.** Synthesis of aromatized board **3-36.**

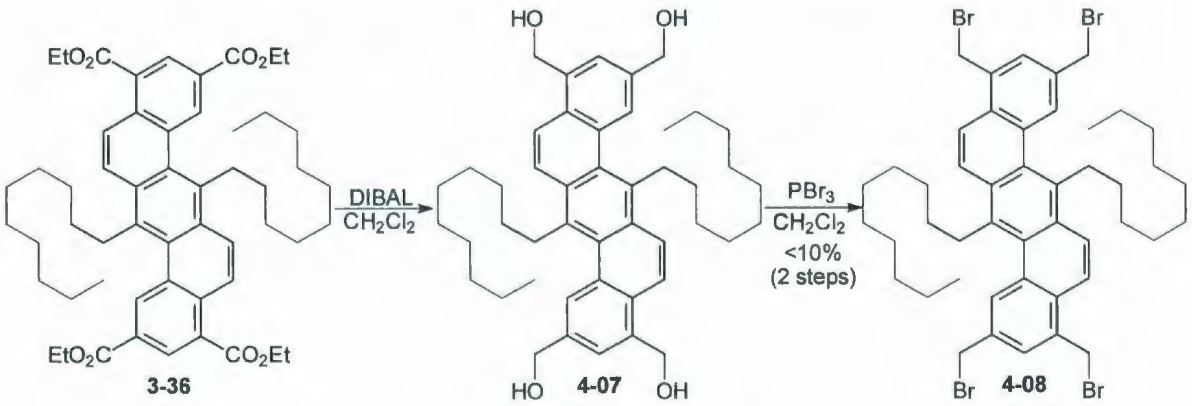


**Scheme 4.07**. Synthesis of tetrabromide **4-08**.

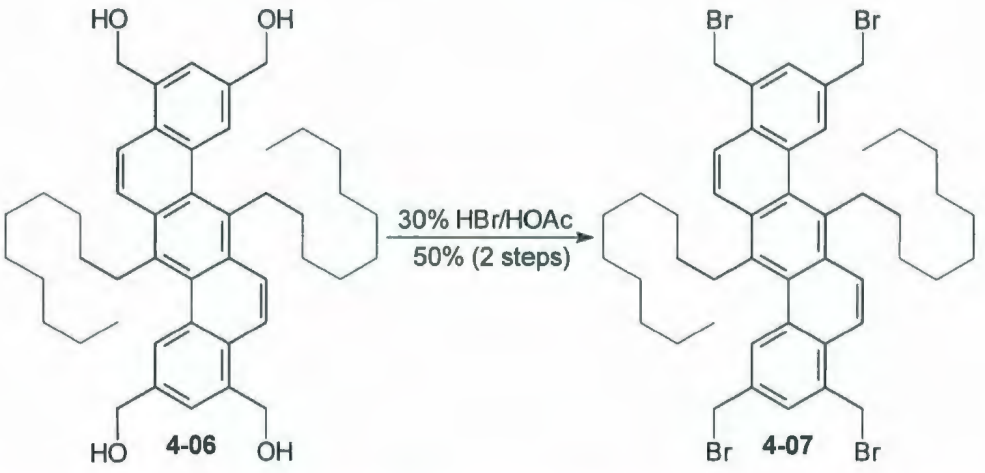


**Scheme 4.08.** Synthesis of tetrabromide **4-08** under optimized conditions.

With **4-08** in hand, the key coupling reaction using sodium sulfide on alumina was attempted. This afforded tetrathiacyclophane **4-09** in 30-50% yield (Scheme 4.09). Although some of the complications that plagued the analysis of the $^1$H NMR spectrum of **3-29** were absent (the ethano units are now etheno units), the $^1$H NMR spectrum of **4-09** was broad and complicated and no useful information could be obtained. Aggregation may be responsible for the poor quality of the spectrum. As with tetrathaicyclophane **3-29**, MS analysis supported the formation of the product. A cluster of peaks corresponding to the desired **4-09** was observed (*m/z*=1349, APCI positive).

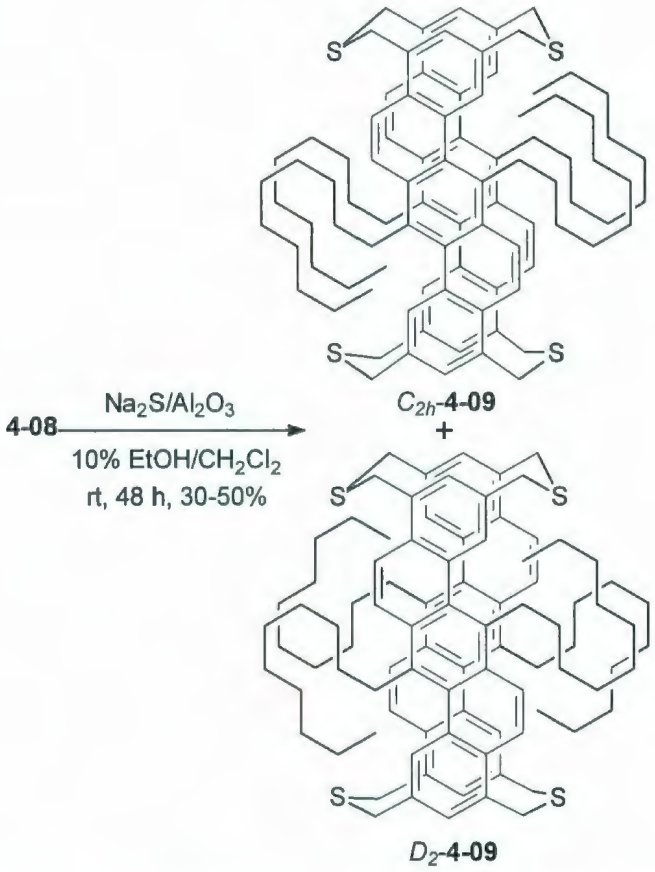


**Scheme 4.09.** Synthesis of tetrathiacyclophane **4-09.**

Fourfold *S*-methylation of tetrathiacyclophanes **4-09** by treatment with Borch reagent was then performed with the intention of generating the corresponding tetrakis(methylsulfonium tetrafluoroborate) salt **4-10** (Scheme 4.10). The crude product was then converted into isomer mixture **4-11** in 16% yield by treatment with *t*-BuOK (thia-Stevens rearrangement). Since the symmetry of **4-11** is identical to that of **3-31** (Scheme 3.12, p. 82), there are still up to 148 isomers present in the mixture (See Appendix 1), and MS analysis was again the only useful method to support the formation of **4-11**. As with compound **3-31** (Figure 3.02, p. 80), a cluster of peaks corresponding to the desired product

**4-10** and clusters of peaks corresponding to the fragments arising from the loss of SMe groups and $CH_2$ groups were observed.

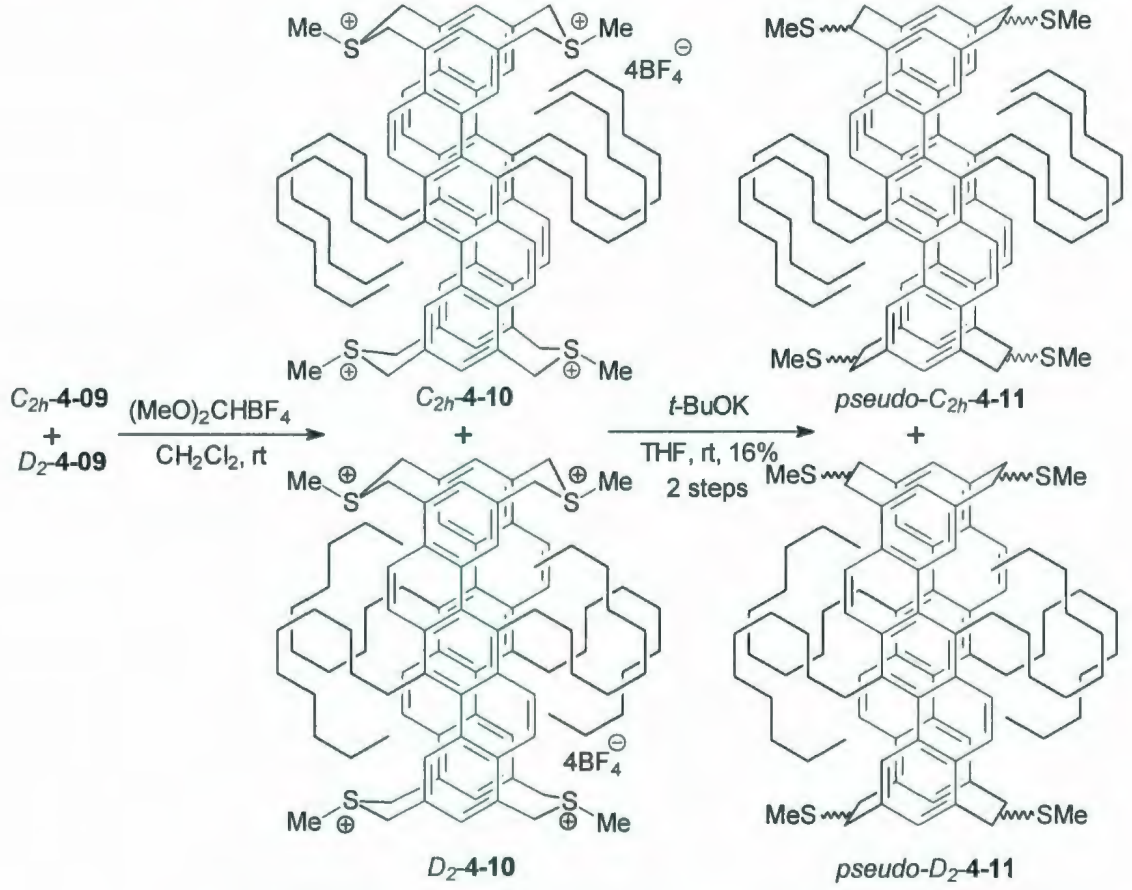


**Scheme 4.10.** Synthesis of compounds **4-11.**

Fourfold *S*-methylation of chromatographed **4-11** with Borch reagent was then performed to generate the corresponding tetrakis(dimethylsulfonium tetrafluoroborate) salt **4-12** (Scheme 4.11). Crude **4-12** was then reacted with *t*-BuOK (Hofmann elimination) to afford cyclophanetetraene **4-13** (60%). Again, MS analysis was the only useful evidence obtained for the formation of **4-13** (*m/z*=1213, APCI positive).

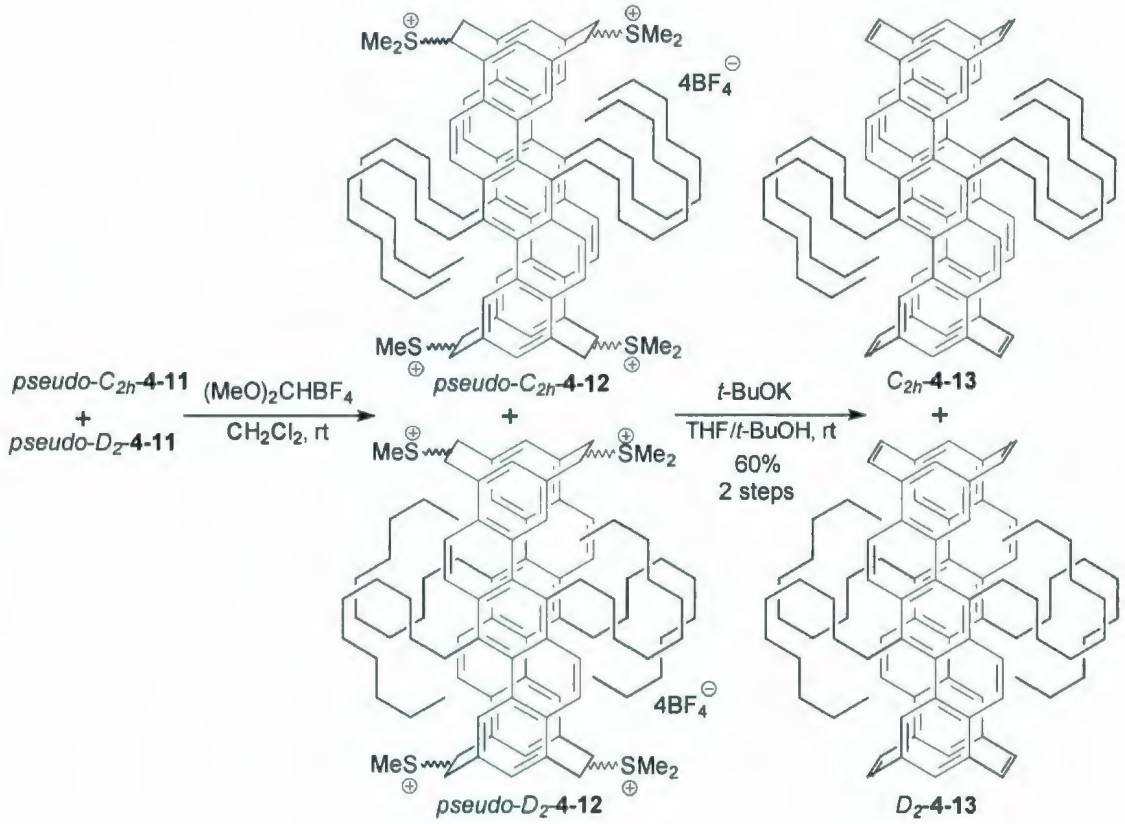


**Scheme 4.11.** Synthesis of cyclophanetetraene **4-13**.

Stage 4 of the general strategy to complete the synthesis of aromatic belts **3-34** was at hand, although only small amounts of material were available. In contrast to the conversion of **3-33** into **3-34**, which required the loss of twelve hydrogen atoms, the key VID reaction of **4-13** required the removal of only four hydrogen atoms. Tetraene **4-13** (~1 mg scale) was reacted with DDQ (10 eq.) in benzene for 60 minutes at room temperature (Scheme 4.12). TLC analysis showed that two new narrowly-separated spots had formed ($R_f \simeq 0.2$, 5% EtOAc/hexanes). MS analysis of the chromatographed sample showed a low

intensity cluster of peaks (*m/z*=1209, APCI positive) (Figure 4.01), which matched the desired aromatic belts **3-34** (calculated isotopic pattern shown in Figure 4.02).[8] Due to the scale of the reaction, no other characterization method (including NMR) gave useful information to support the formation of the desired aromatic belts **3-34**.

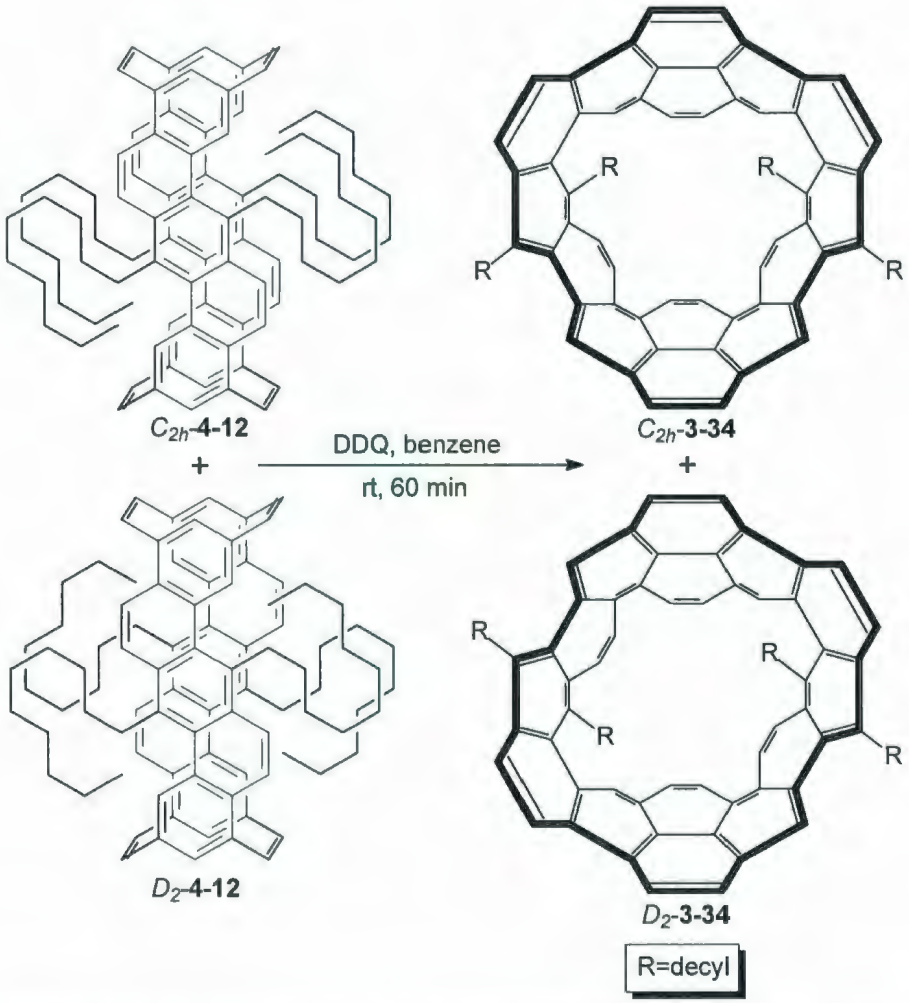


**Scheme 4.12.** Synthesis of aromatic belts **3-34** by the VID reaction.

The synthesis was not performed on a larger scale due to time constraints, because the synthesis is long and has several low-yielding steps. Although $^1$H NMR analysis did not give useful information, and X-ray analysis was not obtained either, on the basis of TLC and mass spectrometric evidence, there can be some optimism that $C_{2h}$-**3-34** and $D_2$-**3-34** (2 new, narrowly separated spots by TLC, correct mass) formed *at room temperature*, and the VID reaction appears to be easily capable of generating belt structures in the last step of the synthesis. Furthermore, the belts appear to have at least some stability at room temperature because the product could be chromatographed. This work also gave cause for optimism about the viability of the Bodwell group's approach to synthesize aromatic belts (based on the VID reaction) and indicated that the use of a partially-saturated molecular board was not necessary to maintain solubility of the synthetic building blocks. In fact, they were probably to blame for the failure to achieve the desired targets at the end (see Chapter 3, p. 85).

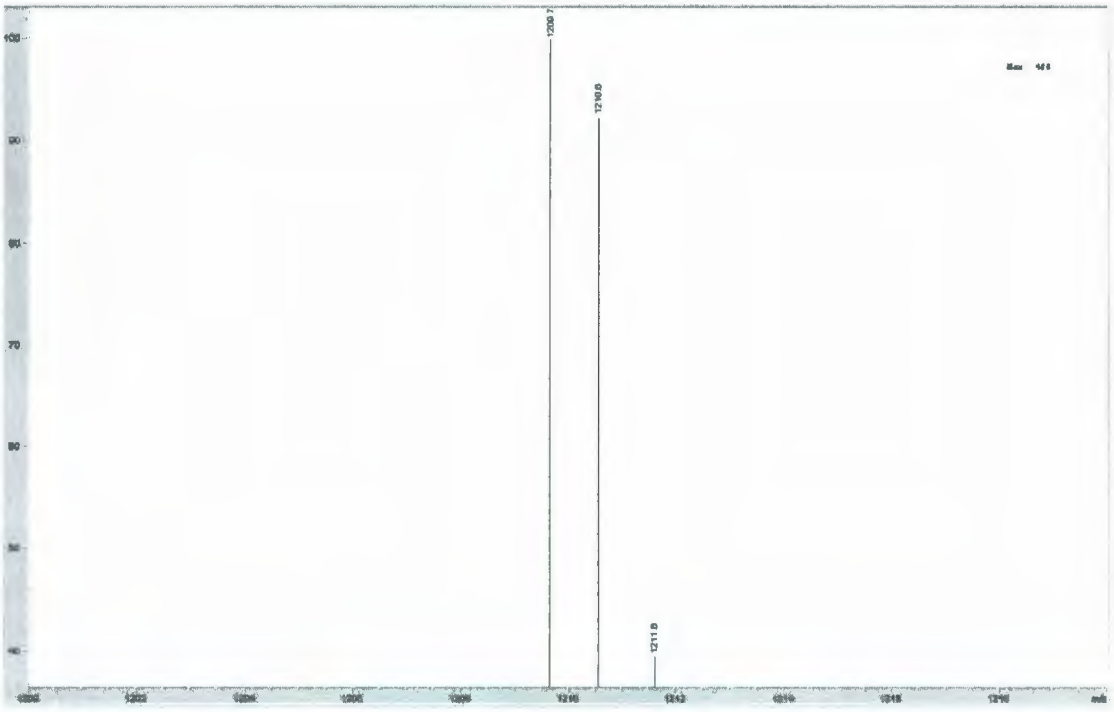

**Figure 4.01.** APCI (positive) mass spectrum of **3-34**.

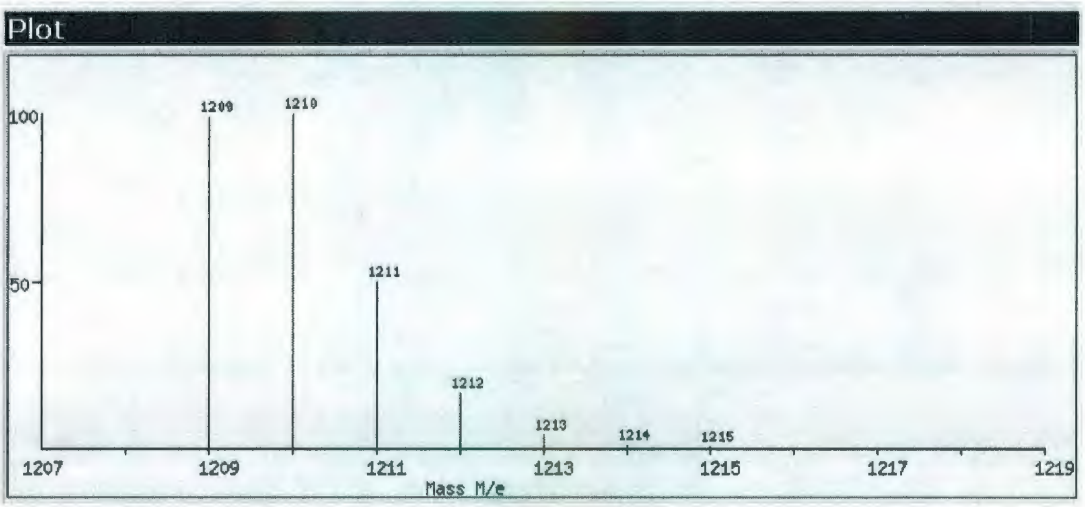


**Figure 4.02.** Calculated isotopic pattern of $C_{92}H_{104}$.

## 4.3 Future Work

In future, substantial improvement of the existing synthesis of the development of a better synthetic route will have to be investigated. Furthermore, future synthetic work should focus on aromatic boards and not partially saturated ones. Molecular boards with larger sizes, and/or having $D_{2h}$ symmetry, e.g., **4-14**, that are building blocks for Vögtle's belts will also be investigated (Figure 4.03). The advantage of synthesizing aromatic belts via such a board is that this approach prevents the formation of two isomers of the belts and its cyclophane precursors. This should thereby facilitate the characterization of these products.

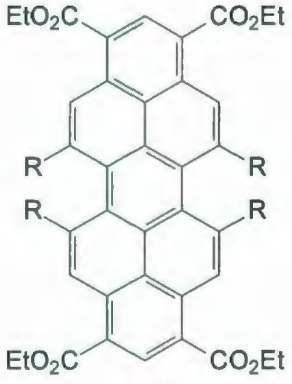


**4-14**

**Figure 4.03**. A $D_{2h}$-symmetric board as a building block of the synthesis of the aromatic belts.

## 4.4 Experimental

**General.** For general procedures, please refer to the section in Chapter 3.

**1,3-Bis(ethoxycarbonyl)-4-(1-(tributylstannyl)vinyl)benzene (4-03).**

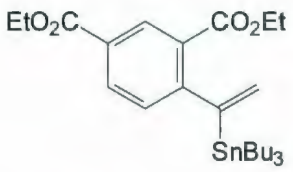


To a solution of 1,3-bis(ethoxycarbonyl)-4-ethynylbenzene (**3-19**) (1.00 g, 4.06 mmol) and $Pd(PPh_3)_2Cl_2$ (0.029 g, 0.0041 mmol) in THF was added $Bu_3SnH$ (1.42 g, 4.87 mmol) dropwise at 0 °C under $N_2$. The reaction was stirred at 0 °C for 45 min and concentrated under reduced pressure. The residue was subjected to column chromatography to afforded **4-03** as a clear colorless liquid (2.13 g, 3.97 mmol, 98%): $R_f$ ($CH_2Cl_2$) = 0.6; $^1$H NMR (500 MHz, $CDCl_3$) δ 8.55 (d, *J*=1.6 Hz, 1H), 8.04 (dd, *J*=8.0, 1.7 Hz, 1H), 7.08 (d, *J*=8.0 Hz, 1H), 5.69 (d, *J*=2.8, 1H), 5.42 (d, *J*=2.8 Hz, 1H), 4.40 (q, *J*=7.1 Hz, 2H), 4.33 (q, *J*=7.1 Hz, 2H), 1.46–1.36 (m, 12H), 1.28–1.24 (m, 6H), 0.91–0.87 (m, 6H), 0.85 (t, *J*=7.3 Hz, 9H); $^{13}$C NMR (500 MHz, $CDCl_3$) δ 166.6, 166.1, 157.9, 155.1, 132.8, 131.4, 128.7, 128.0, 127.4, 124.9, 61.2, 61.1, 29.0, 27.5, 14.48, 14.46, 13.8, 11.2; LCMS (APCI, positive) *m/z* (%):HRMS ($EI^+$): calcd for $C_{26}H_{42}O_4Sn$ 539.2183, found 539.2175.

**7,14-Didecyldibenzo[*a,h*]anthracene-2,4,9,11-tetracarboxylic acid tetraethyl ester (3-36).**

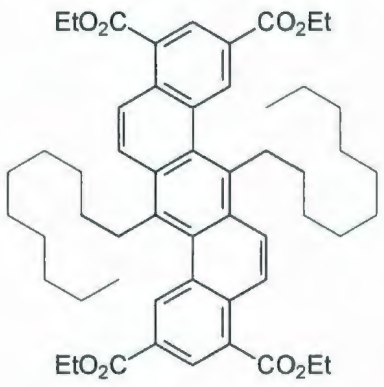


A mixture of 7,14-didecyl-5,6,12,13-tetrahydrodibenzo[*a,h*]anthracene-2,4,9,11-tetracarboxylic acid tetraethyl ester (**3-25**) (960 mg, 1.13 mmol), NBS (recrystallized from $H_2O$ before use, 602 mg, 3.38 mmol), benzoyl peroxide (1 spatula tip) and benzene (50 mL) in a 250 mL round-bottomed flask was irradiated by sodium lamp for 20 min. The solvent was removed under reduced pressure and then the residue was subjected to column chromatography to afford **3-36** as orange oil (0.321 g, 0.379 mmol, 34%). The product was of sufficient purity (>90% by $^1$H NMR) for the use of the next step. For characterization, a small sample was recrystallized from ethanol, which afforded **3-36** as an orange solid (0.201 g, 0.237 mmol, 21%): $R_f$ ($CH_2Cl_2$) = 0.60; mp (ethanol) 78.0–80.0 °C; IR (neat, $cm^{-1}$) 2920 (s), 1718 (s), 1602 (w), 1467 (m), 1318 (m), 1221 (s); $^1$H NMR (500 MHz, $CDCl_3$) δ 9.24 (s, *J*=1.7 Hz, 2H), 8.82 (s, *J*=1.7 Hz, 2H), 8.76 (d, *J*=1.9 Hz, 2H), 8.25 (d, *J*=1.9 Hz, 2H), 4.56 (q, *J*=7.1 Hz, 4H), 4.49 (q, *J*=7.1 Hz, 4H), 3.62-3.55 (m, 4H), 2.28-2.19 (m, 4H), 1.68-1.60 (m, 4H), 1.53 (t, *J*=7.1 Hz, 6H), 1.47 (t, *J*=7.1 Hz, 6H), 1.40–1.25 (m, 24H), 0.89 (t, *J*=7.0 Hz, 6H); $^{13}$C NMR (500 MHz, $CDCl_3$) δ 167.6, 166.3, 134.8, 134.4, 131.7, 130.6, 129.96, 129.93, 127.96, 127.87, 125.5, 123.7, 61.8, 61.6, 33.0, 32.1, 30.4, 30.1, 29.9, 29.7, 29.6, 22.9 (2C), 14.71, 14.66, 14.3; LCMS (APCI, positive) *m/z* (%): 849 (21) 848 (60), 847 (100, $M^+$), 846 (20);

UV/Vis ($CHCl_3$) $\lambda_{max}$ (log $\varepsilon$) nm 293 (4.43), 306 (4.43), 320 (4.43), 335 (4.51), 397 (4.28), 432 (3.88); $\Phi_f$ , 0.60 ($\lambda_{em}$ = 454 nm); HRMS ($EI^+$): calcd for $C_{54}H_{70}O_8$ 846.5071, found 846.5070.

**7,14-Didecyl-2,4,9,11-tetrakis(bromomethyl)dibenzo[*a,h*]anthracene (4-08).**

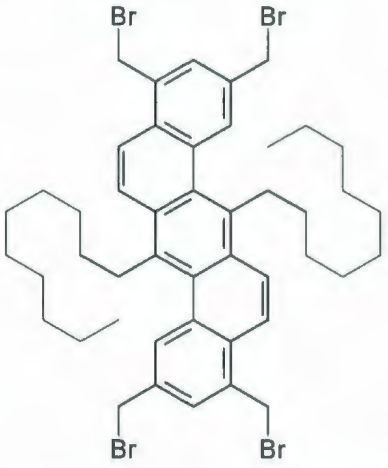


To a mixture of 7,14-didecyldibenzo[*a,h*]anthracene-2,4,9,11-tetracarboxylic acid tetraethyl ester (**3-36**) (366 mg, 0.432 mmol) and $CH_2Cl_2$ (20 mL) was added DIBAL-H in $CH_2Cl_2$ (1.0 M, 6.9 mL) at 0 °C. The mixture was allowed to warm to room temperature and stir overnight. The mixture was quenched by adding water dropwise at 0 °C. The precipitate was collected by suction filtration to afforded **4-07** as a yellow solid. Crude **4-07** was then mixed with 30% HBr in AcOH (50 mL). The mixture was stirred at room temperature for 60 min and then quenched by adding ice-water (25 mL) at 0 °C. The precipitate was collected by suction filtration as a brown solid and subjected to column chromatography to give **4-08** as a yellow solid. This sample was recrystallized from EtOAc, which afforded **4-08** as an orange solid (200 mg, 0.215 mmol, 50%): $R_f$ (30% hexanes in $CH_2Cl_2$) = 0.4; mp (EtOAc) 175.5–177.5 °C; IR (neat) 2921 (s), 2851 (s) 1741 (w), 1455 (m), 1212 (s), 721 (s) $cm^{-1}$; $^1H$ NMR (500 MHz, $CDCl_3$) $\delta$ 8.37 (s, 2H), 8.22 (d, *J*=10.0 Hz, 2H), 8.04 (d, *J*=10.0 Hz, 2H), 7.68 (d, *J*=1.4 Hz, 2H), 5.03 (s, 4H), 4.69 (s, 4H), 3.63–3.59 (m, 4H), 2.21–2.16 (m, 4H),

1.69–1.65 (m, 4H), 1.51–1.47 (m, 4H), 1.33–1.25 (m, 20H), 0.89 (t, *J*=7.1 Hz, 6H); $^{13}C$ NMR (500 MHz, $CDCl_3$) δ 134.5, 133.75, 133.73, 132.3, 130.9(2C), 130.2, 130.1, 129.1, 125.4, 121.8, 33.8, 32.9, 32.1, 30.5, 30.1, 29.92, 29.89, 29.76, 29.6, 22.9, 14.4; LCMS (APCI, positive) *m/z* (%): 935 (21) 934 (30), 933 (65), 932 (45), 931 (100, $M^+$ $(^{81}Br)_2(^{79}Br)_2$), 930 (35), 929 (66), 928 (17), 927 (22); UV/Vis ($CHCl_3$) $\lambda_{max}$ (log ε) nm 302 (4.06); HRMS ($EI^+$): calcd for $C_{46}H_{58}Br_4$ 926.1272, found 926.1257.

**6,13,24,31-tetradecyl-2,19,36,39-tetrathia[2$_4$](2,4,9,11)dibenzo[*a,h*]anthracenophane (*C$_{2h}$*-4-09) and 6,13,23,30-tetradecyl-2,19,36,39-tetrathia[2$_4$](2,4,9,11)(4,2,11,9)dibenzo[*a,h*]anthracenophane (*D$_2$*-4-09).**

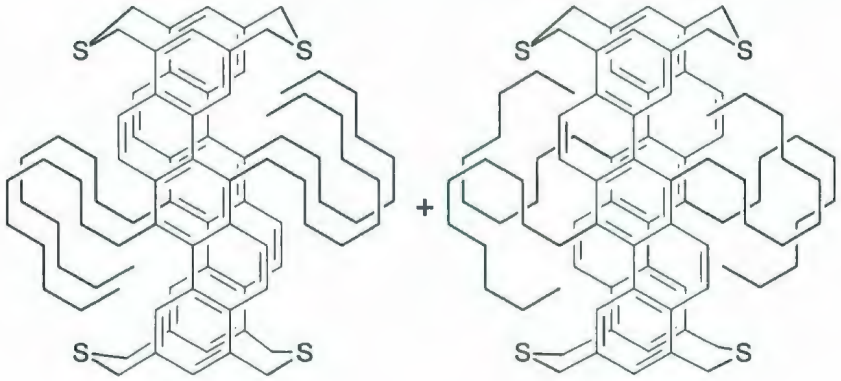


*C$_{2h}$*-4-09 *D$_2$*-4-09

To a mixture of 7,14-didecyl-2,4,9,11-tetrakis(bromomethyl)dibenzo[*a,h*]anthracene (**4-08**) (233 mg, 0.250 mmol) and 10% EtOH (anhydrous) in $CH_2Cl_2$ was added $Na_2S/Al_2O_3$ (1.55 g, 4.01 mmol) in four roughly equal portions over 2 d. The mixture was stirred at room temperature for a further 12 h. Insoluble material was removed by suction

filtration and the filtrate was concentrated under reduced pressure. The residue was subjected to column chromatography to give **4-09** as a yellow solid (70 mg, 0.052 mmol, 41%): $R_f$ (5% EtOAc in hexanes) = 0.4; LCMS (APCI, positive) *m/z* (%): 1354 (33) 1353 (42), 1352 (60), 1351 (57), 1350 (100), 1349 (82, $M^+$). Attempt to obtain a HRMS spectrum was unsuccessful.

**5,12,22,29-tetradecyl-1,17/18,33/34,35/36-tetrakis(methylthio)[2$_4$](2,4,9,11)dibenzo[*a,h*]anthracenophane (*pseudo*-$C_{2h}$-4-11) and 5,12,21,28-tetradecyl-1/2,17/18,33/34,35/36-tetrakis(methylthio)[2$_4$](2,4,9,11)(4,2,11,9)dibenzo[*a,h*]anthracenophane (*pseudo*-$D_2$-4-11).**

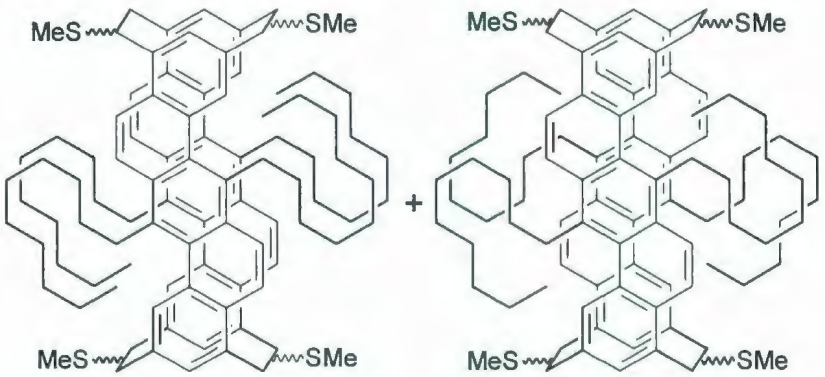


*pseudo*-$C_{2h}$-**4-11** *pseudo*-$D_2$-**4-11**

To a solution of the 6,13,24,31-tetradecyl-2,19,36,39-tetrathia[2$_4$](2,4,9,11)dibenzo[*a,h*]anthracenophane ($C_{2h}$-**4-09**) and 6,13,23,30-tetradecyl-2,19,36,39-tetrathia[2$_4$](2,4,9,11)(4,2,11,9)dibenzo[*a,h*]anthracenophane ($D_2$-**4-09**) (105 mg, 0.0770 mmol) in $CH_2Cl_2$ (20 mL) was added $(MeO)_2CHBF_4$ (125 mg, 0.770

mmol) by syringe at room temperature. The mixture was stirred for 3 h at room temperature and then concentrated under reduced pressure. EtOAc (40 mL) was added and the mixture was stirred at room temperature for 20 min. The precipitate was collected by suction filtration, mixed with THF (5 mL) and concentrated under reduced pressure to remove the trace amount of EtOAc in the system. THF (10 mL) and *t*-BuOK (2.97 g, 26.5 mmol) was then added. The mixture was stirred at room temperature for overnight and then concentrated under reduced pressure. The residue was taken up in $CH_2Cl_2$ (30 mL), washed with $H_2O$ (50 mL × 3), washed with brine (20 mL), dried over $MgSO_4$ and concentrated under reduced pressure. The residue was subjected to column chromatography (0.5 × 5 cm, 5% EtOAc in hexanes), which afforded **4-11** as a yellow solid (17 mg, 0.012 mmol, 16%): $R_f$ (5% EtOAc in hexanes) = 0.4; LCMS (APCI, positive) *m/z* (%): 1411 (40) 1410 (45), 1409 (78), 1408 (72), 1407 (100, $M^+$), 1406 (95), 1405 (93), 1391 (18), 1389 (19), 1363 (23), 1362 (21), 1361 (33), 1360 (22), 1359 (43), 1358 (33), 1357 (37). Attempt to obtain a HRMS spectrum was unsuccessful.

**5,12,22,29-Tetradecyl-(1*Z*,17*Z*,33*Z*,35*Z*)-[2$_4$](2,4,9,11)dibenzo[*a,h*]anthracenophane-1,17,33,35-tetraene (*$C_{2h}$*-4-13), and 5,12,21,28-tetradecyl-(1*Z*,17*Z*,33*Z*,35*Z*)-[2$_4$](2,4,9,11)(4,2,11,9)dibenzo[*a,h*]anthracenophane-1,17,33,35-tetraene (*$D_2$*-4-13).**

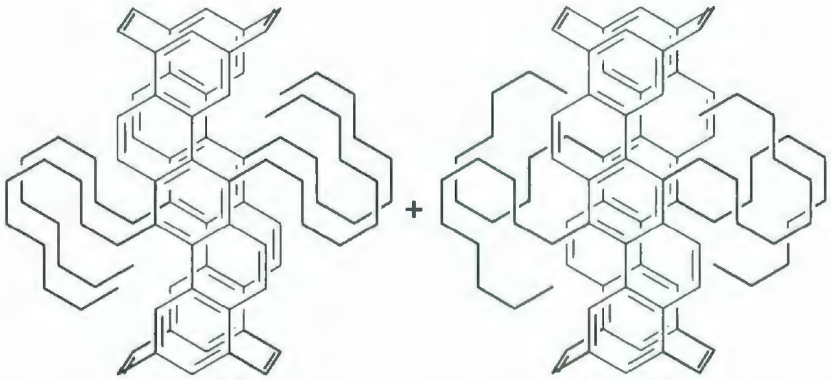

*$C_{2h}$*-**4-13** + *$D_2$*-**4-13**

To a solution of 5,12,22,29-tetradecyl-1,17/18,33/34,35/36-tetrakis(methylthio)[2$_4$](2,4,9,11)dibenzo[*a,h*]anthracenophane (*pseudo-$C_{2h}$*-**4-11**) and 5,12,21,28-tetradecyl-1/2,17/18,33/34,35/36-tetrakis(methylthio)[2$_4$](2,4,9,11)(4,2,11,9)dibenzo[*a,h*]anthracenophane (*pseudo-$D_2$*-**4-11**) (10 mg, 7.1 μmol) in $CH_2Cl_2$ (10 mL) was added $(MeO)_2CHBF_4$ (17 mg, 0.106 mmol) by syringe at room temperature. The mixture was stirred for 5 h at room temperature and concentrated under reduced pressure. The residue was mixed with EtOAc (20 mL). The mixture was stirred at room temperature for 20 min and then concentrated under reduced pressure. THF (5 mL) was added to the residue and then the mixture was concentrated under reduced pressure to remove the trace amount of EtOAc in the system. The residue was mixed with

50% *t*-BuOH in THF (10 mL) and *t*-BuOK (40 mg, 0.355 mmol). The mixture was stirred at room temperature overnight and then concentrated under reduced pressure. The residue was taken up in $CH_2Cl_2$ (50 mL), washed with $H_2O$ (50 mL × 2), washed with brine (20 mL), dried over $MgSO_4$ and concentrated under reduced pressure. The residue was subjected to column chromatography (0.5 × 5 cm, $CH_2Cl_2$), which afforded **4-13** as an oily yellow solid (6 mg, 60%): $R_f$ (5% EtOAc in hexanes) = 0.3 (two narrowly separated spots); LCMS (APCI, positive) *m/z* (%): 1232 (53), 1231 (75), 1230 (91), 1229 (61), 1228 (50), 1216 (56), 1215 (77), 1214 (92), 1213 (100, $M^+$). Attempt to obtain a HRMS spectrum was unsuccessful.

**Belts 3-34.**

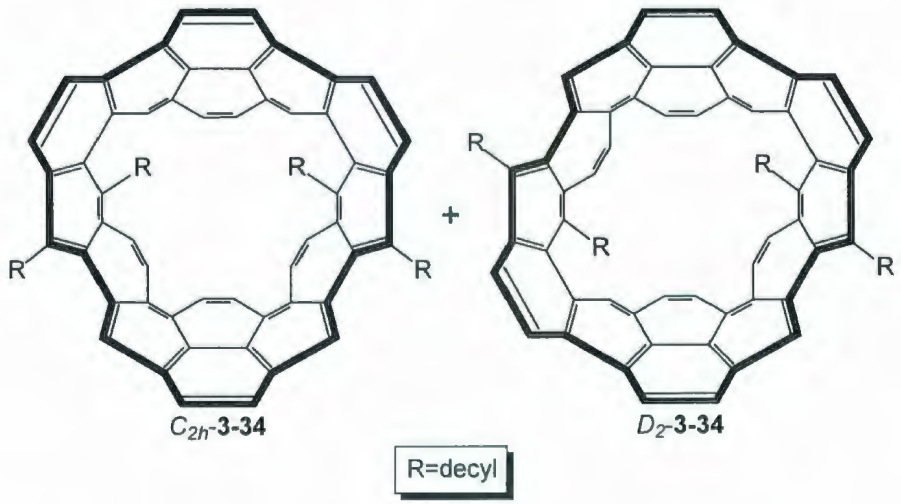


$C_{2h}$-**3-34** $D_2$-**3-34**

A solution of 5,12,22,29-tetradecyl-(1*Z*,17*Z*,33*Z*,35*Z*)-[2$_4$](2,4,9,11)dibenzo[*a,h*]anthracenophane-1,17,33,35-tetraene ($C_{2h}$-**4-13**), 5,12,21,28-tetradecyl-(1*Z*,17*Z*,33*Z*,35*Z*)-

[$2_4$](2,4,9,11)(4,2,11,9)dibenzo[*a,h*]anthracenophane-1,17,33,35-tetraene (*$D_2$*-**4-13**) (1 mg, 0.00008 mmol) and DDQ (6 mg, 0.016 mmol) in benzene (1 mL) was stirred at room temperature for 60 min and then concentrated under reduced pressure. The residue was subjected to column chromatography (pipette column, $CH_2Cl_2$), which afforded **3-34** as an oily yellow solid: $R_f$ (5% EtOAc in hexanes) = 0.2 (two narrowly separated spots); LCMS (APCI, positive) *m/z* (%): 1211 (40), 1210 (92), 1209 (100, $M^+$). Attempt to obtain a HRMS spectrum was unsuccessful.

**4.5 References:**


1. Laarhoven, W. H.; Cuppen, T. J. H. M.; Nivard, R. J. F. *Tetrahedron*, **1970**, *26*, 1069.
2. Blum, J.; Zimmerman, M. *Tetrahedron*, **1972**, *28*, 275.
3. Hammond, G. S.; Saltiel, J.; Lamola, A. A.; Turro, N. J.; Bradshaw, J. S.; Cowan, D. O.; Counsell, R. C.; Vogt, V.; Dalton, C. *J. Am. Chem. Soc.* **1964**, *86*, 3197.
4. Yu, H. M.Sc. Thesis, Memorial University, 2004.
5. Suzuki, H. *Organic Syntheses*; Wiley: New York, **1988**, Collect. Vol. VI, 700.
6. Gallagher, W, P.; Terstiege, I.; Maleczka, R. E. *J. Am. Chem. Soc.* **2001**, *123*, 3194.
7. Maleczka, R. E. Jr.; Lavis, J. M.; Clark, D. H.; Gallagher, W. P. *Org. Lett.* **2000**, *2*, 3655.
8. http://www2.sisweb.com/mstools/isotope.htm Feb. 25, 2009.

# Appendix A

## Calculation of the Number of Possible Isomers of Compounds 3-31 and 4-11

When the backbones of **3-31** adopt average conformations, the point groups of the backbones are $C_{2h}$ and $D_2$. Therefore, the discussion will be divided into two different cases. Two independent strategies will be applied to each case. The first strategy is symmetry-based and the second strategy is a substituent-based approach. For the sake of clarity, solublizing groups are omitted (Figure A1-1).

### A1. $C_{2h}$ backbone

A1.1 Strategy 1

The first strategy involves the following steps:

1. Calculation of the total possible number of isomers.

   On each bridge of the cyclophane molecule, there should be one, and only one substituent attached. Since there are four points of attachment in each of the four ethano bridges (2 *pseudo*-axial and 2 *pseudo*-equatorial, see Figure A1-2), the maximum possible number of stereoisomers is $4^4$=256.

2. Analysis of the symmetry of every possible isomers

   a) In all of these 256 possible isomers, the plane of symmetry of the original $C_{2h}$-symmetric backbone is destroyed. In the absence of any substituents, the two carbon atoms of each ethano bridge are related to one another by the molecular plane of symmetry. When one site of an ethano bridge is substituted, the adjacent site must be unsubstituted.

b) 16 of the 256 possible isomers maintain the $C_2$ axis from the original $C_{2h}$ symmetry of the backbone (Figure A1-3).

c) Another 16 of the 256 possible isomers maintain the center of inversion from the original $C_{2h}$ symmetry (Figure A1-4).

d) All of the ramaining 224 possible isomers (256-16-16) have $C_1$ symmetry.

3. Evaluation of each case shown in Step 2.

a) $C_2$: These 16 possible isomers reduce to 8 pairs of enantiomers (Figure A1-3).

b) $C_i$: These 16 possible isomers reduce to 8 *meso*-compounds (Figure A1-4).

c) $C_1$: The remaining 224 possible isomers (256-16-16) falls into 56 groups of four consisting of in which there are two pairs of equivalent structures, which are enantiomers of one another (Figure A1-5). Thus there are 56 pairs of enantiomers.

4. Totaling of the result in Step 3.

Total number=56+8+8=72 (64 pairs of enantiomers and 8 *meso* compounds)

A1.2 The second strategy (substituent-based) involves the following steps:

1. Separate all possible isomers into 3 groups: a) all subsitituents are adjacent to the same molecular board, b) 1 subsitituent is adjacent to one board and other 3 subsitituents are adjacent to the other board, and c) 2

substituents are adjacent to one board and other 2 substituents are adjacent to the other board.

2. Calculate numbers of isomers in each group.

   a) (4,0) group

      1) Total possible isomers in this case equal to $2^4 \times 2^1 = 32$. This is because when all four substituents are adjacent to one molecular board, each substituent has two possible orientations, i.e., *pseudo*-axial and *pseudo*-equatorial. Thus there are $2^4 = 16$ possible isomers. When the four substituents are adjacent to the other molecular board of the backbone, there are another 16 possible isomers. The total number of the (4,0) group is $2^4 \times 2 = 32$.

      2) 8 out of these 32 possible isomers contain a $C_2$ axis and reduce to 4 pairs of enantiomers (Figure A1-6, **$A_{C2h}$-18** – **$A_{C2h}$-21**). The remaining 24 possible isomers (32–8) have $C_1$ symmetry, and fall into 6 groups of four, each one consisting of two pairs of equivalent structures. Thus there are 6 pairs of enantiomers (Figure A1-6, **$A_{C2h}$-22** – **$A_{C2h}$-27**).

      3) Total number of the (4,0) group: 6+4=10.

   b) (3,1) group

      1) The total number of possible isomers in this case is equal to $4 \times 2^4 \times 2^1 = 128$. This is because there are four possible sites of substitution (meaning that only the position of substitution and

not the stereochemistry is considered) of the single substituent adjacent to one molecular board (the origin of "4" in the equation). In each of these cases, the other three substituents have only one choice. Each substituent has two possible orientations, *pseudo*-axial and *pseudo*-equatorial (the origin of $2^4$ in the equation). Furthermore, the "1" subsituent in the (3,1) group can be adjacent to the other molecular board of the backbone (the origin of "$2^1$" in the equation).

2) As shown in Figure A1-5, 128 possible isomers have $C_1$ symmetry and fall into 32 groups of four, each one consisting of two pairs of equivalent structures. Thus there are 32 pairs of enantiomers.

c) (2,2) group

1) The total number of possible isomers in this group is equal to $6\times2^4=96$. This is because two substituents adjacent to one molecular board have 6 possible substitution patterns (the origin of "6" in the equation). In each of these cases, the other two substituents have only 1 possible substitution pattern. Each of four substituents has two possible orientations, *pseudo*-axial and *pseudo*-equatorial (the origin of $2^4$ in the equation).

2) If two substituents adjacent to one molecular board are considered first (both position and stereoisomers), there are

totally 14 possible parent isomers (Figure A1-7). Each of these 14 parent isomers has 4 possible isomers when the other 2 substituents are added to the other board. Thus there are 56 possible isomers.

3) The number of unique isomers can be calculated by a brute force method. This method is based on the counting of the unique isomers of the 56 possible isomers. This leads to the identification of 22 pairs of enantiomers and 8 *meso*-compounds (Figure A1-8). In Figure A1-8, the left column shows the positions and stereochemistry of the first two substituents adjacent to the front molecular board (parent isomers) and the four structures to the right are those obtained by adding the other two substituents.

3. Totaling of the results from Step 2:

Total number=10+32+30 (22 pairs of enantiomers + 8 *meso*-compounds) = 72 (64 pairs of enantiomers and 8 *meso*-compounds)

**A2. $D_2$ backbone**

A2.1 General analysis

The $D_2$ backbone itself is chiral. Therefore, each possible isomer on one enantiomer of the backbone has one corresponding enantiomer on the other

backbone. Based on this statement, the calculation will be focused on one enantiomer of the $D_2$ backbone.

A2.2 Strategy 1

This strategy is similar to Strategy 1 used for the calculation of isomers derived from the $C_{2h}$ symmetric backbone and involves the following steps:

1. Calculation of the total possibilities of the number of isomers.

   Since there are four points of attachment in each of the four ethano bridges (2 *pseudo*-axial and 2 *pseudo*-equatorial), the maximum possible combined number of stereoisomers is $4^4$=256.

2. Analysis of the symmetry of every possible isomer

   a. 36 out of this 256 maintain one and only one $C_2$ axis of the 3 twofold axes present in the original $D_2$ symmetry (Figure A1-9, **$A_{D2}$-01** – **$A_{D2}$-06**, **$A_{D2}$-11** – **$A_{D2}$-22**). To maintain any one $C_2$ axis, only 2 substituents of the 4 are free to be varied in terms of position and stereochemistry because the position and stereochemistry of the other two substituents is dictated by the twofold axis. Each of the three $C_2$ axes gives 16 possible isomers ($2^4$), in which 12 have $C_2$ symmetry and 4 have $D_2$ symmetry. Thus there are up to 48 possible isomers (3 $C_2$ axes % 16). However, in these 48 possible isomers, the 12 isomers having $D_2$ symmetry reduce to 4 isomers because the consideration of each $C_2$ axis affords the same set of 4 $D_2$ isomers (Figure A1-9, **$A_{D2}$-07** – **$A_{D2}$-10**, shown in FigureA1-9-1,

Figure A1-9-2, and Figure A1-9-3). Therefore, 40 of the 256 possible isomers retain at least one $C_2$ axis (36 have $C_2$ symmetry and 4 have $D_2$ symmetry).

b. All of other 216 possible isomers (256-40) have $C_1$ symmetry.

3. Evaluation of each case shown in Step 2.

   a. $C_2$: These 36 possible isomers reduce to 18 isomers due to equivalence (Figure A1-9, **$A_{D2}$-01** – **$A_{D2}$-06**, **$A_{D2}$-11** – **$A_{D2}$-22**).

   b. $D_2$: These 4 possible isomers do not reduce due to equivalence, leaving 4 isomers (Figure A1-10, **$A_{D2}$-07** – **$A_{D2}$-10**).

   c. $C_1$: These 216 possible isomers (256-36-4) have $C_1$ symmetry, and fall into 54 groups of four, each one consisting of 4 equivalent structures. Thus there are 54 isomers. (Figure A1-11).

4. Totaling of the results from Step 3.

   Total number=18+4+54=76

A2.3 Strategy 2

This strategy is similar to Strategy 2 of calculation of $C_{2h}$ backbone, and involves the following steps:

1. Separate all possible isomers into 3 groups: a) all subsitituents are adjacent to the same molecular board, b) 1 subsitituent is adjacent to one board and other 3 subsitituents are adjacent to the other board, and c) 2 substituents are adjacent to one board and other 2 substituents are adjacent to the other board.

2. Calculate numbers of isomers in each group.

a) (4,0) group

1) The total number of possible isomers in this case is equal to $2^4x2^1=32$. This is because when all four substituents are adjacent to one molecular board, each substituent has two possible orientations, i.e., *pseudo*-axial and *pseudo*-equatorial. Thus there are $2^4=16$ possible isomers. When the four substituents are adjacent to the other molecular board of the backbone, there are another 16 possibilities. The total number of the (4,0) group is $2^4\times2=32$.

2) 8 out of these 32 possible isomers contain a $C_2$ axis and reduce to 4 possible isomers due to equivalence (Figure A1-12, **$A_{D2}$-24 – $A_{D2}$-27**). The remaining 24 possible isomers (32–8) have $C_1$ symmetry, and fall into 6 groups of four, each one consisting of four equivalent structures. Thus there are 6 possible isomers (Figure A1-12, **$A_{D2}$-28 – $A_{D2}$-33**).

3) Total number of the (4,0) group: 6+4=10.

b) (3,1) group

1) The total number of possible isomers in this case is equal to $4\times2^4\times2^1=128$. This is because there are four possible sites of substitution (meaning that only the position of substitution and not the stereochemistry is considered) of the single substituent adjacent to one molecular board (the origin

of "4" in the equation). In each of these cases, the other three substituents have only one choice. Each substituent has two possible orientations, *pseudo*-axial and *pseudo*-equatorial (the origin of $2^4$ in the equation). Furthermore, the "1" subsituent in the (3,1) group can be adjacent to the other molecular board of the backbone (the origin of "$2^1$" in the equation).

2) As shown in Figure A1-11, 128 possible isomers have $C_1$ symmetry and fall into 32 groups of four, each one consisting of four equivalent structures. Thus there are 32 possible isomers.

c) (2,2) group

1) The total number of possible isomers in this group is equal to $6\times2^4=96$. This is because two substituents adjacent to one molecular board have 6 possible substitution patterns (origin of "6" in the equation). In each of these cases, the other two substituents have only 1 possible substitution pattern. Each of four substituents has two possible orientations, *pseudo*-axial and *pseudo*-equatorial (the origin of $2^4$ in the equation).

2) If two substituents adjacent to one molecular board are considered first (both position and stereoisomers), there are totally 14 possible parent isomers (Figure A1-13). Each of these 14 parent isomers has 4 possible isomers when the

other 2 substituents are added to the other board. Thus there are 56 possible isomers.

3) The number of unique isomers can be calculated by a brute force method. This method is based on the counting of the unique isomers of the 56 possible isomers (similar to the previous brute force method), and leads to the identification of 34 isomers (Figure A1-14). In Figure A1-14, the left column shows the positions and stereochemistry of the first two substituents adjacent to the front molecular board (parent isomers) and the four structures to the right are those obtained by adding the other two substituents.

3. Totaling of the results from Step 2:

Total number=10+32+34=76 (76 pairs of enantiomers if the chirality of the backbone is considered)

All 148 possible isomers are shown in Figure A1-15

Structures of all isomers are shown in the following pages. Some isomers have more than one compound number due to equivalence, i.e., **$A_{C2h}$-01** (equivalent to **$A_{C2h}$-18**), **$A_{C2h}$-02** (equivalent to **$A_{C2h}$-19**), **$A_{C2h}$-05** (equivalent to **$A_{C2h}$-21**), **$A_{C2h}$-06** (equivalent to **$A_{C2h}$-20**), **$A_{C2h}$-03** (equivalent to **$A_{C2h}$-c-04**), *ent*-**$A_{C2h}$-03** (equivalent to *ent*-**$A_{C2h}$-c-04**), **$A_{C2h}$-04** (equivalent to **$A_{C2h}$-g-01** and *ent*-**$A_{C2h}$-c-01**), *ent*-**$A_{C2h}$-04** (equivalent to **$A_{C2h}$-c-01**), **$A_{C2h}$-07** (equivalent to **$A_{C2h}$-k-**

**01** and *ent*-**$A_{C2h}$-g-04**), *ent*-**$A_{C2h}$-07** (equivalent to **$A_{C2h}$-g-04**), **$A_{C2h}$-08** (equivalent to **$A_{C2h}$-k-04**), *ent*-**$A_{C2h}$-08** (equivalent to **$A_{C2h}$-n-04** and *ent*-**$A_{C2h}$-k-04**), **$A_{C2h}$-09** (equivalent to **$A_{C2h}$-a-01**), **$A_{C2h}$-10** (equivalent to **$A_{C2h}$-b-03**), **$A_{C2h}$-11** (equivalent to **$A_{C2h}$-f-03**), **$A_{C2h}$-12** (equivalent to **$A_{C2h}$-e-01**), **$A_{C2h}$-13** (equivalent to **$A_{C2h}$-i-04**), **$A_{C2h}$-14** (equivalent to **$A_{C2h}$-h-02**), **$A_{C2h}$-15** (equivalent to **$A_{C2h}$-l-02**), **$A_{C2h}$-16** (equivalent to **$A_{C2h}$-m-04**), **$A_{D2}$-01** (equivalent to **$A_{D2}$-24**), **$A_{D2}$-02** (equivalent to **$A_{D2}$-25**), **$A_{D2}$-03** (equivalent to **$A_{D2}$-c-04**), **$A_{D2}$-04** (equivalent to **$A_{D2}$-26**), **$A_{D2}$-05** (equivalent to **$A_{D2}$-27**), **$A_{D2}$-06** (equivalent to **$A_{D2}$-n-01** and **$A_{D2}$-l-04**), **$A_{D2}$-07** (equivalent to **$A_{D2}$-c-01**), **$A_{D2}$-08** (equivalent to **$A_{D2}$-i-04**), **$A_{D2}$-09** (equivalent to **$A_{D2}$-l-01**), **$A_{D2}$-10** (equivalent to **$A_{D2}$-n-04**), **$A_{D2}$-11** (equivalent to **$A_{D2}$-f-02**), **$A_{D2}$-12** (equivalent to **$A_{D2}$-d-02**), **$A_{D2}$-13** (equivalent to **$A_{D2}$-j-03**), **$A_{D2}$-14** (equivalent to **$A_{D2}$-m-02**), **$A_{D2}$-15** (equivalent to **$A_{D2}$-e-01**), **$A_{D2}$-16** (equivalent to **$A_{D2}$-k-04**), **$A_{D2}$-17** (equivalent to **$A_{D2}$-b-02**), **$A_{D2}$-18** (equivalent to **$A_{D2}$-a-01**), **$A_{D2}$-19** (equivalent to **$A_{D2}$-d-03**), **$A_{D2}$-20** (equivalent to **$A_{D2}$-g-03**), **$A_{D2}$-21** (equivalent to **$A_{D2}$-d-03**), **$A_{D2}$-22** (equivalent to **$A_{D2}$-h-04**).

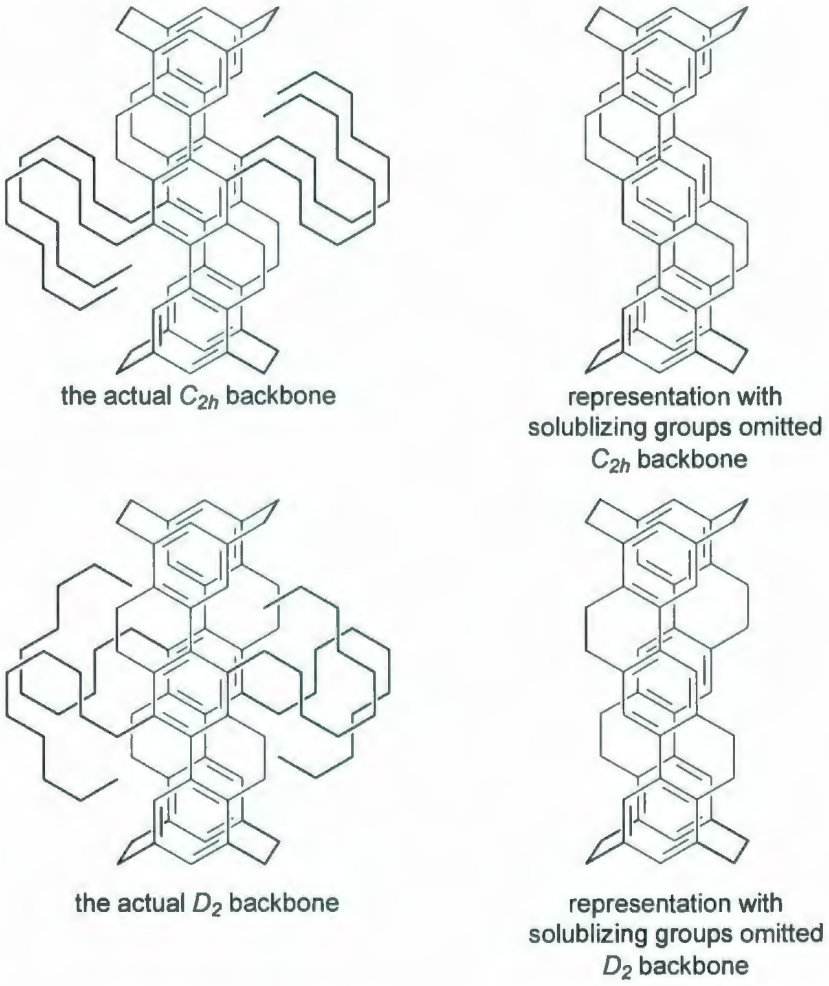


**Figure A1-1.** The representation of $C_{2h}$ and $D_2$ backbones.

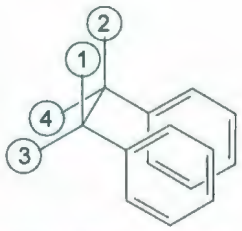


1. *pseudo*-axial, adjacent to the front ring
2. *pseudo*-axial, adjacent to the rear ring
3. *pseudo*-equatorial, adjacent to the front ring
4. *pseudo*-equatorial, adjacent to the rear ring

**Figure A1-2.** Positional and stereochemistry of the substituents.

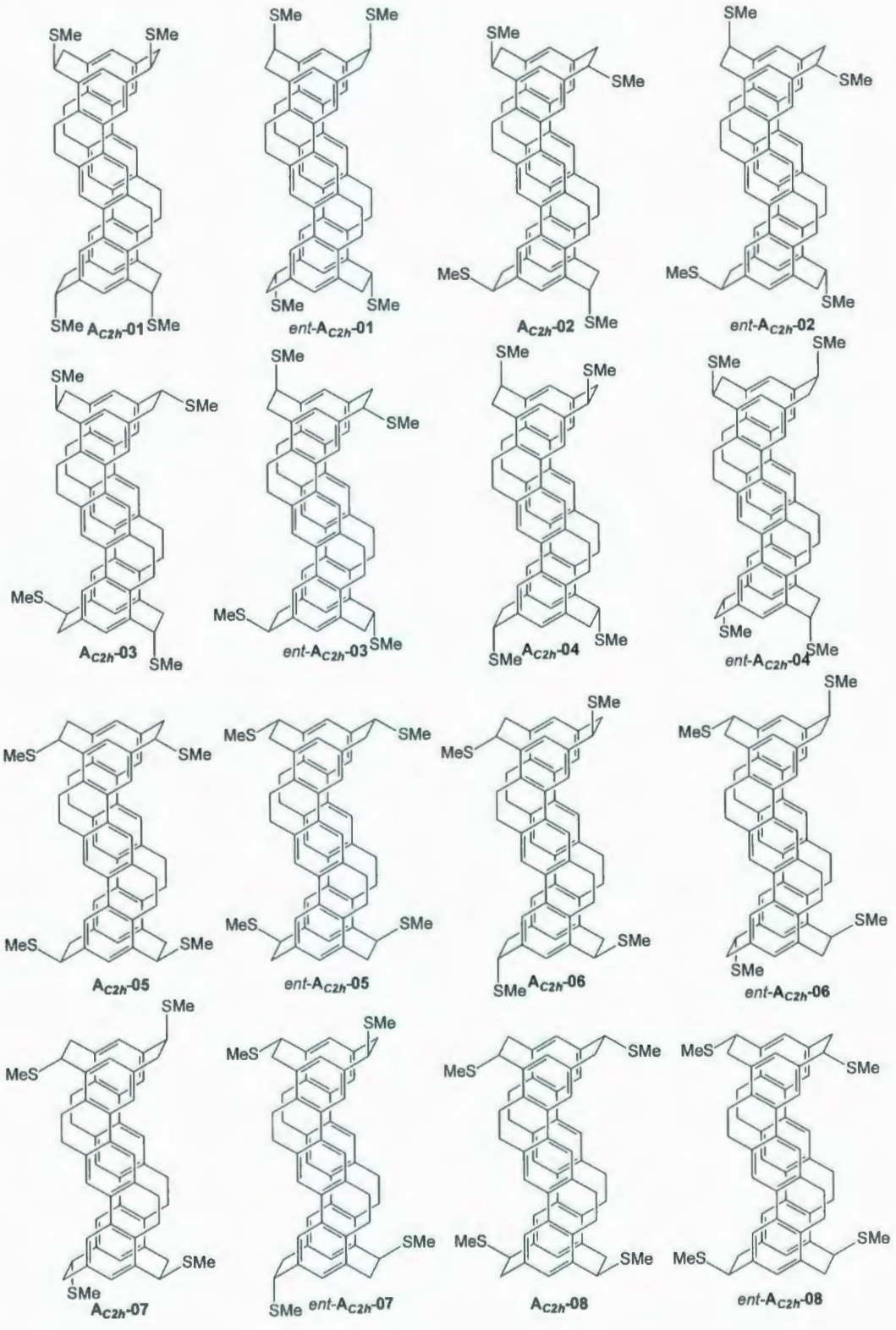


**Figure A1-3.** 8 pairs of enantiomers that have $C_2$ symmetry from $C_{2h}$ backbone.

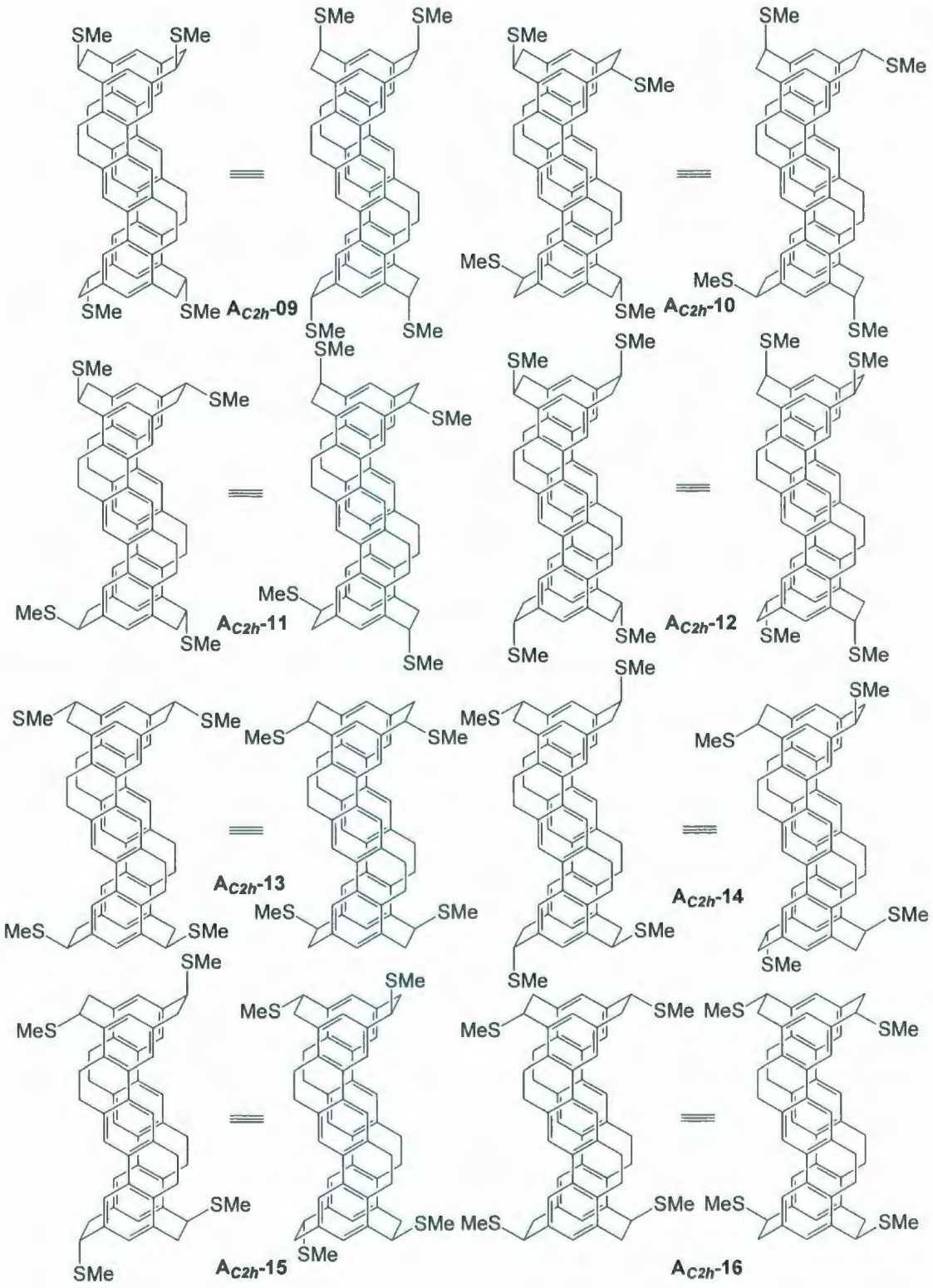


**Figure A1-4.** 8 *meso* possible isomers from $C_{2h}$ backbone.

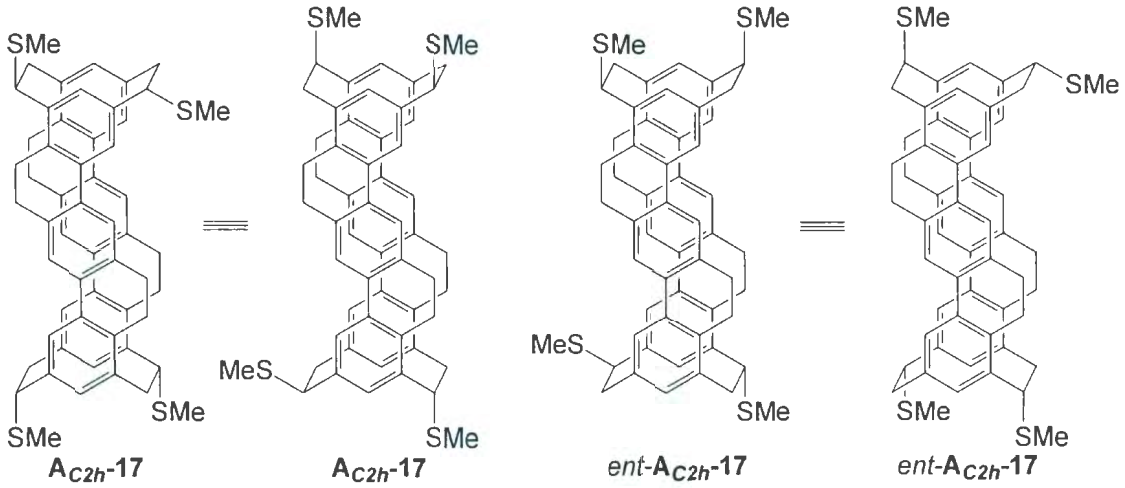


**Figure A1-5.** An example of how 4 possible $C_1$-symmetric isomers reduce to 1 pair of enantiomers.

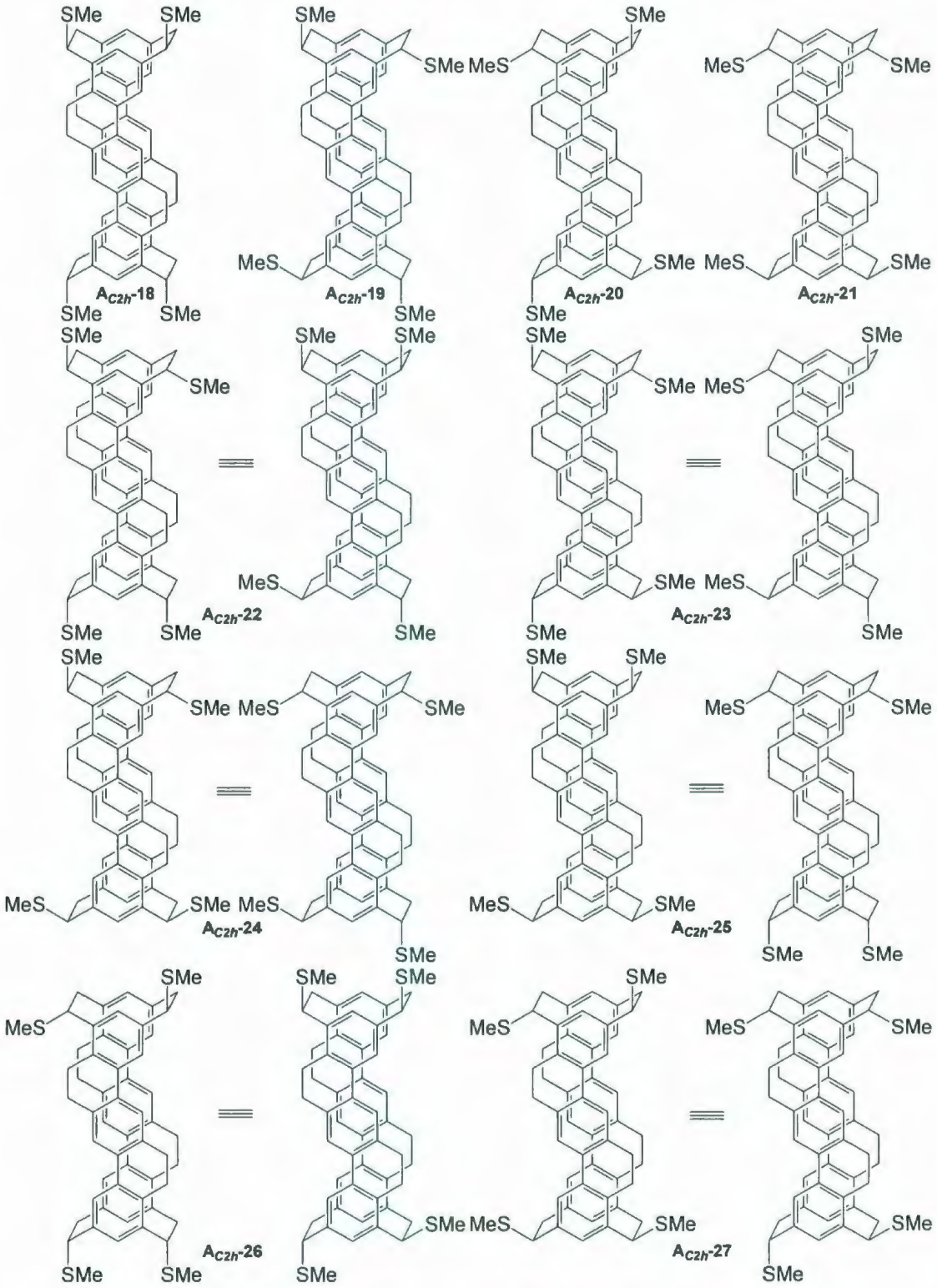


**Figure A1-6.** 10 isomers of the case that 4 substituents are adjacent to one board.

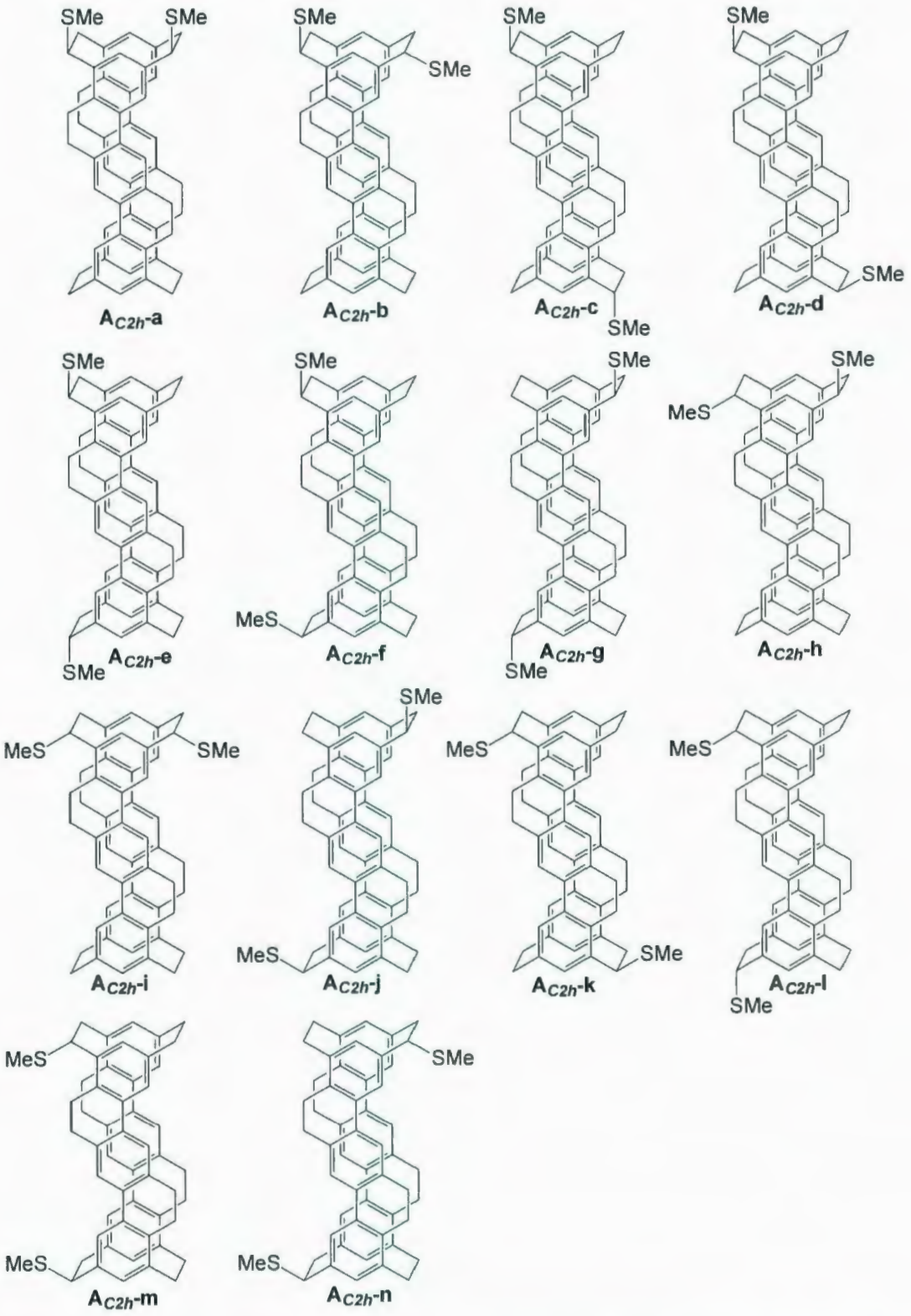


**Figure A1-7.** 14 possible substitution patterns when 2 substituents are added adjacent to one board.

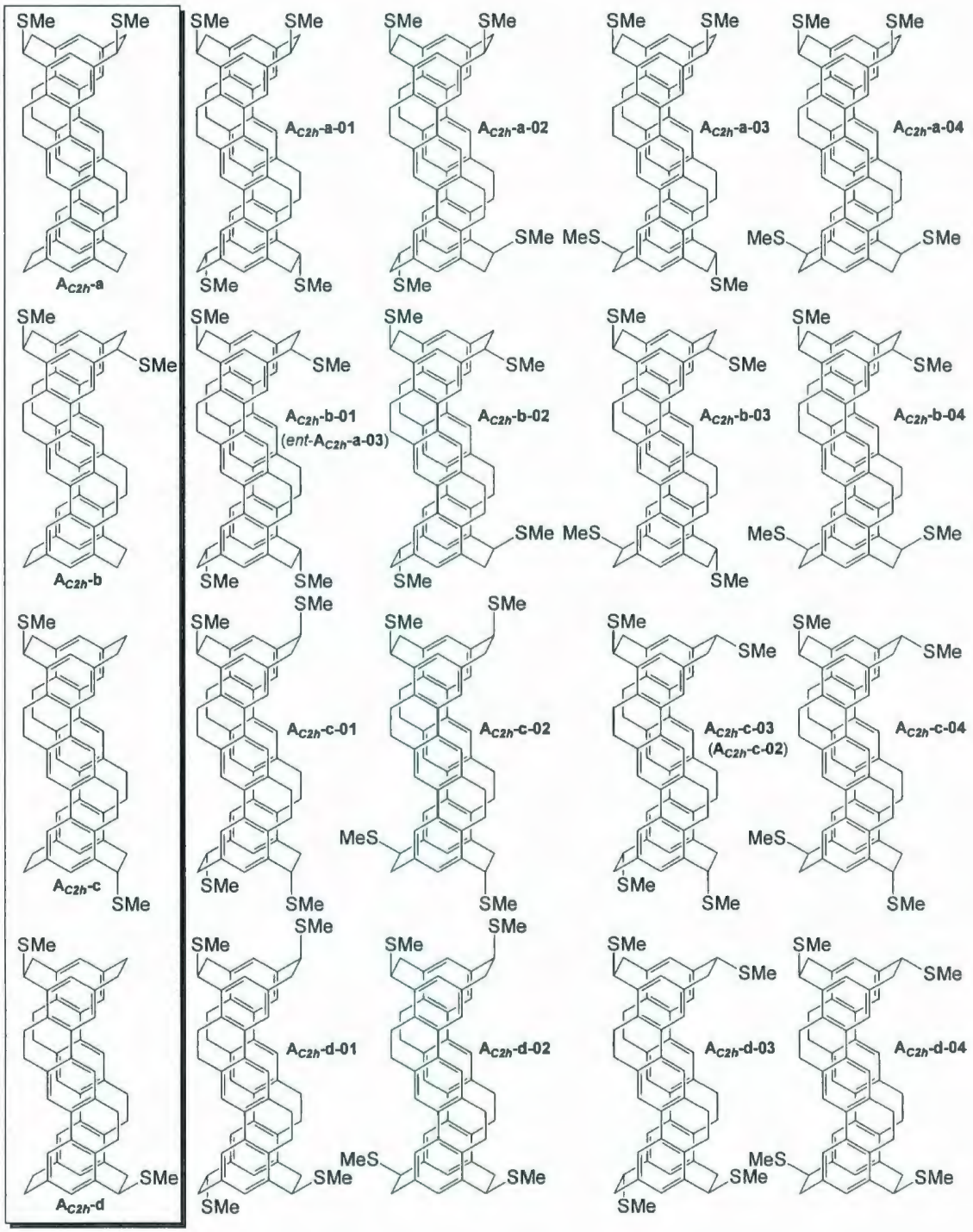


**Figure A1-8-1.** All 56 possible isomers (30 unique structures) (1).

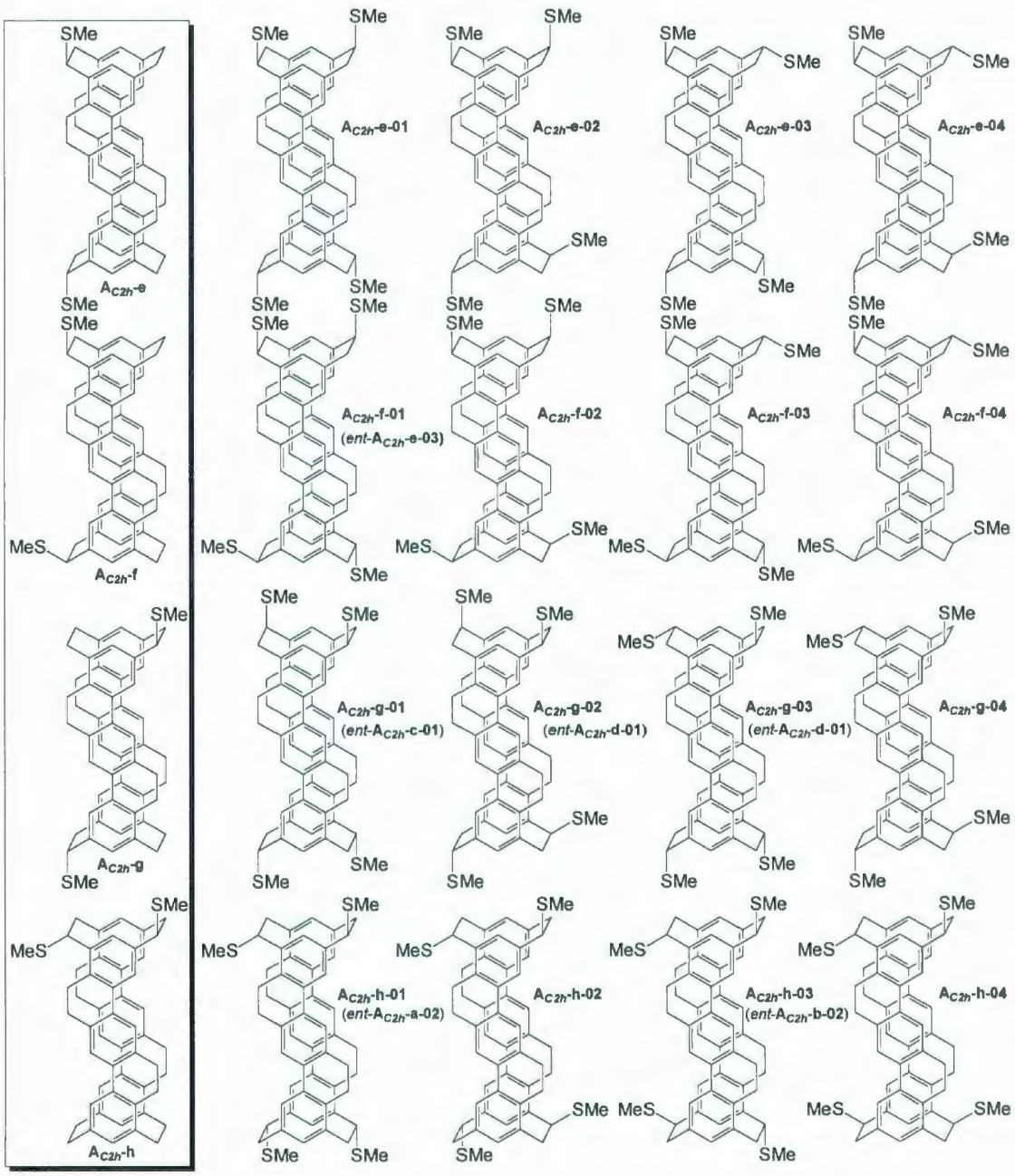


**Figure A1-8-2.** All 56 possible isomers (30 unique structures) (2).

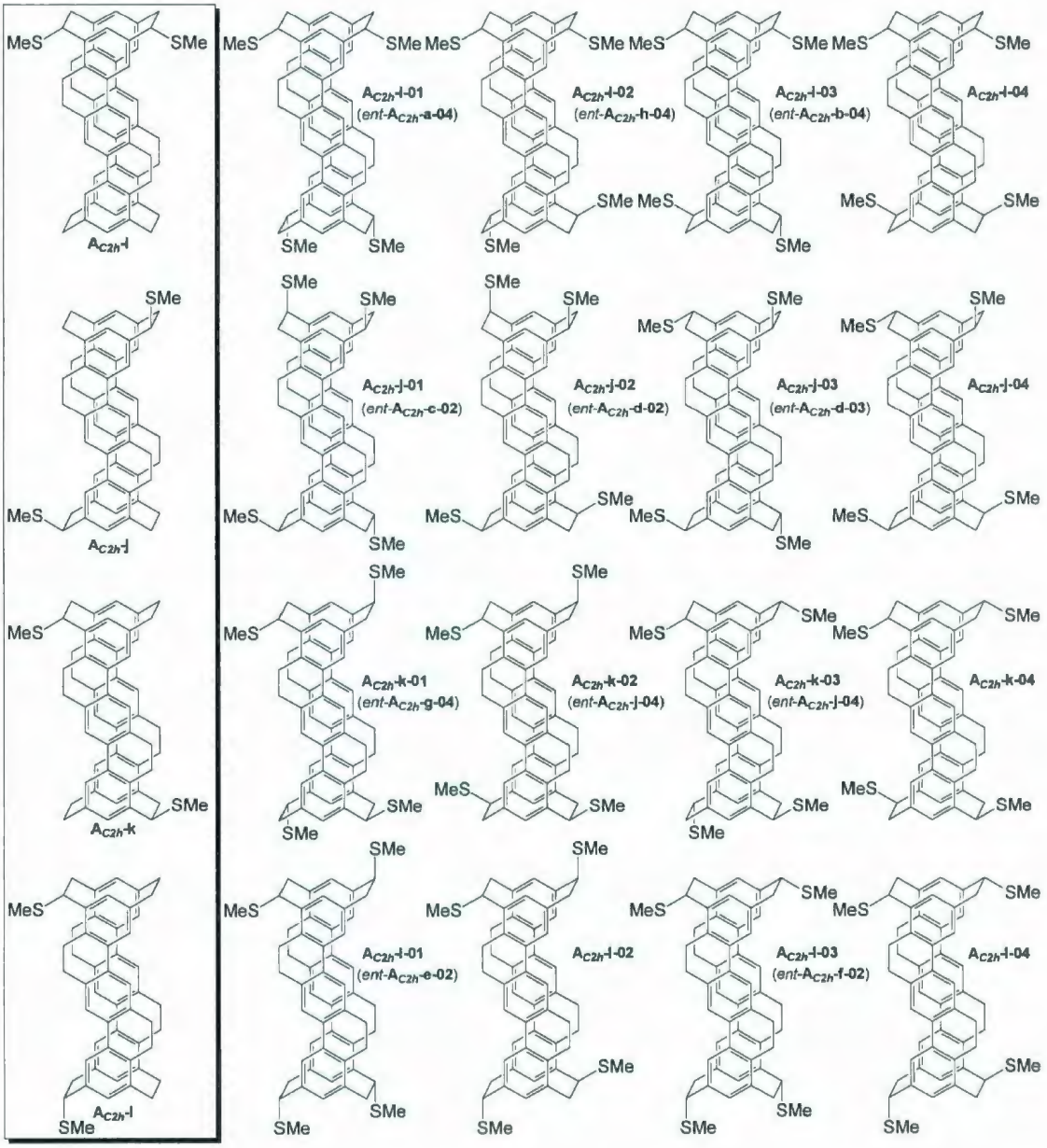


**Figure A1-8-3.** All 56 possible isomers (30 unique structures) (3).

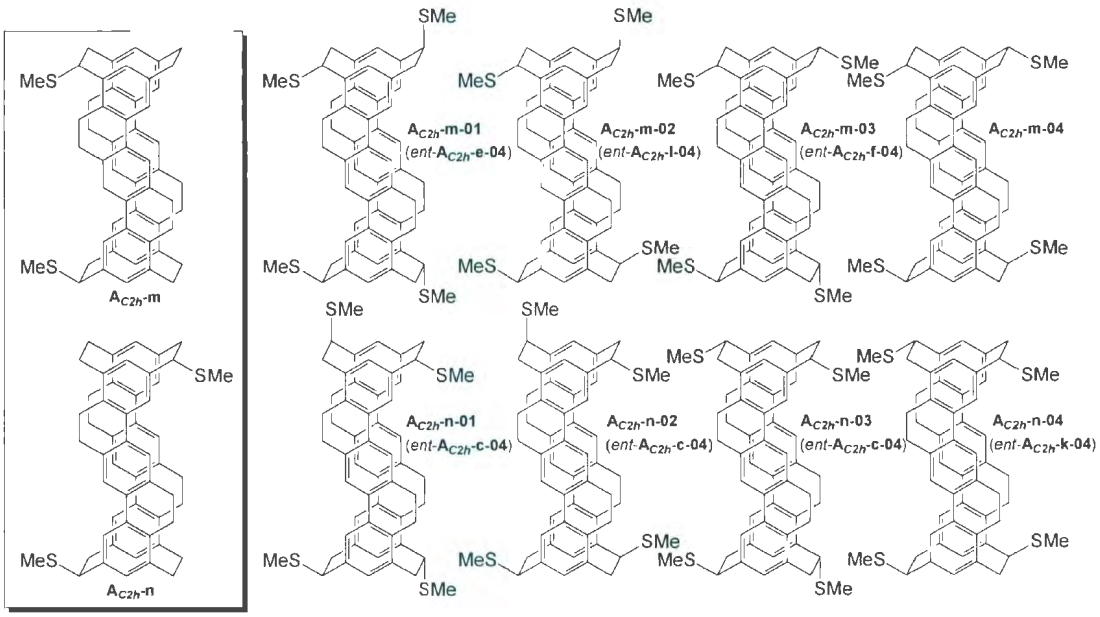


**Figure A1-8-4.** All 56 possible isomers (30 unique structures) (4).

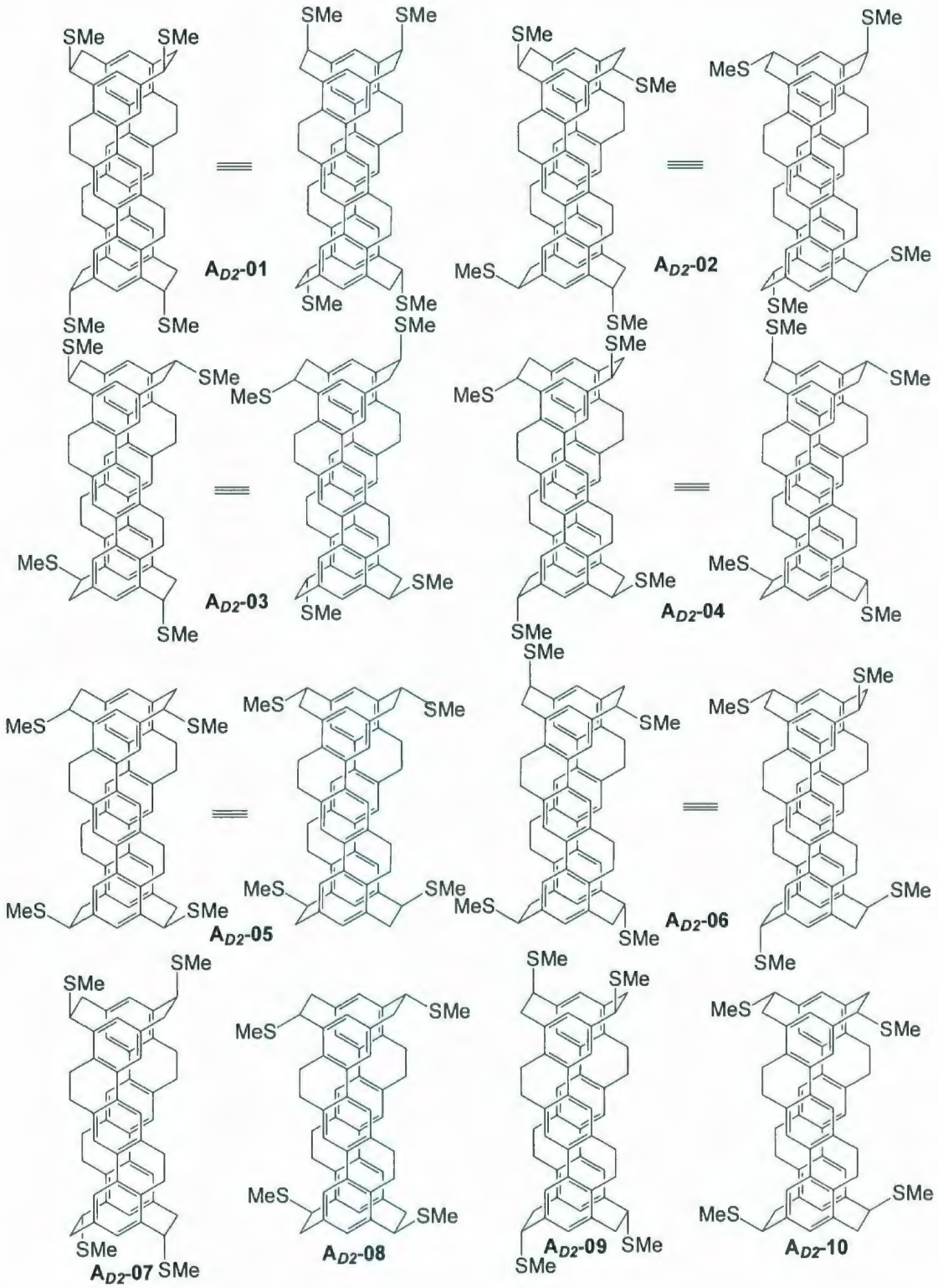


**Figure A1-9-1.** 40 possible isomers that have at least 1 $C_2$ axis (22 isomers) (1).

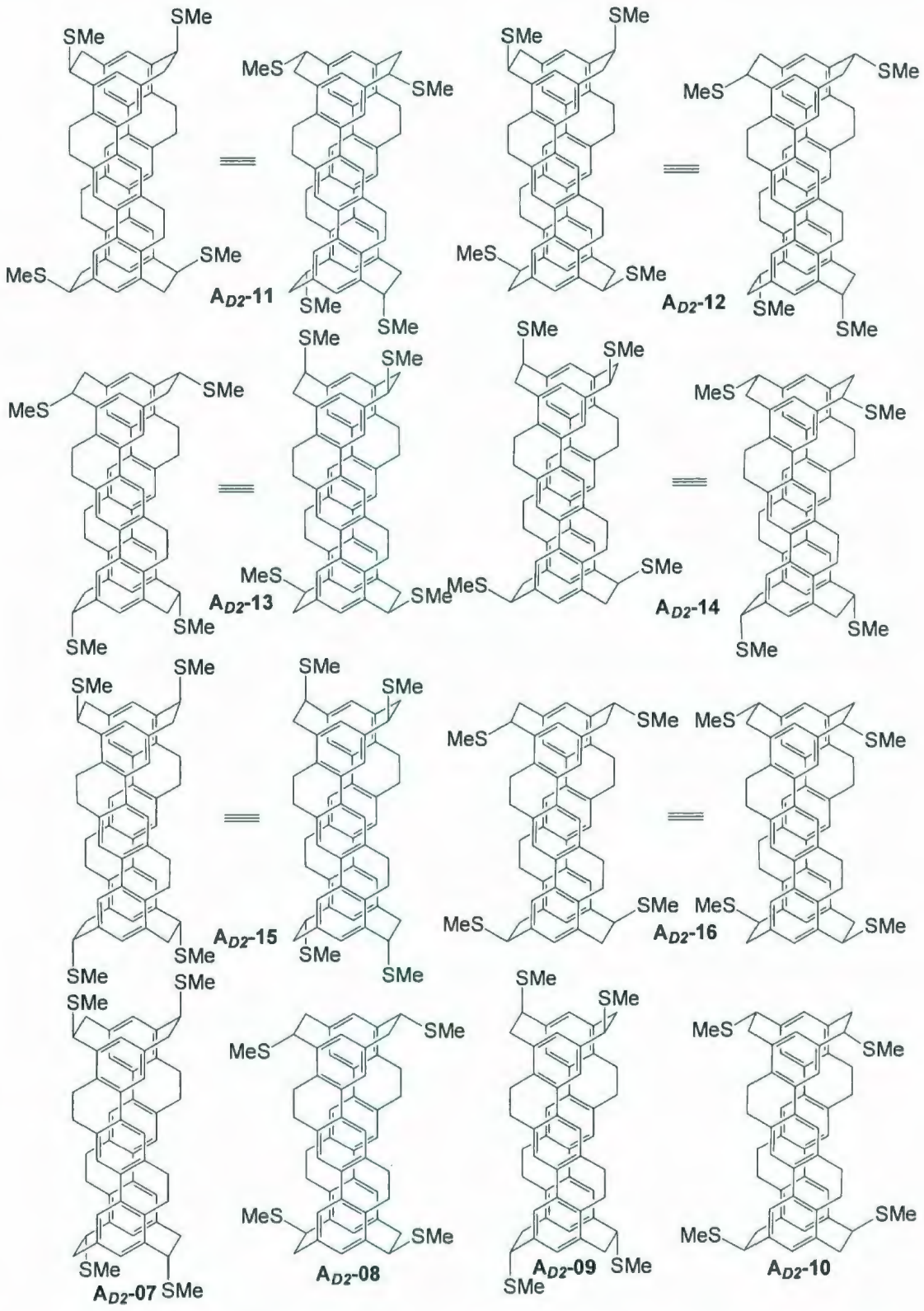


**Figure A1-9-2.** 40 possible isomers that have at least 1 $C_2$ axis (22 isomers) (2).

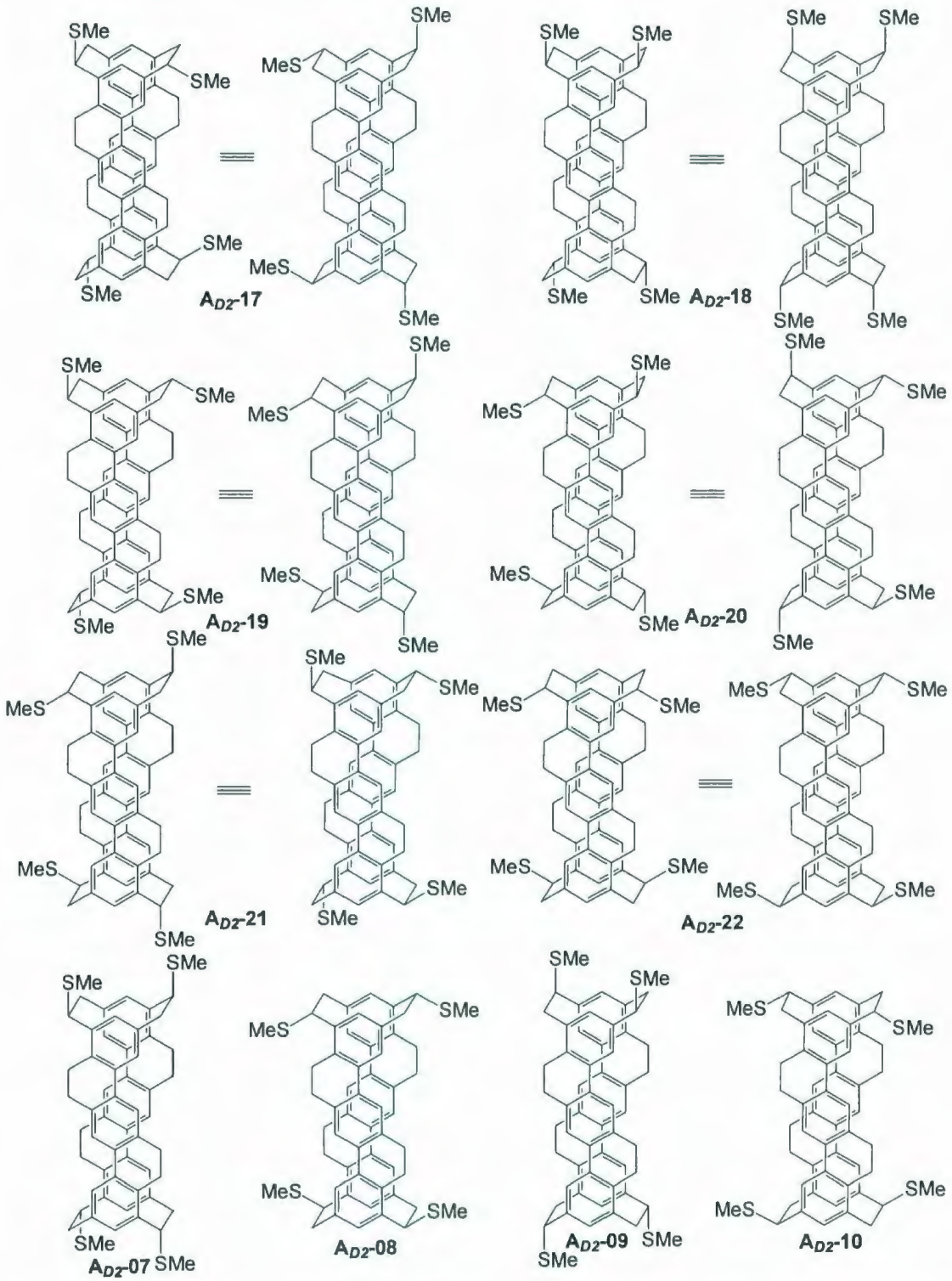


**Figure A1-9-3.** 40 possible isomers that have at least 1 $C_2$ axis (22 isomers) (3).

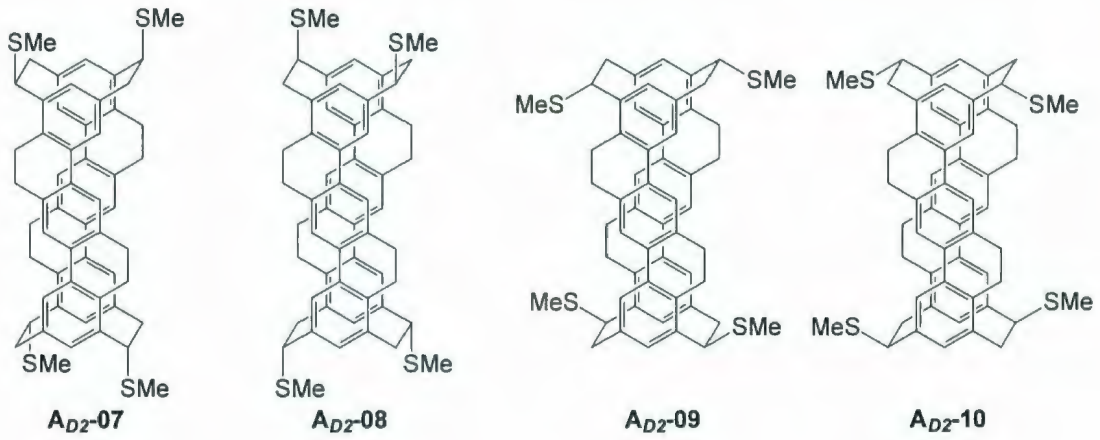


**Figure A1-10.** 4 possible isomers having $D_2$ symmetry (4 isomers).

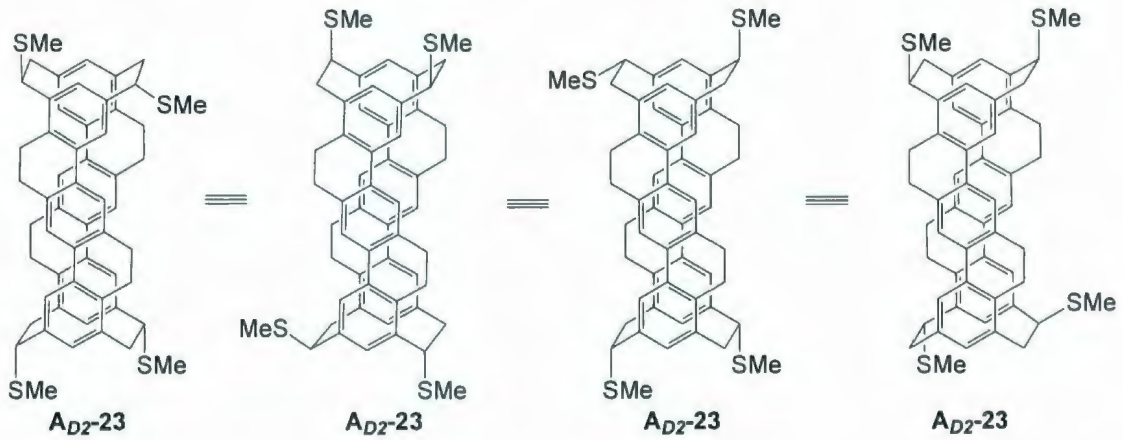


**Figure A1-11.** An example of how 4 possible $C_1$-symmetric isomers reduce to 1 isomer.

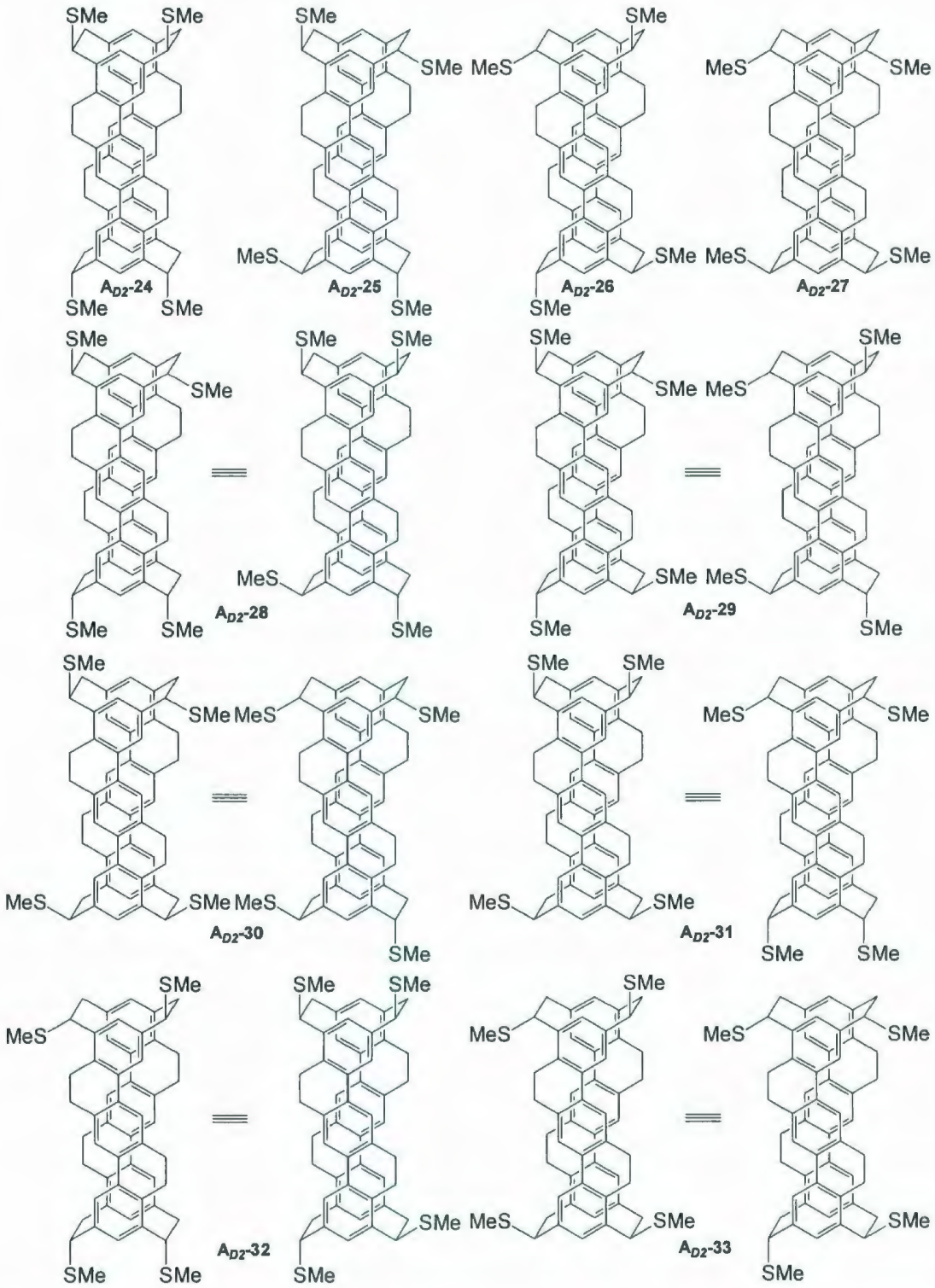


**Figure A1-12.** 10 isomers of the case that 4 substituents are adjacent to one board.

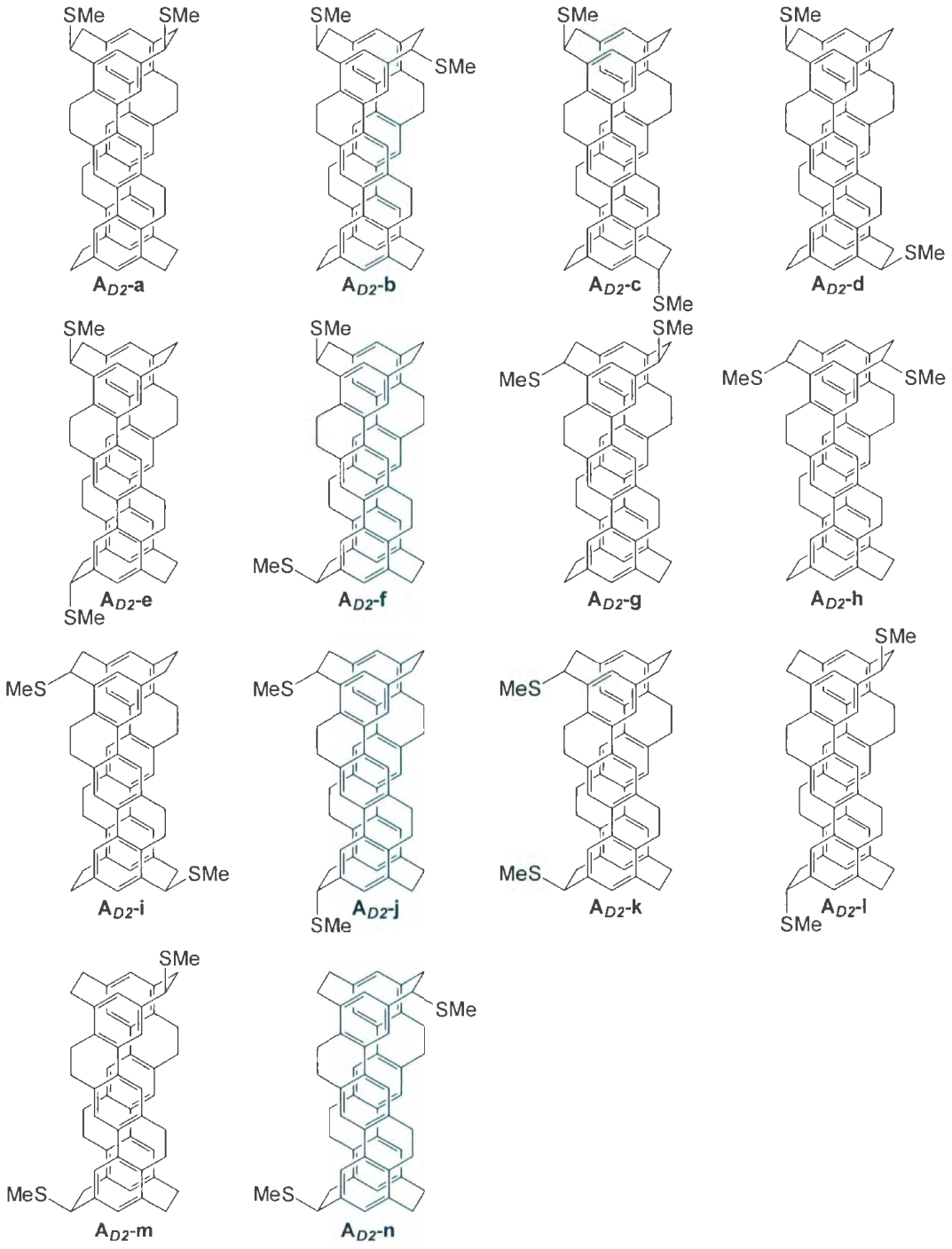


**Figure A1-13.** 14 possible substitution patterns when 2 substituents are added adjacent to one board.

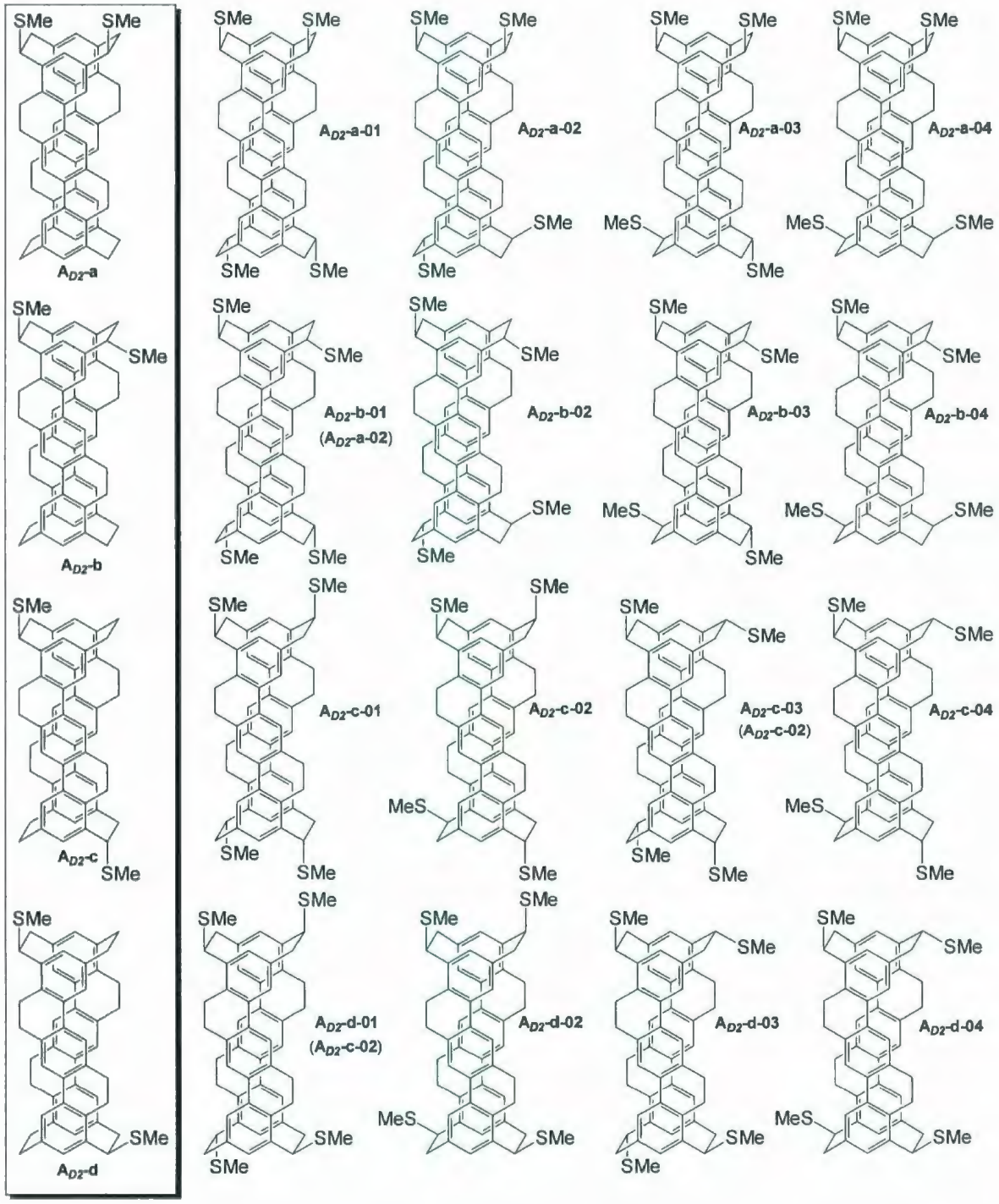


**Figure A1-14-1.** All 56 possible isomers (34 unique structures) (1).

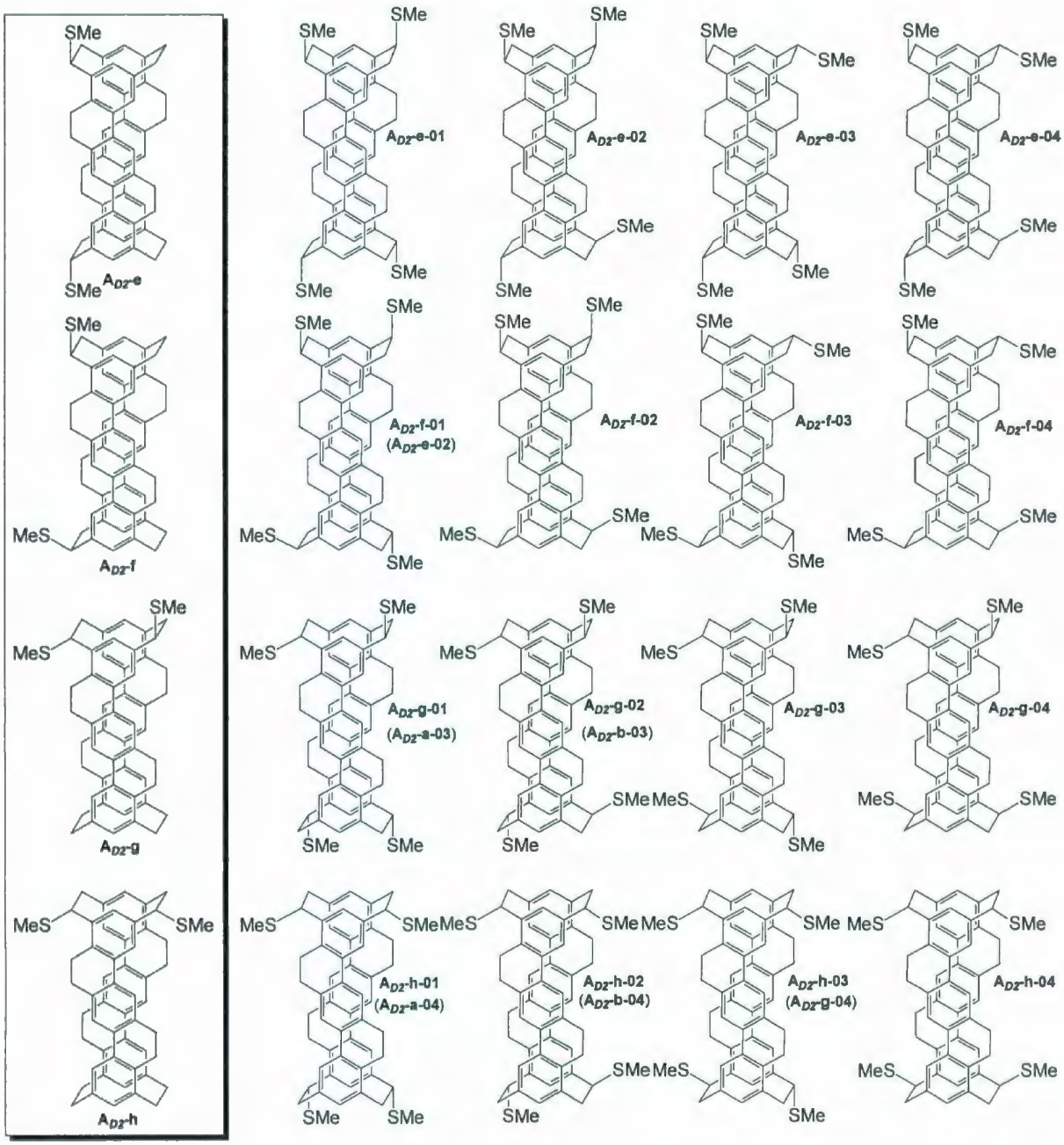


**Figure A1-14-2.** All 56 possible isomers (34 unique structures) (2).

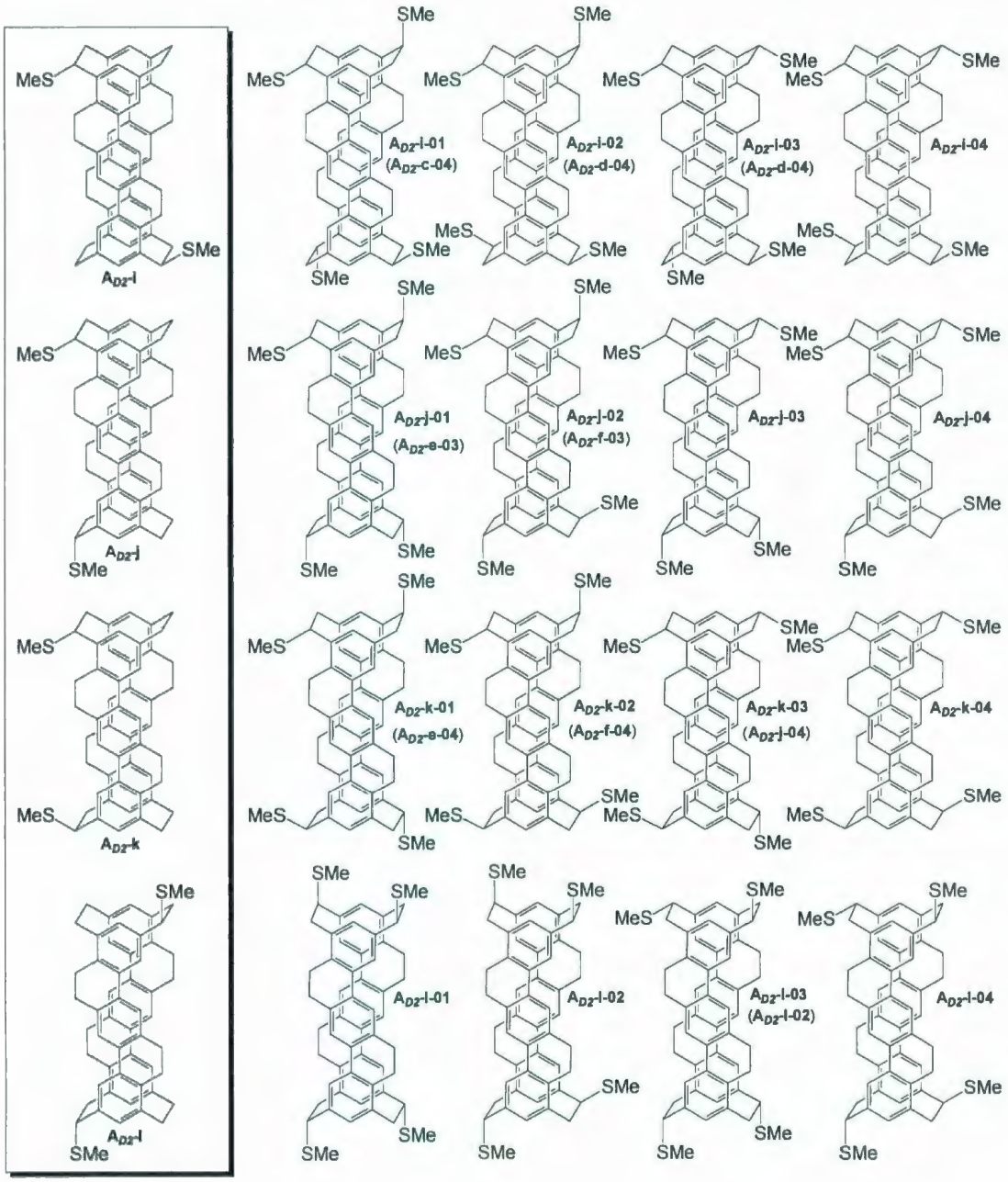


**Figure A1-14-3.** All 56 possible isomers (34 unique structures) (3).

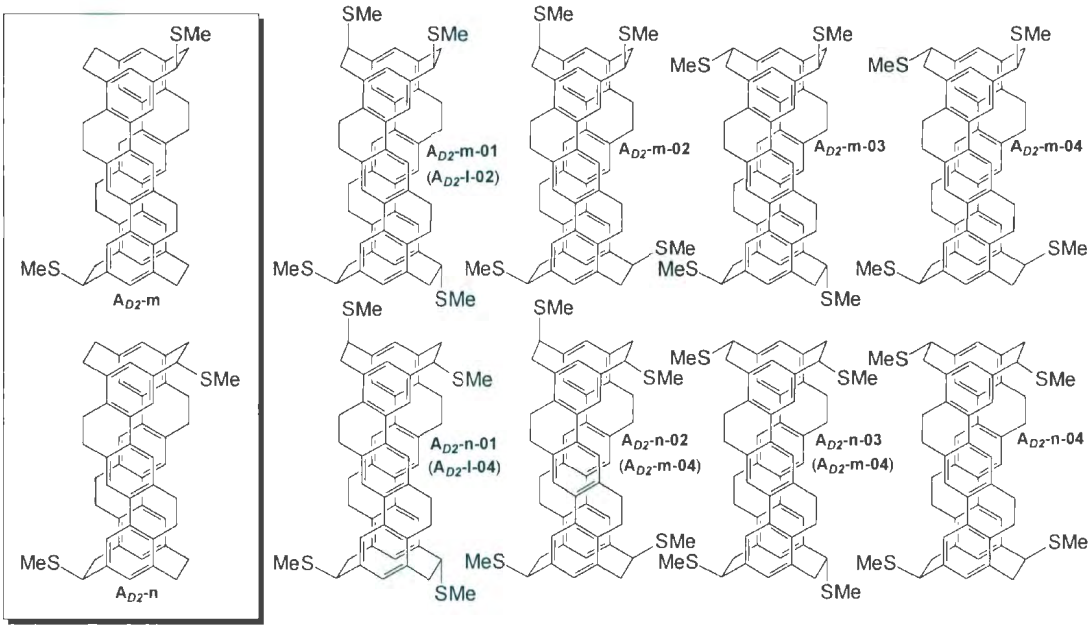


**Figure A1-14-4.** All 56 possible isomers (34 unique structures) (4).

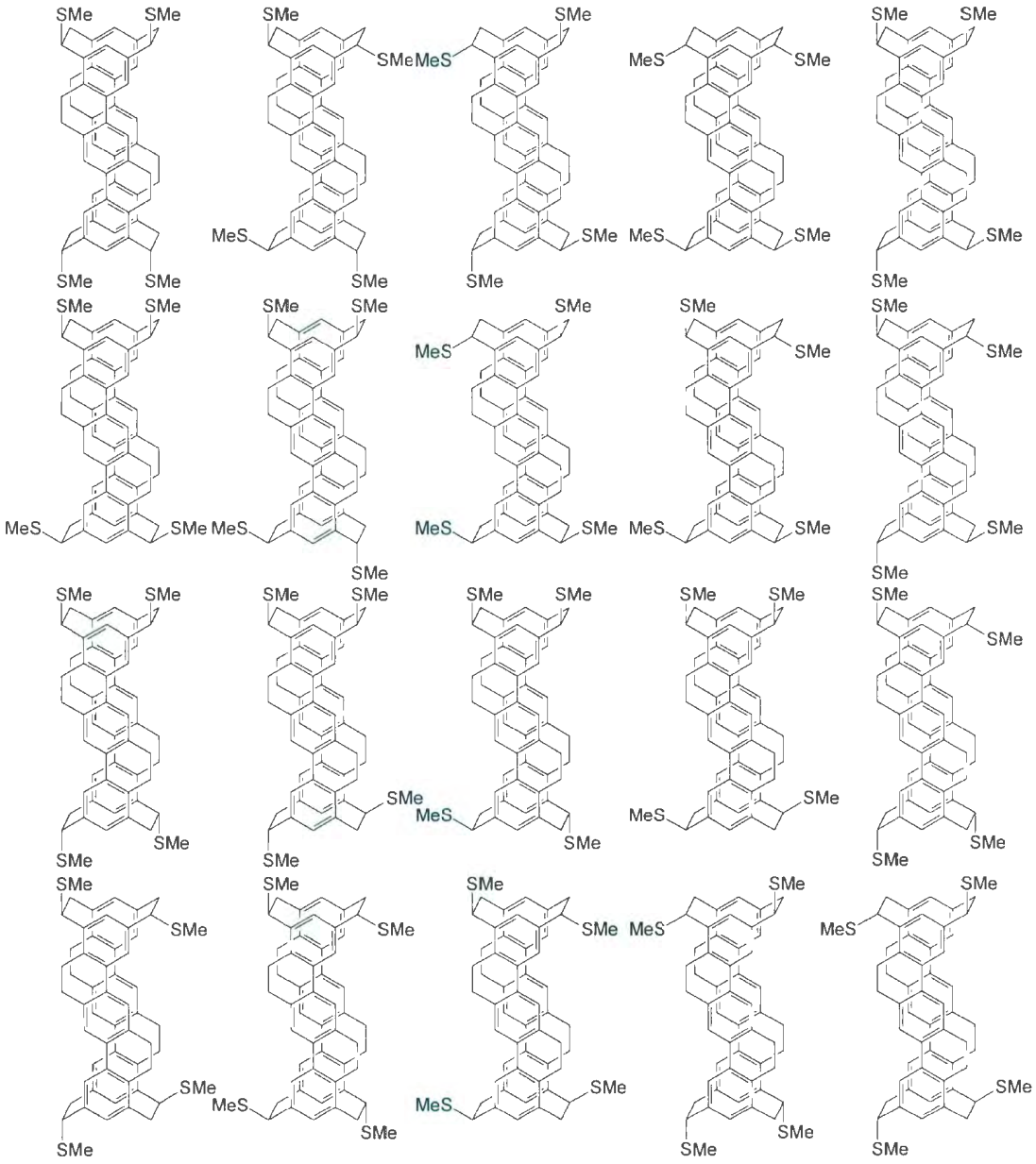


**Figure A1-15-1.** 64 pairs of enantiomers and 8 *meso*-compounds from the $C_{2h}$ backbone (1).

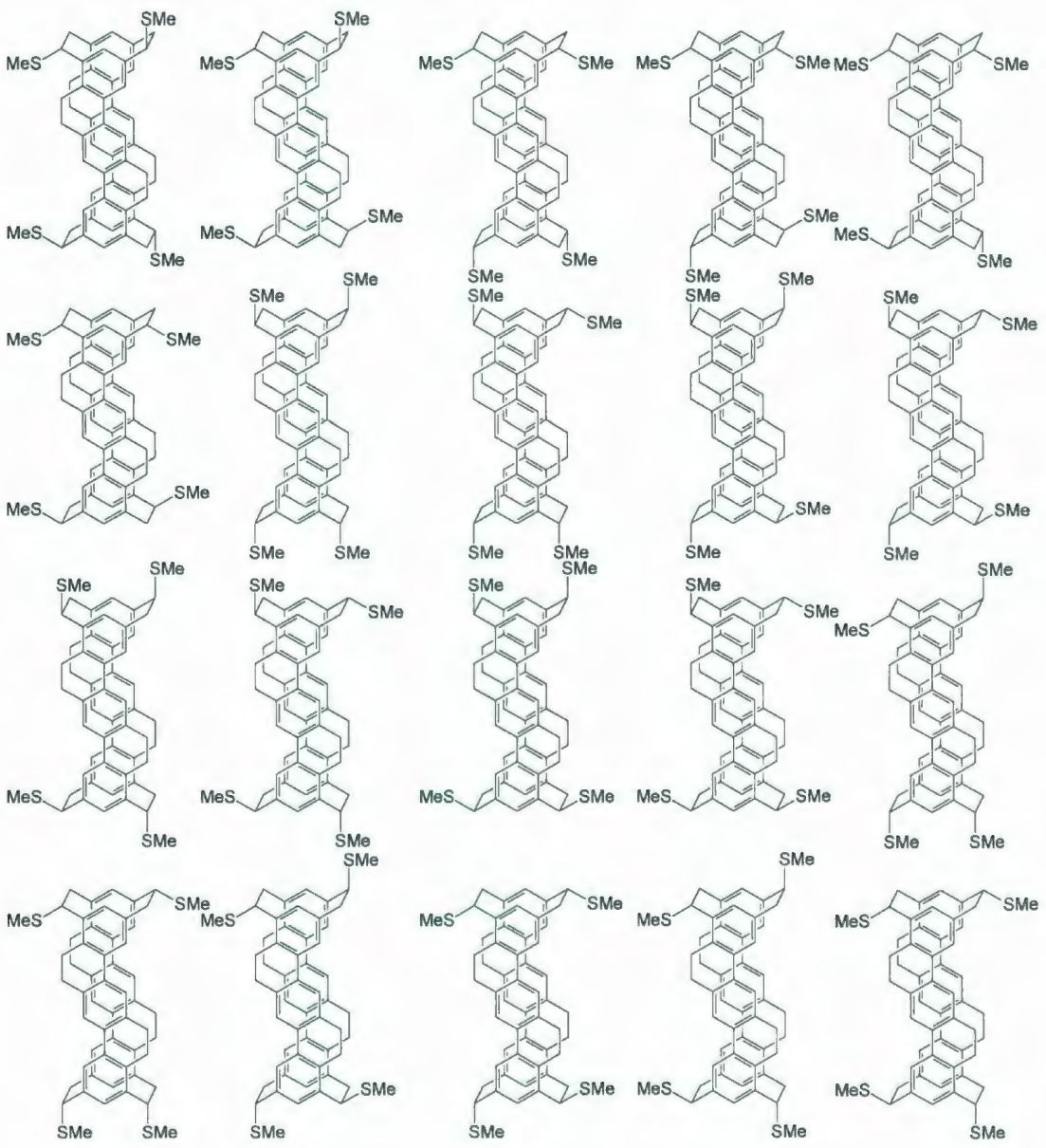


**Figure A1-15-2.** 64 pairs of enantiomers and 8 *meso*-compounds from the $C_{2h}$ backbone (2).

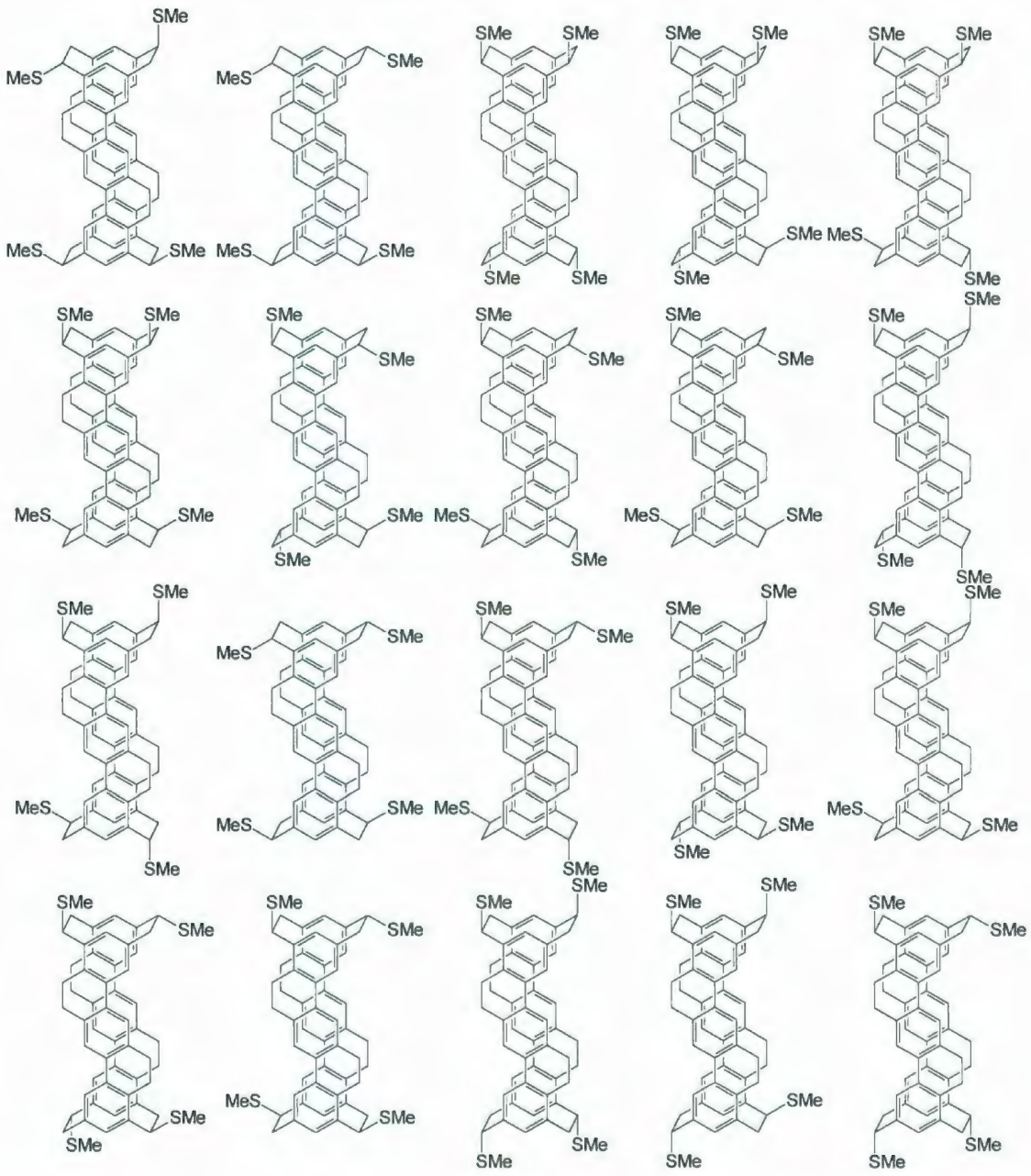


**Figure A1-15-3.** 64 pairs of enantiomers and 8 *meso*-compounds from the $C_{2h}$ backbone (3).

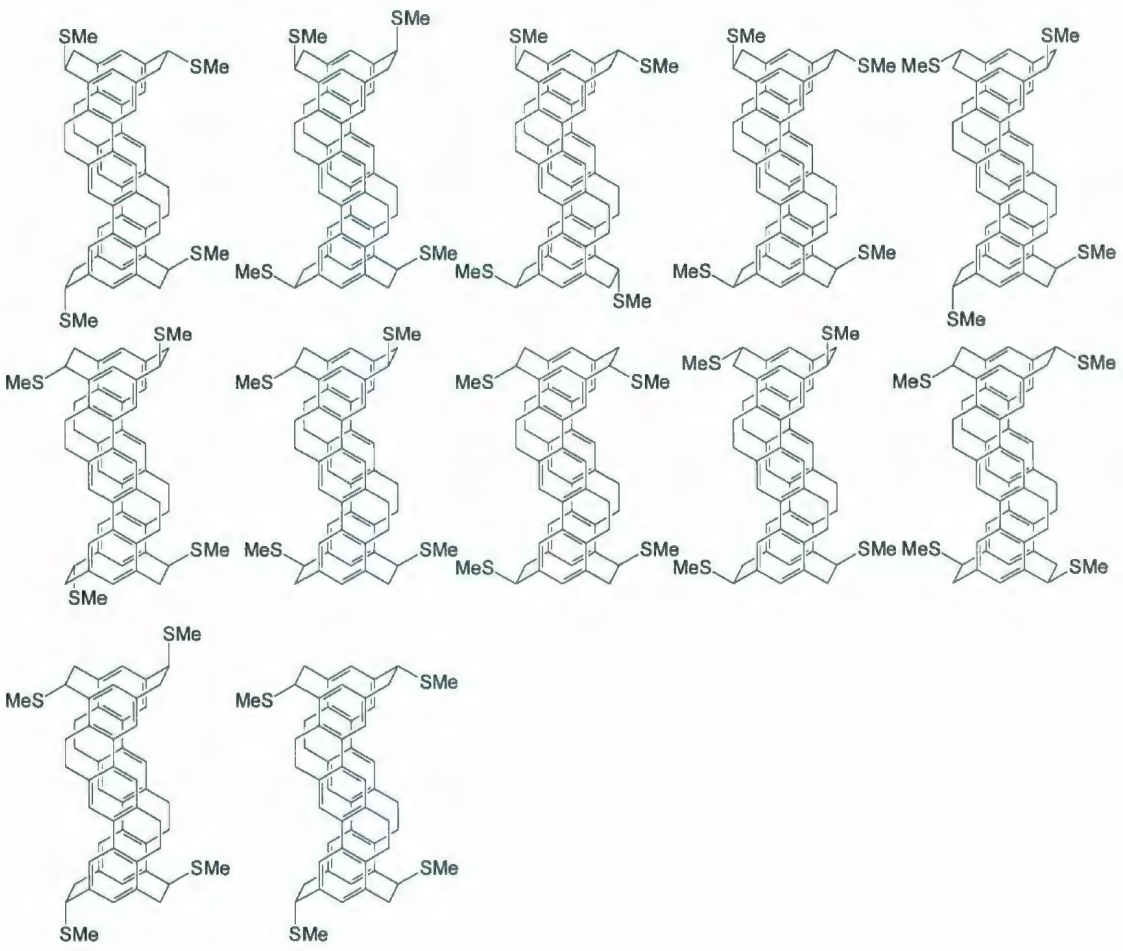


**Figure A1-15-4.** 64 pairs of enantiomers and 8 *meso*-compounds from the $C_{2h}$ backbone (4).

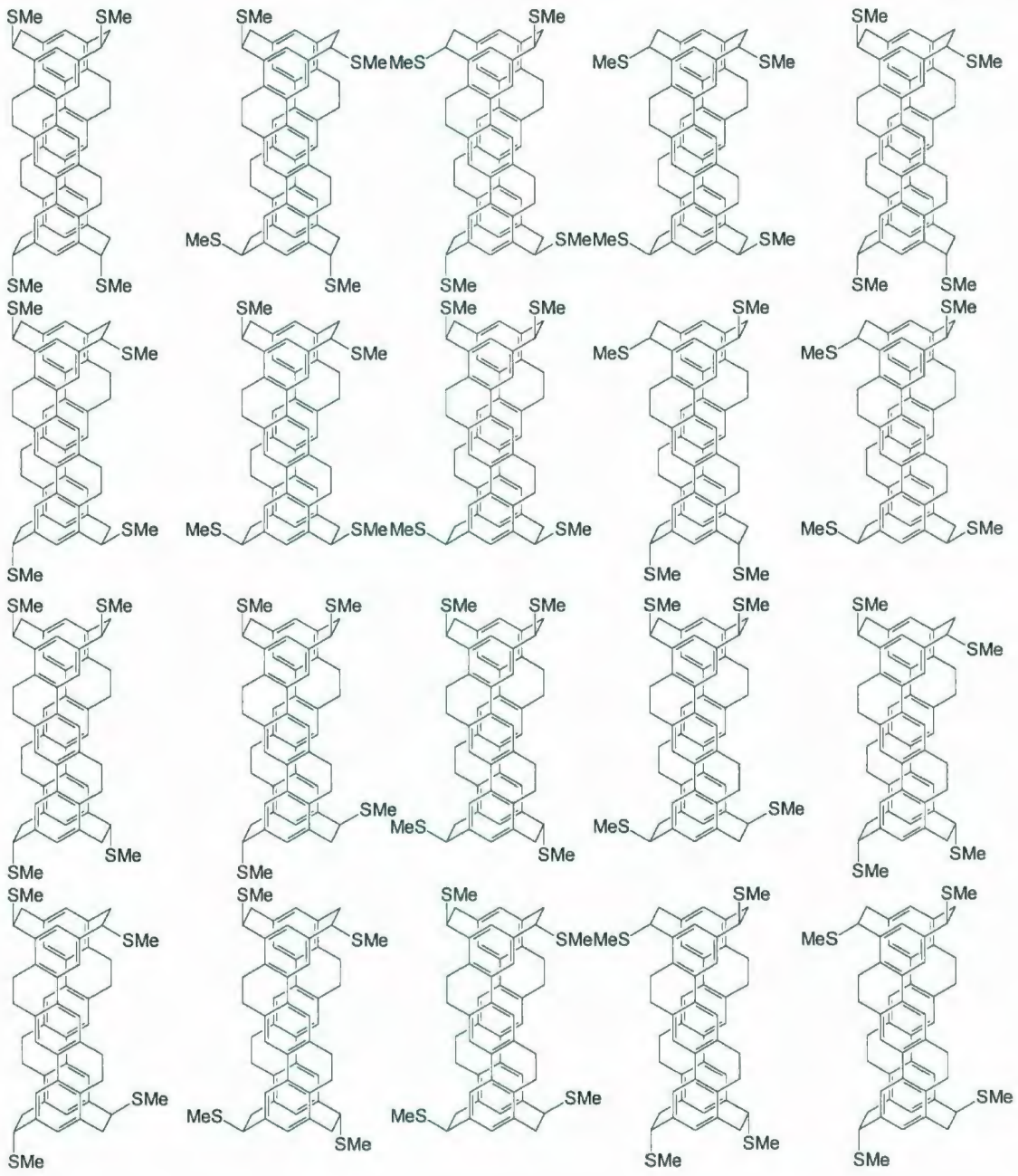


**Figure A1-16-1.** 76 pairs of enantiomers from the $D_2$ backbone (1).

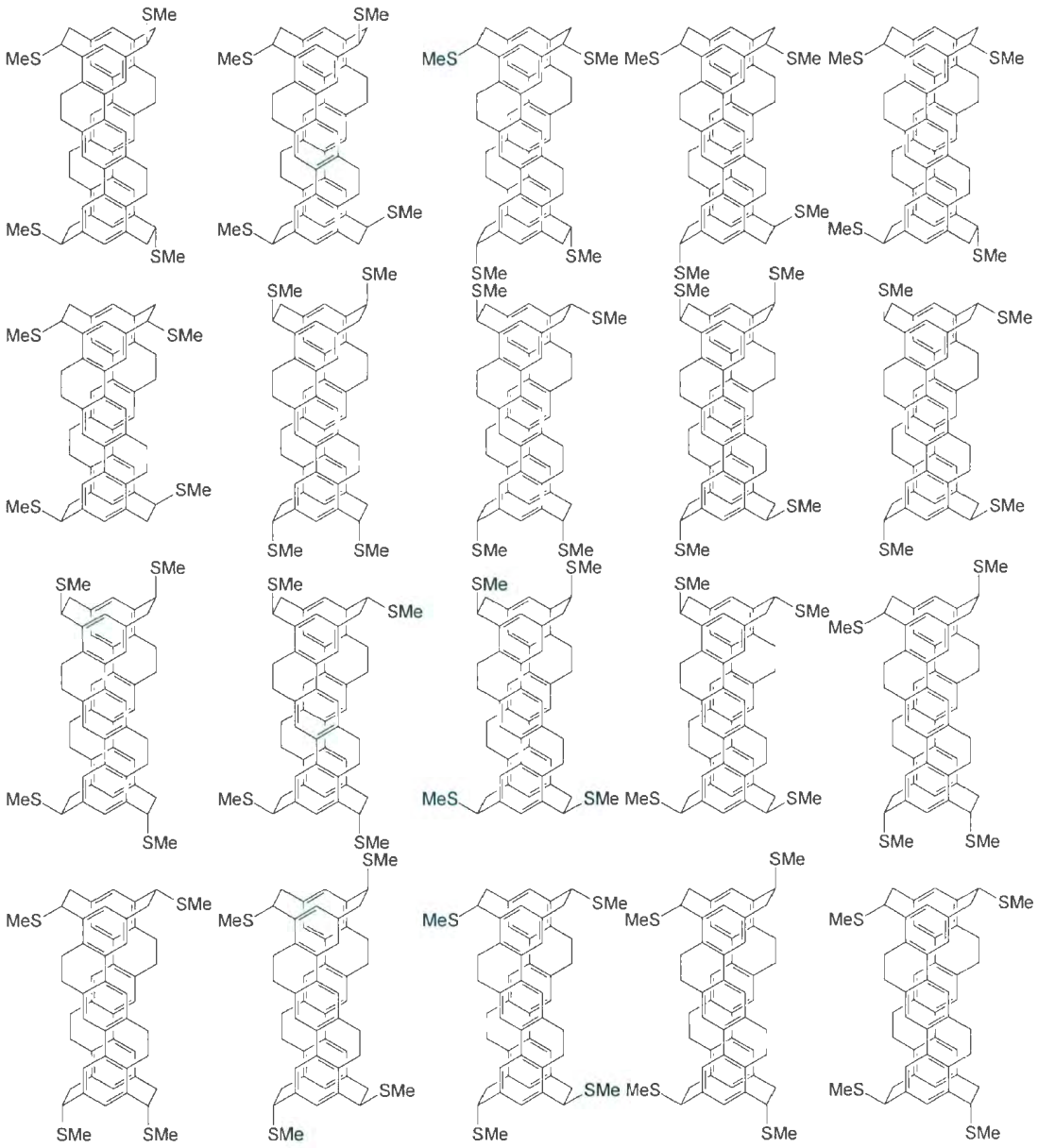


**Figure A1-16-2.** 76 pairs of enantiomers from the $D_2$ backbone (2).

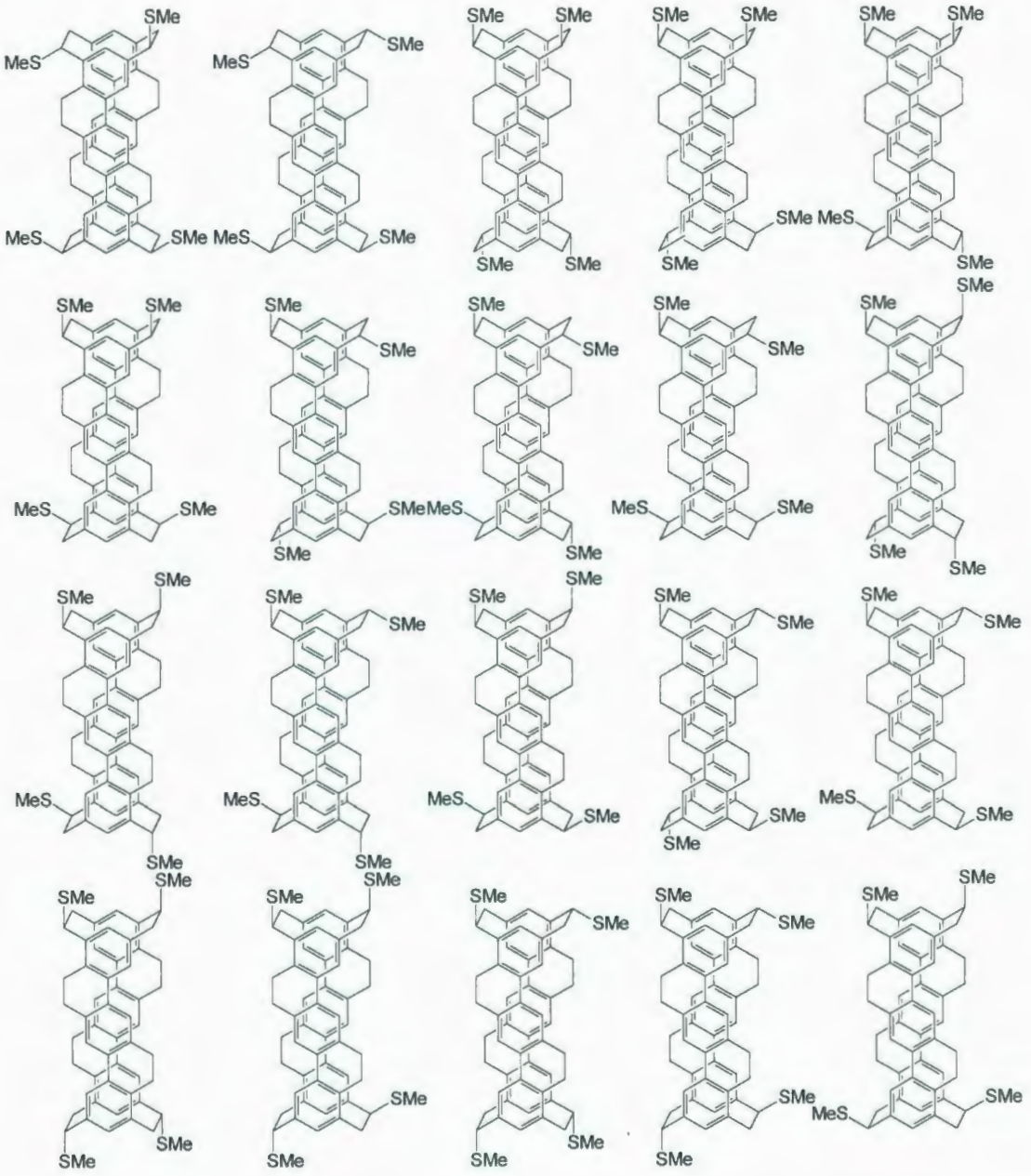


**Figure A1-16-3.** 76 pairs of enantiomers from the $D_2$ backbone (3).

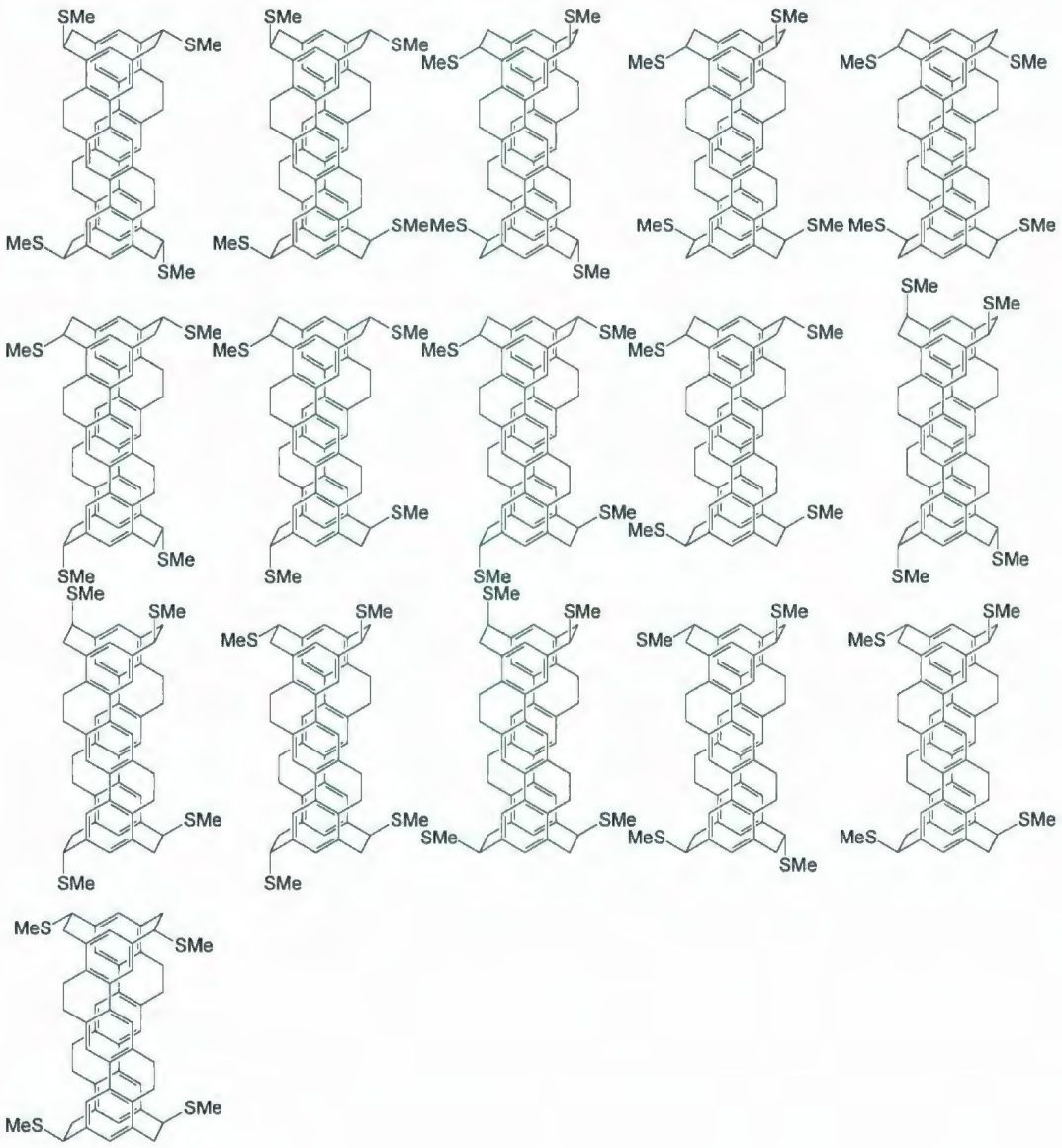


**Figure A1-16-4.** 76 pairs of enantiomers from the $D_2$ backbone (4).

# Appendix B

## Selected NMR Spectra

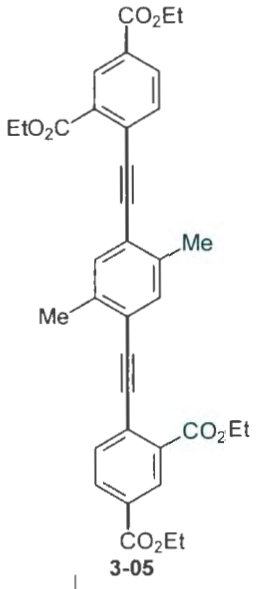


**3-05**




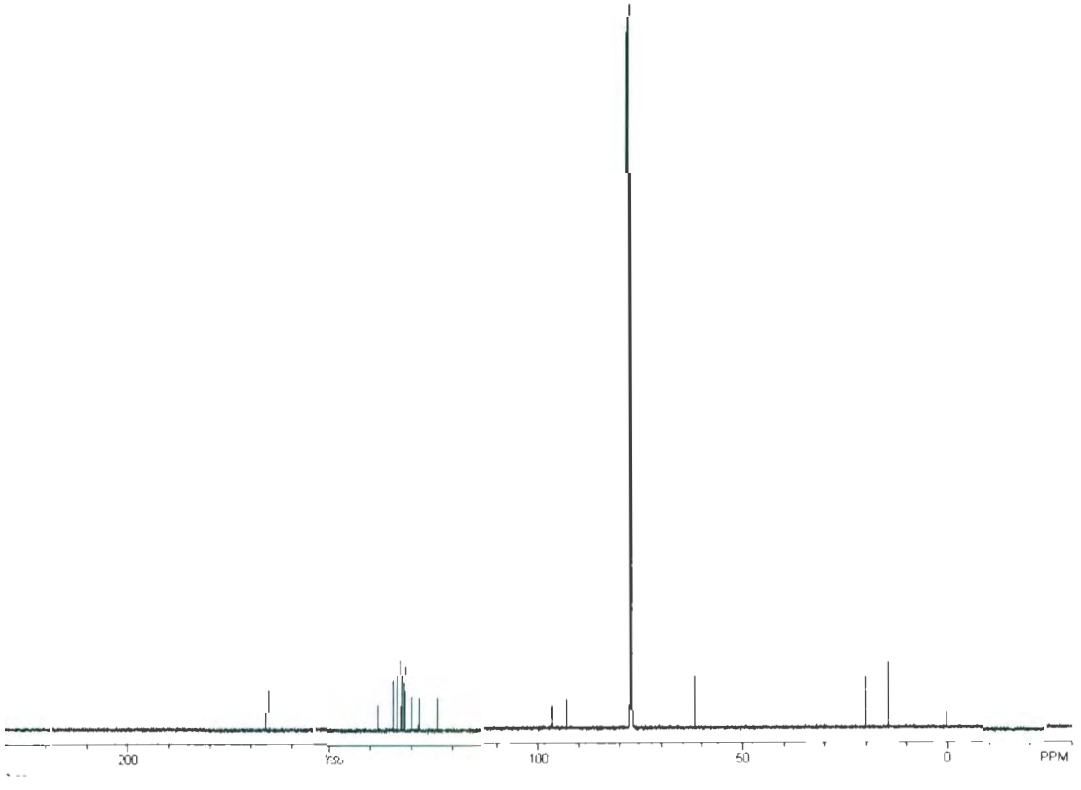

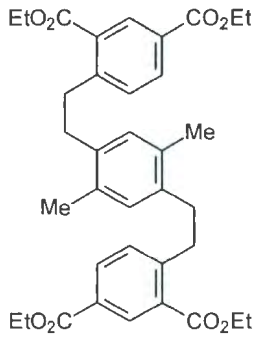


**3-06**




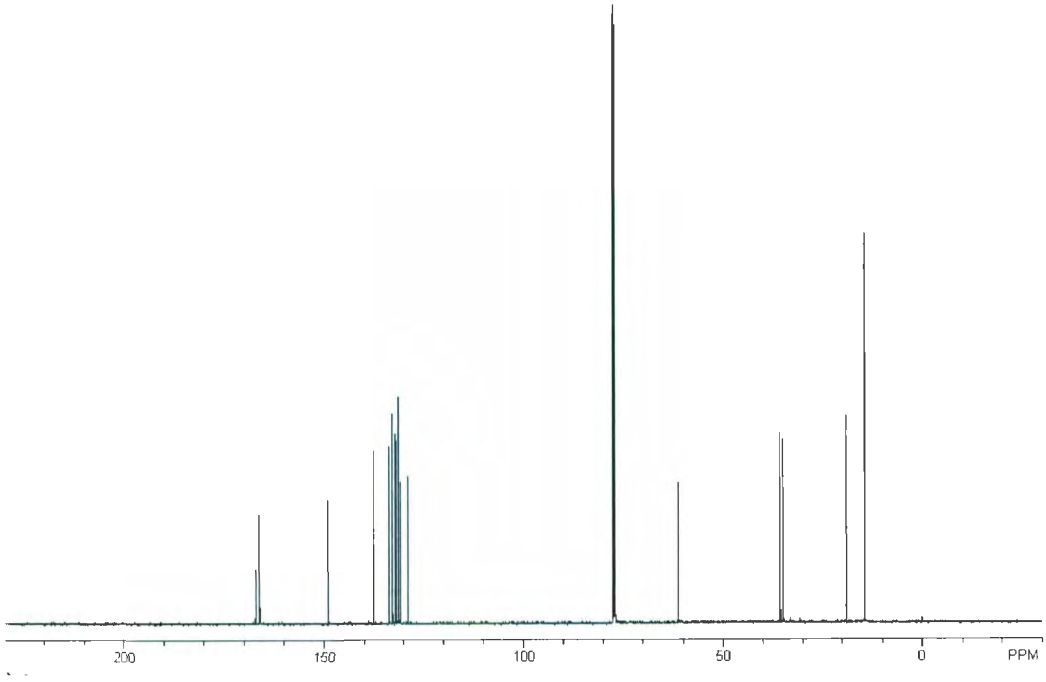

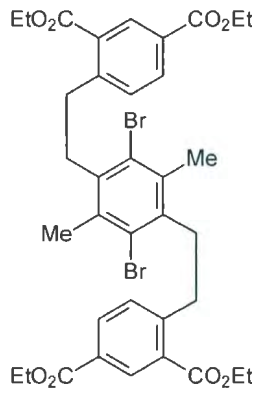
EtO2C
CO2Et
Br
Me
Me
Br
EtO2C
CO2Et

**3-07**


10
8
6
4
2
PPM

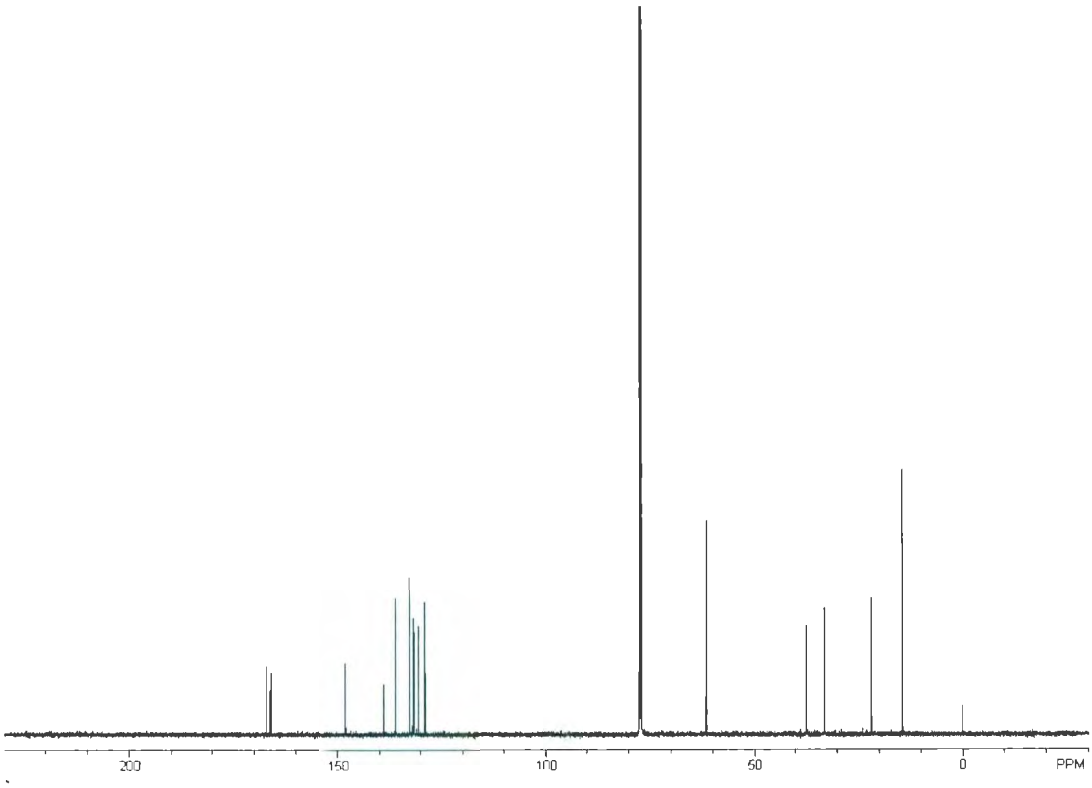
200
150
100
50
0
PPM

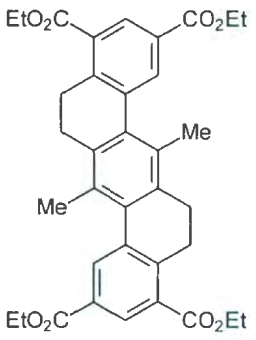


**3-08**




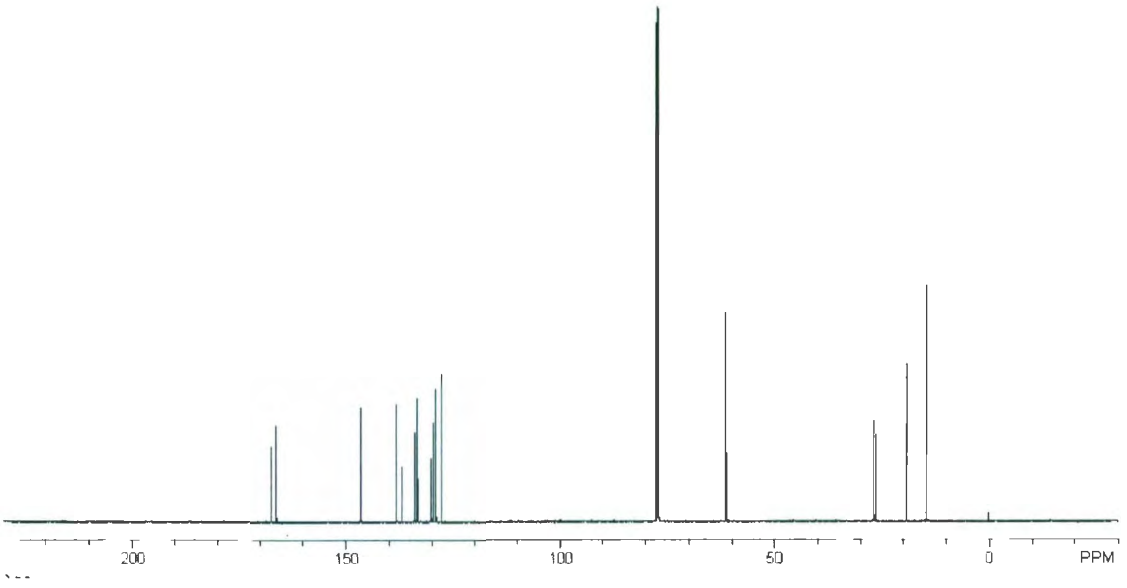

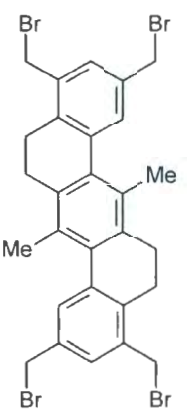


**3-11**

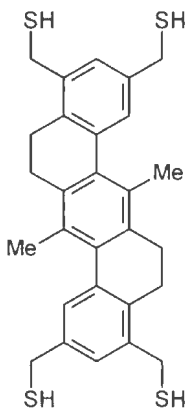


**3-12**

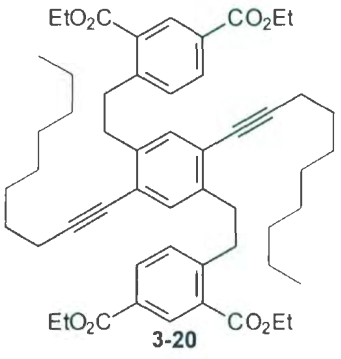


3-20




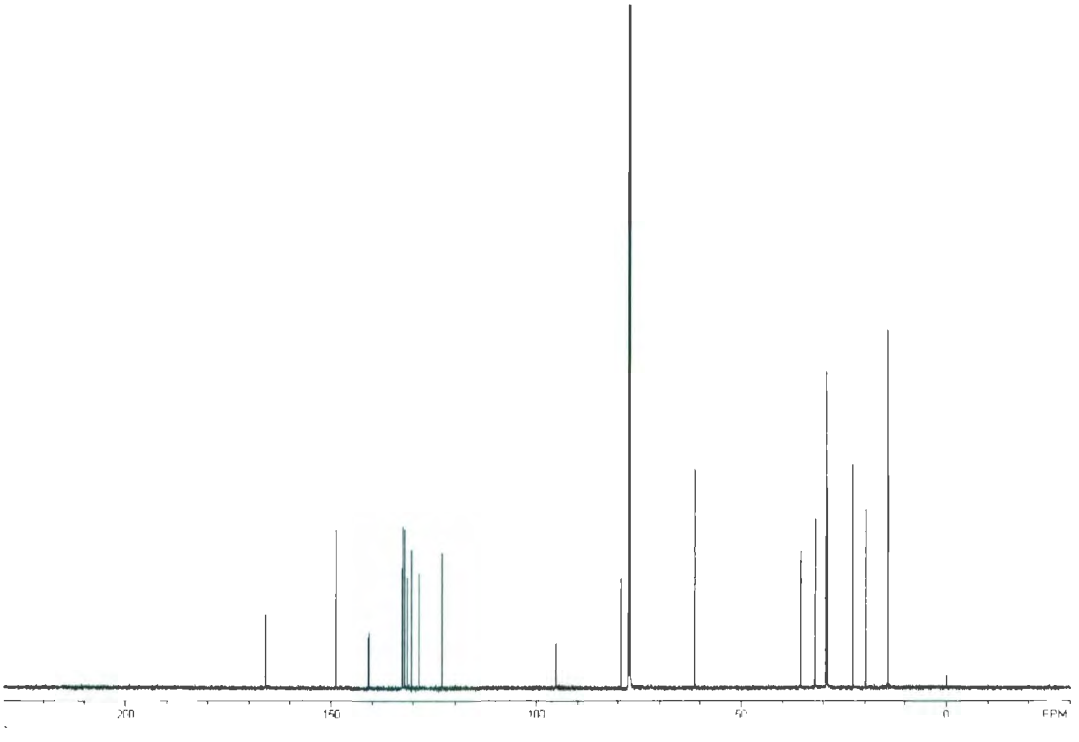

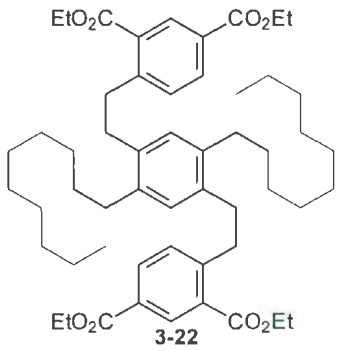


**3-22**




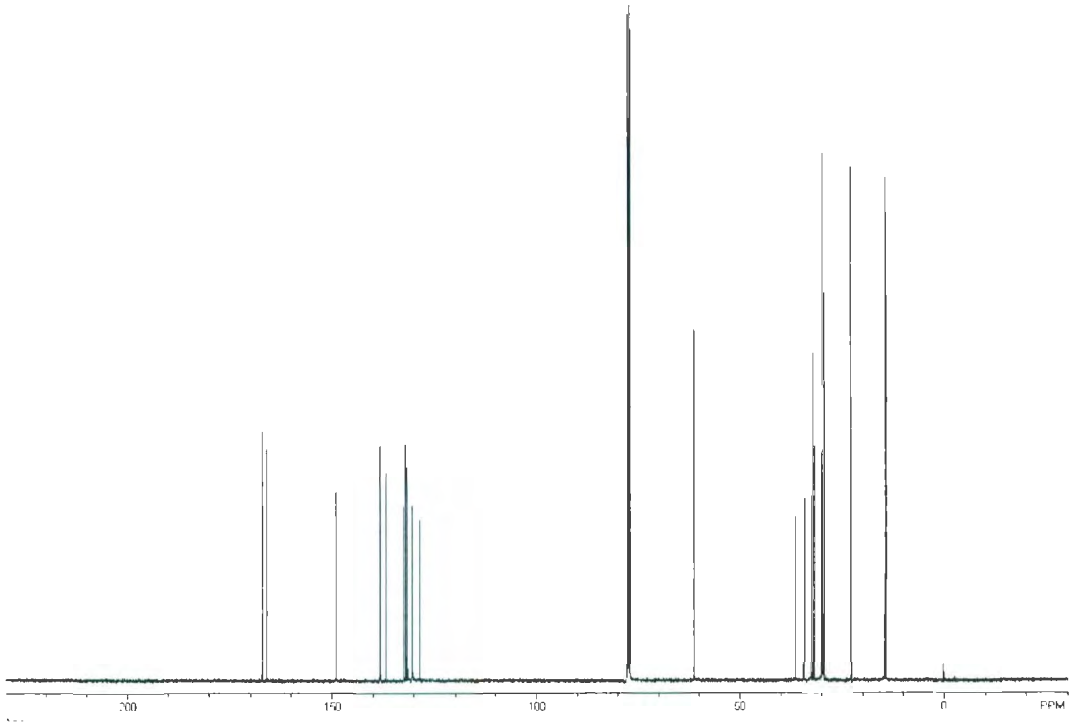

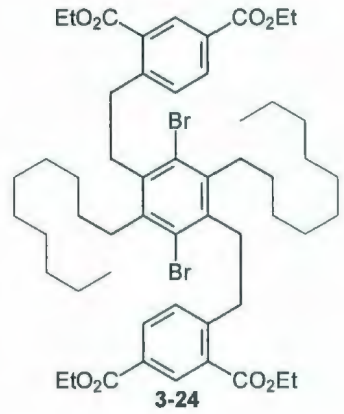


**3-24**




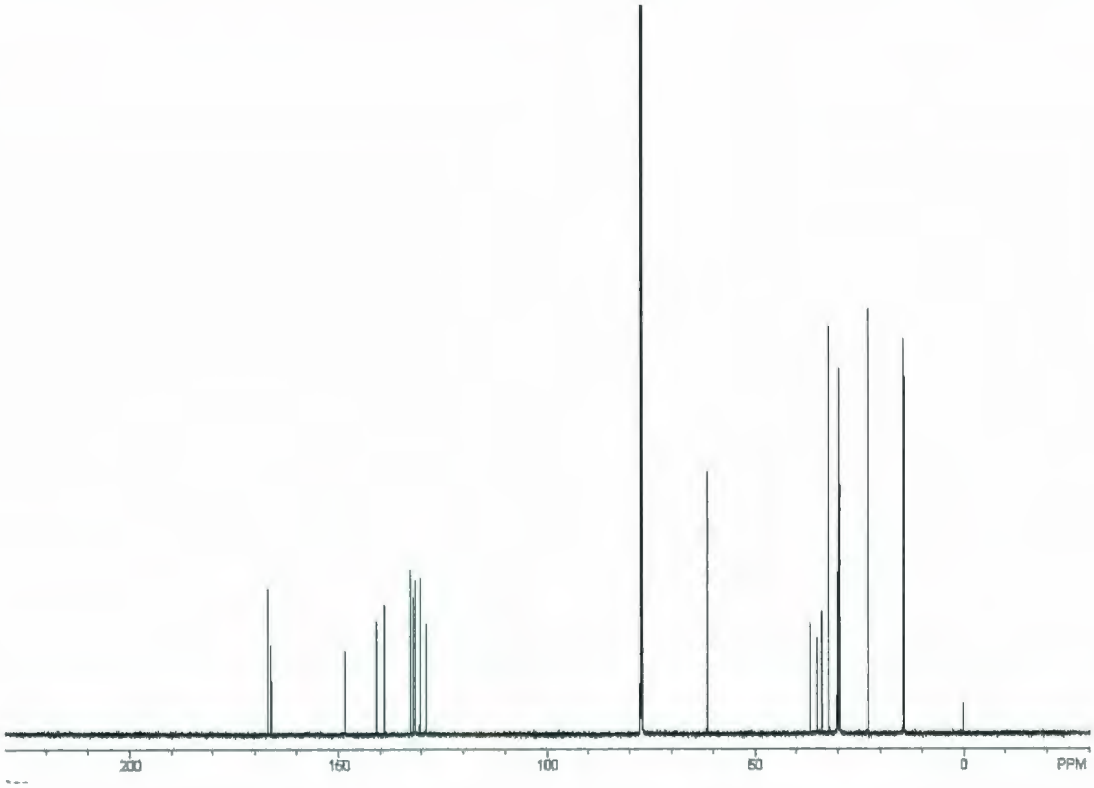

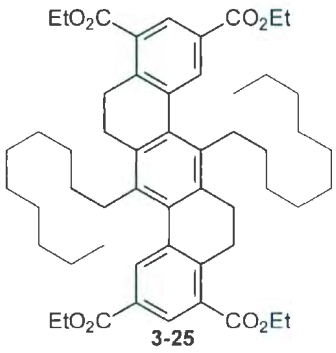


**3-25**

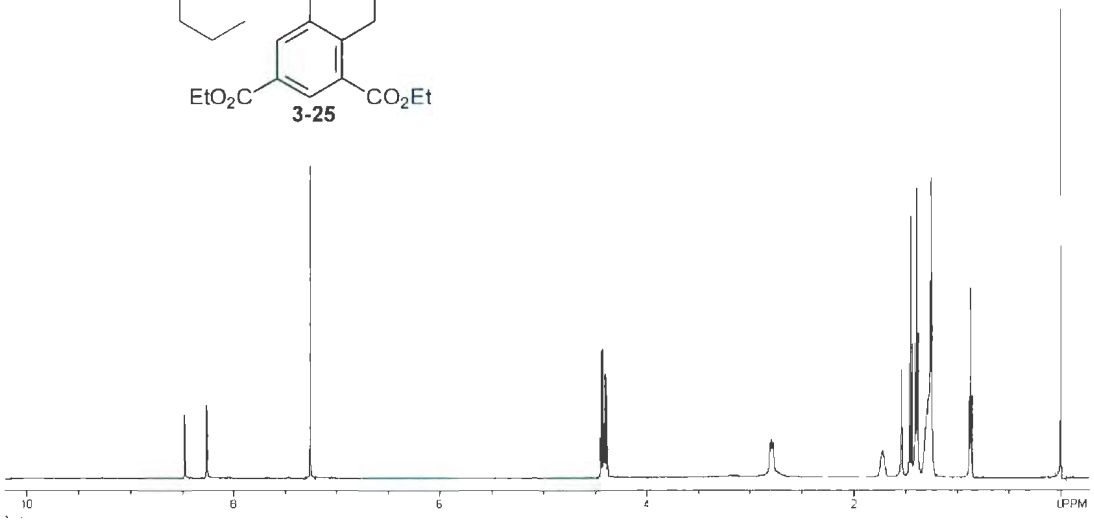


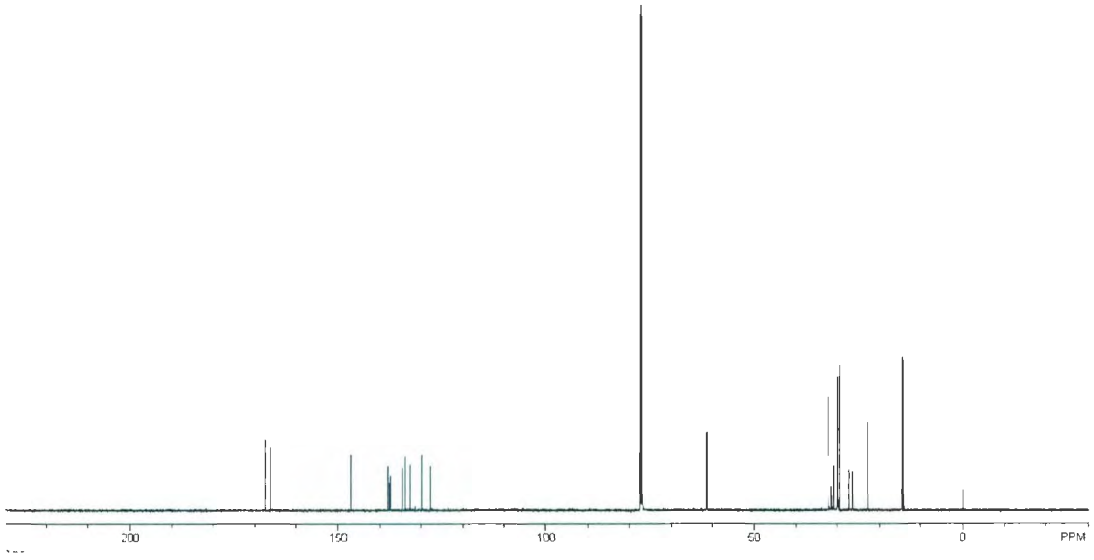

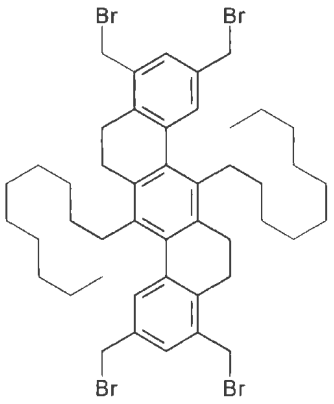


**3-27**




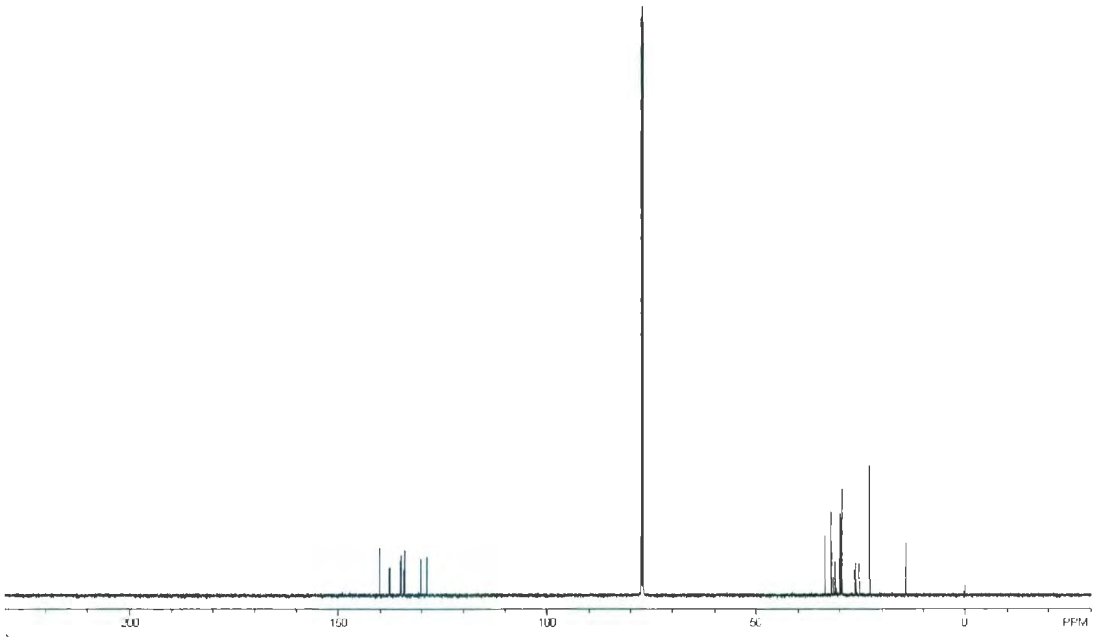

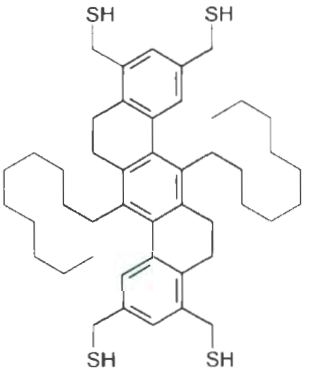


**3-28**



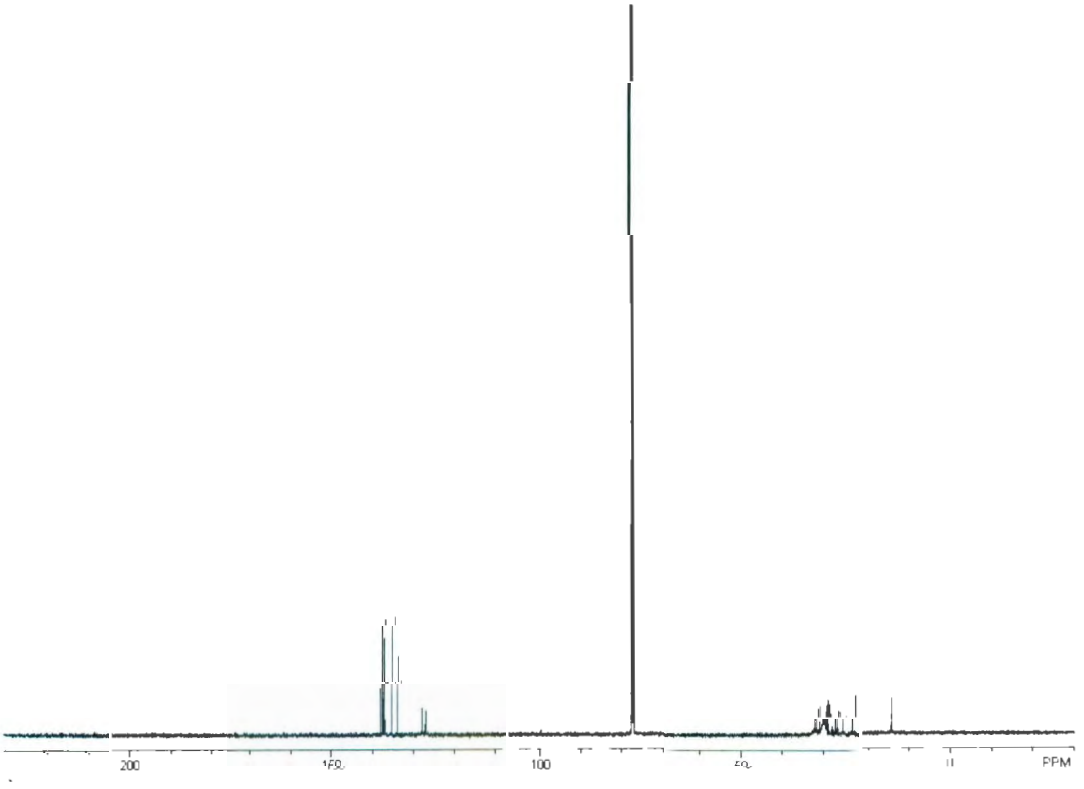

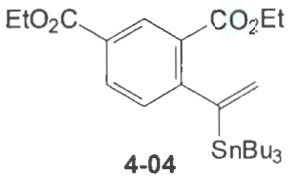


**4-04**




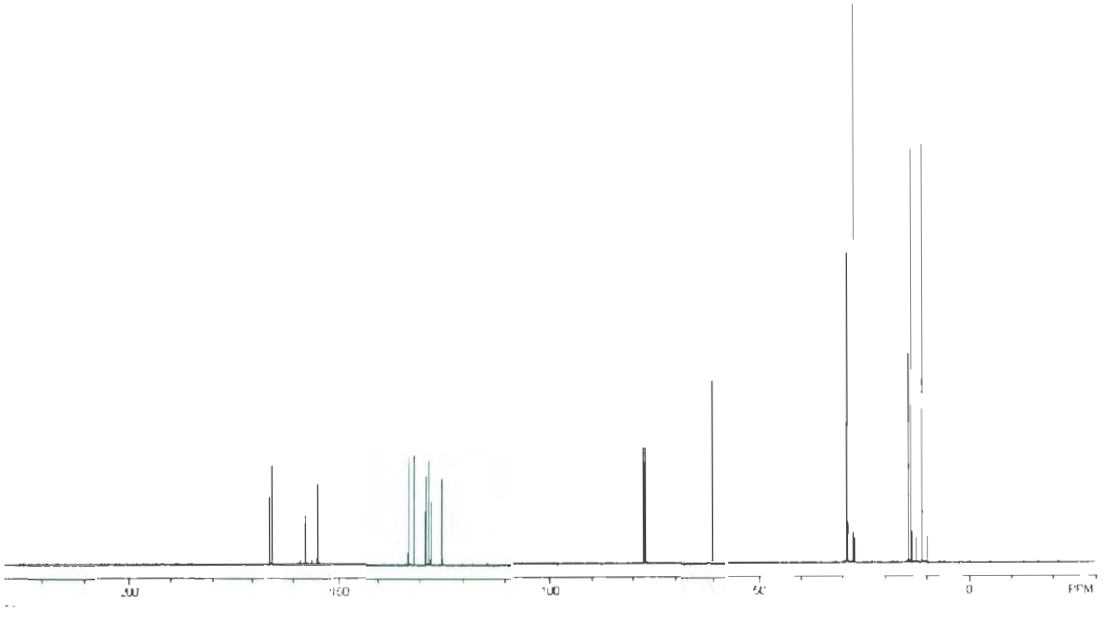

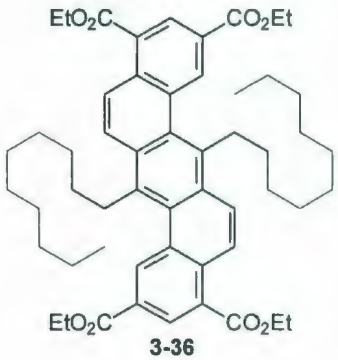


**3-36**

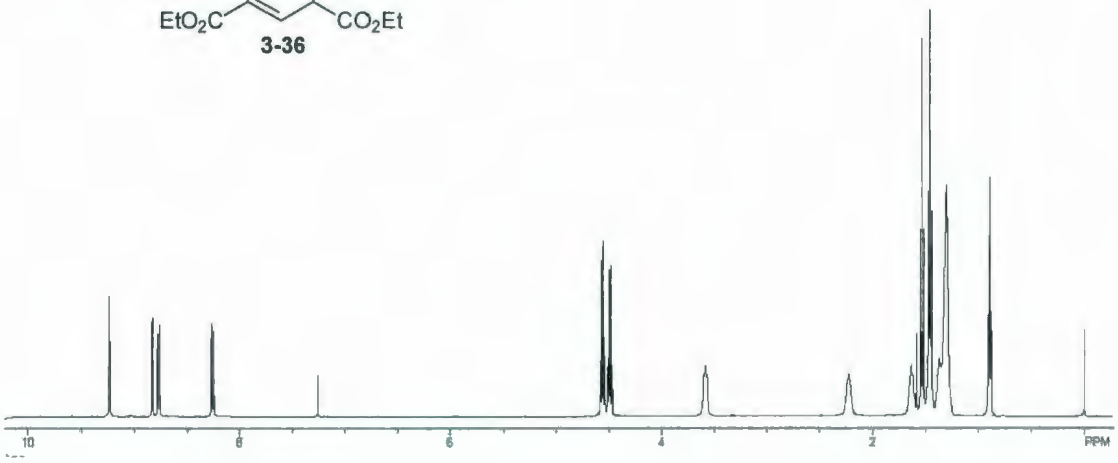


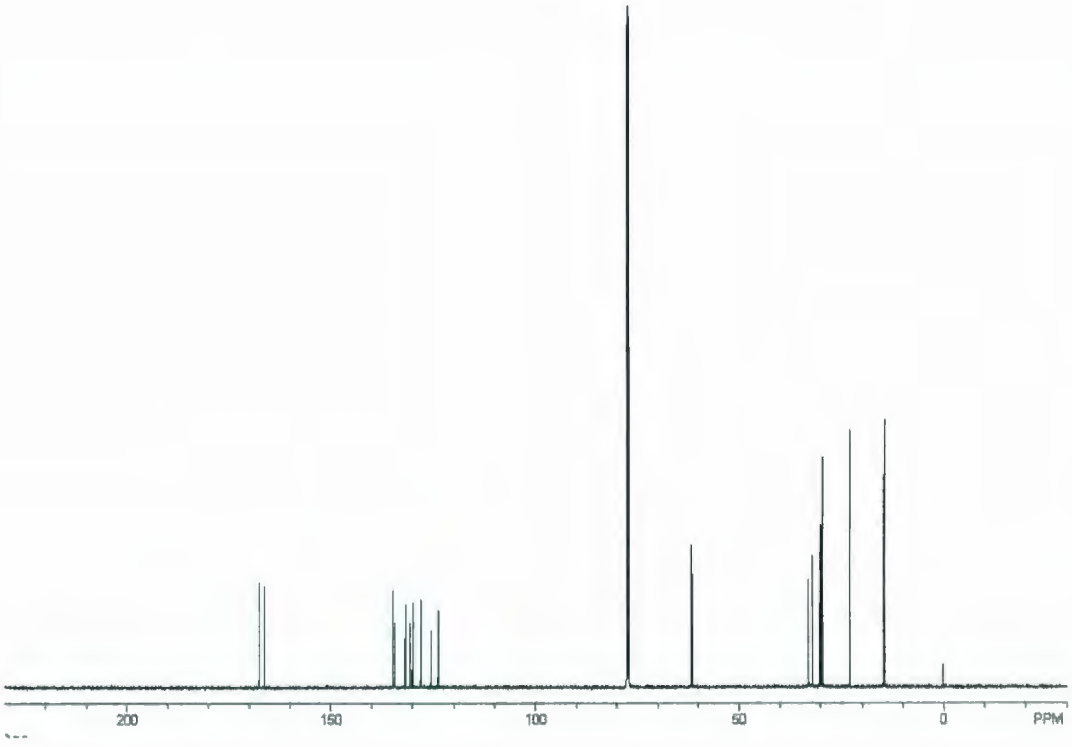

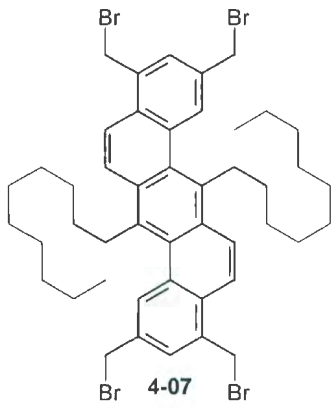


4-07